LN251 74-31

NOT FOR PUBLICATION

分置

Performance of Fuel Failure Detection System in Sodium in-Pile Loop Experiment (II)
—5th to 10th Sodium Circulation Experiments—

Dec., 1974

POWER REACTOR AND NUCLEAR FUEL DEVELOPMENT CORPORATION

This document is not intended for publication.

NOT FOR PUBLICATION
~~SJ250~~ TN251 74-31
Dec., 1974

Performance of Fuel Failure Detection System in Sodium in-Pile Loop Experiment (II)*

--- 5th to 10th sodium circulation experiments ---

Eiji SAKAI,** Masaki KATAGIRI,** Hiroshi ITOH,**
Kenmei HIRANO*** and Yasaburo YAMAZAKI***

Abstract

Performance of four different types of fuel failure detection systems has been studied using a sodium in-pile loop located in Japan Research Reactor 2, Sodium of 8.5-liters circulates through an irradiation section (500 °C), a main-cooler (400 °C), an expansion tank (350 °C), an electromagnetic pump, and a main-heater at a flow rate of 3-liters/min. In the irradiation section, four metallic uranium plates (20%-enriched) of a total amount of U-235 of 9.18-g have been irradiated at a thermal neutron detector consisting of a BF_3- counter system in a graphite moderator (50-cm x 50-cm x 80-cm) detects delayed neutrons from fission products in the expansion tank. The sodium travel time from the irradiation section to the expansion tank was 23.1-sec. at a sodium flow rate of 3-liters/min. Helium cover gas over the sodium in the tank carries gaseous fission products, such as Kr and Xe, to a

---

This is the translation of the report, SJ250 74-~~14~~12, issued in Apr., 1974.

* Work performed by Japan Atomic Energy Research Institute (JAERI) under contract with Power Reactor and Nuclear Fuel Development Corporation.

** Reactor Instrumentation Laboratory Division of Reactor Engineering, JAERI

*** Reactor Safety Laboratory II Division of Reactor Safety, JAERI

precipitator (The Plessey Co., Ltd., Mark XI) by which beta-rays from Rb-88 and Cs-188 collected on a precipitation-wire are detected. The precipitator was modified to measure gamma-ray spectrum from the wire using a 40-cm^3 Ge(Li) detector systems. The helium gas is also guided into a gas-reservoir whose gamma-rays are analysed by another 100-cm^3 Ge(Li) detector system.

The results obtained using the delayed neutron-, precipitator-, and cover-gas reservoir gamma-ray spectrometer-type detection systems during the first to the fourth sodium circulation experiments were already reported in a previous paper (Eiji SAKAI, et al.: JAERI-memo 5287 (May 1973)). The present paper describes the results obtained from the four types of the detection systems mentioned above during the fifth to the tenth sodium circulation experiments in the period from May to December, 1973.

Contents

1. Introduction

In order to test and confirm the performance of a fuel failure detection system consisting of a delayed neutron detector and a precipitator using a sodium in-pile loop (SIL)[1)~3)] located in Japan Research Reactor 2 and also to obtain data for evaluating the performance of the fuel failure detection system of the experimental fast breeder reactor "JOYO", the Fast Breeder Corporation (PNC) entrusted Japan Atomic Energy Research Institute (JAERI) with a study titled "fuel failure detector test in sodium in-pile loop" on October 31, 1972. The content of the study involved the test and evaluation of the performance of the delayed neutron detector and the precipitator provided by PNC. The detailed description of the study is as follows: about the delayed neutron detector, the measurement of the background level caused by radioactive sodium, neon, and fission products from impurity uranium presented in sodium, detection sensitivity and their dependence on reactor power and sodium flow rate and the signal-to-noise ratio were requested. About the precipitator, the measurement of the effect of the background level caused by radioactive nuclides transferred into cover gas helium, detection sensitivity, response characteristics and their dependency on reactor power and cover gas flow rate and the signal-to-noise ratio were requested.

The Reactor Instrumentation Laboratory, Division of Reactor Engineering, and the Reactor Safety Laboratory II, Division of Reactor Safety, JAERI, were entrusted the study. The latter took charge of the sodium in-pile loop operation[1)~3)].

The first contract had been performed during October 31, 1972, and May 31, 1973. The sodium in-pile loop was operated

without fuels and the background caused by the radioactive sodium was measured during November 4 and 14, 1972 (the first sodium circulation experiment). The sodium circulation time was 170 hr 52 min. Then, 20%-enriched metal uranium plates were installed and the second, the third, the fourth sodium circulation experiments were carried out during January 15 and 27, 1973 (sodium circulation time 290 hr 50 min.), February 26 and March 10, 1973 (303 hr), and April 9 and 21, 1973 (300 hr 45 min.), respectively. The results obtained were reported to PNC by a contract report (JAERI-memo 5287[4]), the end of May, 1973. Another study related to the behavior of fission products in sodium using the same sodium in-pile loop was made by the Reactor Safety Laboratory II, JAERI and a report (JAERI-memo 5283[5]) was published, in which the results on FFD-related studies such as fission product transfer from sodium to cover gas were described.

The second contract "fuel failure detector test in sodium in-pile loop (II)" started on May 14, 1973 and terminated on April 30, 1974. The content of the contract included an additional measurement of precipitator wire gamma-ray spectra as well as the content of the first contract. The sodium in-pile loop was operated six times during the second contract period: May 28 to June 9, 1973 (the fifth sodium circulation experiment, 306 hr sodium circulation time), June 18 to 30 (the sixth sodium circulation experiment, 245 hr), July 30 to August 11 (the seventh sodium circulation experiment, 298 hr 1 min.), October 1 to 13 (the eighth sodium circulation experiment, 271 hr 13 min.), November 12 to 24 (the ninth sodium circulation experiment, 295 hr 23 min.), and December 3 to 15 (the tenth sodium circulation experiment,

257 hr 21 min.). The total sodium circulation time was 2,739 hr 18 min.

The present report describes the results obtained during the fifth and the tenth sodium circulation experiments. Chapter 2 describes the outline of the sodium in-pile loop, the delayed neutron detector system, the precipitator, a gamma-ray spectrometer for expansion tank gas, the precipitator wire gamma-ray spectrometer. Chapter 3 outlines the results obtained during the second contract period (the fifth to the tenth sodium circulation experiments) as well as those during the first contract period (the first to the fourth sodium circulation experiments). Chapter 4, 5, 6 present the results obtained by the delayed neutron detection system, the precipitator, and the precipitator wire gamma-ray spectrometer, respectively. In Chapter 7, the detection sensitivity, signal-to-noise ratio, and the minimum detectable area of uranium plates were calculated. Chapter 8 was devoted to the concluding summary. The results of the study on fission product behavior in sodium made during the fifth and the tenth sodium circulation experiments is reported by Yamazaki, et al.[6].

The present delayed neutron detection system was designed by the Fast Breeder Development Project, PNC, and the Reactor Instrumentation Laboratory, JAERI, and manufactured by the Hitachi Shipbuilding Co., Ltd. The precipitator system was designed by the Fast Breeder Development Project, PNC and Tokyo Shibaura Electric Co., Ltd., who manufactured the system. References 7) to 12) were published at various stages of designing, manufacturing, and testing.

During the fifth and the tenth sodium circulation experiments,

Makoto Sawada, Akira Endo, Yoshinori Ishii, and Hiroshi Hara of the Experimental Fast Reactor Division, PNC, participated in some parts of the experiments.

This study will be continued after May, 1974 and the sodium in-pile loop experiment having uranium oxide fuels will start in the mid 1975 when Japan Research Reactor 2 start its operation again.

2. Outline of Experimental Apparatus

The experimental apparatus used in the present study consisted of

1) Japan Research Reactor 2 (JRR-2),

2) a sodium in-pile loop (SIL) whose irradiation section was inserted in a horizontal experimental hole HT-15 in JRR-2 and the circulating liquid sodium carried the fission products released from irradiated uranium metal plates,

3) a delayed neutron detector type fuel failure detection system attached to the sodium in-pile loop by which the delayed neutrons from an expansion tank could be detected,

4) a precipitator type fuel failure detection system attached to the sodium in-pile loop by which Kr and Xe radioactivities in cover gas in the expansion tank could be dtected,

5) a gas reservoir and a Ge(Li) gamma-ray spectrometer which could measure the gamma-rays from fission products in cover gas extracted from the expansion tank, and

6) another Ge(Li) gamma-ray spectrometer which could measure and identify the gamma-rays from radioactive nuclides collected on a precipitator wire.

While Item 5) was not installed in the first sodium circulation experiment and used thenceforth. Item 6) was prepared shortly before the ninth circulation experiment and used in the ninth and the tenth experiments.

The following is the outline of these apparatus. No explanation was given on JRR-2.

2.1 Outline of Sodium In-Pile Loop

The sodium in-pile loop circulates sodium which carries some of the fission products originated from fissile nuclear fuels under neutron irradiation and make the out-of-pile measurement of gamma-rays and delayed neutrons possible. It consisted of a sodium circulation system, a gas system, an operation system for instrumentation, control and safety, and radiation shieldings. Figure 2-1 shows the outline of the apparatus.

The sodium circulation system can be devided into an in-pile system and an out-of-pile system. The in-pile sodium circulation system was constructed in an irradiation plug inserted in a horizontal experimental hole HT-15 in JRR-2. The irradiation plug consisted of an inner tube, an outer tube, and a radiation shielding. Sodium flows in a tube (SUS-304, outer diameter 13.8 mm, inner diameter 9.4 mm) in the inner tube, make direct touch with the nuclear fuels (four metallic plates of 20%-enriched uranium) in an irradiation section of the top of the inner tube and returns through the other tube. The detailed description of the fuels is shown in Table 2-1. The four uranium plates, two of which were chosen from A-type plates and the other two from B-type, were loaded into the irradiation section. The total amount of ^{235}U in the loaded uranium plates was 9.18 gr and the estimated heat generation produced by thermal irradiation was less than 20 W. The averaged thermal neutron flux in the irradiation section was calculated as $5.4 \times 10^{10} n/cm^2 sec$ from the measured saturated radioactivity 0.43 Ci of 7.9 l sodium at 10 MW operation of the reactor (see Yamazaki, et al., JAERI-memo 5283 (May, 1973)). In replacing the nuclear fuels, the tube carrying sodium will be

cut and pulled out together with whole inner tube. The outer tube will be left in the experimental hole until the disassembling of the SIL.

The out-of-pile sodium circulation system consisted of a connecting intermediate section and an air-tight chamber. The two tubes carrying sodium came out of the irradiation plug go through the intermediate section in which they are protected by the inner and outer tubes from the outside and enter the air-tight chamber. All of the out-of-pile equipments related to sodium circulation, i.e., an electromagnetic pump, a main heater, an electromagnetic flowmeter, a main cooler, a cold trap, an expansion tank, a charge tank, a drain tank, a valve for opening and closing sodium flow, a valve for adjusting sodium flow rate, etc., are housed in the air-tight chamber.

Sodium flows out of the irradiation section, goes through the intermediate section to the air-tight chamber in which the sodium is cooled adequately by the main cooler, and enters through the electromagnetic pump into the expansion tank. In the expansion tank, the sodium has a free liquid surface on which helium cover gas touches to the sodium. The sodium stays in the expansion tank for about one min providing the measurement of delayed neutrons. The sodium came out of the expansion tank flows through the automatic valve for opening and closing sodium flow, the electromagnetic pump, the adjusting valve of sodium flow rate into the main heater in which the sodium is heated up to a desired temperature, leaves the air-tight chamber, goes through the intermediate section, and returns to the irradiation section. These equipments were connected by SUS-304 stainless

steel pipings of inner diameter 9.8mm and outer diameter 13.8 mm. All the sodium-touching portions of these equipments were made of SUS-304 stainless steel.

The sodium circulation system has a bypassing purifier system which takes care of sodium impurity control. The purifier system branches off from the main sodium circulation system just after the electromagnetic pump and the sodium to be purified flows through a sodium flow rate adjusting valve, a cold trap, a reheater, and an electromagnetic flowmeter, and returns to the expansion tank. The sodium purity is determined by the cold trap temperature. The sodium system also includes the charge tank that stores new unused sodium and the drain tank for used sodium.

As a protection system for sodium leak accidents, the porting touching sodium have a doubly-wrapped construction which makes it impossible for the sodium to be exposed to the air even when the sodium leaks. Helium gas flows through the gap between the inner and the outer tubes and the gas radioactivity is monitored by a radiation detector. Also, some of the sodium leak detectors are equipped and the sodium will be automatically drained into the drain tank when any sodium leak is found.

The entire volume of the main sodium circulation system is 3.85 liters except the expansion tank (10 liters), that of the purifier system 0.62 liters, and that from the end of the irradiation section to the expansion tank 1.153 liters.

The air-tight chamber hold a negative pressure to prevent from diverging of the contaminated air to the reactor room and has a tightly-closed fire-extinguishable construction when the

sodium leak starts fire.

The gas system consisted of a helium gas system which provided supplying, exhausting, and pressure adjusting of helium gas into the sodium system and the gap between the inner and the outer tubes, a pressurized-air supplying system to operate various types of air-operated valves, and to cool the electromagnetic pump and a cooling-air system to cool inside of the air-tight chamber.

The helium gas including fission products that was exhausted from the sodium system passes or bypasses a precipitation chamber of the fuel failure detection system, flows through a fission product trap, is monitored by a radiation monitor, and then exhausted to the exhausted system of the reactor building. The fission product gas trap is a liquid-nitrogen-cooled coil tubing made of SUS-304 stainless steel in which activated charcoal is filled.

The air inside of the air-tight chamber is monitored by a radiation detector.

The operation system for instrumentation, control, and safety measures and controls automatically the temperature and flow rate of the sodium at various points. It also performs safety actions such as alarm generation, sodium drainage, and reactor scram when needed in case of the abnormal conditions beyond automatic control or of sodium leakage.

Aiming to shield gamma-rays and neutrons, the radiation shielding was constructed by lead and stainless steel for gamma-ray shieldings and boron-loaded paraffin, graphite, boron-compound for neutron shieldings. The irradiation plug was constructed by lead, stainless steel, graphite, and boron-compound. Lead

and boron-loaded paraffin were used on the outside construction of the intermediate section and the air-tight chamber. The shielding-required equipments in the air-tight chamber and the fission product gas trap were covered by lead.

Smoke detectors were also furnished to provide fire detection. Collimators of 15 mm inner diameter were made at twelve positions on the air-tight chamber and four positions on the intermediate section to be used in gamma-ray measurements. An example of such collimators is shown in Fig. 2-2. The collimator positions are shown in Fig. 2-3. Graphite moderator blocks were constructed above the expansion tank, serving for delayed neutron detection.

2.2 Delayed Neutron Detector Type Fuel Failure Detection System[4)]

The delayed neutron detector system of the SIL consists of a graphite moderator system situated above the expansion tank, a neutron detector inserted into the moderator system and electronic equipments, as shown in Fig. 2-1.

The graphite moderator system[4)7)9)] slows down delayed neutrons (average neutron energy 250 ~ 600 keV) emitted from their precursor nuclides included in sodium in the expansion tank to thermal neutrons and provides the neutron measurement by a BF_3 counter or ^{10}B counter whose efficiency is large for thermal neutrons.

The dimension and construction of the expansion tank and the moderator system are shown in Fig. 2-4. The expansion tank is a SUS-304 stainless steel cylinder container of about 20 cm diameter and 38 cm height. The sodium passed the fuel irradiation section flows through the main cooler into the expansion tank and

then to the electromagnetic pump.

The sodium travel time from the end of the irradiated fuels to the inlet of the expansion tank through the main cooler is an important factor that determines the counting rate of the short halflife delayed neutrons, and the exact measurement of the travel time is needed. At present, the measurement is not yet performed so that the travel time was deduced from the calculated sodium volume devided by the sodium flow rate. The results are shown in Table 2-2 in which one can obtain 23.1 sec. for a sodium flow rate of 3.0 liters/min.

The expansion tank wrapped by fineflex felt as temperature insulator was put in a SUS-304 outer cylinder of 30 cm diameter. The outer cylinder was enclosed in a lead shielding which had a 5.0 cm thick lead ceiling. On the ceiling, a 2.5 cm thick SS-41 made lid-plate of the air-tight chamber, a 0.9 cm thick iron plate, a 4 cm thick lead shielding-plate, and a 0.9 cm thick iron plate were laminated, and then the graphite moderator system was set on the top iron plate.

The graphite moderator system was assembled by 25 pieces of the 10cm x 10cm x 80cm graphite blocks. Each of eight of the graphite blocks has a 6cm diameter hole in which a graphite rod of the same diameter can be inserted. When a neutron detector is to be inserted into the moderator, one of the graphite rods (in Positions A, B, C, D, I, J, in Fig. 2-4) must be pulled out for inserting the neutron detector. Most of the measurements were carried out by inserting a neutron detector into Position A. The distance between the center of the detector and the sodium surface in the expansion tank was 70.7 cm. The graphite

moderator blocks were enclosed in a paraffin shielding of 10 cm thickness which shielded neutrons from the outside and thus reduced the background counting rate. As will be described later, the original form of the graphite moderator system shown in Fig. 2-4 was used in the earlier stage of the first sodium circulation experiment in which a background counting rate of 10 cps was observed. At a later period, 10 cm thick boron-loaded paraffin blocks were placed on the wall of the moderator system faced to JRR-2 core and this reduced the background to 5 cps.

Photo 2-1 shows a BF_3 neutron counter and the graphite moderator system. Photo 2-2 shows the graphite moderator system covered by boron-loaded paraffin blocks into which the neutron detector was inserted. The white blocks seen in the two photos are the boron-loaded paraffin blocks. The neutron detectors provided by PNC for the fuel failure detection experiments include five BF_3 counters (20th Century Electronics, Ltd., 40EB-50/70G), four ^{10}B counters (20th Century Electronics, Ltd., PN12EB), two BF_3 counters (Mitsubishi Electric Co., Ltd., ND-8523-A-60), and two BF_3 counters (Mitsubishi Electric Co., Ltd., ND-8537-90), whose characteristics are tabulated in Table 2-3. The neutron detector mainly used was one of 40EB-50/70G made by the 20th Century Electronics, Ltd., with an applied voltage of 3200 V covered by a sheet of polyethylene insulator.

The output pulses of the neutron detector were amplified and analysed using the electronics shown in Fig. 2-4. The neutron detector output was connected by a 2 cm long cable to a preamplifier (JAERI-121A) placed on the ceiling of the SIL,

amplified and led by a 70 m cable to a basement of the reactor room where it was pulse-shaped by a main-amplifier (JAERI-156), pulse-height-analysed by a single channel analyser (JAERI-133A), and its counting rate was measured by a counting-ratemeter (Toyo Electronics Co., Ltd., BM-700) whose output was recorded by a pen recorder (Yokogawa Electric Co., Ltd., 3047). The output of the single channel analyser was also counted by a scaler (JAERI-146) whose counting time was controlled by another scaler (JAERI-146) used as a timer. A high voltage power supply (John Fluke 408B) for the neutron detector was placed in the basement and was connected by a 70 m cable to the preamplifier on the ceiling of the SIL. Photo 2-3 shows the electronics for the delayed neutron detector system. The top equipment on the rack shown at righthand in the photo is the pen recorder under which the electronics (NIM modules) for the delayed neutron detector system are seen. The others are the electronics for the precipitator, which will be described in the next section.

An electronic system shown in the lower part of Fig. 2-5 monitors reactor neutron flux. A BF_3 counter (Mitsubishi Electric Co., Ltd., ND-8537-90) was placed near the SIL intermediate section on the wall of the heavy concrete shielding of JRR-2 core to measure leakage neutrons from the reactor. The time response characteristics of the delayed neutron detector system were measured by studying the timing relation between the outputs of the leakage neutron detector and the delayed neutron detector. The electronics were placed in the basement.

A multichannel pulse height analyser indicated in Fig. 2-5

belongs to the Reactor Instrumentation Laboratory, JAERI, and the detector system were transferred by a 1,000 m long cable from JRR-2 to the analyser that located in the Research Building No.2. Multi-scaler measurement was performed by the multichannel analyser to which the outputs from the detectors for the leakage neutrons, delayed neutrons and gamma-rays were fed in order to measure their timing relation. The analyser used was one of the ND-50/50 manufactured by Nuclear Data Co., Ltd., with a mini-computor PDP-8/L by which the multi-scaler measurement was made using a laboratory-made program.

Table 2-4 shows normal operating conditions of the delayed neutron detector.

2.3 Precipitator Type Fuel Failure Detection System[4)10)11)]

As already shown in Fig. 2-1, helium gas flows on the sodium surface in the expansion tank and fission products with the helium gas from the expansion tank if they transfer from the sodium into the gas. The helium gas moves from the expansion tank to a sodium vapour trap in which sodium vapour can be removed by the stainless steel meshes packed in the trap and flows to the basement room, where it flows through a gas reservoir for gamma-ray spectroscopy and a precipitation chamber to a liquid-nitrogen-filled cold trap by which fission products are removed. It is exhausted from the JRR-2 stack after its radioactivities are checked. The gas reservoir for gamma-ray spectroscopy can be bypassed using valves.

The precipitator used was the Mark XI manufactured by The Plessey Co., Ltd.[10)] The principle of the precipitator is as follows: positively-charged Rb and Cs nuclides produced in the process of the beta-decay of Kr and Xe are collected on a central

wire which has a negative voltage relative to the positive voltage of an outer cylindrical electrode in the precipitation chamber. The beta-rays emitted from the Rb and Cs nuclides collected on the central wire are detected by a scintillation counter. The precipitator detects only Kr and Xe radioactivities out of many kinds of fission products so that it provide a high S/N ratio measurement.

The precipitator and its associated panel placed in the basement are seen in Photo 2-4. An explanation drawing of the construction of the precipitator is shown in Fig. 2-6. The helium gas including fission products enters into and flows through the precipitation chamber. The volume of the precipitation chamber is one liter. The cylinder radius is 7 cm and its length is 6.7 cm. There is a stainless steel wire of 18 m length in the center axis of the precipitation chamber. The wire forms a 2.15 mm diameter helical coil spring which provides a tensile force and is wound on four pulleys. It collects Rb^+ and Cs^+ ions accelerated by the electric field in the chamber. After these ions are collected for a predetermined period (soak time), the wire is driven by a driving motor into the scintillation counter in which a counting is performed in the same period of time (count time). The part of the wire for which the counting is terminated is wound many turns on the pulleys in the precipitator so that the wire radioactivity can decay. Purge gas flows from the scintillation counter to the precipitation chamber so that the fission products in cover gas can not enter into the scintillation counter and contaminate it.

The scintillation counter detecting beta-rays is, as shown

in Fig. 2-7, of tetraphenylbutadien plus terphenyl having a shape of 3.97 mm inner diameter, 6.35 mm outer diameter and 53.97 mm length, which is covered by a light-guide of pyrex-glass and the light-guide touches to a photomultiplier is amplifier (EMI 6097G). The output of the photomultiplier is amplified by a preamplified by a preamplifier and is led by a 15 m long cable to the precipitator electronics located in the middle of the standard rack shown in the lefthandside of Photo 2-3.

Figure 2-8 shows a schematic diagram of the electronics of the precipitator. The pulse count channel serves to amplify the scintillation counter output, in integrate the counted value and to record its integrated value on the chart of a pen recorder. Therefore, a pen follows a series of figure which rises step-like (10 cts per step) and then resets to 0 at the end of its count time on the recorder chart.

The operation of the precipitator is as follows: the soak time can be manually set as 20 sec. to 12 min. During this soak time, the precipitator wire collects Rb and Cs nuclei and them moves into the scintillation counter which detects the wire radio-activities. The time needed for the wire movement is about one sec. This operation repeats again and again.

For the experiment which uses other type of the recording instruments than the pen recorder, the preamplifier output from the scintillation counter can be taken out from the "PULSE HEIGHT CHANNEL" terminal and counted by a scaler as digital signals.

Table 2-5 shows normal operating conditions of the precipitator.

2.4 Gamma-Ray Spectrometer System for Expansion Tank Gas[4)5)]

The identification of the fission product nuclides in the helium gas filled in the space above sodium in the expansion tank is very important to investigate the basic performance of the cover gas type fuel failure detection system such as a precipitator which measures the fission products in cover gas extracted from the SIL. It is also one of the necessary items of the measurement to investigate the transfer of fission products from sodium to helium gas in the expansion tank.

The SIL has a collimator for measuring gamma-ray spectrum of the expansion tank gas which has the same construction as the one for the expansion tank sodium shown in Fig. 2-2. The gamma-rays from the expansion tank gas pass through an inner cylinder (made of 6.5 mm thick SUS-304), a 40.8 mm thick fineflex felt heat insulator, a 10.3 mm thick outer cylinder of SUS-304, a 5 mm thick iron plate of SS-41, successively, and thus a beam of 15 mm diameter of gamma-rays can be taken out from the expansion tank in order to make gamma-ray spectroscopy by a Ge(Li) detector.

The Ge(Li) detector used in the gamma-ray spectroscopy of the expansion tank gas is a 55 cm^3 coaxial detector manufactured by Ortec, Inc., and its main characteristics are shown in Table 2-6.

Photo 2-5 shows the Ge(Li) detector system located in one of the collimators dug on the side-wall of the SIL. The detector is placed on a movable cart which makes the adjustment of the detector position possible.

A schematic diagram of the electronics used for the detector

is shown in Fig. 2-9. The detector output was amplified by a preamplifier (Ortec 120-4B), pulse-shaped by a research amplifier (Ortec-450) and analysed by a 4096 channel pulse height analyser (Toshiba USC-1). It was also fed to a single channel pulse height analyser (Ortec-420). Its counting rate was measured by a counting-ratemeter (Hammer NR-10) whose output was recorded by a pen-recorder (Matsushita Electric Co., Ltd., VP-652A). The output from the single channel pulse height analyser was fed to a delayed gate generator (JAERI-148) whose output was sent to a multichannel pulse height analyser (ND-50/50) located in the Research Building No.2 in order to investigate the relation between the outputs from various neutron detectors and gamma-ray detectors.

2.5 Gamma-Ray Spectrometer for Gas Reservoir Gas[4)]

The cover gas in the expansion tank was taken out from the SIL and sent to the precipitator. Just before the precipitator, a gas reservoir was located to investigate fission products in the helium gas by measuring the gamma-ray spectra with a Ge(Li) detector.

The gas reservoir was set up on the side of the precipitator in the basement as shown in Photo 2-6. It is a SUS-304 cylinder of 95.6 mm diameter and 144 mm length in which a 125 mm long partition plate serves to ensure a smooth flow of helium gas without staying in the corners, as shown in Fig. 2-10. The axis of the cylinder was set horizontally. The thickness of the end plate to which the Ge(Li) detector faces is 4 mm of SUS-304. The thickness less than 4 mm was impossible in the view point of mechanical safety. The inner volume of the gas reservoir is

984.4 cm^3. A lead cylinder of 7.4 cm thickness shields around the reservoir. The top of the Ge(Li) detector was put into a hole of 10.6 cm inner diameter of the lead shielding to shield the gamma-rays coming from the outside of the reservoir. At the lefthandside in Fig. 2-7, the Ge(Li) gamma-ray spectrometer for gas in the reservoir.

The Ge(Li) detector is a 100 cm^3 coaxial detector made by the authors[8] and its characteristics are shown in Table 2-7. The detector output was fed to a preamplifier (Ortec 120-2B), a research amplifier (Ortec 450), a gated bias amplifier (Ortec 444) and a multichannel pulse height analyser (ND-50/50) by which pulse height measurement was performed. Also, to a single channel pulse height analyser (JAERI-133S), A counting-ratemeter (JAERI-161) and a pen-recorder (Matsushita Electric Co., Ltd., VP-625A) to record its counting rate.

2.6 Precipitator Wire Gamma-Ray Spectrometer System

In order to measure gamma-ray spectra of the radioactive nuclides collected on the precipitator wire, a coaxial Ge(Li) detector was made and installed in the space where the photomultiplier of the precipitator had been moved, as shown in Fig. 2-7. The manufacturing and characteristics of the system are described in detail in Chapter 6. The construction is shown in Figs. 6-4, 6-5, and 6-6.

3. Outline of the experiments

Since the first sodium circulation experiment on November 4 to 13, 1972, the Sodium In-Pile Loop had been operated satisfactorily until the tenth sodium circulation experiment completed on December 25, 1973. The total sodium circulation time became 2,739 hr 18 min. Figs. 3-1 and 3-2 show the operation period of JRR-2 and the SIL, the sodium amount loaded, the sodium circulation time of each sodium circulation experiment during the term of the previous contract and the present contract term. Table 3-1 tabulates the subtotaled and totaled sodium circulation times of the experiments.

The results obtained in the first to the fourth sodium circulation experiments, which were reported in Chapter 3 of the previous report (JAERI-memo 5287[4]), will be outlined in Section 3-1 of the present report.

During the term of the present contract, the fifth to the tenth sodium circulation experiments have been carried out (see Fig. 3-2). In the fifth and the sixth sodium circulation experiments, sodium was circulated under the constant operating conditions to study the behavior of fission products synthetically. In the seventh sodium circulation experiment, the sodium flow rate in the purifier system was changed from 0.25 to 1 liter/min. to measure its effect on the fission product behavior. During the shutdown period of the reactor after the seventh experiment had completed, the shielding-wall and the lid of the air-tight chamber of the SIL were removed to sample a part of the sodium from the drain tank. The eighth sodium circulation experiment started after the SIL was assembled again The effect of sodium temperatures of the various

parts on the fission product behavior was measured under a constant flow of sodium circulation. In the ninth and the tenth sodium circulation experiments, the transfer of fission products to helium cover gas was mainly studied.

The sections following Section 3.2 describe the operating conditions of JRR-2 and the SIL, the contents of the experiments, the observed counting rates of the delayed neutron detector and the precipitator for each sodium circulation experiment. Table 3-2 explains the symbols used in the text to describe the SIL operating conditions. In the Table, the figures on the righthand-side show the temperatures and the flow rates of sodium in various parts under stationary operation of the SIL: the sodium temperatures in the irradiation section, main-cooler, expansion tank, cold trap were 500 °C, 380 °C, and 200 °C, respectively. The sodium flow rates of the main circulation system and the purifier system were 3 l/min and 0.5 l/min, respectively. The cover gas pressure (helium) was 100 mmHg gauge.

3.1 Outline of the First to the Fourth Sodium Circulation Experiments

The detailed description of the first to the fourth sodium circulation experiments was given by two previous reports (JAERI-memo 5287[4] and JAERI-memo 5283[5]). Their summary will be described in this section.

(1) The First Sodium Circulation Experiment

The first sodium circulation experiment was carried out with stainless steel plates (SUS-304) as dummy fuels in the irradiation section during 6 and 13 November 1972 (the eighth operation cycle of JRR-2 of FY 1972). Sodium of 7.9 liters

was circulated. The sodium circulation time was 170 hr 52 min.

In the experiment, ^{24}Na gamma-ray counting rate was measured to obtain the saturated radioactivity of ^{24}Na from which an average neutron flux in the irradiation section was calculated. The appropriateness of the irradiation section position in the reactor, the shielding ability and the safety of the apparatus were confirmed. The saturated radioactivity of ^{24}Na in 7.9 l sodium was 0.43 Ci and the average thermal neutron flux was calculated as 5.4×10^{10} n/cm^{2}sec. by taking 0.54 barn as $^{23}Na(n, \gamma)^{24}Na$ reaction cross section. The 440 keV gamma-rays from ^{23}Ne produced by $^{23}Na(n, p)^{23}Ne$ reaction could not be detected. This shows that the fast neutron flux in the irradiation section was too small and no reaction of ^{23}Ne occurred. The surface dose rate of the apparatus was less than 2 mR/hr and fulfilled the design specification.

The background counting rates of the delayed neutron monitor and the precipitator were measured. The delayed neutron monitor gave 10 cps counting rate at 10 MW reactor operation, but, the counting rate was reduced to 5 cps after 10 cm thick blocks of boron-loaded paraffin had been placed to the side wall of the delayed neutron monitor. This counting rate, 5 cps, was considered as the background counting rate of the delayed neutron monitor. The appropriate precipitation chamber voltage had not been known in the first experiment and the proper operating conditions of the precipitator were firstly established when the second circulation experiment gave fission product release. After a continuous operation of the precipitation, the "WIRE DRIVE" mechanism

caused troubles and the precipitator operation was stopped. Uncorrect timing relation of the cams in the control circuit of the wire-driving mechanism was found. The troubles were cured after the adjustment of the cam position.

(2) The Second Sodium Circulation Experiment

After the first sodium circulation experiment was finished, the SIL was disassembled, four plates of 20%-enriched metal uranium (two 1 mm thick, 37.6 mm long, 15.9 mm wide plates and two 1 mm thick, 37.6 mm long, 18.9 mm wide plates; the total amount of ^{235}U, 9.18 g; total surface area 56.45 cm^2) were loaded in the irradiation section (the detailed description of metallic uranium plates is given in Table 2-1). A gas reservoir for gamma-ray spectrometry was placed just before the precipitator.

The second sodium circulation experiment was carried out during 15 and 27 January, 1973 (the 10th operation cycle of JRR-2 in FY 1972). The sodium circulation time was 290 hr 50 min. The circulating sodium was 8.5 l and the conditions of the stationary operation were as follows.

Irradiation section temperature (TRCA-1-1):	500 °C
Main-cooler outlet temperature (TRCA-2-1):	400 °C
Cold trap outlet temperature (TRCA-3-1):	200 °C
Sodium flow rate in the main circulation system (FRCA-1):	3 l/min.
Sodium flow rate in the purifier system (FRCA-2):	0.5 l/min.
He cover gas pressure:	100 mmHg
He cover gas flow rate (25 °C):	200 cm^3/min.

Gamma-ray spectroscopy of fission products was made

through collimeters. Fission product behavior in sodium, counting rate change and response characteristic change of the fuel failure detection systems were measured by varying cover gas flow rate, main circulation system sodium flow rate, cold trap outlet temperature, etc.

The counting rate of the delayed neutron monitor increased upto 1,500 cps when JRR-2 power was increased to 10 MW at the reactor start-up on 15 January, 1973. Thereafter, the delayed neutron counting rate increased gradually as sodium circulation time increased and reached 2,100 cps just before the reactor shut down on 27 January, 1973. On 19 January, sodium in the SIL was drained during 10 MW operation and the delayed neutron counting rate was counted as 6.2 cps. This counting rate was thought as background counting rate of the delayed neutron monitor. By using the delayed neutron counting rate, 1884.3 cps, measured on 17 January and the background counting rate, 6.2 cps, measured on 19 January, the detection sensitivity, S/N ratio, and minimum detectable area of uranium plates were calculated.

$$\text{the detector sensitivity} = \frac{\text{delayed neutron counting rate (cps)}}{\text{uranium plate area } (cm^2) \times \text{reactor power(MW)}} = 3.3\,\text{cps}/cm^2\text{MW} \quad \text{---- (3.1)}$$

$$\text{S/N ratio} = \frac{\text{delayed neutron counting rate (cps)} - \text{background counting rate (cps)}}{\text{background counting rate (cps)}} = 302.9 \quad \text{---- (3.2)}$$

$$\text{minimum detectable area of uranium plate} = \frac{\text{uranium plate area } (cm^2)}{S/N \text{ ratio}} = 0.186\ cm^2 \quad \text{---- (3.3)}$$

When new sodium was loaded after the sodium drain on 19 January, the delayed neutron counting rates were almost the same before the sodium drain and after the new sodium loading. Therefore, the gradual increase of the delayed neutron counting rate was found not to be due to metallic uranium circulating in the sodium. It might be explained by gradual increase of the surface area of the metallic uranium.

The precipitator counting rate dependence on the chamber voltage was measured and the chamber voltage necessary to obtain the saturated counting rate was found to be above 70 V. Thenceforth, a chamber voltage of 500 V was decided to be used. The precipitator counting rate change was measured as a function of purge gas flow rate. A purge gas flow rate of 50 cm^3/min was found to be adequate. By using the background count, 10^2 cts, obtained on 15 January for cover gas flow rate 200 cm^3/min. and soak/count time 1 min, and the precipitator count 10^6 cts obtained on 27 January, the following three values were calculated;

$$\text{the detection sensitivity} = \frac{\text{precipitator counting rate (cps)}}{\text{uranium plate area } (cm^2) \times \text{reactor power (MW)}} = 29.5\ (cps/cm^2\text{-}MW) \quad \text{---- (3.4)}$$

$$S/N \text{ ratio} = \frac{\text{precipitator counting rate (cps)} - \text{background (cps)}}{\text{background (cps)}} = 10^4 \quad \text{---- (3.5)}$$

$$\text{minimum detectable area of uranium plate} = \frac{\text{uranium plate area } (cm^2)}{S/N \text{ ratio}} = 5.65 \times 10^{-3} cm^2 \quad \text{---- (3.6)}$$

The sensitivity and S/N ratio for the precipitator are larger than those for the delayed neutronmonitor and the precipitator can detect smaller area of uranium plates than the delayed neutron monitor cam.

(3) The Third Sodium Circulation Experiment

The third sodium circulation experiment was carried out during 26 February and 10 March, 1973 (the 12th operation cycle of JRR-2, FY 1972). The sodium circulation time was 303 hr.

In this experiment, the response characteristics of the precipitator at reactor start-up was measured with a cover gas flow rate of 500 cm^3/min. Thenceforth, fission product behavior in the expansion tank liquid phase and gas phase, in the cold trap, the delayed neutron counting rate change, the nuclide determination and concentration change of the fission products reached the precipitator, etc., were measured for various conditions such as cover gas flow change cover gas pressure change from 100 mmHg to 700 mmHg, the irradiation section temperature change down to 400 °C, the sodium flow rate change from 4.5 l/min to 0 l/min, the cold trap temperature change down to 130 °C, etc.

The delayed neutron counting rate increased from 1,900 cps (or 26 February) to 2,900 cps (10 March). When the sodium flow rate was changed from 0.5 to 4.5 l/min, the delayed

neutron counting rate increased as sodium flow rate increased because of shorter travel time of sodium from the irradiation section to the expansion tank. The delayed neutron counting rate change was measured for various sodium temperature in the irradiation section and main-cooler. The delayed neutron counting rate varied as temperature varied. When the sodium temperature in the main-cooler was lowered, the gamma-ray counting rate from the main-cooler increased: therefore, gamma-ray emitting nuclides were found to adher on the main-cooler when the temperature was lowered. The response characteristics of the delayed neutron counting rate were measured by multi-scaler method for reactor start-up and shut-down. The delayed neutron counting rate change was delayed by 20 ~ 40 sec. after the reactor neutron counting rate change and the delay times between 20 and 40 sec. were almost the same as 23.1 sec., a calculated sodium travel time from the irradiation section to the expansion tank. The decay of the delayed neutron counting rate after the reactor shut-down could be decomposed into the two lines of halflives 22 sec. and 57 sec. so that the first group (halflife 57 sec, 87 Br) and the second group (halflife 22 sec., mainly 88 Br) delayed neutrons must have been measured. The delayed neutron counting rate didn't change for cover gas pressure change from 100 to 700 mmHg.

As the result of precipitator count measurement for reactor start-up, the precipitator count delayed by about 40 min. from the reactor output change for a cover gas flow rate of 200 $cm^3/min.$ and reached a constant value after 150 min.: the fission products in the cover gas needs 40 min. from the expansion tank to the

precipitator. The decay measurement of the precipitator counting rate for the stopped-wire showed a halflife of 17.8 min. which was of the radionuclides of ^{88}Rb adhered on the wire. The measurement of the cover gas gamma-ray spectrum in the gas reservoir by a Ge(Li) detector revealed the pressure of ^{85m}Kr, ^{87}Kr, ^{99}Kr, ^{138}Xe, ^{88}Rb, ^{138}Cs, and ^{135}Xe.

(4) The Fourth Sodium Circulation Experiment

The fourth sodium circulation experiment was carried out during 19 and 21 April, 1973 (the 1st operation cycle of JRR-2, FY 1973). The sodium circulation time was 300 hr 45 min.

In the first part of the experiment, the fission product concentration change in the main cooler and the delayed neutron counting rate change weasured by changing the main-cooler outlet temperature. Then, fission product transfering behavior and the delayed neutron counting rate change were measured by varying sodium flow rate from 1.5 to 4.5 l/min. Also, fission product collection was measured for cold trap outlet temperature down to 130 °C.

The delayed neutron counting rate increased to 5,700 cps on the first day (9 April) of the fourth sodium circulation experiment. This counting rate showed on abrupt increase when compared with 2,900 cps obtained on the last day of the 3rd sodium circulation experiment (10 March) and suggested an abrupt change of the metallic uranium surface. A possible explanation is that this abrupt increase of the delayed neutron counting rate was caused by the possible oxidation of the metallic uranium surface due to air introduced into the sodium circulation system of the SIL by helium pressure drop. The delayed

neutron counting rate increased gradually upto 7,800 cps which was obtained on the last day of the fourth experiment (21 April). The measurement of the delayed neutron counting rate decaying after a sudden stop of sodium circulation for 5 to 10 sec., of the delayed neutron counting rate decaying after reactor shut-down for the sodium flow rate 3 l/min., and 5 l/min., of the counting rate dependence on reactor power, and of the correlation between the delayed neutron counting rate and fission products in cover gas had been made.

Also, the measurement of precipitation counting rate at reactor start-up, of the precipitator counting rate dependence on soak/count time, of the background counting rate, etc., had been carried out.

3.2 The Fifth Sodium Circulation Experiment*

* Makoto Sawada of the Fast Breeder Reactor Development Project, Oarai Engineering Center, PNC, joined in experiment.

The fifth sodium circulation experiment was carried out during 28 May and 9 June, 1973 (the third operation cycle of JRR-2, FY 1973). The sodium circulation time was 306 hr 50 min. The operating conditions of JRR-2 and SIL are shown in Fig. 3-3.

In this experiment, sodium was circulated at the constant stationary conditions: gamma-ray spectrometry of the main cooler, expansion tank, cold trap, sodium valves, and sodium tubes, delayed neutron measurement, and precipitator measurement were carried out to investigate fission product behavior collectively. The experimental conditions were as follows:

irradiation section temperature (TRCA-1-1)	:	500 °C
main-cooler outlet temperature (TRCA-2-1)	:	400 °C
expansion tank temperature (TRA-6-5)	:	352~355 °C
cold trap outlet temperature (TRCA-3-1)	:	200 °C
main-circulation system sodium flow rate (FRCA-1)	:	3 l/min.
purifier system sodium flow rate (FRCA-2)	:	0.5 l/min.
helicum cover gas pressure	:	100 mmHg
helium cover gas flow rate (25 °C)	:	200 cm^3/min.

The experiment was performed as follows:

27 May	20:50	The system preheating started.
28 May	00:12	Sodium charging started.
	00:17	Sodium charging finished (Sodium amount 8.5 l) Sodium circulation started (The purifier system was plugged.)
	00:43	The purifier system was opened.
	01:30	The stationary operation of SIL was reached.
	08:45	Bypassing of the precipitator was terminated.
21 May	09:22	The reactor started up.
	10:03	The reactor thermal power 10kW was reached.
	10:09	The reactor thermal power started to increase.
	10:14	The reactor thermal power reached 1 MW.
	10:22	The reactor thermal power started to increase.
	10:25	The reactor thermal power reached 3 MW.
	10:35	The reactor thermal power started to increase.
	10:36	The reactor thermal power reached 5 MW.
	10:45	The reactor thermal power started to increase.
	10:46	The reactor thermal power reached 8 MW.

	10:55:30	The reactor thermal power started to increase.
	10:56	The reactor thermal power reached 10 MW.
3 June	17:04	Electric power failed and recovered instantly. The reactor scrammed. The signals of sodium-drain, main-heater cut-off, and electromagnetic pump off were sent out. But, the sodium drain valves were in manual position because of thunderstorm so that the sodium drain didn't occurred.
	17:10	Sodium circulation restarted.
	17:14	The reactor restarted up.
	17:36	The reactor thermal power reached 10 MW.
	17:41	The SIL recovered the stationary operation.
9 June	15:00	The reactor shut down.
	19:40	Sodium circulation terminated, Helium cover gas circulation stopped.
	19:13	Sodium was drained manually.
	19:25	Cooling of the air-tight chamber started.
	~ 22:00	Cooling of the air-tight chamber terminated. Purge gas flow stopped.

The objects of the experiment on the fuel failure detection systems are as follows; for the continuous stationary operating conditions of the SIL.

1) to measure the long-term change of the counting rates of the delayed neutron monitor and the precipitator.

2) to measure the halflife of the radioactivities adhered on the precipitator wire at the precipitation-chamber voltages of 500 V and 0 V. The cover gas flow rate was 200 cm^3/min.

3) to measure the precipitator counting rate dependence on soak time.

4) to investigate the pulse height distribution of beta-rays by varying the applied voltage of the precipitator photomultiplier.

About Item 1), the measurement was performed during the entire period of the experiment (28 May to 9 June) (see Fig. 3-5). The measurement continued until 10 June because of slow decaying of the precipitator counts. The gamma-ray spectrometry of the gas reservoir (1 l) was performed by using a 100 cm^3 Ge(Li) detector, but, the measurement was terminated after the gamma-ray counting rate became too large to be counted.

The delayed neutron counting rate increased from 2,500 cps to 8,100 cps, as shown in Fig. 3-4. This counting rate was a line expected from 5,700 cps to 7,800 cps obtained in the fourth sodium circulation experiment. The counting rate discontinuity such as that observed between the third and the fourth sodium circulation experiments was not seen and the possibility of dismembering metallic uranium plates was denied.

The precipitator was operated at a chamber voltage of 500 V, soak time 30 sec, cover gas flow rate 200 cm^3/min. The counting rate was almost constant and 10^6 cts, as shown in Fig. 3-5.

About Item 2), the measurement at chamber voltage 0 V was made on 30 May, and at 500 V on 6 May. It was found that ^{88}Rb (halflife 17.8 min.) was counted at 500 V and 0 V chamber voltages. Also, it was found that the background counting rate, 22.5 cps, was still in existence often many hours had elapsed: the explanation of 22.5 cps needs more experimental results.

For Item 3), the counting rate was measured on 30 May by

varying soak time from 30 sec. to 10 min. and it was confirmed that the precipitator counting rate was proportional to soak time.

For Item 4), the pulse height distributions of ^{88}Rb beta-rays were measured by varying the discriminator level at photo. multiplier voltages of 1,100 V and 1,350 V. From the results, it was found that the pulse height dependence on the photomultiplier voltage was very large. The energy calibration of the pulse height was performed using a ^{90}Sr source on 18 May during the reactor stoppage period.

3.3 The Sixth Sodium Circulation Experiment*

* Makoto Sawada of the Fast Breeder Reactor Development Project, Oarai Engineering Center, PNC, joined in this experiment.

In this experiment, sodium was circulated at the constant operating conditions and gamma-ray spectrometry of the main-cooler, expansion tank, cold trap, sodium valves, and sodium tubes, delayed neutron measurement, precipitator measurement, etc., were made to investigate fission product behavior collectively. The experimental conditions were as follows:

Irradiation section temperature (TRCA-1-1)	:	454 °C
Main-cooler outlet temperature (TRCA-2-1)	:	400 °C
Expansion tank temperature (TRA-6-5)	:	356 °C
Cold trap outlet temperature (TRCA-3-1)	:	200 °C
Main-circulating system sodium flow rate (FRCA-1)	:	3 l/min.
Purifier system sodium flow rate (FRCA-2)	:	0.5 l/min.
Helium cover gas pressure	:	100 mmHg
Helium cover gas flow rate (25 °C)	:	200 cm^3/min.

The experiment was carried out as follows:

20 June	09:40	The entire system preheating started.
	13:13	Sodium charging started.
	13:20	Sodium charging terminated (Sodium amount 8.5 l). Sodium circulation started (the purifier system plugged).
	13:50	Sodium was drained to mend plugged purifier system
	13:55	Sodium recharging started.
	13:58	Sodium recharging terminated (Sodium amount 8.5 l). Sodium circulation started (the purifier system was plugged).
	14:20	Sodium was drained to mend plugging of the purifier system.
	14:23	Sodium recharging started.
	14:24	Sodium recharging terminated. (Sodium amount 8.5 l). Sodium circulation started (The purifier system opened).
	~ 15:00	The stationary operation reached.
	20:04	The reactor started.
	20:22	The reactor thermal power reached 10 kW.
	20:31	The reactor thermal power started to increase.
	20:35:45	The reactor thermal power reached 1 MW.
	20:40:40	The reactor thermal power started to increase.
	20:43	The reactor thermal power reached 3 MW.
	20:50	The reactor thermal power started to increase.
	20:51:35	The reactor thermal power reached 5 MW.
	21:04:40	The reactor thermal power started to increase.
	21:05:35	The reactor thermal power reached 8 MW.

	21:18	The reactor thermal power started to increase.
	21:18	The reactor thermal power reached 10 MW.
21 June	18:01	Helium cover gas flowed through the precipitator bypassing line.
22 June	15:00	Helium cover gas flowed through the precipitator line.
	17:03	Helium cover gas flow through the precipitator bypassing line.
23 June	09:30	Helium cover gas flowed through a precipitator line.
	14:03	Helium cover gas flowed through a precipitator bypassing line.
	20:57	The reactor scrummed by a voltage drop due to thunder bolt. The main heater and the electro-magnetic pump were cut off. Sodium was not drained because the sodium drain valve was in manual position.
	21:10	Sodium circulation restarted.
	21:12	The reactor started up.
	21:32	The reactor thermal power reached 10 MW.
	21:50	The stationary operation of the SIL recovered.
25 June	11:04	Helium cover gas flow rate was changed to 500 cm^3/min. Helium cover gas was switched to the precipitator line.
	11:34	Helium cover gas flow rate was changed to 200 cm^2/min.

	12:00	Helium cover gas was switched to the precipitation bypassing line.
28 June	10:32	Helium cover gas flow rate was changed to 500 cm^3/min.
		Helium cover gas was switched to the precipitator line.
	12:00	Helium cover gas was switched to the precipitator bypassing line.
	12:11	Helium cover gas flow rate was changed to 200 cm^3/min.
30 June	morning	Helium cover gas was switched to the precipitator bypassing line.
	15:00	The reactor was shut down.
	19:37	Helium cover gas was stopped.
	19:39	Sodium circulation terminated.
	19:40	Sodium was drained manually.
	19:55	Cooling of the air-tight chamber started.
~	22:00	Cooling of the air-tight chamber terminated.
		Precipitator purge gas flow was stopped.

Main items of the sixth experiments on the fuel failure detection systems were as follows:

The delayed neutron counting rate increased from 7,800 cps to 8,500 cps as shown in Fig. 3-7.

The following experiments were performed on the precipitator.

1) In order to investigate the origin of the precipitation counting rate at 0 MW reactor operation, the precipitator count was measured by varying soak/count time at precipitation-chamber voltages

of 500 V and 0 V. The count was constant within a statistical error for every case. This means that the back ground count was not caused by fission products in cover gas.

2) During 22 and 30 June, the precipitator response characteristics were measured by opening a valve situated just before the precipitator. The experiments were made at the cover gas flow rates of 200 cm^3/min. and 500 cm^3/min. The precipitator response characteristics were also measured by putting the gas reservoir in series with the precipitator.

3) In order to measure radionuclides adhered on the precipitator wire at a cover gas flow rate of 500 cm^3/min, decaying of the precipitator counting rate were measured for the stopped wire on which fission products had been collected at a chamber voltage of 500 V. It was found that the nuclides adhered on the wire were ^{88}Rb and ^{138}Cs after the decay curve was analysed.

3.4 The Seventh Sodium Circulation Experiment*

* Makoto Sawada and Akira Endo of the Fast Breeder Reactor Development Project, Oarai Engineering Center, PNC, joined in this experiment.

The seventh sodium circulation experiment was carried out during 30 July and 11 August 1973 (the 6th operation cycle of JRR-2, FY 1973). The total sodium circulation time was 298 hr 1 min. Fig. 3~9 shows the operating conditions of JRR-2 and SIL.

In the seventh experiment, the sodium flow rate of the main circulation system was raised to 4 l/min. and the fission product behavior in the entire system was collectively investigated. The effects of the purifier system sodium flow rate on fission product collection on the cold trap and fission product transfer to

helium cover gas were measured by varying the flow rate of the purifier system from 0.25 to 1 l/min.

The initial experimental conditions were as follows:

Irradiation section temperature (TRCA-1-1)	:	490 °C
Main-cooler outlet temperature (TRCA-2-1)	:	400 °C
Expansion tank temperature (TRA-6-5)	:	356 °C
Cold trap outlet temperature (TRCA-3-1)	:	200 °C
Main-circulation system sodium flow rate(FRCA-1)	:	4 l/min.
Purifier system sodium flow rate (FRCA-2)	:	0.5 l/min.
Helium cover gas pressure	:	100mmHg
Helium cover gas flow rate (25 °C)	:	200mmHg

The experiment was performed as follows:

30 July	02:20	Preheating of the entire system started.
	06:45	Sodium charging started.
	06:58	Sodium charging terminated (Sodium amount 8.5 l). Sodium circulation started, but the purifier system was plugged.
	07:00	The purifier system was opened.
	08:46	The reactor started up.
	~ 09:00	The reactor scrammed due to noise.
	09:06	The reactor restarted up.
	09:34	The reactor power reached 10 kW.
	09:39	The reactor power started to increase.
	09:44	The reactor power reached 1 MW.
	09:55	The reactor power started to increase.
	09:58	The reactor power reached 5 MW.
	10:14	The reactor power started to increase.
	10:16	The reactor power reached 10 MW.

31 July	12:00	The reactor power changed to 9.5 MW.
	16:20	Helium cover gas was switched to the precipitator-bypassing line.
1 Aug.	~10:00	Helium cover gas was switched to the precipitator line.
3 Aug.	12:16	The reactor power changed to 9 MW.
4 Aug.	16:42	Sodium flow rate in the purifier system was changed to 1 l/min.
6 Aug.	15:26	The purifier system sodium flow rate was changed to 0.25 l/min.
	15:46	The purifier system sodium flow rate was changed to 0.30 l/min.
	16:07	The purifier system sodium flow rate was changed to 0.35 l/min.
	16:28	The purifier system sodium flow rate was changed to 0.75 l/min.
	16:31	The reactor scrummed by the voltage drop due to thunderbolt. The main-heater and the electromagnetic pump were cut off. Sodium was not drained because the drain valve was switched to manual operation).
	16:33	Sodium circulation started.
	16:40	The reactor started up.
	17:02	The reactor power reached to 9 MW.
8 Aug.	17:39	The reactor scrammed.
	17:58	The reactor started.
	18:07	The reactor power reached 9 MW.
9 Aug.	15:02	The reactor power was changed to 8.5 MW.

9 Aug.	17:04	The sodium flow rate in the purifier system was changed to 0.35 l/min.
	17:05	The sodium flow rate in the purifier system was changed to 0.40 l/min.
	21:37	The reactor scrammed due to the control rod insertion.
	21:56	The reactor started up.
	22:08	The reactor power reached 8.5 MW.
	22:50	The reactor scrammed.
	23:04	The reactor started up.
	23:17	The reactor power reached 8.5 MW.
11 Aug.	12:50	The reactor scrammed due to the control rod insertion.
	16:56	Sodium circulation terminated. Helium cover gas circulation terminated.
	16:59	Sodium was drained manually.
	17:25	Cooling of the air-tight chamber started.
	~ 20:00	Cooling of the air-tight chamber terminated. Precipitator purge gas flow terminated.

Change in the delayed neutron counting rate and precipitator count observed in the seventh experiment are shown in Figs. 3-10 and 3-11. The main items of the experiments on the fuel failure detection systems are as follows:

1) While the response characteristics of the delayed neutron monitor measured at the reactor start-up in the previous experiment were obtained for a sodium flow rate of 3 l/min, the sodium flow rate in the main circulation system in this experiment was 4 l/min. Therefore, the response characteristics of the delayed

neutron counting rate for 4 l/min. sodium flow rate could be measured at the reactor start-up. But, the reactor started up very slowly to the maximum power of 10 MW and the response characteristics appropriate to analysis could not be obtained. The date of the measurement was 30 July.

2) In the fifth sodium circulation experiment (see Section 3.2), it was observed that the precipitator count became 22.5 cps after many hours had elapsed. This value, 22.5 cps, gave the background counting rate. In order to investigate the origin of 22.5 cps, the following experiment was performed on 1 August. When the radioactivities on the wire and in the precipitator decayed thoroughly after the cover gas valve was closed, the valve was opened suddenly to introduce cover gas into the precipitation chamber without driving the wire. The counting rate was at first 2 cps, then gradually increased to 25 cps at 1 hr later (see Fig. 5-13). This result shows that the background counting rate was due to gamma-rays from fission products in cover gas (see Section 5.8).

3) After the experiment of Item 2) finished, the effect of purge gas flow rate on the background counting rate was experimented. The counting rates were almost constant and 25 cps for the purge gas flow rates from 125 cm^3/min to 25 cm^3/min. The counting rate increased to 35 cps when the flow rate was changed to 12.5 cm^3/min. This means that a part of the fission products in cover gas may flow into the scintillator at 12.5 cm^3/min. (see Section 5.10).

4) The increase rate of the delayed neutron counting rate in one sodium circulation experiment was obtained. In this experiment,

the increase rate in 9 days was 1.10 for a sodium flow rate of 4 l/min. This was 4% larger than 1.07, the increase rate observed in the previous experiment operated at 3 l/min. It may be suggested that the surface of the metallic uranium fuels roughened when the flow rate increase.

3.5 The Eighth Sodium Circulation Experiment*

* Yoshinori Ishii of the Fast Breeder Reactor Development Project, Oarai Engineering Center, PNC, joined in the experiment.

The shielding and the top rid plate on the air-tight chamber of the SIL were disassembled on 14 September (The reactor was in recess). The neutron detection efficiency of the delayed neutron monitor was found to be 1.2×10^{-4} count/n from the experiment using a RaD-Be neutron source (9 m Ci) (see Section 4.2).

The eighth sodium circulation experiment was carried out during 1 and 13 October 1973 and the sodium circulation time was 271 hr 13 min. The operating conditions of JRR-2 and SIL are shown in Fig. 3-12.

In the eighth experiment, fission product transferring behavior to helium cover gas and fission product behavior in the loop were studied for 3 l/min. main-circulation system flow rate and 0.5 l/min. purifier system flow rate by varying the cold trap temperature from 200 °C. Then, the fission product transferring behavior to helium cover gas was measured by varying the main-cooler outlet temperature from 389 °C to 429 °C and the expansion tank temperature from 336 °C to 378 °C. The initial experimental conditions were as follows:

Irradiation section temperature (TRCA-1-1) : 500 °C

Main-cooler outlet temperature (TRCA-2-1)	:	400 °C
Expansion tank temperature (TRA-6-5)	:	355 °C
Cold trap outlet temperature (TRCA-3-1)	:	150 °C
Main-circulation system sodium flow rate (FRCA-1)	:	3 l/min.
Purifier system sodium flow rate (FRCA-2)	:	0.5 l/min.
Helium cover gas pressure	:	100 mmHg
Helium cover gas flow rate (25 °C)	:	200 cm^3/min

The experiments were made as follows.

1 Oct. 00:30 Preheating of the entire system started.

06:57 Sodium charge started.

07:00 Sodium charge terminated (sodium amount 8.5 l). Sodium circulation started, but the purifier system plugged.

07:23 The purifier system opened.

08:10 The stationary operation reached.

09:08 The reactor started up.

09:26 The reactor power reached 10 kW.

09:34 The reactor power started to increase.

09:42 The reactor power reached 1 MW.

10:24 The reactor power started to increase.

10:27 The reactor power reached 5 MW.

10:47 The reactor power started to increase.

10:49 The reactor power reached 10 MW.

10:51 The reactor scrammed.

11:04 The reactor started up.

11:20 The reactor power reached 10 MW.

12:15 The purifier system sodium flow rate was reduced to 0.1 l/min.

	14:42	Sodium of 0.78 l was manually drained from the purifier system by applying a helium gas pressure of 1 kg/cm^2G because the purifier system sodium flow rate could not be recovered.
	14:48	Sodium circulation started (the purifier system opened).
	15:10	Sodium circulation terminated. Charging of 0.78 l sodium started.
	15:12	Sodium charging terminated (the total sodium amount became 8.5 l).
	~ 16:00	The stationary operation reached (TRCA-3-1 = 200 °C)
2 Oct.	17:28	The reactor power suddenly decreased due to D_2O leak-detector alarm.
	17:38	The reactor power started to increase.
	17:51	The reactor power reached 10 MW.
	19:45	Cold trap outlet temperature started to increase.
	20:00	Cold trap outlet temperature reached 215 °C.
	20:06	Cold trap outlet temperature reached 220 °C.
	20:16	Cold trap outlet temperature reached 230 °C.
	20:28	Cold trap outlet temperature reached 240 °C.
	20:46	Cold trap outlet temperature reached 250 °C.
4 Oct.	16:22	Helium cover gas flow through the precipitator-bypassing line.
5 Oct.	~ 10:00	Helium cover gas was switched to the precipitator line.
6 Oct.	11:29	Temperatures of the main-cooler, cold trap, and expansion tank started to decrease.

	11:38	Main-cooler outlet temperature 390 °C, cold trap outlet temperature 240 °C.
	11:50	Main-cooler outlet temperature 383 °C, cold trap outlet temperature 214 °C
	12:00	Main-cooler outlet temperature 382 °C, cold trap outlet temperature 204 °C
	12:10	Cold trap outlet temperature 200 °C
8 Oct.	15:11	Main-cooler outlet temperature and expansion tank temperature started to increase.
	15:15	Main-cooler outlet temperature 420 °C
	15:17	Main-cooler outlet temperature 424 °C, expansion tank temperature 360 °C.
	15:30	Main-cooler outlet temperature 429 °C, expansion tank temperature 372 °C.
	16:03	Main-cooler outlet temperature 430 °C, expansion tank temperature 377 °C.
	16:33	Main-cooler outlet temperature 428 °C, expansion tank temperature 377 °C.
11 Oct.	09:45	The reactor shut down.
	10:50	Sodium circulation was terminated. Sodium was manually drained.
	10:57	Helium cover gas circulation terminated.
	11:05	Cooling of the air-tight chamber started.
	~ 14:00	Cooling of the air-tight chamber terminated.
	~ 17:00	Precipitator purge gas flow stopped.
12 Oct.	09:20	Preheating of the entire system started.
	14:00	Sodium charge started.

12 Oct. 14:03 Sodium charging terminated (sodium amount 9.5 l).
Sodium circulation started (the purifier system plugged).

15:30 Sodium was manually drained because of the plugged purifier system.

15:50 Sodium charging started.

15:51 Sodium charging terminated (sodium amount 9.5 l). Sodium circulation started. (the purifier system plugged).

16:36 The reactor started up.

16:55 The purifier system opened.

17:03 The reactor thermal output power reached 5 MW.

17:07 The reactor thermal output power reached 10 MW.

17:27 Everything became stabilized except helium cover gas. Helium cover gas pressure = 150 mmHg.

18:22 Helium cover gas pressure = 130 mmHg

12 Oct. 19:07 Helium cover gas pressure = 100 mmHg

13 Oct. 15:00 The reactor shut down.

19:12 Sodium circulation terminated.
Helium cover gas circulation stopped.

19:14 Sodium was manually drained.

19:35 Cooling of the air-tight chamber started.

~ 22:00 Cooling of the air-tight chamber finished.
Precipitation purge gas flow stopped.

The delayed neutron counting rate and the precipitator count in this experiment are shown in Figs. 3-13 and 14.

Main items of the experiments during this period were as

follows:

1) Sodium was manually drained at 10:50 on 11 October and the total amount of sodium in the SIL was 8.5 l. The sodium amount was increased to 9.5 l which increased the sodium amount in the expansion tank from 4 l to 5 l. The delayed neutron counting rate increased about 6% due to 1 l sodium increase in the expansion tank (see Section 4.3).

2) The precipitator count change was measured as a function of cold temperature. The cold temperature was increased from 200 °C to 250 °C at 17:45 ~ 20:46 on 2 October. The cold trap temperature was decreased from 250 °C to 200 °C at 11:29 ~ 12:00 on 6 October. From these experiments, it was found that the precipitator count change was very small; the amount of the fission products adhered on the cold trap hand to be very small compared with the total amount of fission products in SIL (see Section 4.4).

3) The precipitator counting rate change was measured as a function of the precipitation chamber voltage between +500 V and -500 V on 5 October. When the precipitator was operated at a soak/count time of 60 sec, the counting rates were 100519 cps at 500 V, 4820 cps at 0 V, and 364 cps at -500 V. The precipitator counted even at -500 V (see Section 5.4).

4) The halflife measurement of the radioactivities adhered on the wire at -500 V for 200 cm^3/min. cover gas flow rate was carried out on 5 October. It was found that only radioactivities having a halflife of 17.8 min. were observed: this radionuclide was ^{88}Rb (see Section 5.6).

5) The measurement of the response characteristics of the

precipitator was made at the reactor shutdown on 13 October. The SIL was in the stationary operation and the cover gas flow rate was 200 cm^3/min. The soak/count time of the precipitator was 60 sec. The precipitator counting rate didn't decrease just after the reactor shut down at 15:00 and started to decrease at 16:39 (99 min. later). This means that the cover gas travel time from the expansion tank to the precipitator was 99 min. (see Section 5.12).

3.6 The Ninth Sodium Circulation Experiment

The ninth sodium circulation experiment was made during 12 and 24 October 1973 (in the 9th operating cycle of JRR-2, FY 1973). The sodium circulation time was 295 hr 23 min. The operation conditions of JRR-2 and SIL are shown in Fig. 3-15.

In the present experiment, gamma-ray spectrometry of the precipitator wire and fission product transferring behavior to helium cover gas were carried out at a constant flow rate of the purifier sodium and a constant helium cover gas pressure by varying the expansion tank temperature from 310 °C, and the helium cover gas flow rate from 0 to 300 cm^3/min. When the expansion tank temperature changed, temperatures of the irradiation section, main-cooler outlet, cold trap outlet, etc., changed and these effects were investigated. Also, the halflife measurement of the gamma-ray spectrum peaks was made for stopping the sodium circulation for a while. The initial experimental conditions were as follows:

Irradiation section temperature (TRCA-1-1)	:	487 °C
Main-cooler outlet temperature (TRCA-2-1)	:	300 °C
Expansion tank temperature (TRA-6-5)	:	310 °C

Cold trap outlet temperature (TRCA-3-1)	:	200 °C
Main-circulation system sodium flow rate(FRCA-1)	:	1 l/min.
Purifier system sodium flow rate (FRCA-2)	:	0.5 l/min.
Helium cover gas pressure	:	100mmHg
Helium cover gas flow rate (25 °C)	:	200cm^3/min.

The experiments were carried out as follows:

12 Oct. 01:00 Preheating of the entire system started.

06:52 Sodium charging started.
Sodium charging terminated (8.5 l sodium)
Sodium circulation started (the purifier system plugged).
Sodium was manually drained.

06:52 Sodium was tried to be charged through the purifier system, but failed.
Sodium was manually drained.

08:20 Sodium was tried to be charged through the purifier system, but failed.
Sodium was manually drained.
Sodium was charged successfully through the purifier system (8.5 l sodium).

08:20 Sodium circulation started (the purifier system opened).

09:19 The reactor started up.

09:33 The reactor thermal output power reached 10 kW.

09:46 The reactor thermal output power reached 1 MW.

09:58 The reactor thermal output power reached 5 MW.

10:08 The reactor thermal output power reached 10 MW.

20:16 The electromagnetic pump stopped.

		The sodium flow rates of the main circulation system and the purifier system were both 0 l/min.
	20:20	The sodium flow rate of the purifier system was changed to 0.07 l/min.
12 Oct.	20:25	The sodium flow rate of the purifier system was changed to 0.1 l/min.
	20:27	The sodium flow rate of the main-circulation system was changed to 0.25 l/min.
	20:28	The sodium flow rate of the main-circulation system was changed to 0.1 l/min.
	20:30	The sodium flow rate of the main-circulation system was changed to 0.3 l/min.
	20:31:30	The sodium flow rate of the main-circulation system was changed to 0.25 l/min.
	20:39	The sodium flow rate of the main-circulation system was changed to 3 l/min., of the purifier system to 0.5 l/min.
	21:24	Helium cover gas flow stopped.
13 Oct.	18:40	Helium cover gas flow rate was changed to 100 cm^3/min.
14 Oct.	17:49	Helium cover gas flow rate was changed to 200 cm^3/min.
15 Oct.	01:00	Sodium was automatically drained due to an abnormal temperature of the main-heater outlet (TRCA-5-ILL). This was caused by the movement of the setting point during the recorder chart change.

	03:00	Sodium charging started.
	03:03	Sodium charging terminated (8.5 l sodium).
	03:45	Everything became almost stabilized.
	16:25	Helium cover gas flow rate was changed to 300 cm^3/min.
16 Oct.	16:41	Sodium circulation stopped. Both the sodium flow rates of the main circulation system and the purifier system were 0 l/min.
	16:44	The sodium flow rate of the purifier system was changed to 0.1 l/min.
	16:52	The sodium flow rate of the purifier system was changed to 0.26 l/min.
	17:05	The sodium flow rates of the main-circulation system and the purifier were changed to 3 l/min. and 0.5 l/min, respectively.
	18:14	Helium cover gas flow stopped.
17 Oct.	16:33	Helium cover gas flow rate was changed to 100 cm^3/min.
18 Oct.	15:47	Helium cover gas flow rate was changed to 200 cm^3/min.
19 Oct.	17:15	Helium cover gas flow rate was changed to 300 cm^3/min.
20 Oct.	15:17	Sodium circulation stopped. The sodium flow rates of the main circulation system and the purifier system were both 0 l/min.
	15:26	The sodium flow rate of the purifier system was changed to 0.07 l/min.
	15:35	It was changed to 0.05 l/min.

	15:40	It was changed to 0.1 l/min.
	15:45	It was changed to 0.5 l/min. FRCA-3=3 l/min.
	16:39	Helium cover gas flow stopped.
21 Oct.	20:04	Helium cover gas flow rate was changed to 100 cm^3/min.
22 Oct.	18:08	It was changed to 500 cm^3/min.
23 Oct.	02:10	It was changed to 200 cm^3/min.
	14:30	It was changed to 300 cm^3/min.
24 Oct.	15:00	The reactor shut down.
	19:01	Sodium circulation stopped.
		Helium cover gas flow stopped.
	19:02	Sodium was manually drained.
	19:17	Cooling of the air-tight chamber started.
	~ 22:00	Cooling of the air-tight chamber terminated.
		Precipitator purge gas flow stopped.

The delayed neutron counting rate and the precipitator count obtained during the ninth sodium circulation experiments made in this period were as follows:

1) Gamma-rays from the nuclides adhered on the precipitator wire were measured on 22 and 23 October using a 41 cm^2 Ge(Li) detector newly manufactured. The measurement was performed at the stationary operation of the SIL for 500 cm^3/min. and 100 cm^3/min. cover gas flow rates. The nuclides found at 500 cm^3/min. were ^{85m}Kr, ^{87}Kr, ^{88}Kr, ^{138}Xe, ^{88}Rb and ^{138}Cs. The last two nuclides, ^{88}Rb and ^{138}Cs, were the nuclides adhered on the wire, but, it could not determined whether Kr and Xe isotopes were from the wire or background. At 100 cm^3/min.

cover gas flow rate, no ^{138}Cs was found.

2) The precipitator counting rate change was measured at 100, 200, 300 cm^3/min. cover gas flow rates on 13 to 16 October. The operating conditions of the SIL were 450 °C irradiation section temperature, 380 °C main-cooler temperature, 330 °C expansion tank temperature, and 3.0 l/min. sodium flow rate. The precipitation counting rate change was measured at 100, 200, and 300 cm^3/min. cover gas flow rates on 17 to 20 October: the SIL operating conditions were 500 °C irradiation section temperature, 425 °C main-cooler temperature, and 391 °C expansion tank temperature. From these measurements, the cover gas travel time from the expansion tank to the precipitator was found to be about 80 min. at a cover gas flow rate of 200 cm^3/min.

3.7 The Tenth Sodium Circulation Experiment

The tenth sodium circulation experiment was carried out on 3 to 12 December 1973 (in the 10th operating cycle of JRR-2, FY 1973). The sodium circulation time was 257 hr 21 min. The operating conditions of JRR-2 and SIL are shown in Fig. 3-18.

In this experiment, gamma-ray spectrometry of the precipitator wire as well as fission product transferring behavior to helium cover gas were investigated at 0 to 500 cm^3/min. helium cover gas flow rate, 3 to 5 l/min. main-circulation system sodium flow rate, and 0.4 to 1 l/min. purifier system sodium flow rate. The initial experimental conditions was as follows:

Irradiation section temperature (TRCA-1-1)	:	480 °C
Main cooler outlet temperature (TRCA-2-1)	:	433 °C
Expansion tank temperature (TRA-6-5)	:	400 °C

Cold trap outlet temperature (TRCA-3-1)	:	200 °C
Main circulation system sodium flow rate(FRCA-1)	:	5 l/min.
Purifier system sodium flow rate (FRCA-2)	:	0.5 l/min.
Helium cover gas pressure	:	100 mmHg.
Helium cover gas flow rate (25 °C)	:	300 cm^3/min.

The experiment was performed as follows:

3 Dec.	00:30	Preheating of the entire system started.
	06:55	Sodium charging started.
	07:00	Sodium charging completed (8.5 l sodium). Sodium circulation started, but the main circulation system and the purifier system plugged.
	07:03	Sodium was manually drained.
	07:10	Sodium charging started.
	07:13	Sodium charging completed. Sodium circulation started (Both systems opened).
	08:10	Sodium was added to have 8.5 l totally.
	09:00	The reactor started up.
	09:25	The reactor thermal output power started to increase.
	09:24	The reactor thermal output power reached 100 kW.
	09:43	The reactor thermal output power started to increase.
	09:45	The reactor thermal output power reached 500 kW.
	09:55	The reactor thermal output power started to increase.
	09:56	The reactor thermal output power reached 1 MW.
	10:08	The reactor thermal output power started to increase.
	10:13	The reactor thermal output power reached 5 MW.
	10:27	The reactor thermal output power started to increase.
	10:29	The reactor thermal output power reached 10 MW.

4 Dec.	11:00	The reactor shut down.
		Helium cover gas flow stopped.
		Sodium was manually drained.
	11:20	Cooling of the air-tight chamber started.
	~ 14:00	Cooling of the air-tight chamber completed.
5 Dec.	09:15	Preheating of the entire system started.
	14:24	Sodium charging started.
	14:26	Sodium charging terminated (8.5 l sodium).
		Sodium circulation started (both systems opened).
	19:41	The reactor started up.
	19:56	The reactor thermal output power reached 10 kW.
	19:59	The reactor thermal output power started to increase.
	20:10	The reactor thermal output power reached 10 MW.
6 Dec.	18:02	Helium cover gas flow rate was changed to 100 cm^3/min.
7 Dec.	16:40	It was changed to 200 cm^3/min.
8 Dec.	16:36	The main circulation system sodium flow rate, irradiation section temperature, main cooler outlet temperature, expansion tank temperature were changed to 3 l/min, 500 °C, 400 °C, and 355 °C, respectively.
9 Dec.	04:48	The reactor scrammed by the control rod insertion.
10 Dec.	09:30	The purifier system sodium flow rate and the helium cover gas flow rate were changed to 0.4 l/min. and 500 cm^3/min., respectively.
	10:00	The reactor started up.
	10:21	The reactor thermal output power reached to 10 MW.

10 Dec.	16:05	Helium cover gas flow rate was changed to 200 cm^3/min.
11 Dec.	10:00	The purifier system sodium flow rate was changed to 0.6 l/min.
12 Dec.	09:15	It was changed to 0.8 l/min.
	12:00	The reactor scrammed by the control rod insertion.
	12:37	The reactor thermal output power reached 10 MW.
	12:43	The reactor scrammed by the control rod insertion.
	13:00	The reactor shut down.
13 Dec.	18:21	Helium cover gas flow rate was changed to 500 cm^3/min.
	19:09	The reactor started up.
	19:34	The reactor thermal output power reached 10 MW.
14 Dec.	03:50	Helium cover gas was changed to 200 cm^3/min.
	13:30	The purifier system sodium flow rate was changed to 1 l/min.
15 Dec.	15:00	The reactor shut down. Sodium was manually drained. Helium cover gas flow stopped.
	15:20	Cooling of the air-tight chamber started.
	19:45	Cooling of the air-tight chamber finished.
16 Dec.	~09:00	Precipitator purge gas flow stopped.

The delayed neutron counting rates and the precipitator counts obtained in the 10th sodium circulation experiment are shown in Figs. 3-19 and 20. The main experiment in this period was to make gamma-ray spectrometry of the precipitator wire. The experiment was performed on 13 and 14 December. The SIL was operated

stationarily with a cover gas flow rate of 500 cm^3/min. and a purge gas flow rate of 125 cm^3/min. The gamma-ray peak counting rate of the wire was measured as a function of soak/count time, and precipitation chamber voltage: The halflife of the adhered nuclides and the background were measured. Then, gamma-ray counting rate dependence on soak/count time was measured: it was found that the gamma-ray counting rate was proportional to soak/count time. From the halflife measurement of the nuclides adhered on the wire, it was concluded that ^{88}Kr did not adhere on the wire (see Section 6.5).

4. Experimental Results Obtained by Delayed Neutron Detector Type Fuel Failure Detection System

In the fifth sodium circulation experiment, the delayed neutron detection type fuel failure detection system operated without any problem except 2 to 3 troubles. All the troubles were terminal of BF_3 counter, as explained below. A BF_3 counter did not generate output pulses when the bias voltage 3,200 V was applied on 20 May, 1973, the first day in the sixth sodium circulation experiment: the reactor room temperature was 26 °C, humidity 86%. Since this kind of troubles was considered as the results of insulation worsening of the counter signal terminal, preamplifier input terminal (MHV), or coupling capacitor in the preamplifier (3 kV, 1,000 pF, two condensers in series) by high humidity, the suspected parts were cleaned by aceton, dried with an electric drier, and silicagel was placed near the high voltage terminal of the counter and the preamplifier input terminal. This caused normal output pulses from the BF_3 counter and made it work all right until the last day of the sixth sodium circulation experiment. In the seventh sodium circulation experiment, the output pulses of the BF_3 counter disappeared on 5 August, the seventh day of the experiment: the applied voltage was reduced to 0 V and left as it was until 6 August. The counter operated normally when 3,200 V was applied at 9:20 on 6 August. At 18:45 on the same day, the amplitudes of the output pulses became unstable and this was thought as the results of insulation degradation. The voltage was reduced to 2,700 V and the gain of the amplifier was increased (coarse gain x 256, fine gain 3.00, discrimination level 2.00) to compensate the reduction of gas amplification factor.

The results of the investigation made on 7 August exhibited that the pulse amplitude distribution of the counter output became unstable at above 2,800 V. The BF_3 counter (20th Century Electronics, Ltd., 40 EB 70/50 G #4) was replaced by a new one because insulation of the high voltage terminal of the old counter was thought to become worsened. The new BF_3 counter was 20th Century Electronics, Ltd. 40 EB 70/50 G #2. The neutron detection efficiency of this new BF_3 counter was the same as that of the old counter within 1%. The applied voltage for the new counter was decreased to 3,000 V. This counter operated normally until the last day of the seventh sodium circulation experiment. On the first day in the eighth sodium circulation experiment, the delayed neutron monitor did not work: the preamplifier had a trouble and was replaced by a new one. The counting rates before and after the preamplifier replacement were the same. Thenceforth, the delayed neutron monitor behaved normally until the last day of the tenth sodium circulation experiment. As described above, the mulfunctioning of the delayed neutron monitor was caused by high voltages applied on BF_3 counters in every case, and was the results of insulation degradation of cables, connectors, AC-coupling capacitors in the preamplifier caused by high temperature and humidity. It is necessary to pay severe attention on designing and standards of these parts. Also, the use of neutron detectors such as ^{10}B counters which can be operated by applying lower voltages should be taken into consideration.

The experimental results and some of the analytical results obtained during the fifth and the tenth sodium circulation experiments are described as follows:

Long-term change in delayed neutron counting rate (4.1)

Detection efficiency of delayed neutron monitor (4.2)

Delayed neutron counting rate dependence on expansion tank sodium amount (4.3)

Delayed neutron counting rate dependence on purifier cold trap temperature (4.4)

Delayed neutron counting rate dependence on purifier sodium flow rate (4.5)

Decaying of delayed neutron counting rate after sudden stop of circulating sodium (4.6)

Calculation of fission rate and fission product release rate (4.7)

Calculation of response characteristics of delayed neutron monitor at reactor start-up (4.8)

Counting rate of delayed neutron monitor for different neutron detectors (4.9)

The results obtained on the delayed neutron monitor in the first to the fourth sodium circulation experiments were described in Chapter 4 of JAERI-memo 5287.[4)]

4.1 Long-Term Change in Delayed Neutron Counting Rate

The delayed neutron counting rate increased as sodium circulation time increased in the second to the fourth sodium circulation experiments as described in Section 4.2 of JAERI-memo 5287.[4)] It increased from 1,500 cps to 2,100 cps in the second sodium circulation experiment, from 1,900 cps to 2,900 cps in the third experiment, and from 5,700 cps to 7,500 cps in the fourth experiment. The reason why the counting rate obtained in the first day of the fourth experiment was larger than that in the last day of the third experiment was not clearly understood, but, there was a

possibility of oxidizing the surface of the metallic uranium plates and this oxidization might cause the increase of fission product release from uranium to sodium. Except this abnormal case, it was found that the counting rate observed on the last day of a previous sodium circulation experiment was almost the same as that on the first day of the next circulation experiment.

Delayed neutron counting rates obtained during the fifth and the tenth sodium circulation experiments are shown in Figs. 3-4, 7, 10, 13, 16 and 19. The counting rate gradually increased and discontinuity of the counting rate such as that observed between the third and the fourth experiments was not observed.

Fig. 4-1 shows a general picture of the delayed neutron counting rate change during the first and the tenth sodium circulation experiments taking the sodium circulation time as the axis of abscissa. In Fig. 4-1, a discontinuity of the delayed neutron counting rate are clearly seen between the third and the fourth experiments. The level of the delayed neutron counting rate were a little bit higher in the seventh and the eighth experiments: this was caused by 4 l/min. sodium flow rate. In the other experiments, the sodium flow rate was 3 l/min. The reason why the delayed neutron counting rate for 4 l/min. sodium flow rate was higher than that for 3 l/min. was explained in Section 4.10 of JAERI-memo 5287.[4)]

The increase rate of the delayed neutron counting rate was calculated for the fifth and the seventh sodium circulation experiments in which the operating conditions of JRR-2 and SIL were relatively stationary and is shown in Table 4-1. The counting rates used in the calculation were taken from the counting rates

in 9 days in the stationary operation starting from the second day. The first day of the experiment usually showed a large change. The increase rates in 9 days were 1,070 and 1,064 in the fifth and the sixth experiments, respectively. In both the experiments, the irradiation section temperatures were different, but the increase rates did not differ so much. Therefore, it can be said that the increase rate of the delayed neutron counting rate was not effected by the sodium temperature in the irradiation section. The increase rate of the delayed neutron counting rate in 9 days in the seventh sodium circulation experiment was calculated as 1,110 and larger than those of the fifth and the sixth experiments. In the seventh experiment, the sodium flow rate was 4 l/min. while it was 3 l/min. in the other experiments. Therefore, it can be said that the increase rate of the delayed neutron counting rate increased as the sodium flow rate increased. When one assumes that the increase of the counting rate corresponds to the increase in effective area of metallic uranium, it can be concluded that roughening of the metallic uranium surface depends on the sodium flow rate.

Fig. 4-1 shows a change of the precipitator count during the second and the tenth experiments, but the soak/count times of 30 sec. and 60 sec. were taken and the direct comparison can not be made. The precipitator counts obtained for 30 sec. soak/count time can be converted to those for 60 sec. These results will be described in Section 5.14.

4.2 Detection Efficiency of Delayed Neutron Detection System

The shielding wall and the ceiling plate of the air-tight chamber of the SIL were disassembled to sample sodium in the drain tank of the SIL in the reactor stoppage period between the seventh

and the eighth experiments. As theresults, the measurement of the delayed neutron detection system became possible by placing a neutron source around the expansion tank. The experiment were performed on 14 August, 1973. The neutron source used was 9mCi of RaD-Be (of the Reactor Instrumentation Laboratory, JAERI), and its neutron emission rate was measured to be 1.8 x 10^4 n/sec. compared with a RaD-Be source of 2 Ci of the Health Physics Division, JAERI. Since the neutron source could not be placed inside of the expansion tank, it was placed three points of the outside of the lead shield enclosing the expansion tank, as shown by 1 2 3 in Fig. 4-2 and the neutron counting rate of the delayed neutron monitor was measured. The points, 1 , 2 , 3 , had a height between the sodium level of 4 l sodium and the bottom of the tank. The neutron counting rates obtained by placing the neutron source at 1 , 2 , and 3 were 2.20 cps, 1.73 cps, and 2.70 cps, respectively, and the average became 2.15 cps. Therefore, the neutron detection efficiency became

$$2.15 \text{ cps}/1.8 \times 10^4 \text{n/sec} = 1.2 \times 10^{-4} \text{ count/n.}$$

This detection efficiency may be different from the delayed neutron detection efficiency from fission products in the expansion tank when one considers the energy difference of delayed neutrons (average 250 ~ 600 keV) and RaD-Be neutron source (average 4 ~ 5 MeV) and also the difference of neutron emitting places.

Isao Fujii, et al., reported in their report ("Fuel Failure detection system by delayed neutron monitoring-Out-of-pile test of detector-monitor system", J201 71-24 (September 1971) (in Japanese)[9]) the results of the experiment obtained by an Am-Be neutron source placed at 20 cm in front of the 10 cm thick lead of

the SIL delayed neutron monitor (50 cm x 50 cm x 80 cm graphite moderator enclosed by a 5 cm air space plus 5 cm thick boron-loaded paraffins; delayed neutrons entered through 10 cm thick lead layer placed on 50 cm x 80 cm face). In the real delayed neutron monitor of the SIL, the distance between the sodium level and the lead was 45 cm and the direct comparison could not be made.

In the same report,[9] the authors compared the detection efficiency obtained from the Am-Be neutron source with that obtained from the delayed neutron measurement by using 14 MeV neutrons on ^{238}U. They concluded that the detection efficiency obtained from delayed neutrons (average energy 250 ~ 450 ReV) was about 2 to 3 times as large as that from the Am-Be source neutrons (average energy 2 MeV) (see reference 9), p. 72, Table-10). Since average neutron energy from RaD-Be is 4 ~ 5 MeV and higher than 2 MeV of Am-Be neutrons, the detection efficiency for RaD-Be neutrons is considered to be smaller than that for delayed neutrons.

4.3 Dependence of Delayed Neutron Counting Rate on Sodium Amount in Expansion Tank

The SIL was usually operated by charging 8.5 l sodium in the main-circulation system, thus 4 l sodium in the expansion tank. It is interesting to know whether the delayed neutron counting rate does change or not as the sodium amount in the expansion tank changes. When one assumes that the amount of fission products released from metallic uranium is constant and independent of the sodium amount, and that the flow rate and the temperature of sodium do not change, then, the delayed neutron

counting rate will increase as the increase of the sodium amount in the expansion tank because a longer stay of sodium in the expansion tank makes delayed neutrons having longer halflives count.

In the eighth sodium circulation experiment, sodium in the SIL was drained at 10:50 on 11 October. Before then, 8.5 l sodium was charged, thus 4 l sodium was in the expansion tank. The amount of sodium in the expansion tank increased to 5 l by charging 9.5 l sodium into the main-circulation system at 15:51 on 12 October. The delayed neutron counting rate became 11063 cps at 14:45 on 13 October when the stationary operation became stabilized. This counting rate corresponds to about 6% increase when compared with 10423 cps for 4 l sodium in the expansion tank (the measured value at 9:45 on 5 October) while the operation conditions such as sodium temperature, flow rate, etc., were the same except the amount of sodium in the expansion tank. It is considered that the delayed neutron counting rate increase was caused by the increase of sodium staying time in the expansion tank due to 1 l increase of sodium.

4.4 Dependence of Delayed Neutron Counting Rate on Cold Trap Temperature in Purifier System

According to the experimental result of gamma-ray spectrometry of the cold trap of the SIL (Y. Yamazaki, et al., JAERI-memo 5283 (May 1973)[5], Section 4.5), the cold trap collected many kinds of fission products. Since delayed neutron emitting nuclides were not included in the fission products collected on the cold trap, the delayed neutron counting rate does not change even when the cold trap temperature is changed.

At 19:45 on 2 October, 1973, the cold trap temperature started to increase from 200 °C to 250 °C and reached 250 °C at 20:46. The delayed neutron counting rate increased from 10013 cps to 10252 cps, but the increase was 2% and very small.

4.5 Dependence of Delayed Neutron Counting Rate on Sodium Flow Rate in Purifier System

When the sodium flow rate in the purifier system decreases, the sodium stay in the expansion tank become shorter, thus the delayed neutron counting rate is expected to decrease. The sodium flow rate in the purifier system in the stationary SIL operation was 0.5 l/min.

When the sodium flow rate in the purifier system was increased from 0.5 l/min. to 1 l/min. at 16:45 on 4 August, 1973, the delayed neutron counting rate decreased about 1% from 10176 cps to 10083 cps. The delayed neutron counting rate increased about 2% from 9912 cps to 10130 cps when the sodium flow rate was decreased from 1 l/min. to 0.5 l/min. at 15:26 on 6 August. From these results, it is concluded that the sodium flow rate change in the purifier system changes delayed neutron counting rate.

4.6 Decay of Delayed Neutron Counting Rate on Sodium Flow Rate in Purifier System

Decaying of the delayed neutron counting rate after a sudden stop of sodium circulation by cutting the power of the electromagnetic pump off when the SIL was operated stationarily. Fig. 4-3 shows a decay curve of the delayed neutron counting rate after a sudden cut-off of the electromagnetic pump power when sodium was circulated at 3 l/min. In the figure, the time of the

sudden cut-off of the power is denoted by t = 24 sec. The time needed between the cut-off the electromagnetic pump power and the shut-off of the valve by pushing the button of the sodium flow rate adjusting valve was less than 5 sec. from the indication of the sodium flow meter. This decay curve of the delayed neutron counting rate could be decomposed into two lines having halflives of 57 sec. (the first group) and 22 sec. (the second group) as shown in the figure, and the counting rates of the first group and the second group delayed neutrons became 960 cps and 6600 cps, respectively.

Similar measurements were made at 4.5, 1.5, 0.5 l/min. sodium flow rates and the measured decay curves were decomposed into various groups of delayed neutrons. The delayed neutron counting rates of various groups were calculated as shown in Table 4-2. The third group of delayed neutrons (halflife 6.2 sec.) appeared only for 4.5 l/min. sodium flow rate. It should be pointed out that at 0.5 l/min. sodium flow rate the temperatures of various parts of the SIL could not be maintained and the temperatures of the main cooler and the expansion tank decreased.

By using the delayed neutron counting rates of the first and the second groups shown in Table 4-2, the fission rate and fission product release fraction from metallic uranium can be calculated. The results will be described in Section 4-7.

4.7 Calculation of Fission Rate and Fission Product Release Fraction

As described in Section 4.6, the delayed neutron counting rates of the first and the second groups were calculated, as shown in Table 4-2. By considering the decay and correcting the delayed

neutron counting rates, fission rate and fission product release fraction can be calculated. Let assume that the delayed neutron emitting nuclides are transferred in ta sec. (= the volume, 1153 cm^3, between the irradiation section and the expansion tank inlet/ sodium flow rate) from the irradiation section through the main-cooler to the expansion tank and that the delayed neutron emitting nuclides do not adhere on the tube wall and arrive at the expansion tank. Then, the delayed neutron emitting nuclides decreased by $e^{-\lambda_i t_a}$, where λ_1 is the decay constant of the i-th group of delayed neutrons.

When one assume that it takes tb sec. (= expansion tank 4 ℓ sodium volume 4 l/sodium flow rate) from the inlet to the outlet in the expansion tank, and that only the delayed neutrons generated in the expansion tank can be detected by the delayed neutron detection system of the detection efficiency ε (cts/n), then one can obtain the counting rate, Ni (cps), of the delayed neutron detection system as the initial counting rate times.

$$e^{-\lambda_i t_a} \times \varepsilon \times \int_0^{t_b} \lambda_i e^{-\lambda_i t} \, dt = \varepsilon \times e^{-\lambda_i t_a} \times (1 - e^{-\lambda_i t_b})$$

One can also assume that it takes tc sec. (= sodiume in the loop/sodium flow rate) for sodium to one circulation. Therefore, the counting rate will be increased by taking account of the longer halflife nuclides emitting delayed neutrons. This increase rate becomes

$$1 + e^{-\lambda_i t_c} + e^{-2\lambda_i t_c} + e^{-3\lambda_i t_c} + \cdots\cdots$$

Therefore, the counting rate of the delayed neutron detection system, Ni (cps) becomes the initial counting rate times.

$$\varepsilon \times e^{-\lambda_i t_a} \times (1 - e^{-\lambda_i t_b}) \times (1 + e^{-\lambda_i t_c} + e^{-2\lambda_i t_c} + e^{-3\lambda_i t_c} + \cdots\cdots)$$

Since the delayed neutron counting rates of the first and the second groups measured by the delayed neutron detection system, Ni (cps), were given in Table 4-2, delayed neutrons emitted by the delayed neutron emitting nuclides released from the uranium plates to sodium in one sec, ni (neutrons/sec) is given by

$$n_i = \frac{N_i}{\varepsilon \times e^{-\lambda_i t_a} \times (1 - e^{-\lambda_i t_b}) \times (1 + e^{-\lambda_i t_c} + e^{-2\lambda_i t_c} + e^{-3\lambda_i t_c} + \cdots\cdots)} \quad \cdots\cdots (4.1)$$

The first column of Table 4-3 shows the delayed neutron counting rates of the first and the second groups for 4.5, 3.0, 1.5 l/min. sodium flow rates calculated in Section 4.6 and the second column shows the delayed neutrons in one second at the irradiation section which were calculated using Equation (4.1).

The constants used in the calculation are as follows:
Delayed neutron detection efficiency of the delayed neutron detection system was taken as

$$\varepsilon = 1.2 \times 10^{-4} \text{ count} / \text{n}$$

as explained in Section 4.2.

As the decay constants, λ_i the following values were used.[14)] For the first group (halflife 57 sec.),

$$\lambda_1 = 0.0124 \text{ sec}^{-1}$$

and for the second group (halflife 22 sec.),

$$\lambda_2 = 0.0305 \text{ sec}^{-1}$$

The travel times of sodium from the irradiation section to the expansion tank inlet, ta, were 15.4, 23.1, and 46.1 sec. for 4.5,

3.0, and 1.5 l/min., respectively, as shown in Table 2.2.

The sodium staying times in the expansion tank, tb, were 48.0, 68.6, 120 sec for 4.5, 3.0, 1.5 l/min., sodium flow rates, respectively. These values were calculated from the expansion tank volume, 4 l, divided by the sodium flow rates of the main-circulation system plus of the purifier system.

The times needed for sodium to circulate once can be calculated basically from the sodium volume in the loop divided by the sodium flow rate, but, the sodium flow rate of the purifier system should be taken into account. The times became 83.13, 120.98, 223.3 sec. for 4.5, 3.0, 1.5 l/min., sodium flow rates of the main-circulating system, respectively.

Thus calculated numbers of delayed neutrons in one second (numbers in the second column of Table 4-3) divided by the numbers of delayed neutrons emitted from one fission, α_i (delayed neutron yield) give the numbers of fissions. The delayed neutron yields, α_i , of the first and the second groups were taken as[14)]

$$\alpha_1 = 0.00052$$

$$\alpha_2 = 0.00346$$

and the numbers of fissions in one second in the irradiation section sodium were calculated as shown in the third column. The first group delayed neutrons were $(4.54 \sim 4.68) \times 10^{10}$ and the second group delayed neutrons were 3.9×10^{10} for 4.5, 3.0, and 1.5 l/min. sodium flow rates. These numbers are almost independent of the sodium flow rates. This means that the amount of delayed neutron emitting nuclides adhered on the inner wall of the loop is independent of the sodium flow rates. The numbers of fissions calculated from the first group delayed neutrons, 3.9×10^{10}/sec,

did not coincide with those from the second group delayed neutrons, $(4.54 \sim 4.68) \times 10^{10}$/sec; this origin was not known. It is confirmed that the first and the second group delayed neutrons have different energy distributions (see reference 14), Fig. 5). If one assumes that the delayed neutron detection system has larger detection efficiency for lower energy neutrons, the numbers of fissions calculated from the first group delayed neutrons must become larger, but the experiment showed an inverse result. This may be caused by the different release rates of ^{87}Br (the first group) and of ^{137}I (the second group).

It is necessary to know the number of fissions occurred in metallic uranium in order to calculate the fission product release fraction which shows what percentage of fission products is released from metallic uranium into sodium. But the number of fissions in metallic uranium is not known. If one assumes 10W as the heat generated in 46.1 g of 20% enriched metallic uranium plates at 10 MW thermal output power of the reactor (see Y. Yamazaki, et al., JAERI-memo 5283[5], Section 5.3), the number of fissions for 10W becomes 3.1×10^{11}/sec. because the number of fissions per W is 3.1×10^{10}/sec. The fourth column in Table 4-3 shows the release fraction. The release fractions of the first and the second group delayed neutron emitting nuclides become 12.0% and 15.0%, respectively. The difference in the two values was of the different numbers of fissions, but the origin is not known. This release fraction is ten times as large as $1.5 \sim 2.0$ % calculated from fission product gamma-ray spectrometry in sodium made at various placed in the loop in the eighth sodium circulation experiment (Y. Yamazaki, et al[6]). This ten times difference was caused by the inadequate

value used as the detection efficiency of the delayed neutron detection system. The used value, 1.2×10^{-4} count/n is the result of the measurement using the RaD-Be neutron source. As described in Section 4.2, neutron energy of the RaD-Be source is 10 times as high as that of delayed neutrons: therefore, the real detection efficiency for delayed neutrons is expected to be at least several times as high as 1.2×10^{-4} count/n. The measurement of the delayed neutron detection efficiency of the detection system or Monte Carlo calculation of the efficiency seems to be necessary.

4.8 Calculation of Response Characteristics of Delayed Neutron Detection System at Reactor Start-Up

In Section 4.7 of JAERI-memo 5287[4], the experimental results on response characteristics of the delayed neutron detection system at the reactor start-up were reported. Fig. 4.8 in JAERI-memo 5287[4] shows the experimental results obtained in 7 March, 1973 and exhibits the counting rate change of the reactor neutrons and of the delayed neutrons measured by the delayed neutron detection system. The reactor power increased from 0 MW to 10 MW with one rush and was very appropriate for analysis. Figure 4.9 in JAERI-memo 5287[4] shows the normalized values of the counting rates of reactor neutrons and delayed neutrons taking the saturation values as 1. The subject of this section is whether the response characteristics shown in Fig. 4-9 can be explained by a calculation using one model.

We assume that the number of delayed neutron emitting nuclides released from uranium plates to sodium in the irradiation section is proportional to the number of reactor neutrons

without delay. This means that the delayed neutron emitting nuclides released from the surface of metallic uranium plates into sodium were emitted by the recoil mechanism of fissions and that the nuclides were not the ones diffused out from the inside of the uranium plates by diffusion mechanism. Let assume that the reactor neutron counting rate increases following a function, $n(t)$, after the reactor starts up at t=0. Then, the number of delayed neutron emitting nuclides in the irradiation section, $D(t)$, becomes

$$D(t) = K\, n(t),$$

where K is a constant.

Fig. 4-4 shows a picture of the movement of the delayed neutron emitting nuclides from the irradiation section to the expansion tank. The delayed neutron emitting nuclides released into sodium in the irradiation section decaying by a decay constant λ ($= 0.693/T_{\frac{1}{2}}$) were carried through the main-cooler to the expansion tank at ta sec. We assume that the probability of adhesion of the delayed neutron emitting nuclides onto the inner walls of tubes and the main-cooler between the irradiation section and the expansion tank is negligibly small. (In the real experiments, as shown in Section 4.12 of JAERI-memo 5287[4], the delayed neutron counting rate decreased as the main-cooler temperature decreased. This means that a part of the delayed neutron emitting nuclides adhered on the main-cooler wall and didn't arrive at the expansion tank). Then, the number of the delayed neutron emitting nuclides at the expansion tank inlet is given by

$$Kn(t-t_a)e^{-\lambda t_a}$$

If on assumes that the delayed neutron detection system located above the expansion tank can detect only delayed neutrons generated in the expansion tank, the delayed neutron counting rate, N(cps), is 0 in the times between 0 and ta. i.e.,

(1) for $0 < t < t_a$ $\qquad N = 0 \qquad \cdots\cdots\cdots (4.2)$

The delayed neutron counting rate starts to increase as the delayed neutron emitting nuclides starts to fill into the expansion tank. The delayed neutron counting rate, N(t), at t = (ta + t'), t' sec. after sodium starts to fill the expansion tank, is given by

$$N(t)=\lambda\varepsilon\int_0^{t-t_a} Kn(t-t_a-t')\,e^{-\lambda t_a}\,e^{-\lambda t'}\,dt'$$

Where (cts/n) is the delayed neutron detection efficiency of the delayed neutron detection system, i.e.,

(2) for ta t tb,

$$N(t)=\lambda\varepsilon\int_0^{t-t_a} Kn(t-t_a-t')\,e^{-\lambda t_a}e^{-\lambda t'}\,dt' \qquad \cdots\cdots\cdots (4.3)$$

After the time, t = (ta + tb), when the delayed neutron emitting nuclides start to flow out of the expansion tank, the delayed neutron counting rate, N(t), becomes

$$N(t)=\lambda\varepsilon\int_0^{t_b} Kn(t-t_a-t')\,e^{-\lambda t_a}e^{-\lambda t'}\,dt'$$

i.e.,

(3) for $ta + tb \leqq t < ta + tc$,

$$N(t)\lambda\varepsilon\int_0^{t_b} Kn(t-t_a-t')\,e^{-\lambda t_a}e^{-\lambda t'}\,dt' \qquad \cdots\cdots\cdots (4.4)$$

where tc is the time when the reactor neutron counting rate becomes constant. Therefore, the time (ta + tc) means that at

this time the effect of the constant counting rate of the reactor neutrons starts to appear in the expansion tank.

For $(ta + tc) < t < (ta + tb + tc)$, the delayed neutron emitting nuclides in the expansion tank can be decomposed into two kinds: the nuclides emitted during the increase of reactor neutron counting rate and those during the constant counting rate of reactor neutrons. The delayed neutron counting rate for the former case is given by,

$$\lambda\varepsilon\int_{t-(t_a+t_c)}^{t_b} Kn(t-t_a-t')e^{-\lambda t_a}e^{-\lambda t_a}e^{-\lambda t'}dt'$$

and for the later case,

$$n(t) = 1,$$

therefore, the counting rate becomes

$$\lambda\varepsilon\int_0^{t-(t_a+t_c)} K e^{-\lambda t_a}e^{-\lambda t'}dt'$$

Thus,

(4) for $(ta + tc) < t < (ta + tb + tc)$, the delayed neutron counting rate becomes

$$N(t)=\lambda\varepsilon\int_0^{t-(t_a+t_c)} Ke^{-\lambda t_a}e^{-\lambda t'}dt'+\lambda\varepsilon\int_{t-(t_a+t_c)}^{t_b} Kn(t-t_a-t')\,e^{-\lambda t_a}e^{-\lambda t'}dt' \quad \cdots\cdots\cdots (4.5)$$

(5) for $t > (ta + tb + tc)$, the reactor neutron counting rate becomes constant and

$$n(t) = 1.$$

and its effect prevails the entire expansion tank. Thus, the delayed neutron counting rate becomes

$$N(t)=\lambda\varepsilon\int_0^{t_b} Ke^{-\lambda t_a}e^{-\lambda t'}dt'=\varepsilon Ke^{-\lambda t_a}(1-e^{-\lambda t_b}) \qquad \cdots\cdots\cdots(4.6)$$

and is a constant value.

Fig. 4-9 of JAERI-memo 5287[4] is shown as Fig. 4-5 of the present report. The reactor neutron counting rate shown by triangles in Fig. 4-5 is taken as n(t) and let calculate the delayed neutron counting rate, N(t), using the above mentioned equations to see whether this N(t) coincides with the measurement. From the experimental conditions in Fig. 4-5,

ta = 23.1 sec.

tb = 4 x 60/(3 + 0.5) = 68.6 sec.

are obtained for 3 l/min. main-circulation system flow rate and 0.5 l/min. purifier system flow rate. Delayed neutrons contributed to the delayed neutron counting rate were found to be of the first and the second groups as described in Sections 4.6 and 4.7. The decay constants of the two groups are given by,

$\lambda_1 = 0.0124\ \text{sec}^{-1}$

$\lambda_2 = 0.0305\ \text{sec}^{-1}$

The ratios of the delayed neutrons of the first and the second groups to the sum of delayed neutrons of the two groups are 13.1% and 86.9%, respectively, from the delayed neutron yield data.[14]

At first, λ_1, ta, and tb are put into Equation (4.6), then,

$$N_1(t)=\varepsilon Ke^{-0.0124\times 23.1}(1-e^{-0.0124\times 68.6})$$

$$=\varepsilon K\times 0.7509\times(1-0.4271)$$

$$=0.4302\,\varepsilon K$$

By putting λ_2 , ta, and tb into Equation (4.6)

$$N_2(t) = \varepsilon K e^{-0.0305\times 23.1}(1-e^{-0.0305\times 68.6})$$

$$= \varepsilon K \times 0.4943 \times (1-0.1234)$$

$$= 0.4333\,\varepsilon K$$

Then, the sum of the delayed neutron counting rates of the first and the second groups becomes

$$N(t) = \varepsilon K(0.4302\times 0.131 + 0.4333\times 0.869)$$

$$= 0.4329\,\varepsilon K$$

When N(t) is normalized as 1

$$N(t) = 1$$

then,

$$\varepsilon K = 2.3100 \qquad \cdots\cdots (4.7)$$

Let calculate using Equation (4.4).

$$t_a + t_b = 23.1 + 68.6 = 91.7 \text{ sec}$$

and the time when the reactor neutron counting rate becomes constant is 290 sec, as shown in Fig. 4-5,

$$t_a + t_c = 23.1 + 290 = 313.1 \text{ sec}$$

Therefore, the time range in which Equation (4.4) can establish is

$$91.7 \text{ sec} < t < 313.1 \text{ sec}$$

The reactor neutron counting rate increased linearly between 100 sec. and 200 sec., as shown in Fig. 4-5, n(t) can be expressed by

$$n(t) = Ae^{\beta t} \qquad \cdots\cdots (4.8)$$

Therefore, Equation (4.4) becomes

$$N(t)=\lambda\varepsilon K\int_0^{t_b} n(t-t_a-t')\,e^{-\lambda t_a}\,e^{-\lambda t'}\,dt'$$

$$=\lambda\varepsilon K\int_0^{t_b} A e^{\beta(t-t_a-t')}\,e^{-\lambda t_a}\,e^{-\lambda t'}\,dt'$$

$$=\frac{\lambda\varepsilon KA}{\lambda+\beta}\cdot e^{-(\lambda+\beta)t_a}\left[1-e^{-(\lambda+\beta)t_b}\right]e^{\beta t} \qquad \cdots\cdots\cdots (4.9)$$

From Fig. 4-5, becomes

$\beta = 0.0289\ \mathrm{sec}^{-1}$

At t = 100 sec, A becomes 1.5×10^{-2} in Fig. 4-5, then Equation (4.8) becomes

$$n(100\,\mathrm{sec}) = Ae^{0.0280\times 100}$$

$$= 17.993A$$

$$= 1.5\times 10^{-2}$$

Therefore,

$$A = \frac{1.5\times 10^{-2}}{17.993} = 0.8336\times 10^{-3}$$

Thus, Equation (4.8) becomes

$$n(t) = 0.8336\times 10^{-3} \qquad \cdots\cdots\cdots (4.10)$$

By putting the first group constant, Equations (4.7) and (4.10) into Equation (4.9)

$$N_1(t)=\frac{0.0124\times 2.31\times 0.8336\times 10^{-3}}{0.0124+0.0289}\,e^{-(0.0124+0.0289)\times 231}$$

$$\times\left[1-e^{-(0.0124+0.0289)\times 636}\right]e^{0.0289\,t}$$

$$=\frac{0.02388\times 10^{-3}}{0.0413}\times 0.3852\times 0.94117\times e^{0.0289\,t}$$

$$= 0.2096\times 10^{-3}\ e^{0.0289\,t}$$

$$N_2(t)=\frac{0.0305\times 2.31\times 0.8336\times 10^{-3}}{0.0305+0.0289}e^{-(0.0305+0.0289)\times 23t}$$

$$\times\left[1-e^{-(0.0305+0.0289)\times 686}\right]e^{0.0289t}$$

$$=\frac{0.05873\times 10^{-3}}{0.05940}\times 0.2536\times 0.984\,e^{0.0289t}$$

$$=0.2467\times 10^{-3}\,e^{0.0289t}$$

Therefore, the delayed neutron counting rate, N(t), becomes

$$N(t)=(0.131\times 0.2096+0.869\times 0.2467)\times 10^{-3}\,e^{0.0289t}$$

$$=0.2381\times 10^{-3}\,e^{0.0289t} \qquad \cdots\cdots\cdots (4.11)$$

By putting t = 100 sec. and 200 sec. into Equation (4.11),

$$N(100\,\text{sec}) = 4.2842\times 10^{-3}$$

$$N(200\,\text{sec}) = 7,709\times 10^{-2}$$

These calculated values are plotted in Fig. 4-5. The calculated values delayed a little from the measured values, but, both are not so different.

Equations (4.3) ~ (4.6) can be solved by putting any function, n(t), as the reactor neutron counting rate into computer.

4.9 Counting Rate of Delayed Neutron Detection System Having Various Types of Neutron Detectors

The delayed neutron detector used in the first to the seventh sodium circulation experiments was 20th Century Electronics, Ltd. 40 EB 70/50 G #4. The experiment was made on 31 May, 1973 to know the effect of the neutron detector on the delayed neutron counting rate. The neutron detectors were three BF_3 counters

40 EB 70/50 G of 20th Century Electronics, Ltd., one BF_3 counters ND-8523-A60 of Mitsubishi Electric Company, and three ^{10}B counters PN 12 EB of 20th Century Electrics, Ltd. Signals from the BF_3 counter amplified by the preamplifier JAERI-121B are pulse-shaped in the spectroscopy amplifier JAERI-156 and sent to a 256 channel pulse height analyser. The output amplitudes from the amplifier were about 7 V and the pulses above 4 V were counted. For ^{10}B counters, the pulses above 1 V were counted. The results of the experiments on various types of the neutron detectors are shown in Table 4-4. The three BF_3 counters 40EB70/50G had almost the same characteristics. The delayed neutron counting rate of the BF_3 counter ND-8523-A60 of Mitsubishi Electric Company was about one fourth as large as that of 40EB 70/50G. ^{10}B counters PN12EB gave 7% delayed neutron counting rate of 40EB70/50G.

Table 4-4 shows the specification given by the manufacturer and ratio of sensitivity to that of 40EB70/50G. Sensitivity ratios of the specification coincided with the counting rate ratios for ND-8523-A60, but did not coincide for the three ^{10}B counters.

5. Experimental Results Obtained by Precipitator Type Fuel Failure Detection System

The precipitator type fuel failure detection system operated normally during the fifth and the tenth sodium circulation experiments except some troubles. The "WIRE DRIVE" of the precipitator stopped two or three times on 6 August 1973 in the seventh circulation experiment. This could be caused by the instant variation of the electric power voltage by considering the instant darkening of the room lights. This never happened, thenceforth. The precipitator measurement was not made on 22, 23 November, and 13, 14 December, to remove the photomultiplier from the precipitator. On 14 December, in the tenth circulation experiment, the main amplifier circuit to amplify the photomultiplier signals exhibited a trouble and the measurement was postponed. As the results of investigation, the first stage transistor (VT1 in Fig. 3(611/DA/04112) of Precipitator Manual by the Plessey Co.[10]) in the main amplifier (PULSE COUNT CHANNEL) was found to be burnt out and it was replaced by an equivalent transistor*.

The experimental results obtained by the precipitator during the fifth and the tenth circulation experiments and their analysis will be described as follows:

Leakage current vs applied voltage characteristics of precipitation chamber (Section 5.1)

Sodium amount adhered on inner wall of precipitation chamber (Section 5.2)

Pulse height distribution of beta-rays from precipitator wire (Section 5.3)

Dependence of precipitator counting rate on chamber

voltage (Section 5.4)

Radioactive nuclides adhered on wire at chamber voltage 0 V (Section 5.5)

Radioactive nuclides adhered on wire at chamber voltage -500 V (Section 5.6)

Radioactive nuclides adhered on wire at cover gas flow rate 500 cm^3/min. (Section 5.7)

Precipitator counting rate due to gamma-rays from fission products in cover gas in precipitation chamber (Section 5.8)

Background counting rate of precipitator during reactor not in operation (Section 5.9)

Effect of purge gas flow rate on background counting rate when wire was not driven (Section 5.10)

Precipitator response characteristics (Section 5.11)

Decay of precipitator counting rate after reactor shut down (Section 5.12)

Effect of cold trap temperature on precipitator counting rate (Section 5.13)

Correspondence of precipitator counting rate to delayed neutron counting rate (5.14)

* Tatsuo Miyazawa, et al., of the Toshiba Research and Development Center, Tokyo Shibaura Electric Co., Ltd., repaired.

5.1 Leakage Current vs. Applied Voltage Characteristics of Precipitation Chamber

Leakage current between the high voltage terminal and the ground of the precipitator was measured by Keithley 602B electrometer (battery operation). The object was to investigate whether an electric discharge occurred in the chamber gas or whether the insulation worsening due to sodium vapor adhered on the chamber inner wall occurred. The overcurrent protection circuit of the high voltage supply in the precipitator was supposed to cut the high voltage when the leakage current exceeded 5 uA.

In Section 5.3 of JAERI-memo 5287[4], the results of the leakage current measurement in the first sodium circulation experiment (on 15, 27 January, 1973) were reported: the leakage current didn't differ before and after the first circulation experiment and was 5 uA at 1900 V. It decreased to 3 uA at 1900 V when the chamber was disassembled and washed with purified water before the second circulation experiment. It didn't change very much before and after the second circulation experiment.

Leakage current vs. applied voltage characteristics were measured on 28 January, 1974 after the first to the tenth sodium circulation experiments finished (the total sodium circulation time was 2739 hr 18 min.). The cover gas flow rate and pressure were 200 cm^3/min. and 100 mmHg, respectively. The results are shown in Fig. 5-1. The leakage current was 2.5×10^{-8} A at 800 V and smaller than 1.2×10^{-6} A (for the first circulation experiment). No insulation degradation was observed due to sodium adhesion onto the chamber inner wall and, on the contrary, the insulation characteristics were improved.

The above description was about the leakage current measurement with the ordinary polarity voltage (+ high voltage on the high voltage terminal). Fig. 5-2 shows the leakage current measured by applying negative voltages on the high voltage terminal and exhibits a current vs. voltage characteristic symmetrical to the point (0 V, 0 A).

5.2 Sodium Amount Adhered on Inner Wall of Precipitation Chamber

The precipitation chamber was disassembled on 13 December 1972 after the first sodium circulation experiment finished. The materials adhered in the chamber were washed out with purified water and the sodium amount in the water was measured. The results were reported in JAERI-memo 5287[4], p. 26 (May, 1973). Similar experiment was performed in the tenth sodium circulation experiment. The measurement using atomic absorption spectroscopy was made by Tatsuo Miyazawa, et al., of the Toshiba Research and Development Center*.

* The authors wish to give a deep appreciation to Tatsuo Miyazawa and Katsumi Kubo.

The precipitator was moved to the Toshiba R & D Center on 29 January, 1974. It was disassembled on 20 February, 1974. Radioactivity measurement made using a GM and a NaI(Tl) survey meter before the disassembly gave counting rates less than background (20 cps). Gamma-ray spectrometry of the smeared samples from the various parts of the disassembled precipitator gave no meaningful result. The results of the sodium amount measurement using an atomic absorption spectrometer (Toshiba-Beckman NF-1B) are shown in Table 5-1. For a comparison purpose, the sodium amount measured after the first circulation experiment is also added.

The places of the measurement shown in Table 5-1 are explained in Fig. 5-3. The total amount of the adhered sodium measured after the tenth sodium circulation experiment was found to be 0.655 g. 0.1855 g on the drum, 0.1022 g on the inlet and the outlet for sample gas, and 0.0896 g on the wire. The sodium amount measured after the tenth circulation experiment is only twice of that after the first experiment (0.3364 g) while the sodium circulation time at the end of the tenth experiment is more than 10 times of that at the end of the first experiment: the reason is not understood yet.

5.3 Pulse Height Distribution of Beta-Rays from Precipitator Wire

The Mark XI precipitator of the Plessey Co., Ltd., detects the fission products adhered on the wire using a combination of beta-ray detecting scintillator and a photomultiplier. The scintillator has a dimension of 3.97 mm inner diameter, 6.35 mm outer diameter, and 53.95 mm length made of tetraphenylbutadien + terphenyl, and is enclosed by a light guide of pyrex-glass which connected to a photomultiplier (EMI 6097 G). After the photomultiplier outputs are amplified by a preamplifier and a main amplifier, they are connected to a discriminator by which they are converted to digital signals and counted by a scaler. It is already shown that the nuclides adhered on the wire is ^{88}Rb when the precipitator is operated at a chamber voltage of 500 V and a cover gas flow rate of 200 cm^3/min. (see JAERI-memo 5287[4], Section 5.7 and Fig. 5-6). Therefore, beta-ray pulse height distribution measured at 200 cm^3/min. cover gas flow rate is considered to be of ^{88}Rb. The pulse heights of beta-rays from the wire were measured by changing the discriminator level on 7 June, 1973 when the

precipitator was operated at a cover gas flow rate of 200 $cm^3/min.$, purge gas flow rate of 50 $cm^3/min.$, cover gas pressure of 100 mmHg, and chamber voltage of 500 V. The solid line in Fig. 5-4 shows beta-ray counting rate dependence on discriminator level measured at 1350 V photomultiplier voltage. This line means an integration curve of the pulse counting rate having heights above the discriminator level. The differences of the succeeding measurement points were calculated and plotted as a dotted line (differential curve). This differential curve shows the pulse height distributions of beta-rays from ^{88}Rb. In the ordinary measurements all pulses having heights above 1.1 V were counted: this 1.1 V is found to be an appropriate voltage to discriminate noise and give the maximum beta-ray detection efficiency. To know how this discriminator level corresponds to beta-ray energy, the pulse height distribution of beta-rays from ^{90}Sr 6 Ci (maximum energy 0.546 MeV) was measured and shown in Fig. 5-4. In this distribution, the pulse heights was too large and the pulses corresponded to 0.546 MeV became larger than 11 V of discriminator level. Therefore, the energy calibration of the discriminator level could not be made.

The photomultiplier voltage was decreased to 1100 V in order to make pulse height smaller and make the pulse height corresponding to the maximum energy of beta-rays of ^{88}Rb (5.3 MeV) smaller than 11 V and the results of the measurement of ^{88}Rb pulse height distribution are shown in Fig. 5-6. From the differential curve, the maximum pulses are considered to have 8 V pulse height. Fig. 5-7 shows the pulse height distribution of beta-rays from ^{90}Sr at 1100 V photomultiplier voltage. From Fig. 5-7, it is shown that the maximum height pulses of beta-rays from ^{90}Sr have about 3 V.

When Figs. 5-6 and 5-7 are compared, 5.3 MeV beta-rays from ^{88}Rb corresponds to 8 V whereas 0.546 MeV beta-rays from ^{90}Sr corresponds to 3 V. The pulse heights differ only 2.5 times while the energy difference is 10 times. One of the reasons is that ^{88}Rb and ^{90}Sr sources were located at different positions. The nuclides, ^{88}Rb, adhered on the wire which located on the center axis of the hollow cylinder scintillator while ^{90}Sr calibration source located outside of the cylinder scintillator and the beta-rays from ^{90}Sr entered from the outer surface of the scintillator. Another reason is that the radial thickness of the hollow scintillator is 2.38 mm and too thin to absorb high energy beta-rays and only one part of the energy is given to the scintillator: this make pulse height smaller. If one assumes that the scintillator is made of only terphenyl having a density of 1.23, the maximum range of 0.5 MeV beta-rays is calculated as about 1 mm, and of 5 MeV about 21 mm. Therefore, beta-rays from ^{90}Sr lose their energy completely in the scintillator whereas beta-rays from ^{88}Rb (maximum energy 5.3 MeV) lose only a part of the energy in the scintillator and give pulse height only 2.5 times as large as that of ^{90}Sr. Incidentally it may remark that the beta-ray energy losing the complete energy in 2.38 mm thick scintillator is 0.8 MeV.

The beta-ray energy corresponding to 1.1 V discriminator level as shown in Fig. 5-4 can be calculated as follows. If one assumes that the maximum beta-ray energy 0.546 MeV of ^{90}Sr loses its entire energy, the maximum pulse height 3 V as shown in Fig. 5-7 corresponds to 0.546 MeV. Figs. 5-7 and 5-5 measured the same pulse height distribution of beta-rays from ^{90}Sr, thus, Fig. 5-5 must have shown the pulse height distribution of lower

energy side of Fig. 5-7. In Fig. 5-5, the integral curve changed from 10^3 cps as discriminator level changed from 4.8 V to 10.4 V (difference = 10.4 - 4.8 = 5.6 V) while it is necessary for a change from 10^3 cps to 10^2 cps to change from 0 V to 0.9 V. Therefore, the discriminator level shown in Fig. 5-5 was extended 6.2 times (= 5.6/0.9) as large as the level shown in Fig. 5-7., i.e., the discriminator level,

$$3\,\mathrm{V} \times 6.2 = 18.6\,\mathrm{V}$$

shown in Fig. 5-5 corresponds to beta-ray energy 0.546 MeV. Since the discriminator levels are equal in Figs. 5-4 and 5-5, the discriminator level, 1.1 V, shown in Fig. 5-4 must correspond to

$$\frac{1.1 \times 0.546}{18.6} = 0.032\ \mathrm{MeV}$$

Beta-rays of energies larger than 32 keV had been counted at 1350 V photomultiplier voltage.

5.4 Dependence of Precipitator Counting Rate on Chamber Voltage

In Section 5.4 in JAERI-memo 5287[4], the experimental results of the precipitator counts as a function of chamber voltage are described and shown in Fig. 5-3. Even at 0 V chamber voltage the precipitator showed counts and it was found that ^{88}Rb adhered on the wire from the decay measurement (see Section 5.5 of the present report). It is interesting to know whether ^{88}Rb adheres on the wire or not when an inverse polarity of the applied voltage is applied (negative voltage on the high voltage terminal). To determine this, the precipitator counting rate was measured by varying the chamber voltage from +500 V to -500 V. When negative voltages are applied on the chamber, the decrease of the precipitator counting rate is expected, therefore attention should

be paid to produce errors as little as possible: for examples, attention should be paid to residual radioactive nuclides adhered on the wire. The experiment should start using the wire having very little radionuclides after many hours had elapses. Also, the measurement should be performed before the wire turns more than once because the residual radioactivity becomes large and brings errors to the measurement. The number of the measurements during one turn of the wire can be measured by counting the number of wire drive until the precipitator counting rate increases. A chamber voltage of 500 V was applied only for 2 min. on the wire with no radioactivity in order to adhere ^{88}Rb on the wire and, from that time on, with a chamber voltage of -500 V the precipitator was operated at soak/count time 23 sec. The number of the wire drive before the wire circulated once was found to be 99. The residual radioactivity of ^{88}Rb (halflife 17.8 min.) after one circulation of the wire for soak/count time 20 sec. is calculated as

$$\exp\left(-\frac{0.69315\times 20\times 99}{17.8\times 60}\right)=0.2731$$

and is 27.3% of the initial radioactivity. For soak/count time 1 min., the number becomes

$$\exp\left(-\frac{0.69315\times 1\times 99}{17.8}\right)=0.0204$$

and 2.04% of the initial radioactivity will be left and will be summed onto the measured value. For soak/count times 2 min., 3 min., the residual radioactivities become 4.15×10^{-4}, 8.44×10^{-6}, respectively.

The precipitator counting rate measurement was made on 5 October, 1973 for chamber voltages from -500 V to +500 V. The

reactor was operated at 10 MW, the SIL was in stationary operation at cover gas flow rate 200 cm^3/min., purge gas flow rate 50 cm^3/min., and soak/count time 1 min. The experimental results are shown in Fig. 5-8. The precipitator counting rates for chamber voltages 500 V, 0 V, -500 V were 1 x 10^5 cps, 4500 cps, 380 cps, respectively. Each counting rate included 22.5 cps, the counting rate of gamma-rays from fission products in the chamber which was described later in Section 5.8. The ratio of 380 cps to 1 x 10^5 cps becomes 0.38%. This 0.38% is smaller than 2.04%, the residual radioactivity after one turn of the wire. Therefore, a large error can be brought if the measurement is not made before one turn of the wire. The counting rate ratio at chamber voltages 500 V to 0 V becomes

$$1\times10^5/4500=22.2$$

If one assumes that only ^{88}Rb collided with the wire adheres onto the wire at 0 V chamber voltage whereas all ^{88}Rb in the chamber are collected on the wire at 500 V chamber voltage, the ratio of the counting rates measured at chamber voltages 500 V to 0 V becomes the ratio of the cross sections of the chamber (14 cm x 6.7 cm) to the wire. The wire cross section is given by 0.215 cm (outer diameter of the helical coil) x percentage of the wire cross section in the helical coil x 6.7 cm. When one assumes that the percentage of the wire cross section in the helical coil is 1, then, the cross section ratio becomes

$$14/0.215=65.1$$

Since the percentage of the wire cross section in the helical coil is less than 1, the cross section ratio of the chamber to the wire becomes larger than 65 while the counting ratio for 500 V

chamber voltage to 0 V was measured as only 22.2. It is not easily understood that ^{88}Rb nuclides other than those collided with the wire can be collected at chamber voltage 0 V. Therefore, the collection efficiency of ^{88}Rb to the wire may be smaller than 33% for chamber voltage 500 V. The collection of ^{88}Rb to the wire will be retarded at chamber voltage -500 V, thus make the wire counting rate smaller.

5.5 Radioactive Nuclides Adhered on Wire at Chamber Voltage 0 V

As described in Section 5.4 and shown in Fig. 5-3 in JAERI-memo 5287[4], even at chamber voltage 0 V some counting rates were observed and the value of the counting rate was about 1/20 of that obtained for 500 V chamber voltage. The origin of this counting rate was left not to be understood. In order to investigate this origin, the decay of the counting rate of the stopped wire was measured after the precipitator operation at 0 V chamber voltage. The results are shown in Fig. 5-9 by circles in the lower curve. A constant counting rate, 22.5 cps, was observed 150 mm after the wire was stopped. When one subtracts 22.5 cps from the circles, one obtains black dots and the halflife becomes 16.5 min. Appropriate nuclides having 16.5 min. halflife could not be found except ^{88}Rb (halflife 17.8 min.) when compared with the measurement of gamma-ray spectra of cover gas in the reservoir just before the precipitator (see JAERI-memo 5287, Section 5.8). Therefore, it can be concluded that the wire collects ^{88}Rb even at 0 V chamber voltage: ^{88}Rb adheres on the wire if ^{88}Rb collides with the wire. The fact that ^{88}Rb adhered even at -500 V chamber voltage will be described in Section 5.6.

As described above, ^{88}Rb (halflife 17.8 min.) adheres on

the wire at 0 V. It is interesting to know whether the amount of adhered ^{88}Rb is proportional to the staying time of the wire in the chamber (i.e., soak time) or not. Circles in Fig. 5-10 show the precipitator counting rate change for soak/count time change at 0 V chamber voltage. Dark dots show the results of correction taking account of the dead time of the precipitator electronic circuit (double pulse resolution $= 2.4 \times 10^{-6}$ sec., see JAERI-memo 5287[4], Section 5.6), and the counting rate decrease due to halflife (17.8 min.) of ^{88}Rb. Since the counting rate increased proportionally to soak/count time, it can be said that the amount of ^{88}Rb adhered on the wire is proportional to the staying time of the wire in the chamber.

5.6 Radioactive Nuclides Adhered on Wire at Chamber Voltage -500 V

As explained in Section 5.4 and shown in Fig. 5-8, the precipitator exhibited a certain counting rate at chamber voltage -500 V and the counting rate was 380 cps for soak/count time 1 min. In order to determine the radioactive nuclides which gave this counting rate, the decay measurement on the stopped wire was made. Fig. 5-11 shows the experimental results for cover gas flow rate 200 cm^3/min., and purge gas flow rate 50 cm^3/min. The nuclides, ^{88}Rb, of halflife 17.8 min., were confirmed.

5.7 Radioactive Nuclides Adhered on Wire at Cover Gas Flow Rate 500 cm^3/min.

It is important to determine the radionuclides counted by the precipitator. It is already known that almost all nuclides adhered on the wire at cover gas flow rate 200 cm^3/min., are ^{88}Rb (JAERI-memo 5287[4], Section 5.7, Fig. 5-6). Other nuclides

can be expected to be detected and the decay of the beta-ray counting rate of the stopped wire was measured. Circles in Fig. 5-12 plotted the counting rates from which the background 22.5 cps was subtracted. When a component of ^{88}Rb (halflife 17.8 min.) (solid line) was subtracted from the decay curve, the points shown by the black dots were obtained and the halflife of the black dot points became 32.2 min., which coincided with the halflife of ^{138}Cs. Needless to say, ^{138}Cs is the nuclide beta-decayed from ^{138}Xe. The first part of the data shown by black dots in Fig. 5-12 became decreased: this was the results of too much subtraction of 17.8 min. halflife component in analysis. The beta-ray counting rate at t = 0 min. for ^{88}Rb and ^{138}Cs were calculated as 37000 cps and 1500 cps, respectively. Therefore, it is found that ^{138}Cs as well as ^{88}Rb adhered on the wire when the cover gas flow rate was increased to 500 cm^3/min., whereas only ^{88}Rb adhered on the wire at 200 cm^3/min. cover gas flow rate and 500 V chamber voltage. For 500 cm^3/min. cover gas flow rate, the ratio of the radioactivities of ^{88}Rb to ^{138}Cs becomes

$$37,000/1,500 = 26$$

5.8 Precipitator Counting Rate due to Gamma-Rays from Fission Products in Cover Gas in Precipitation Chamber

When the decay of beta-rays from the wire was measured to identify the nuclides adhered on the wire, the constant counting rate was found after many hours had elapsed (see JAERI-memo 5287[4], Section 5.7, Fig. 5-6). To confirm this, the decay measurement of the beta-rays was made after the wire collected ^{88}Rb at 200 cm^3/min., cover gas flow rate, 500 V chamber voltage and 30 sec. soak/count time. Circles in Fig. 5-9 show the

results: the counting rate became a constant, 22.5 cps, at 250 min. after the wire stopped. Black dots were obtained after the constant counting rate, 22.5 cps, was subtracted from the measurement (circles) and gave a halflife of 17.8 min. (^{88}Rb).

Similarly, a constant counting rate, 22.5 cps, was obtained after 150 min. at chamber voltage 0 V and the values (black dots) obtained by subtracting 22.5 cps from the measurements (circles) showed 16.5 min. halflife: this nuclide corresponded to ^{88}Rb (see Section 5.5).

It is important to know the origin of this residual 22.5 cps after many hours have elapsed at chamber voltages 500 V and 0 V. At first, the precipitator count was measured at chamber voltage 0 V without driving the wire and with no cover gas flow for 10 MW reactor operation and stationary SIL operation. The counting rate was 2 cps. Secondly, the cover gas was started to flow through the precipitation chamber at 200 cm^3/min. without driving the wire at chamber voltage 0 V: the counting rate started to increase and reached to a constant value, 22.5 cps, after 1 hr, as shown in Fig. 5-13. This time, 1 hr, seems to be the time needed for fission product concentration in gas in the precipitation chamber to become constant. The counting rate, 22.5 cps, observed in Fig. 5-9 is considered to be given by the gamma-rays of the fission products in the precipitation chamber which passed through the wire-driving hole and the shield between the chamber and the scintillator*. This shows the necessity of paying attention to

* As a method to confirm this, the pulse height distribution of the scintillator output should be compared with the beta-ray distribution given in Fig.5-4. The measurement will be made in the future.

designing of the wire-driving hole, shielding between the chamber and the scintillator, position of the scintillator in order to reduce background.

5.9 Background Counting Rate of Precipitator during Reactor Not in Operation

The precipitator gave counting rate even at no reactor operation. One of the reasons is the presence of long-lived radionuclides adhered on the precipitator wire. In order to investigate this possibility, the precipitator counting rate was measured as a function of soak/count time (23 sec., 60 sec., 120 sec.) at chamber voltages 500 V and 0 V during reactor power 0 MW before the reactor started up. The experiment was made on 28 May, 1973 during SIL stationary operation with cover gas flow rate 200 cm^3/min. and purge gas flow rate 50 cm^3/min. The experimental results are shown in Fig. 5-14. The precipitator counting rates were 0.65 cps at precipitation chamber voltages 0 V and 500 V and did not depend on soak/count time. As described in Section 5.6 of JAERI-memo 5287[4], the precipitator counting rate will be proportional to soak/count time if the beta-rays from the wire are counted whereas it will be constant if radiations from other sources than the wire are counted. Therefore, this 0.65 cps is not caused from the nuclides collected on the precipitator wire and is considered to be caused from radioactivities present outside or inside of the precipitator or from the electric noises.

5.10 Effect of Purge Gas Flow Rate on Background Counting Rate When Wire Was Not Driven

In Section 5.5 of JAERI-memo 5287[4], the results on the effect of purge gas flow rate on the precipitator counting rate were

explained. The precipitator counts for chamber voltages 500 V and 0 V were measured for 200 cm^3/min. cover gas flow rate by varying purge gas flow rate from 12.5 cm^3/min. to 125 cm^3/min. as shown in Fig. 5-4 of JAERI-memo 5287[4]. Also, it was concluded that fission products in cover gas did not enter into the scintillator to contaminate it. To reconfirm this, the following experiment was carried out.

The precipitator counting rates were measured by varying only purge gas flow rate from 12.5 cm^3/min. to 125 cm^3/min.: The reactor operated at 10 MW, SIL was in the stationary operation, the cover gas flow rate was 200 cm^3/min., the precipitator chamber voltage was 0 V, and the wire was not driven. The results are shown in Fig. 5-15. For an initial purge gas flow rate of 50 cm^3/min, the counting rate was 24 cps. This counting rate was due to fission product gamma-rays in cover gas in the chamber counted by the scintillator. At 11:33, the purge gas was changed to 125 cm^3/min., but the counting rate did not vary. At 11:36, the purge gas flow rate was changed to 25 cm^3/min., then, the counting rate increased to 26 cps with a delay of 1 min. At 11:44, the purge gas flow rate was decreased to 12.5 cm^3/min., then, the counting rate increased to 36 cps with a delay of 1 min. At 11:51, when the flow rate increased to 25 cm^3/min., the counting rate decreased to 25 cm^3/min., the counting rate decreased to 31 cps. At 11:56, the flow rate increased to 50 cm^3/min., but, the counting rate kept 31 cps. From the measurement, a part of cover gas entered into the scintillator at a purge gas flow rate of 12.5 cm^3/min., and the fission products in cover gas were suspected to contaminate the scintillator. For purge gas flow rates

larger than 25 cm^3/min., this kind of suspicion can not be considered. Therefore, it is more safer to flow purge gas more than 25 cm^3/min. for a cover gas flow rate of 200 cm^3/min. to prevent a possibility of contamination of the scintillator.

5.11 Precipitator Response Characteristics

As described in Section 5.8 of JAERI-memo 5287[4], there is a total volume of

$$7.24\,\ell + 1.54\,\ell = 8.78\,\ell$$

between the expansion tank outlet and the precipitator inlet including a sodium vapor trap (7.24 l) and piping (1.54 l). Therefore, the travel time of fission products in cover gas to arrive at the precipitator is calculated as

$$8.78 / 0.2 = 43.9 \text{ min}$$

for a cover gas flow rate of 200 cm^3/min. This cover gas travel time becomes

$$8.78 / 0.5 = 17.6 \text{ min}$$

even for 500 cm^3/min.

Since the total volume between the expansion outlet and the precipitator inlet becomes 9.76 l when the gas reservoir (0.98 l) is inserted before the precipitator, the cover gas travel times can be calculated as 48.8 min. and 19.5 min., respectively, for cover gas flow rates of 200 cm^3/min. and 500 cm^3/min.

Fission products released from metallic uranium were carried by sodium to the expansion tank 23.1 sec. later at a sodium flow rate of 3.0 l/min., and fission products such as Kr and Xe were transferred from sodium to cover gas in the expansion tank from which Kr and Xe were carried out to the precipitator. Therefore, the precipitator counting rate followed after the reactor output

power by a delayed time of at least the cover gas travel time. It is necessary to add the time needed for the concentration of Kr and Xe in cover gas in the precipitator to become constant before the precipitator counting rate change finished. Change in the counting rate of the cover gas gamma-ray spectrometer and of the precipitator was shown in Figs. 5-9, 10, 11, and 12 of JAERI-memo 5287[4] and the figures showed the response of the cover gas system including the sodium vapor trap and piping and did not show the response of the precipitator itself. In order to measure the response of the precipitator itself, the travel time of cover gas should be very short, thus smaller volumes of the sodium vapor trap and pipings are needed. Reconstruction of the cover gas system is very difficult practically, thus, was not made. In stead of the reconstruction, the following method was used to measure the response of the precipitator itself: i.e., the precipitator was bypassed by closing a valve just before the precipitator. Then, the valve was opened to flow cover gas into the precipitation chamber when the fission product concentration became constant after many hours had elapsed from the reactor start-up. This made the response characteristic measurement of the precipitator possible.

The response characteristics of the precipitator was measured on 22, 23, 25, and 28 June 1973. The reactor was operated at 10 MW, the SIL was under stationary operation, the chamber voltage of the precipitator was 500 V and the soak/count time was set to 20 sec. The curve A shown in Fig. 5-16 shows the precipitator counting rate change after cover gas started to flow into the precipitator by opening the valve just before the precipitator at

200 cm^3/min. cover gas flow rate and 50 cm^3/min. purge gas flow rate. It started to increase just after the introduction of cover gas and saturated after 60 min. The precipitation chamber had 1.03 l volume and it took 60 min. to have a constant concentration of fission products. Curves B and C shows the precipitator counting rate change after cover gas was introduced into the gas reservoir in series with the precipitator by opening the valve before the gas reservoir.

The time difference of the rising parts of Curves B and C was about 13 min. and this was due to a time delay brought by insertion of the gas reservoir before the precipitator. This delay of 13 min. is 2.65 times as large as 4.9 min., the value obtained from a simple calculation of the gas reservoir volume (980 cm^3) divided by the cover gas flow rate 200 cm^3/min. Also, Curve B increased just after the opening of the valve, and this was caused by the presence of fission products in cover gas of the gas reservoir. Curve C was obtained after the valve was opened when the fission products in cover gas of the gas reservoir decayed sufficiently.

Curves A and B in Fig. 5-17 shown the precipitator counting rate change after the valve was opened. The cover gas flow rate was 500 cm^3/min. and the purge gas flow rate was 125 cm^3/min. Curve A shows the results obtained when cover gas flowed only through the precipitator whereas Curve B shows the results obtained when cover gas flowed through the gas reservoir and the precipitator. The time difference of the rising parts of Curves A and B was 4.3 min., which was 2.2 times as large as the value calculated from the gas reservoir volume 980 cm^3 divided by cover gas flow rate 500 cm^3/min. Curves C and D in the figure are the

same curves shown as A and C in Fig. 5-16.

The delays of the response characteristics of the precipitator by placing the gas reservoir before the precipitator measured at cover gas flow rates 200 cm^3/min. and 500 cm^3/min. are 2.65 and 2.2 times as large as the simply calculated values, respectively, and this fact needs a future investigation.

5.12 Decay of Precipitator Counting Rate After Reactor Shut Down

In Section 5.8, JAERI-memo 5287[4], the response characteristics were measured at the reactor start-up. As shown in Fig. 5-11, the precipitator counts started to change with 90 min. delay after the reactor start-up. This delay was caused by the time needed for fission products in cover gas to arrive at the precipitator. How does the precipitator counting rate change when cover gas flow continues after the reactor shut down? The amount of radioactive cover gas (Kr and Xe) transferred to cover gas in the expansion tank will decrease after the reactor shut down. This change will appear as a precipitator counting rate change several min. later. The precipitator count change was measured after the reactor shut down on 13 October, 1973. The SIL continued its stationary operation, cover gas and purge gas continued to flow at 200 cm^3/min. and 50 cm^3/min., and the precipitator continued its operation at soak/count time 60 sec. The precipitator count was 6×10^6 at 15:00 when the reactor shut down. It increased gradually until 16:39 and became nearly constant. After 16:39, the precipitator count started to decrease and became $\frac{1}{2}$ of the stationary value at 4 hr 30 min. after the reactor shut down. The time needed for the precipitator counting

rate to start to decrease, 99 min., corresponds to the time needed for cover gas to travel from the expansion tank to the precipitator, and this coincides with the time elapsed between the reactor start-up and the start time of the precipitator count increase, 90 min. These values, 99 min. and 90 min., are twice as large as 43.9 min., the value calculated from the volume 8.78 l between the expansion tank outlet and the precipitator inlet divided by the cover gas flow rate 200 cm^3/min.

5.13 Effect of Cold Trap Temperature on Precipitator Counting Rate

The results of gamma-ray spectroscopy of the cold trap showed that a considerable amount of ^{88}Kr and ^{138}Xe was collected on the cold trap and their amount depended on the cold trap temperature (Y. Yamazaki, et al.: JAERI-memo 5283[5] (May, 1973), Section 5.5 and Section 5.10). The nuclides ^{88}Kr and ^{138}Xe, transferred into cover gas and gave the precipitator count. Therefore, the amount of Kr and Xe in the cover gas will change and the precipitator counting rate will change when the cold trap temperature changes. In order to confirm this, the cold trap temperature was decreased from 250 °C to 200 °C and the effect on the precipitator counting rate was investigated on 6 October, 1973. The results are shown in Fig. 5-19. It was confirmed that the precipitator counting rate changed with 90 min. delay after the change in fission product concentration in the expansion tank (Section 5.12), thus, the precipitator counting rate should have changed at 13:10 which was 90 min. later than 11:40 when the cold trap temperature decreased from 250 °C to 200 °C. But it did not show any change.

When the cold trap temperature increases from 200 °C to 250 °C, Kr and Xe absorbed on the cold trap melt out into sodium, transfer to cover gas, and give the precipitator counting rate. The precipitator counting rate did not change in the experiments of the cold trap temperature increase from 200 °C to 250 °C.

From these measurements, it is concluded that the precipitator counting rate did not show any change for the cold trap temperature change between 200 °C and 250 °C and that this was caused by the very little amount of Kr and Xe absorbed on the cold trap compared with the amount of Kr and Xe in sodium.

5.14 Correspondence of Precipitator Counting Rate to Delayed Neutron Counting Rate

As shown in Section 4.1 and Fig. 4-1, the delayed neutron counting rate increased as sodium circulation time increased. The precipitator counting rate, also, increased and the increase rates of the delayed neutron and the precipitator counting rates are expected to be equal.

The delayed neutron and the precipitator counting rates measured at equal conditions of the SIL and the precipitator operation were picked up and compared, as shown in Table 5-2 and Fig. 5-20. JRR-2 was operated at 10 MW, the SIL irradiation section 500 °C, main cooler 400 °C, expansion tank 350 °C, sodium flow rate 3 l/min., cover gas flow rate 200 cm^3/min., purge gas flow rate 50 cm^3/min. cover gas pressure 100 mmHg, soak/count time 60 sec. The delayed neutron counting rate in the 4th circulation experiment was measured at 4.5 l/min. and it was corrected to the value for 3.0 l/min. using the relation shown in Fig. 4-14 of JAERI-memo 5287. The precipitator

counting rates measured at soak/count times 23 sec. and 30 sec. were corrected to those at 60 sec., using a proportionality of the precipitator counting rate to soak/count time (Fig. 5-10). The ratio of the counting rates of the precipitator to the delayed neutron monitor is about 8.7 and constant, as shown in Table 5-2 and Fig. 5-20. This ratio did not change when the irradiation section temperature decreased from 500 °C to 400 °C or 14 April.

6. Precipitator Wire Gamma-Ray Spectrometer

6.1 Precipitator Wire Gamma-Ray Spectrometer

The precipitator Mark XI made by the Plessey Co. detects beta-rays from the radionuclides adhered on the wire using an organic scintillator as a detector. This detector can detect beta-rays very efficiently, but it has an inconvenience that identification of radionuclides needs halflife measurement for the stopped wire. One way of identifying radionuclides is to measure gamma-ray spectrometry of the wire. For examples, gamma-rays from ^{88}Rb and ^{138}Cs are as shown in Figs. 6-1 and 6-2. Spectrometry of these gamma-rays makes nuclide identification possible and gives a confirmation of not measuring the radionuclides (^{23}Ne, ^{24}Na, ^{41}Ar, etc.) other than fission products.

To measure gamma-rays from the wire, a gamma-ray measuring port as shown in Fig. 6-3 can be added to the precipitator and a gamma-ray detector can be inserted to the port. By using this, gamma-rays and beta-rays can be measured simultaneously. This drawing was sent by the Plessey Co., Ltd., but, the use and the experiments made by the Plessey Co., Ltd., are not reported yet.

In our study, we removed a photomultiplier connected with an organic scintillator for beta-ray measurement and installed a Ge(Li) detector to measure gamma-ray spectra from the wire. Therefore, the gamma-rays through the organic scintillator and the light-guide are to be measured. Since the diameter of the hole was determined, a special Ge(Li) detector suit in the hole is to be made.

6.2 Cryostat construction

The type and size of the cryostat is limited by the photo-multiplier hole. The cryostat should have a vertical feed type: The liquid nitrogen Dewan is one the Ge(Li) detector which is fastened to the lowest end of the cold finger. The aluminum cap diameter of the cryostat should be less than the hole diameter (2.06" = 5.23 cm). The time allowed for manufacturing cryostat was short, therefore, we decided to design a cryostat to suit with a CR-17 Dewar (Union Carbide). Fig. 6-4 shows a drawing of cryostat-Dewar combination. The preamplifier, high voltage filter, and Ge(Li) detector are also shown. The CR-17 Dewar can store 17 l of liquid nitrogen. Fig. 6-5 shows the cryostat mounted on the precipitator.

The details of the cryostat are shown in Fig. 6-6. Liquid nitrogen from the CR-17 Dewar enters into a stainless tube of 3 mm diameter and 0.3 mm thickness and cools a copper cold finger welded in the lower end. Under the cold finger, an aluminum box including a Ge(Li) detector is fastened through a 3 mm thick boron nitride plate. A 0.3 mm thick aluminum foil is placed in front of the detector and shields heat radiation from the parts at room temperature. Stainless steel (SUS-304) and aluminum (cap) were used. A vacuum valve (ryolab SV-1-06-5S2, a high voltage terminal NEC hermetic seal A711, a 7 pin hermetic seal NEC-S101C were used. "O" rings were made of viton. In order to keep vacuum, molecular sieve 5A (NEC-Varian) was enclosed in a mesh cage and cooled to liquid nitrogen temperature. The n^+-layer of the detector was electrically connected to the aluminum box and a teflon-coated wire connected the box with the

high voltage terminal. Onto the p-layer of the detector a needle was pushed by a spring, and this needle was connected to one pin of the 7 pin hermetic seal. This one pin was connected to the FET gate in the preamplifier. The stray capacitance between the pin and the ground was 5 pF and between the high voltage terminal and the ground 60 pF.

A copper-constantan thermocouple was fastened to the top end of the aluminum box and gave a temperature less than 85 ^{o}K. It took 15 min. to reach 77 ^{o}K after liquid nitrogen was fulled.

The consumption of liquid nitrogen was 4 l/day and holding time of 17 l liquid nitrogen was 4 days. The boiling of liquid nitrogen could be heard by ear, but the noise due to boiling was not observed.

6.3 Coaxial Ge(Li) Detector Fabrication

Since the outer diameter of the cryostat was limited to 50 mm, the diameter of Ge(Li) detector was decided to be 38 mm. A crystal was bought from Hoboken*. The crystal was No. 132 in List B Czochralski pulled-gallium doped-111 orientation (6 July, 1973). The characteristics of the crystal are as follows: diameter 41.6 ~ 42.0 mm, length 5.6 cm, weight 421 g, resistivity 19.6 ~ 29.5 cm, EPD 1800 ~ 2900 cm^{-2}, carrier lifetime 860 sec, etch pit uniformity xx, Li drift mobility xxx, rating xxx.

The crystal arrived on 23 August. The crystal surface was lapped and shaped to 41.3 mm diameter and 56.2 mm length. Lithium diffusion was made at 420 ^{o}C in vacuum for 8 min. and gave 1 mm thick n^{+} layer.

* Mettallurgie Hoboken, Hoboken, Belgium

Lithium drift was made in n-pentane. The drift continued by applying 200 ~ 400 V (~ 500 mA) for 35 days during 30 August and 3 October. The diameter of p^+-layer was found to be 13.5 ~ 14.0 mm from the result of copper-staining. The detector was kept in dry ice until the cryostat manufacturing completed.

On 9 November, the detector was taken out from dry ice, shaped to 38 mm diameter and 46 mm length and Li diffused. Lithium drift was again made during 9 November and 14 November in n-pentane. The leakage current was 200 mA at 300 V. Drift was continued at 20 mA 200 V around at room temperature during 14 and 19 November.

The crystal was put into the cryostat and clean-up procedure was performed two or three times and completed on 22 November. One of the reasons that two or three times clean-up procedures were needed was a contamination of the i-layer surface due to electric discharge caused by applied voltage at lower vacuum.

6.4 Spectrometer Performance

Leakage current and capacitance vs. applied voltage characteristics of the detector are shown in Figs. 6-7 and 6-8. The leakage current and capacitance at 1000 V were 1.0×10^{-10} A and 31 pF, respectively. This capacitance included 5 pF of stray capacitance of wiring and hermetic seal. Therefore, the capacitance of the detector itself became 26 pF. The dimensions of the detector estimated from the copper-staining are shown in Fig. 6-9 and the calculated capacitance became 29.6 pF. The detecting volume of the detector (i-region volume) was calculated ad 40.6 cm^3 from the dimensions shown in Fig. 6-9.

The gamma-ray detection characteristics of the detector

were measured using the electronics shown in Fig. 6-10. The total absorption peak detection efficiency, energy resolution, peak/compton ratio were measured by placing standard sources at 25 cm in front of the detector. The results are shown in Figs. 6-11, 12, and 13. The absolute peak detection efficiency was 6.9×10^{-5} for 1332 keV gamma-rays at 1200 V applied voltage. It corresponds to 5.75% of the detection efficiency (1.2×10^{-3}) of 3" x 3" NaI (Tl) scintillation detector. FWHM energy resolution was 2.6 keV. The peak/compton ratio was 45:1. Detection efficiencies decreased as gamma-ray energies decreased below 150 keV. This was caused by the absorption due to the aluminum cap (1 mm thick) and aluminum foil.

When the Ge(Li) detector was placed in the precipitator system, the distance between the front face of the detector and the wire center was 25.75 mm as shown in Fig. 6-14. The gamma-rays from the wire pass through the scintillator of 3.97 mm inner and 6.35 mm outer diameters (tetrobutadien + torphenyl), surrounding light guide made of pyrex glass (minimum thickness 10.92 mm), and the aluminum cap (1 mm thick) and entered into the Ge(Li) detector.

6.5 Measurement of Precipitator Wire Gamma-Ray Spectrum

The photomultiplier tube was taken out and the Ge(Li) detector was placed to measure gamma-rays from the wire. Preliminary experiments were made on 22 and 23 November in the ninth sodium circulation experiment and regular experiments on 13 and 14 December in the tenth experiment.

At 11:00 on 22 November, the Ge(Li) detector was placed in the precipitator and energy calibration was performed using

^{57}Co, ^{137}Cs, and ^{60}Co. The wire gamma-ray measurement started at 13:00. The cover gas pressure was 100 mmHg, flow rate 100 cm^3/min., purge gas flow rate 50 cm^3/min., soak/count time 2 min., chamber voltage 500 V. The gamma-ray spectrum was measured for 30 min. At 15:30, the chamber voltage -500 V was applied to prevent adhesion of fission products onto the wire and, after the fission products decayed, gamma-ray background was measured for 30 min. at 16:20. From these measurements, ^{88}Rb (most strongest), ^{85m}Kr, ^{87}Kr, and ^{88}Kr were detected for a cover gas flow rate of 100 cm^3/min. At 18:08, the cover gas flow rate increased to 500 cm^3/min. At 19:30, the precipitator was operated at soak/count time 1 min. and a chamber voltage of 500 V and gamma-rays from the wire was measured. At 20:50, the soak/count time was changed to 30 sec., and gamma-rays from the wire were detected for 30 min. to measure counting rate change dependence on soak/count time. At 22:47, the chamber voltage was changed to -500 V and, after the wire gamma-rays decayed, the background gamma-rays were measured for 30 min. at 00:20 on 23 November. From these measurements at a cover gas flow rate of 500 cm^3/min., ^{85m}Kr, ^{87}Kr, ^{88}Kr, ^{88}Rb, and ^{138}Cs were detected and ^{88}Rb and ^{138}Cs were much stronger.

In the 10th circulation experiment, the measurement was performed as follows: on 13 December, the gamma-ray background was measured at chamber voltage -500 V, cover gas flow rate 500 cm^3/min., purge gas flow rate 125 cm^3/min. without moving the wire before the reactor start-up. The reactor started up at 19:09, and started to increase at 19:26, and

reached 10 MW at 19:34. Gamma-rays were measured for 1000 sec. at 19:26. Since the travel time of cover gas from the expansion tank to the precipitator was about 20 min. as shown in Section 5.8 and Fig. 5-12 of JAERI-memo 5287[4], the gamma-ray spectrum measured for 1000 sec. at 19:26 showed the background for 10 MW reactor operation. Gamma-rays of 1293 keV from ^{41}Ar were strongly measured.

The background was measured for 1000 sec. without moving the wire at 23:11 after the gamma-ray counting rate increased to a constant value. The pulse height distribution as shown in Fig. 6-15(A) was obtained. Since, in this measurement, the wire was not driven at all, the background had to be obtained. At 00:23 on 14 December, the gamma-ray pulse height distribution, as shown in Fig. 6-15(B), was obtained for 1000 sec. counting at soak time 1 min. with 500 V chamber voltage. When compared (A) and (B) of Fig. 6-15, both exhibited ^{85m}Kr, ^{87}Kr, ^{88}K, ^{88}Rb, ^{128}Xe, and ^{178}Cs, but their peak counting rates were different.

Counting rate dependence on soak/count time was measured by changing soak/count time as 38 sec., 23 sec. with 500 V chamber voltage. Then, chamber voltage was changed from 10 V to 1000 V with a constant soak/count time of 23 sec. and counting rate dependence on chamber voltage had been measured during 01:20 and 03:20.

The decay of gamma-ray spectra from the wire was measured for 200 sec. at 30 min. or 60 min. intervals during 03:47 and 05:47 after the wire had stopped and the halflife of each peak was induced.

At 03:50, the cover gas flow rate was changed from 500 cm^3/min. to 200 cm^3/min. and the purge gas flowed at 125 cm^3/min. At 07:05, 1000 sec. measurement at chamber voltage 500 V was made by varying soak/count time as 1 min., 2 min., 3 min., and the peak counting rate dependence on soak/count time was investigated. The measurement finished at 08:20.

The results of gamma-ray peak counting rates were calculated and will be explained in order of halflife measurement of the gamma-ray peak counting rate, dependence on soak/count time, and dependence on chamber voltage.

The results of decay measurement of each peak for the stopped wire are shown in Fig. 6-16. Gamma-ray peak of ^{138}Cs decayed following 32.2 min. Gamma-ray peak of ^{88}Rb decayed initially following 17.8 min. halflife. Gamma-ray peak of ^{88}Kr (halflife 2.8 hr) did not decay. This means that ^{88}Kr gamma-rays did not come from the wire and come from the background.

Another experiment showing ^{88}Kr background is the measurement of the gamma-ray peak counting rate dependence on soak time. As explained in Section 5.6 of JAERI-memo 5287 (May, 1973)[4], the counting rate is proportional to soak time when the radioactivities from the wire is being measured whereas it does not depend on soak/count time when the radioactivities of the background is being measured. Fig. 6-17 shows the gamma-ray peak counting rate dependence on soak/count time measured at 200 cm^3/min. cover gas flow rate with 500 V chamber voltage: the counting rates of ^{88}Rb, ^{138}Cs were proportional to soak time whereas ^{88}Kr did not depend on soak time. Therefore, it can be said that ^{88}Kr came from the background.

The collection efficiency of Rb^+ and Cs^+ ions will change when the precipitation chamber voltage changes. Beta-ray count dependence on chamber voltage was described in Section 5.4 and Fig. 5-3 of JAERI-memo 5287[4]. From gamma-ray peak counting rate measurement, ^{88}Rb and ^{138}Cs can be separated and the measurement of the collection characteristics of Rb and Cs ion on the wire becomes possible. It is an interesting study to investigate collection characteristics of each ion separately. Fig. 6-18 shows gamma-ray peak counting rate dependence or chamber voltage for ^{88}Rb and ^{138}Cs. When compared with the results shown in Fig. 5-3 of JAERI-memo 5287[4], it is different that the gamma-ray counting rate did not decrease at 10 V chamber voltage. This was caused by strong background, i.e., insufficient gamma-ray shielding between the Ge(Li) detector and the storage drum on which the wire was wound, as shown in Fig. 6-5, and in sufficient shielding of gamma-rays from the upper part of the cryostat gave strong and varying background and made the correction difficult. Therefore, attention should be paid on gamma-ray shielding around the Ge(Li) detector when designing the wire gamma-ray spectrometer. Especially, the distance between the detector and the drum should be large and a sufficient shielding should be added. In this respect, background will decreased in gamma-ray measuring port shown in Fig. 6-3 because the distance between the drum and the detector is large.

It is confirmed that only ^{88}Rb (halflife 17.8 min.) could be detected from the decay measurement of beta-ray counting rate of the stopped wire for cover gas flow rate 200 cm^3/min. (Fig. 5-6, JAERI-memo 5287[4]). From the gamma-ray spectrum measurement

using Ge(Li) detector, ^{138}Cs as well as ^{88}Rb were observed as shown in Fig.6-17. For examples, gamma-ray peak counting rate of 989 keV of ^{88}Rb was 243 cps and 463 keV gamma-ray peak of 463 keV of ^{138}Cs gave 0.72 cps at 1 min. soak time. The gamma-ray branching ratio of 893 keV in ^{88}Rb and of 463 keV in ^{138}Cs are 0.13 and 0.23, respectively and the gamma-ray detection efficiencies were 1×10^{-4} and 1.9×10^{-4} at 25 cm source-to-detector distance from Fig. 6-11. If one assumes that the detection efficiency ratio does not change for distances of 25 cm and 2.575 cm (Fig. 6-14). The ratio of the amounts of ^{88}Rb and ^{138}Cs becomes

$$\frac{24.3 \times 0.23 \times 1.9 \times 10^{-4}}{0.13 \times 0.72 \times 1 \times 10^{-4}} = 113.7$$

While only ^{88}Rb was detected by the beta-ray scintillator, ^{138}Cs as well as ^{88}Rb were detected by the Ge(Li) detector. It can be said that the ability of identifying nuclides is higher at gamma-ray spectrometry than at beta-ray measurement.

The ratio of the amounts of ^{88}Rb to ^{138}Cs adhered on the wire at 500 cm^3/min. cover gas flow rate and 1 min. soak/count time can be calculated using the results of the gamma-ray peak counting rate measurement and it becomes

$$\frac{32.9 \times 0.23 \times 1.9 \times 10^{-4}}{0.13 \times 18.52 \times 1 \times 10^{-4}} = 5.97$$

If one calculates this ratio from the decay measurement of beta-ray counting rate measured at 500 cm^3/min. flow rate and 30 sec. soak/count time (see Fig. 5-12), this becomes

$$\frac{4 \times 10^4 \text{ cps}}{1.5 \times 10^3 \text{ cps}} = 26$$

This value 26 is 4.4 times as large as 5.97. The origin

of this difference is not known: It is also not decided whether this values were actually different at the times of gamma-ray spectrometry (14 December, 1973) and beta-ray measurement (28 June, 1973). It is necessary to measure beta-rays and gamma-rays at the same time in order to make this situation clear.

6.6 Detection Sensitivity, S/N ratio, and Minimum Detectable Area of Uranium-Plates of Precipitator Wire Gamma-Ray Spectrometer

The detection efficiency, S/N ratio, and minimum detectable area of uranium plates of the delayed neutron monitor and of the precipitator were given in Sections 4.13 and 5.9 of JAERI-memo 5287[4]. Let calculate these values of the precipitator-wire gamma-ray spectrometer.

The results of gamma-ray peak counting rates of ^{88}Rb and ^{138}Cs for cover gas flow rates 500 cm^3/min. (Fig. 6-15, 1000 sec. counting at 01:23 on 14 December, 1973) and 200 cm^3/min. (at 07:05 on 14 December 1973) were used. The reactor was operated at 10 MW and the SIL was under stationary operation. The chamber voltage was 500 V, purge gas flow rate 125 cm^3/min., soak time 1 min., counting time 1000 sec. As the background counting rate measured by the precipitator wire gamma-ray spectrometer at 10 MW reactor operation and stationary SIL operation, the results obtained at the time when fission products in cover gas did not reach the precipitator chamber yet was used: i.e., background gamma-rays as shown in Fig. 6-19 measured for 1000 sec. at 19:50 on 13 December, 1973 was used. Gamma-rays of 1274 keV from ^{41}Ar were strong at 10 MW reactor

operation. In the figure, the peak at 262 keV can not be identified. The background at 200 cm^3/min. flow rate is thought to be the same as that at 500 cm^3/min. when considered the character of the background. Table 5-1 shows the results.

The detection sensitivity of the precipitator gamma-ray spectrometer was defined as

$$\frac{\text{gamma-ray peuk counting rate(cps)}}{\text{uranium plate area}(cm^2) \times \text{reactor power(MW)}}$$

and S/N ratio as

$$\frac{\text{gamma-ray peuk counting rute(cps)-background(cps)}}{\text{backgrund(cps)}}$$

The minimum detectable area of uranium plates was defined as

$$\frac{\text{uranium plate area}(cm^2)}{\text{S/N ratio}}$$

From the experimental results shown in Table 5-1, 1836 keV gamma-ray peak of ^{88}Rb has the highest detection sensitivity and S/N ratio: They are 0.38 cps/cm^2.MW and 2.2×10^4 for 200 cm^3/min. cover gas flow rate. The minimum detectable area becomes 2.6×10^{-3} cm^2. Since there is ^{41}Ar background, the S/N ratios for gamma-ray energies less than 1274 keV can not become high.

It is not easy to compare these values obtained by the precipitator wire gamma-ray spectrometer with those by the delayed neutron monitor and by the precipitator. The former results used the data taken in the tenth circulation experiment whereas the latter two results used the data taken in the second experiment. The former results gave about five times as large as the latter results.

7. Detection Sensitivity, S/N-Ratio, and Minimum Detectable Area of Uranium Plates of Gas Reservoir Gamma-Ray Spectrometer

As described in Section 5.8 of JAERI-memo 5287[4], the cover gas gamma-ray spectrometer (see Section 2.5 of this report) is confirmed to be very effective way of determing the amount of fission products in cover gas, and useful to explain the precipitator characteristics. The delayed neutron counting rate became 7500 cps in the fourth sodium circulation experiment and the fission products in cover gas became too strong. The counting rate exceeded 20 kcps and this increased the effective leakage current to shift the operating point of the first FET, thus, the preamplifier output pulses disappeared. It was necessary to decrease the volume of cover gas reservoir in order to reduce gamma-ray counting rates, but the reconstruction of the gas reservoir was not actually made. Therefore, the cover gas gamma-ray spectrometer was not used after the fourth circulation experiment.

Let calculate the detection efficiency, S/N ratio, and minimum detectable area of uranium plates for the gas reservoir gamma-ray spectrometer.

Fig. 7-1(A) shows the gamma-ray pulse height distribution of fission products in cover gas in the gas reservoir obtained by the gas reservoir gamma-ray spectrometer. The counting time was 500 sec. The reactor was operated at 10 MW, the SIL was under stationary operation: Sodium temperatures of the irradiation section and the expansion tank were 500 °C and 350 °C. Sodium flow rate was 3 l/min. Cover gas flow rate was 500 cm^3/min. The gamma-rays from ^{85m}Kr, ^{87}Kr, ^{88}Kr, ^{135}Xe,

^{138}Xe, ^{88}Rb, and ^{138}Cs, were observed.

The pulse height distribution shown in Fig. 7-1(B) was taken at the time when the fission products in cover gas did not reach to the gas reservoir at 10 MW reactor operation and showed the back ground gamma-ray spectra: ^{137}Cs, ^{65}Zn, ^{60}Co, ^{40}K, and ^{41}Ar were detected. Using these peak counting rates, the detection sensitivity, S/N ratio, and minimum detectable area of uranium plates were calculated as shown in Table 7-1.

The detection sensitivity is given by

$$\frac{\text{gamma-ray peak counting rate (cps)}}{\text{uranium plate area (cm}^2\text{) x reactor output (MW)}}$$

and S/N ratio by

$$\frac{\text{gamma-ray peak counting rate (cps) - background (cps)}}{\text{back ground (cps)}}$$

The minimum detectable area of uranium plates is given by

$$\frac{\text{uranium plate area (cm}^2\text{)}}{\text{S/N ratio}}$$

As shown in Table 7-1, 2392 keV gamma-ray peak gave the highest S/N ratio which was 2.9×10^4 for cover gas flow rate 200 cm^3/min. The detection sensitivity and minimum detectable uranium plate area for this gamma-ray were 0.21 $cps/cm^2.MW$ and 1.9×10^{-3} cm^2, respectively. As shown in Fig. 7-1(B), the background had gamma-rays low than 1460 keV of ^{40}K. Therefore, large S/N ratio can be obtained by measuring gamma-lays of higher energy than 1460 keV.

Gamma-rays 249.8 keV from ^{135}Xe gave the maximum peak counting rate and the detection sensitivity was 2.4 cps/cm^2.MW at 200 cm^3/min. cover gas flow rate. Since ^{135}Xe has 9.2 hr halflife, ^{135}Xe did not appear at the reactor start-up and appeared 10 hr later.

8. Concluding Summary

In this contract period (4 May, 1973 ~ 30 April, 1974), the sodium in-pile loop had been operated in the fifth to the tenth sodium circulation experiments. The time schedule was as shown in Fig. 3-2 and the total sodium circulation time became 1673 hr 51 min. The total sodium circulation time became 2739 hr 51 min. if we calculated it from the first to the tenth experiments. In this long period, the SIL had been operated without any severe accident or technical trouble. JRR-2 operation has been stopped since January, 1974 to repair the heavy water leaking. As the result, the SIL operation has been also postponed. The irradiation section was cut and disassembled in April 1974 and the metallic uranium plates loaded as fuels will be taken out and the burn up measurement as well as the surface roughness observation are planed in Hot Laboratory of JAERI.

When JRR-2 starts operation after one and a half years, the SIL experiment will restart with uranium oxide in the irradiation section.

The experimental results obtained by the delayed neutron detection system in the fifth to the tenth sodium circulation experiments are as follows:

1) The delayed neutron detection system had been operated without any trouble except high voltage leak of BF_3 counters during the fifth and the tenth sodium circulation experiments. The leakage of high voltage occurred at the connection part between the counter and the preamplifier due to high temperature and humidity. A voltage of 3200 V was applied on BF_3 counters. This trouble could be repaired by performing appropriate procedures.

It is necessary to develop high sensitivity neutron detectors able to operate at low applied voltages as well as to prevent high voltage leaking.

2) The delayed neutron counting rate increased from 6500 cps to 12000 cps gradually during the fifth and the tenth circulation experiments. This is considered as a result of increase in the effective surface area of metallic uranium. The observation of roughness of the metallic uranium surface will be performed at the Hot Laboratory.

3) The neutron detection efficiency measurement of the delayed neutron detection system using a RaD-Be neutron source (9 mCi) gave 1.2×10^{-4} count/n. Whereas neutron energy of the RaD-Be source is about 4MeV, energies of delayed neutrons are 250 to 600 keV. Therefore, the detection efficiency of delayed neutrons is expected to become several times larger than 1.2×10^{-4} count/n. It is necessary to measure the detection efficiency of delayed neutrons or to make Monte Carlo calculation.

4) The delayed neutron counting rate did not change as the cold trap temperature changed from 200 °C to 250 °C.

5) The delayed neutron counting rate did change as the sodium flow rate in the purifier system changed. This was caused by the sodium staying time change in the expansion tank.

6) Decay of the delayed neutron counting rate was measured after a sudden stop of sodium circulation by cutting off the electromagnetic pump power and the decay curve was decomposed into the first and the second groups of delayed neutrons.

From this result, the number of fissions released from metallic

uranium and release fraction of fission products from metallic uranium to sodium had been calculated. The release fraction became 12.6% to 15.0% if one assumes 10 W as the heat generation of metallic uranium. This value is about seven times as large as that calculated from the gamma-ray spectrum measurement made by Y. Yamazaki, et al.[6], 1.5 to 2.0%. One of the explanation of this large difference is that the delayed neutron detection efficiency, 1.2×10^{-4} count/n, used in the calculation is for RaD-Be neutron source and the actual delayed neutron detection efficiency should have a value several times as large as 1.2×10^{-4} count/n. Since even the calculation of the release fraction using the data obtained by gamma-ray spectrum measurement is considered to have an error, the actual release fraction measurement should be made from the absolute measurement of the burn-up of metallic uranium.

7) A calculation was made on the rising characteristics of delayed neutron counting rate at the reactor start-up using the actual increase of reactor neutron counting rate. The result of the calculation almost coincided with the measurement.

8) The counting rates of the delayed neutron detection system were measured by using various types of neutron detectors.

The experimental results obtained by the procipitator during the fifth and the tenth sodium circulation experiments are as follows:

1) The precipitator was operated without any trouble during the fifth and the tenth circulation experiments. On 14 December, 1973, nearly the end of the tenth sodium circulation experiment, output signals from the photomultiplier disappeared due to a failure of the main amplifier circuit of the precipitator. The

first stage transistor was found to burn out and was replaced by a new equivalent transistor (This replacement was made by Tatsuo Miyazawa, et al., of the Toshiba R & D Center). The total operation time of the precipitator was longer than 2739 hr 18 min., the total sodium circulation time during the first and the tenth circulation experiments.

2) The precipitator and its associated electronics moved to the Toshiba R & D Center on 29 January, 1974 after the 10th sodium circulation experiment terminated. The precipitator will be used in the experimental fast breeder reactor "JOYO" as an actual fuel failure detection system in Oarai Engineering Center, PNC, after it is connected to a new electronics system designed by the Toshiba R & D Center.

3) From the results of the measurement made on the leakage current vs. applied voltage characteristics of the precipitation chamber, it was found that no worsening of insulation due to sodium vapor adhesion was observed during the first and the tenth circulation experiments. The amount of sodium adhered on the inside of the precipitator was found to be 0.655 g by atomic absorption spectrometry.

4) Energy calibration of the pulse height distribution of beta-rays from the precipitator wire was made using a ^{90}Sr source. Pulses corresponding to beta-rays above 32 keV were found to be counted when 1350 V was applied on the photomultiplier.

5) Dependence of the precipitator counting rate on chamber voltages from -500 V to +500V was investigated. The nuclides adhered on the wire at -500 V to +500 V chamber voltages were found to be ^{88}Rb for a cover gas flow rate of 200 cm^3/min.

The counts obtained at -500 V and 0 V were 1/300 and 1/22.2 of the counts obtained at +500 V.

6) At a cover gas flow rate of 500 cm^3/min., the nuclides adhered on the wire were ^{138}Cs as well as ^{88}Rb.

7) The result of investigation of the background counting rate of the precipitator showed that the background increased when cover gas was introduced into the precipitation chamber. This was caused by the gamma-rays from the radioactive nuclides in cover gas which passed through the shielding and the wire-driving-hole and were detected by the scintillator.

8) A background counting rate, 0.7 cps was observed when the reactor was not in operation.

9) The count of the precipitator increased slightly at a purge gas flow rate of 12.5 cm^3/min. when it was measured at 200 cm^3/min. cover gas flow rate by varying the purge gas flow rate from 12.5 to 125 cm^3/min. This may be caused by the scintillator contamination. It is more safer to flow purge gas more than 25 cm^3/min.

10) The result of investigation of the response characteristics of the precipitator count at the reactor start-up showed that the time when the precipitator count started to increase delayed from the reactor start-up and its delays were about 90 min. and 35 min. for the cover gas flow rates of 200 cm^3/min. and 500 cm^3/min., respectively. These values were about two times as large as the values calculated from the volume of the cover gas circuit divided by the cover gas flow rate.

11) The effect of the cold trap temperature in the purifier system on the precipitator counting rate was not observed.

12) The precipitator counting rate increased as the delayed neutron

counting rate increased.

The experimental results obtained by the precipitator wire gamma-ray spectrometer are as follows:

1) A 41 cm^3 coaxial Ge(Li) detector (outer diameter 36.5 mm, length 45.5 mm, p^+-core diameter 9.0 mm) was made and mounted into a cryostat. For 1333 keV gamma-rays, energy resolution was 2.6 keV: the peak detection efficiency was 5.75% of that of 3" x 3" NaI(Tl) detector at a source to detector distance of 25 cm.

2) This Ge(Li) detector was placed in a hole for the photomultiplier of the precipitator and detected gamma-rays from the nuclides adhered on the wire. The distance between the front face of the detector and the wire axis was 25.57 mm.

Gamma-ray spectra of ^{88}Rb and ^{138}Cs which adhered on the wire had been measured. At the same time, ^{85m}Kr, ^{87}Kr, and ^{88}Kr gamma-rays had been measured as background.

3) From the results of the measurement of gamma-ray peak counting rate as a function of soak/count time and chamber voltage, and of the decay measurement, it was found that a complete shielding was necessary between the wire-storing drum and the Ge(Li) detector and also around the detector.

4) The detection sensitivity, S/N ratio, and minimum detectable area of uranium plates of the precipitator wire gamma-ray spectrometer were calculated from the results obtained at cover gas flow rates 500 cm^3/min. and 200 cm^3/min. for soak/count time 1 min. The results are shown in Table 5-1. The detection efficiency, thus S/N ratio, are the highest for 1836 keV gamma-ray peak of ^{88}Rb.

The experimental results obtained by the gas reservoir gamma-ray spectrometer are as follows.

1) The gas reservoir gamma-ray spectrometer was confirmed to be very effective to determine the amount of fission products in cover gas in the second and the third circulation experiments. Gamma-ray counting rate exceeded 20 kcps and too strong to be measured after the 4th sodium circulation experiment. The gas reservoir volume should have been decreased to 1/10, but this reconstruction was not done. The gas reservoir gamma-ray spectrometer had not been used during the fourth and the tenth sodium circulation experiments.

2) The detection efficiency, S/N ratio, and minimum detectable area of uranium plates were calculated for the gas reservoir gamma-ray spectrometer, based on the data obtained in the third sodium circulation experiment. It was found that the detection sensitivities and S/N ratios were high for gamma-ray peaks of 2392 keV and 1836 keV (^{88}Kr), 18361 keV (^{88}Rb), and 249.8 keV (^{135}Xe) measured at 200 cm^3/min. At 500 cm^3/min. cover rays described above showed high detection sensitivities and S/N ratios.

Experiments to be performed in a contract "FFD sodium in-pile loop test", next year, are as follows:

Concerning the delayed neutron detection system, the measurement of delayed neutron counting rate using various neutron detectors of Japanese make, the measurement of delayed neutron counting rate of polyethylene moderator system which replaces the graphite moderator, etc., will be made. Uranium oxide fuels will be used in the

irradiation section.

About the precipitator, characteristics of new precipitators of Japanese make will be measured. These new precipitators have ports for measuring gamma-ray spectra in which Ge(Li) detectors will be fitted.

Above the gas reservoir gamma-ray spectrometer, a gas reservoir of variable volume will be manufactured to handle various counting rates of fission product gamma-rays in cover gas. Also, digital subtract units will be manufactured to count only counting rates of predetermined peaks in gamma-ray spectra.

The SIL experiments will restart in midyear 1975 when JRR-2 starts its operation. Uranium oxide fuels will be loaded and fission product release and transfer will be investigated. These results of the experiments will be compared with those obtained during the first to the tenth experiments using metallic uranium fuels.

Acknowledgement

We would like to express our great appreciation to many people who help us: especially, to Messrs. Tomohide Sukegawa, Hiroshi Taki, Fusao Shiba, Tomotoshi Nishikizawa, Toshiyuki Kuroyanagi, Isao Nihei, Yoshio Fukaya, Takashi Sudo, Isao Sumiya of the SIL operation group, Shunji Honma, Junsaku Tsunoda, and other members of the JRR-2 operation and the Radiation Control Section. Messrs. Tatsuo Miyazawa and Katsumi Kubo of the Toshiba Research and Development Center are gratefully appreciated for their supports on the precipitator maintenance and sodium amount measurement.

References

1) JAERI: Sodium in-pile loop (SIL) operation manual (October 1972) (in Japanese)

2) Yasaburo Yamazaki, Kenmei Hirano, Tomohide Sukegawa, et al.: Out-of-pile test of sodium in-pile loop (SIL), JAERI-memo 5206 (February 1973) (in Japanese)

3) Yasaburo Yamazaki, Kenmei Hirano, Tomohide Sukegawa, et al.: Sodium in-pile loop (SIL) experiment- Progress Report No.1 (April 1971 to March 1972), JAERI memo 5209 (March 1973) (in Japanese)

4) Eiji Sakai, Masaki Katagiri, Kenmei Hirano, and Yasaburo Yamazaki: Performance of fuel failure detection system in sodium in-pile loop experiment (I) - 1st, 2nd, 3rd, and 4th sodium circulation experiments, JAERI memo 5287 (May 1973) (in Japanese)

5) Yasaburo Yamazaki, Kenmei Hirano, Tomohide Sukegawa, et al.: Study on the behavior of fission products in sodium (I) - First, second, third, and fourth sodium circulation experiments, JAERI me
memo 5283 (May 1973) (in Japanese)

6) Yasaburo Yamazaki, Kenmei Hirano, Tomohide Sukegawa, et al.: Study on the behavior of fission products in sodium (II) - the fifth to the tenth sodium circulation experiments, JAERI memo 5694 (April 1974) (in Japanese)

7) Chiyoji Kawaguchi, Eiji Sakai, Hiroshi Gotoh, Hideyuki Yagi, and Masaki Katagiri: A preliminary experiment on the delayed neutron detection system of JFBR, JAERI memo 4137 (March, 1970) (in Japanese)

8) Eiji Sakai, Masaki Katagiri, and Chiyoji Kawaguchi: A study of fuel failure detector - Two-crystal-summing Ge(Li) gamma-ray

spectrometer, JAERI memo 4315 (January 1971) (in Japanese)

9) Isao Fujii, Hisashi Kamei, Tamon Inoue, Tatsuo Miyazawa, and Koichi Onodera: Fuel failure detection system by delayed neutron monitoring - Out-of-pile test of detector-monitor system, J 201 71-24 (September 1971) (in Japanese)

10) The Plessey Co., Ltd.: Technical Handbook for the Burst Can Detector System

11) Hisashi Kamei, Tatsuo Miyazawa, Kiyoshi Kasama, Koichi Onodera, and Katsumi Kubo: Fuel failure detection system by cover gas monitoring - Preliminary test of a charged-wire precipitator, SJ 201 72-25 (August 1972) (in Japanese)

12) Masayoshi Ohno, et al.: The performance test of vapor traps for the experimental fast breeder "JOYO" failed fuel pin detection system, SJ 201 72-37 (November 1972) (in Japanese)

13) Eiji Sakai and Tanemichi Kitahara, ed.: Proceedings of "Fuel Failure Detection" Symposium - January 31, 1969 -, JAERI memo 4157 (October 1970) (in Japanese)

14) Eiko Takekoshi, Hideo Kuroi, and Shinichi Igarashi: Present status of delayed neutron study, Journal of the Atomic Energy Society of Japan, 14, (7), 325 (1972) (in Japanese)

TABLE CAPTIONS

PHOTO CAPTIONS

Photo 2-1 A BF_3-counter extracted from the graphite moderator

Photo 2-2 The graphite moderator with boron-loaded paraffin blocks on the top of Sodium In-pile Loop apparatus

Photo 2-3 Precipitator panel and electronic equipments of precipitator and delayed neutron detector system

Photo 2-4 Precipitator and its panel

Photo 2-5 A Ge(Li) gamma-ray detector system inserted in a collimator looking at a part of the cold trap in Sodium In-pile Loop apparatus

Photo 2-6 Gas reservoir with a lead shield for gamma-ray spectrometry of cover gas

Photo 2-7 A Ge(Li) gamma-ray detector system used in the gamma-ray spectrometry of gas reservoir and electronic equipments for the precipitator and delayed neutron detector

FIGURE CAPTIONS

Table 2-1 Dimensions of enriched uranium plates

Isotropic ratio measured by Goodyear Atomic Corporation,U.S.A.

U-234 0.1 w%, U-235 19.95 w%, U-236 0.13 w%, U-238 79.82 w%

Chemical analysis measured by Furukawa Denki Kogyo KK.

B 0.2ppm, Si 340ppm, Al 20ppm, Fe 220ppm, Mg 100ppm,Mn 20ppm,

Mo 50ppm, Ni≤10ppm, Ag≤0.1ppm, Cd 0.3ppm, C 500ppm

Type	Plate No.	Thickness(mm) 1	2	3	Average	Width(mm) 4	5	6	Average	Length(mm) 7	8	Average	Area(mm^2)	Weight(g)
A	1	0.955	0.965	0.95	0.9567	15.88	15.89	15.865	15.8783	37.51	37.51	37.51		10.43
	2	0.955	o.965	0.965	0.9617	15.875	15.87	15.85	15.8650	37.55	37.57	37.51		10.48
	3	0.970	0.980	0.970	0.9733	15.865	15.87	15.87	15.8683	37.55	37.56	37.555		10.56
	4	0.965	0.970	0.970	0.9683	15.85	15.86	15.89	15.8667	37.595	37.61	37.6025		10.64
					Average 0.9650				Average 15.8696			Average 37.557	Average 1295.1425	Average 10.5275
B	1	0.96	0.98	0.97	0.9700	18.87	18.865	18.86	18.8650	37.57	37.55	37.56		12.38
	2	0.96	0.96	0.955	0.9583	18.85	18.87	18.90	18.8733	37.59	37.60	37.595		12.54
	3	0.98	0.98	0.97	0.9767	18.86	18.88	18.875	18.8717	37.54	37.51	37.525		12.66
	4	0.94	0.975	0.95	0.9550	18.89	18.89	18.87	18.8833	37.62	37.60	37.61		12.34
					Average 0.9650				Average 18.8733			Average 37.5725	Average 1527.1745	Average 12.4800

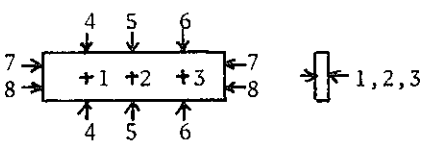

Total exposed area of two sheets of A and two sheets of B

56.446 cm^2

Table 2-2 Calculated sodium travelling time from the end of the fuel plates to the inlet of the expansion tank

Sodium flow rate (l/min)	Sodium travelling time (sec)*
0.5	138
0.75	92.3
1.0	69.2
1.25	55.4
1.5	46.1
1.75	39.5
2.0	34.6
2.25	30.8
2.5	27.7
3.0	23.1
3.5	19.8
4.0	17.3
4.5	15.4
5.0	13.8
5.5	12.6
6.0	11.6

* Calcutation was performed using the following volumes of sodium in various parts.

the end of fuel plates to irradiation section outlet	14.5 cm^3
irradiation section outlet to main cooler inlet	484 cm^3
main cooler	492 cm^3
main cooler outlet to expansion tank inlet	146 cm^3
expansion tank inlet nozzle	16.0 cm^3
total sodium volume	1153 cm^3

Table 2-3 Characteristics of neutron detectors

	20th Century Electronics Ltd BF_3 counter 40EB-50/70G	Mitsubishi Electric Co. Ltd BF_3 counter ND-8537-90	Mitsubishi Electric Co. Ltd BF_3 counter ND-8523-A-60	20th Century Electronics Ltd ^{10}B counter PN12EB
Diameter (mm)	50	25	14	25.4
Overall length (mm)	540	648	172	238
Sensitive length (mm)	400			120
Counting gas	BF_3	BF_3	BF_3	$Ar\text{-}CO_2$
Gas pressure (cmHg)	70	90	60	40
Operating temperature (°C)	100			220
Operating voltage (V)	3200	3000	2150	880
Neutron sensitivity(cps/nv)	73	17	0.32	3.0
Electrode capacitance (pF)	60			

Table 2-4 Operating conditions of delayed neutron detector

Neutron detector	20th Century BF_3 counter 40EB70/50G #4 3200V
Detector position	The lowest position in graphite moderator (Position A, in Fig.2-3)
Preamplifier	JAERI-121A gain x10
Main amplifier	JAERI-156 negative input, coarse gain x 64, fine gain x 3.0, time constant 1.6 usec, bipolar output
Single channel pulse height analyser	input bipolar, integral, discriminator level 4.0
Counting ratemeter	Toyo Denshi BM-700A, positive input, time constant 3sec, range as required
High voltage supply	John Flukes 408B, + 3200V
Pen recorder	YEW-3047, 50mV range, chart speed as required

Table 2-5 Precipitator operating conditions
(The Plessey Co.Ltd., Mark XI)

Cover gas pressure (He)	100mmHg G
Cover gas flow rate (He)	200cm^3/min
Purge gas flow rate (He)	50cm^3/min
Photomultiplier voltage	1.3kV
Precipitator chamber voltage	500V
Soak/count time	as required

Table 2-6 Characteristics of Ge(Li) gamma-ray detector used in gamma-ray spectrometry of gas in the expansion tank

Manufacturer	ORTEC,U.S.A.
Crystal diameter	46.25 mm
Crystal length	38.o mm
Drift length	17.8 mm
Sensitive volume	54.7 cm^3
Capacitance	20.5 pF at 1000V
Fwhm energy resolution	2.1 keV for 1.33 MeV gamma-rays
Peak detection efficiency	9 % relative to 3"x3" NaI(Tl) for 1.33 MeV gamma-rays measured at source-to-detector distance of 25cm.

Table 2-7 Characteristics of Ge(Li) gamma-ray detector used in gamma-ray spectrometry of cover gas in gas reservoir

Fabricated by JAERI	
Crystal diameter	40.5 mm
p^+-core diameter	10.5 mm
n^+-layer thickness	1.o mm
Crystal length	87 mm
Sensitive volume	100 cm^3
Operating voltage	2500 V
Leakage current	1 nA at 2500 V
Detector capacitance	84 pF
Fwhm energy resolution	5.0 keV for 1.33 MeV gamma-rays
Peak detection efficiency	1.37×10^{-4} for 1.33 MeV gamma-rays measured at source-to-detector distance of 25 cm.

Table 3-1 Sodium circulation time during the first to the tenth sodium circulation experiment

Number of sodium circulation experiment	Sodium circulation time in each circulation experiment	Total sodium circulation time
1st	170 hr 52 min	170 hr 52 min
2nd	290 hr 50 min	461 hr 42 min
3rd	303 hr	764 hr 42 min
4th	300 hr 45 min	1065 hr 27 min
5th	306 hr 50 min	1372 hr 17 min
6th	245 hr 3 min	1617 hr 20 min
7th	298 hr 1 min	1915 hr 21 min
8th	271 hr 13 min	2186 hr 34 min
9th	295 hr 23 min	2481 hr 57 min
10th	257 hr 21 min	2739 hr 18 min

Table 3-2 Explanation of symbols related to temperature, flow rate and gas pressure in various parts of Sodium In-pile Loop and their values for stationary operation

Symbol	Explanation	Stationary value
TRCA-1-1	Sodium temperature of irradiation section (°C)	500
TRCA-2-1	Sodium temperature of main cooler outlet (°C)	400
TR-2-2	Sodium temperature of main cooler inlet (°C)	
TRCA-3-1	Sodium temperature of cold trap outlet (°C)	200
TR-3-2	Sodium temperature of cold trap inlet (°C)	
TRCA-4-1	Sodium temperature of reheater outlet (°C)	
TR-6-3	Sodium temperature of the middle part #1 of cold trap (°C)	
TR-6-4	Sodium temperature of the middle part #2 of cold trap (°C)	
TRA-6-5	Sodium temperature of expansion tank (°C)	380
FRCA-1	Main sodium flow rate (l/min)	3.0
FRCA-2	Cold trap flow rate (l/min)	0.5
PI-3	Cover gas pressure in expansion tank (mmHg G)	100

* Values for stationary operation of Sodium In-pile Loop

Table 4-1 Long range increase rate of delayed neutron counting rate

Number of sodium circulation experiment		5th	6th	7th
Sodium flow rate(1/min)		3	3	4
Irradiation section temperature (°C)		500	450	490
Main cooler temperature(°C)		400	400	400
Expansion tank temperature(°C)		350	355	355
Reactor output power(MW)		10	10	10
Delayed neutron counting rate (cps)	1st measurement day	7679	7981	10404
	10 days after	8216	8495	11550*
Delayed neutron counting rate increase in 9 days		1.070	1.064	1.110

* Calculated from the counting rate 10395 cps observed at the reactor power 9 MW.

Table 4-2 Calculated counting rates of delayed neutrons of different half-lives from the observed counting rates decaying after a sudden stop of sodium flow

Sodium flow rate (l/min)	Calculated sodium travelling time from irradiation section to expansion tank (sec)	Delayed neutron counting rate observed before sudden stop of sodium flow(cps)	Counting rate of delayed neutrons of each group (cps)		
			1st group ($T_{1/2}$=57sec)	2nd group (22sec)	3rd group (6.2sec)
4.5	15.4	10010	1010	7600	140
3.0	23.1	7560	960	6600	0
1.5	46.2	4540	840	3700	0
0.5	138.6	868	322	546	0

Table 4-3 Calculation of fission rate and fission product release fraction

	Half-life (sec)	Sodium flow rate		
		4.5 l/min	3.0 l/min	1.5 l/min
Delayed neutron counting rate (cps)	23	7.60×10^3	6.60×10^3	3.70×10^3
	57	1.01×10^3	9.60×10^2	8.40×10^2
Delayed neutrons in sodium at irradiation section (n/sec)	23	1.62×10^8	1.62×10^8	1.57×10^8
	57	2.03×10^7	2.03×10^7	2.03×10^7
Fission rate in sodium at irradiation section (fissions/sec)	23	4.68×10^{10}	4.68×10^{10}	4.54×10^{10}
	57	3.90×10^{10}	3.90×10^{10}	3.90×10^{10}
Release fraction* (%)	23	15.0	15.0	14.6
	57	12.6	12.6	12.6
Ratio of delayed neutrons of 23 sec half-life to 57 sec in sodium at irradiation section		0.125	0.125	0,129

* Total number of fissions in 1 sec was taken as 3.1×10^{11} fissions per sec.

Table 4-4 Comparison of delayed neutron counting rate of various types of neutron counters

Counter type	Manufacturer Model Ser.No.	Bias voltage (V)	Manufacturer's specification neutron sensitivity (cps/n)	(relative)	Delayed neutron counting rate (cps)	(relative)
BF_3 counter	Twentieth Century 40EB70/50G #4	3200	73	1.0	3838	1.0
BF_3 counter	Twentieth Century 40EB70/50G #1	3200	73	1.0	4394	1.145
BF_3 counter	Twentieth Century 40EB70/50G #2	3200	73	1.0	3872	1.009
BF_3 counter	Mitsubishi ND-8523-A60	3150	17	0.232	917	0.239
B^{10} counter	Twentieth Century PN12EB #722	825	3	0.041	241	0.062
B^{10} counter	Twentieth Century PN12EB #691	825	3	0.041	266	0.069
B^{10} counter	Twentieth Century PN12EB #692	825	3	0.041	229	0.073

Table 5-1 Sodium amount deposited on various parts in the precipitation chamber measured by atomic absorption spectrometer*

	Sampled position (See Fig. 5-3)	Sodium amount measured after the first sodium circulation experiment (micrograms)	Sodium amount measured after the tenth sodium circulation experiment (micrograms)
1	Pulley		0.0207
2	High tension plate #1	0.0264	0.0105
3	Insulation plate #1	0.0030	0.0175
4	High tension plate #2	0.0256	0.0341
5	Insulation plate #2	0.0019	0.0102
6	Sample gas inlet and outlet	0.1570	0.1022
7	Inside wall of chamber housing		0.1252
8	Wire storage drums		0.1855
9	Wire	0.1225	0.1855
10	Inside wall of storage drum cover		0.0595
	Total sodium amount	0.3364	0.6550
	Background		0.0040
	Detectable limit		0.0020

* The measurement was performed by Tatsuo Miyazawa,et al.,at Toshiba Research and Development Center.

Table 5-2 Counting rates of delayed neutrons and precipitator and their ratios

Irradiation section temperature 500°C, main cooler 400°C, expansion tank 350°C, sodium flow rate 3 l/min, cover gas 200 cc/min, purge gas 50 cc/min, cover gas pressure 100 mmHg, soak/count time 60 sec.

Number of sodium circulation experiment	2	3	4	5	6	7	8	9	10
Date in 1973	Jan.20	Feb.28	Apr.12	May 29	Jun.21	Aug.10	Oct.2	Nov.23	Dec.11
Delayed neutron counting rate (cps)	1800	2700	7036*1)	7692	7912	10025	10249	10124	13105
Precipitator counting rate (cps)	18000	22960*2)	60994*3)	63660*4)	69984	85214	96366	87239	93725
Precipitator counting rate / Delayed neutron counting rate	10.0	8.5	8.7	8.3	8.8	8.5	9.4	8.7	7.2

*1) Calculated from the counting rate observed at sodium flow rate 4.5 l/min.

*2) at soak/count time 28 sec.

*3) at soak/count time 30 sec.

Table 6-1 Performance of precipitator-wire gamma-ray spectrometer

(Precipitation chamber voltage 500V, soak time 1 min)

Gamma-ray energy (keV)	Nuclide	Abundance	Half life (min)	Counting rate (cps) 500* cc/min	Counting rate (cps) 200** cc/min	Background*** (cps)	Sensitivity (cps/cm^2 MW) 500* cc/min	Sensitivity (cps/cm^2 MW) 200** cc/min	S/N ratio 500* cc/min	S/N ratio 200** cc/min	Minimum detectable area U-plates (cm^2) 500* cc/min	Minimum detectable area U-plates (cm^2) 200** cc/min
463	Cs-138	0.23	32.2	19.1	1.07	0.054	0.34	0.019	350	20	0.16	2.82
898	Rb-88	0.13	17.8	33.7	25.4	0.054	0.60	0.045	630	470	0.09	0.12
1009	Cs-138	0.25	32.2	9.4	0.48	0.029	0.17	0.0085	330	17	0.17	3.32
1426	Cs-138	0.21	32.2	18.0	1.04	0.004	0.32	0.018	4600	270	0.012	0.21
1836	Rb-88	0.73	17.8	28.6	21.5	0.001	0.51	0.38	29000	22000	0.0019	0.0026

* Data was obtained in 1000sec from 1:23 on December 14,1973.

** Data was taken in 1000sec from 7:05 on December 14,1973.

*** Data was measured in 1000sec from 19:50 on December 13,1973. Wire was not driven.

Table 7-1 Performance of gas reservoir gamma-ray spectrometer

Gamma-ray energy (keV)	Nuclide	Abundance	Half life	Counting rate (cps) 500* cc/min	Counting rate (cps) 200** cc/min	Background*** (cps)	Sensitivity ($cps/cm^2 MW$) 500* cc/min	Sensitivity ($cps/cm^2 MW$) 200** cc/min	S/N ratio 500* cc/min	S/N ratio 200** cc/min	Minimum detectable area of U-plates (cm^2) 500* cc/min	Minimum detectable area of U-plates (cm^2) 200** cc/min
151.0	Kr-85m	0.74	4.4hr	275	628	0.21	0.49	1.11	1330	3050	0.042	0.019
196.1	Kr-88	0.378	2.8hr	350	588	0.09	0.62	1.04	3800	6390	0.015	0.0088
249.8	Xe-135	0.91	9.2hr		1338	0.07		2.37		20000		0.0028
402.8	Kr-87	0.84	76min	397	314	0.04	0.70	0.56	9450	7480	0.006	0.0075
434.6	Xe-138	0.545	17min	97.6	2.1	0.05	0.17	0.004	1880	40.4	0.03	1.4
898.0	Rb-88	0.13	17.8min	49.9	94.9	0.02	0.088	0.17	2770	5270	0.02	0.011
1426.0	Cs-138	0.73	32.2min	106	3.9	0.01	0.188	0.007	10600	3900	0.0053	0.14
1836.1	Rb-88	0.21	17.8min	45.0	88.4	0.004	0.08	0.16	11300	22100	0.005	0.0026
2195.9	Kr-88	0.15	2.8hr	23.1	47.1	0.004	0.04	0.083	5780	11800	0.0098	0.0048
2392	Kr-88	0.38	2.8hr	62.5	116	0.004	0.11	0.21	15600	29000	0.0036	0.0019

* Data was taken in 500sec from 14:16 on February 26,1973.

** Data was taken in 500sec from 8:10 on March 2,1973.

*** Data was taken in 500sec from 10:15 on February 26,1973.

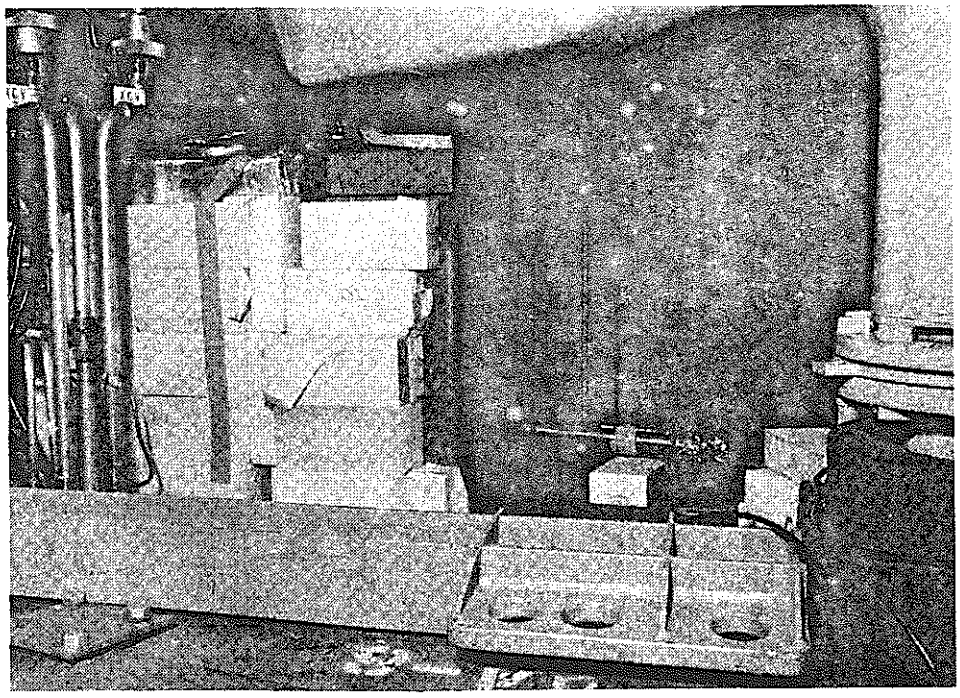

Photo 2—1 A BF_3 counter extracted from the graphite moderator.

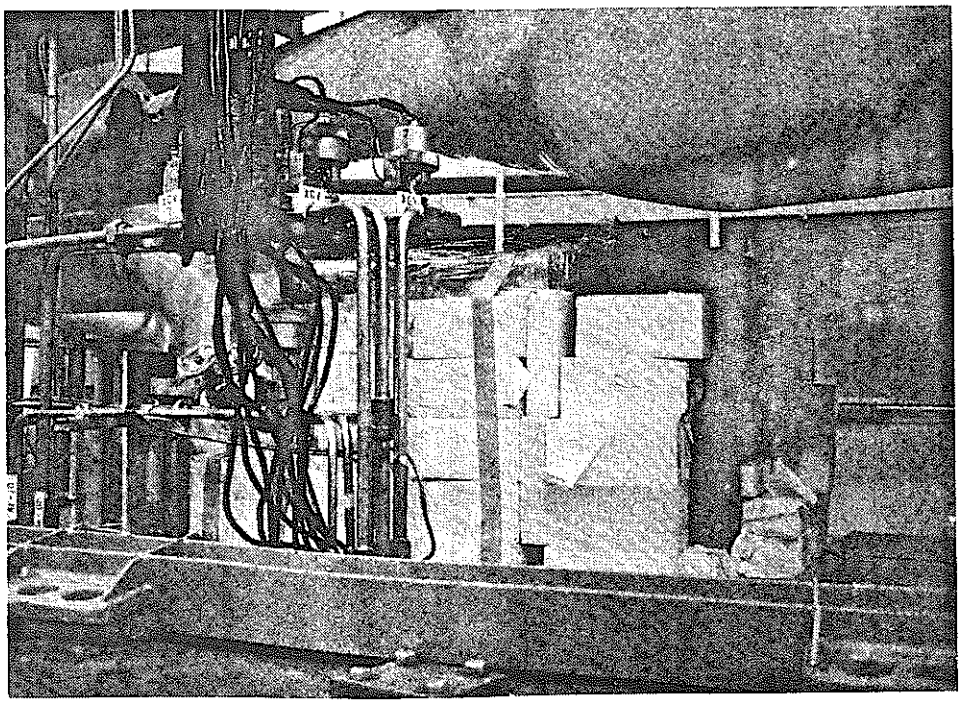

Photo 2—2 The graphite moderator with boron-loaded paraffin blocks on the top of Sodium In-pile Loop apparatus.

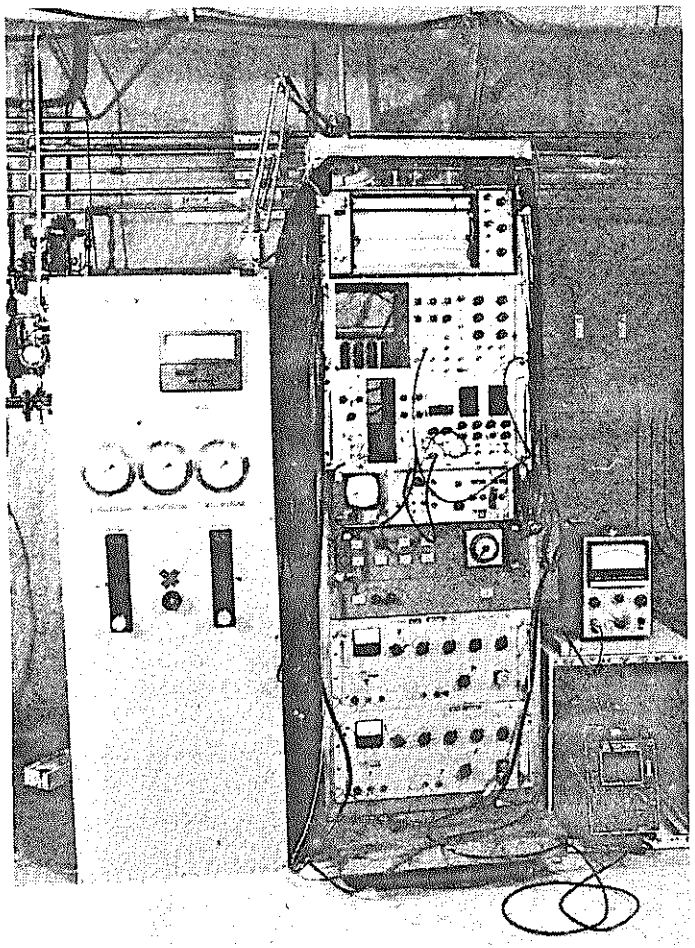

Photo 2－3　Precipitator panel and electronic equipments of precipi- tator and delayed neutron detector system.

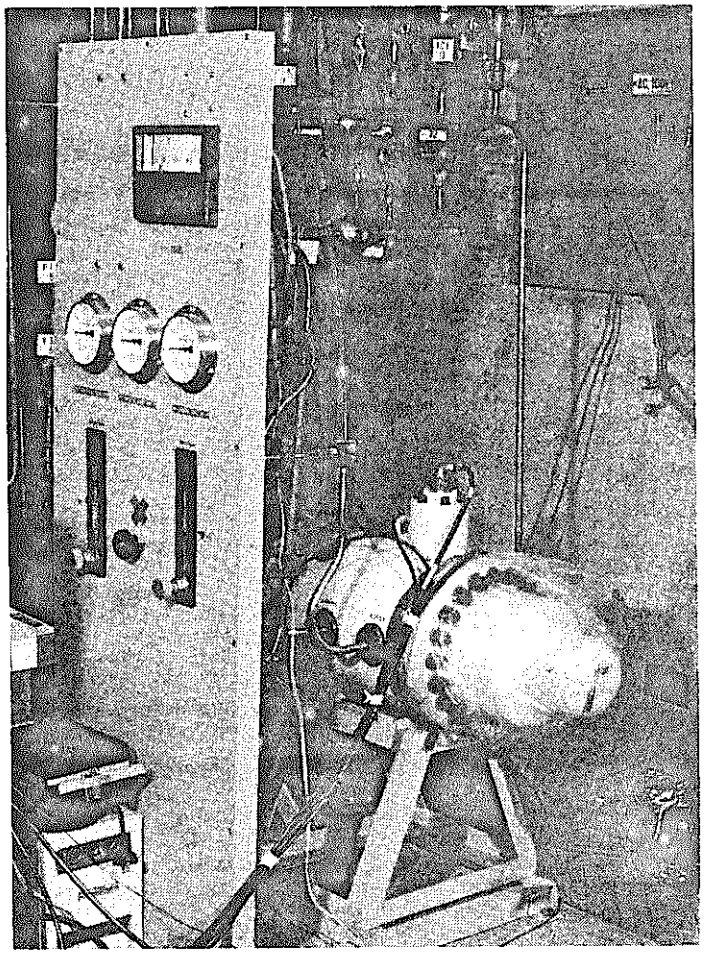

Photo 2－4　Precipitator and precipitator panel.

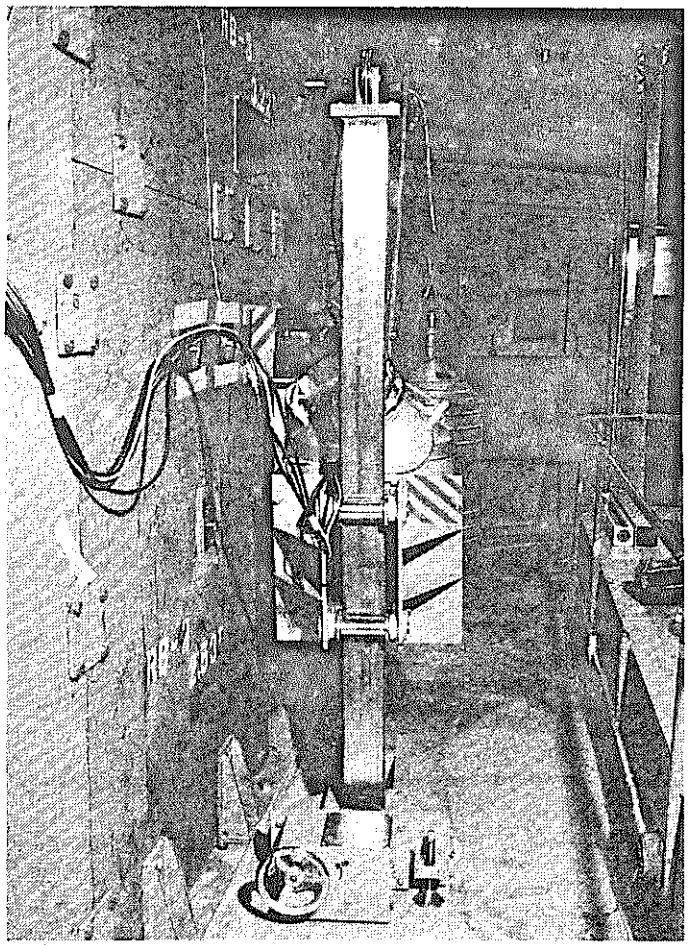

Photo 2−5 A Ge(Li) gamma-ray detector system inserted in a collimator looking at a part of the cold trap in Sodium In-pile Loop apparatus.

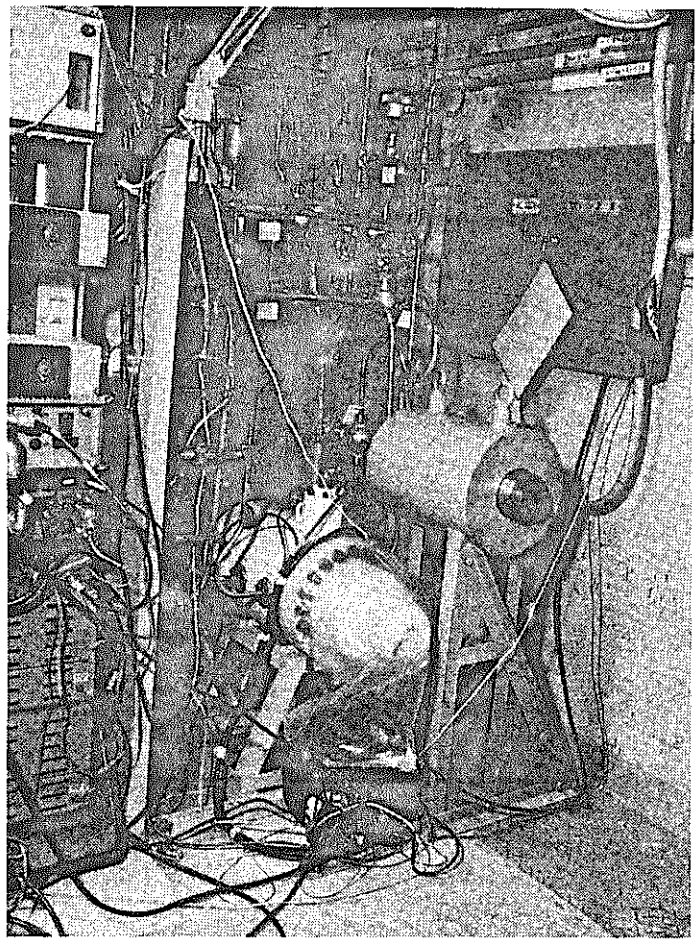

Photo 2−6 Gas reservoir with a lead shield for gamma-ray spectrometry of cover gas.

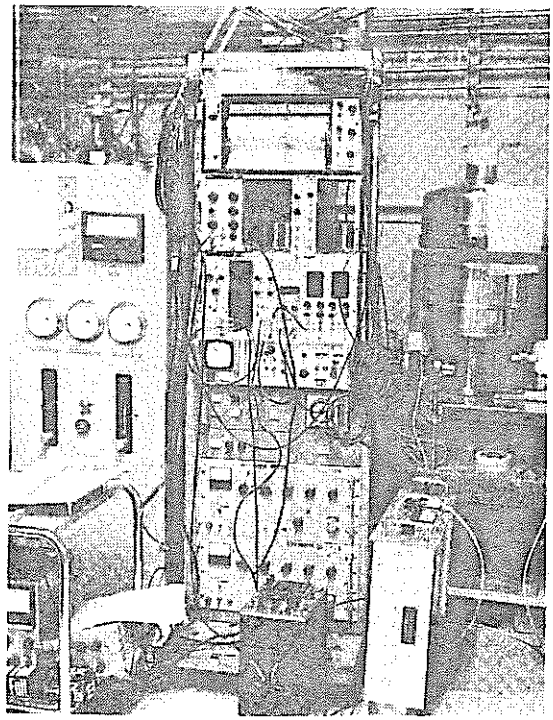

Photo 2—7 A Ge(Li) gamma-ray detector system used in the gamma-ray spectrometry of gas reservoir and electronic equipments for the precipitator and delayed neutron detector.

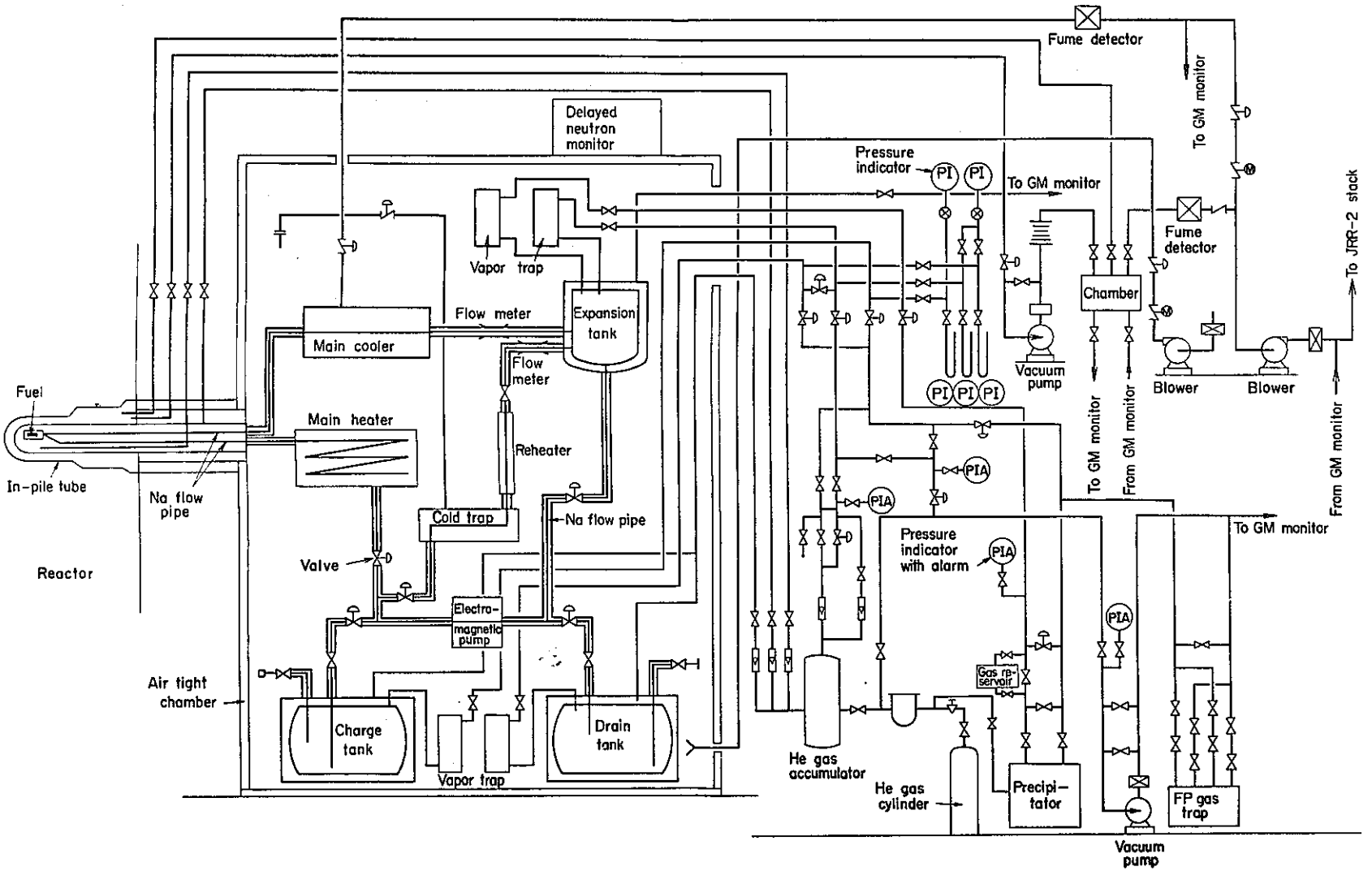

Fig. 2-1 Schematic diagram of Sodium In-pile Loop

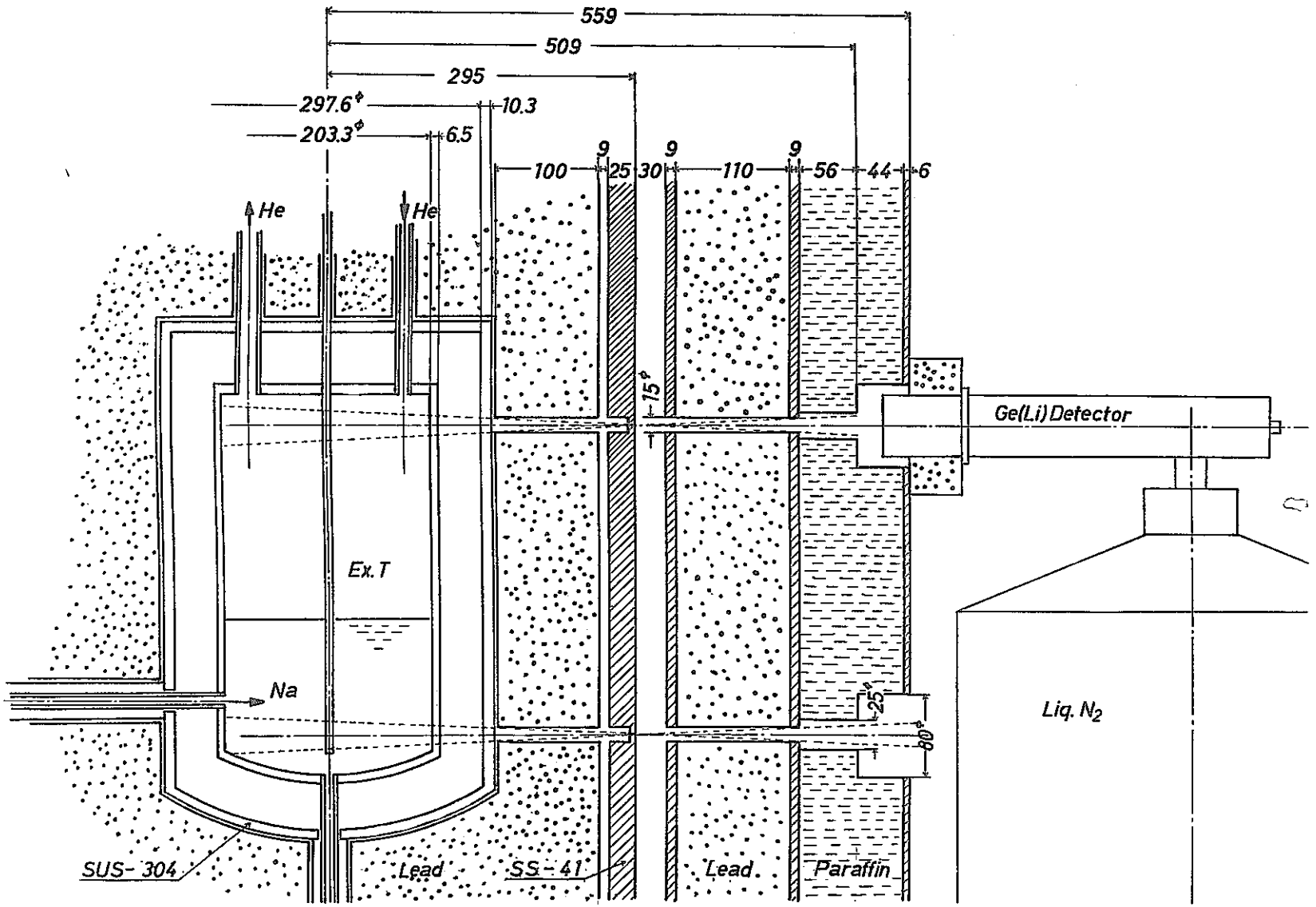

Fig. 2-2 Dimensions of the collimators for measuring gamma-rays from expansion tar

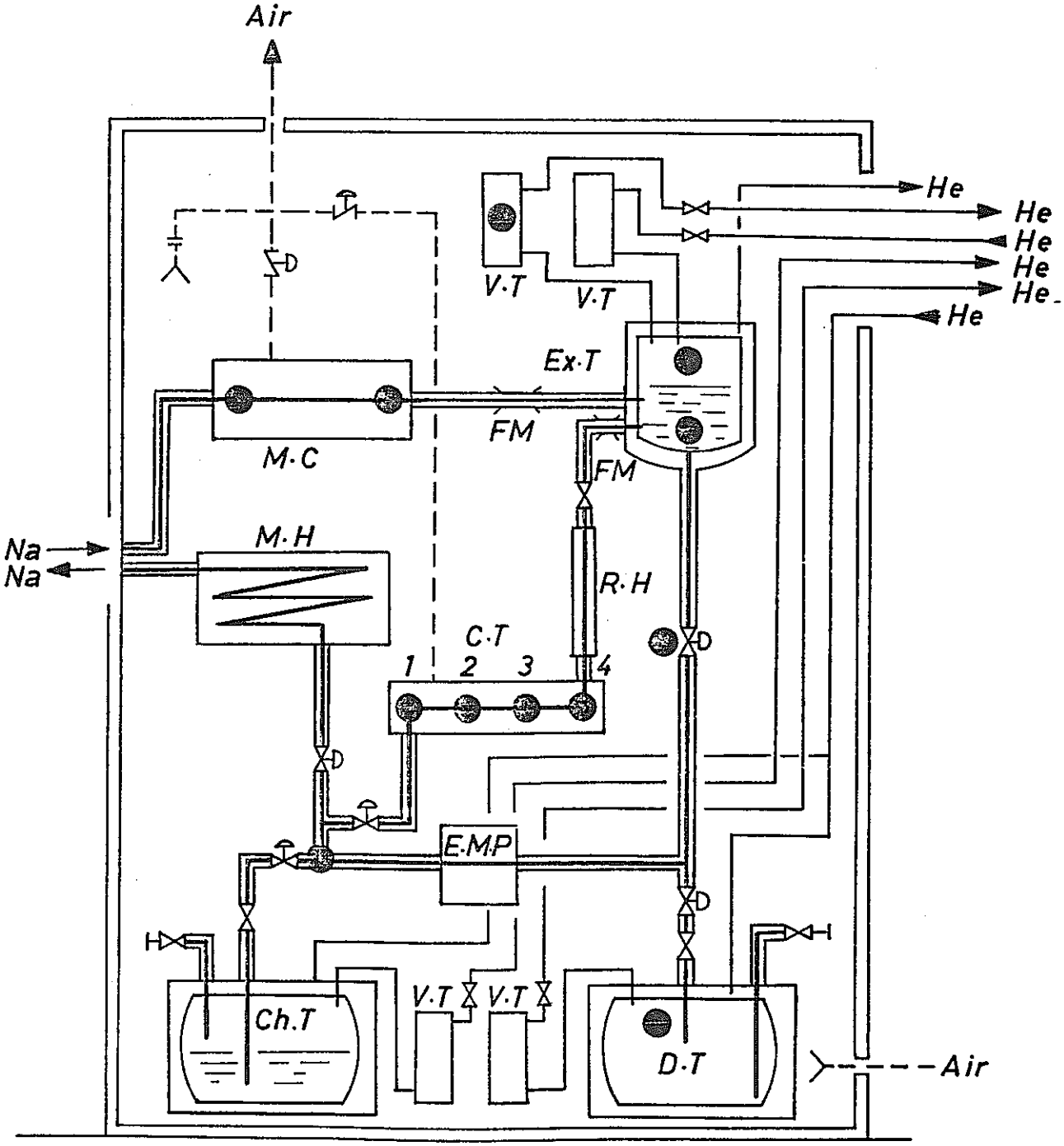

Fig. 2-3 Positions of collimators

(Sodium in-pile loop)

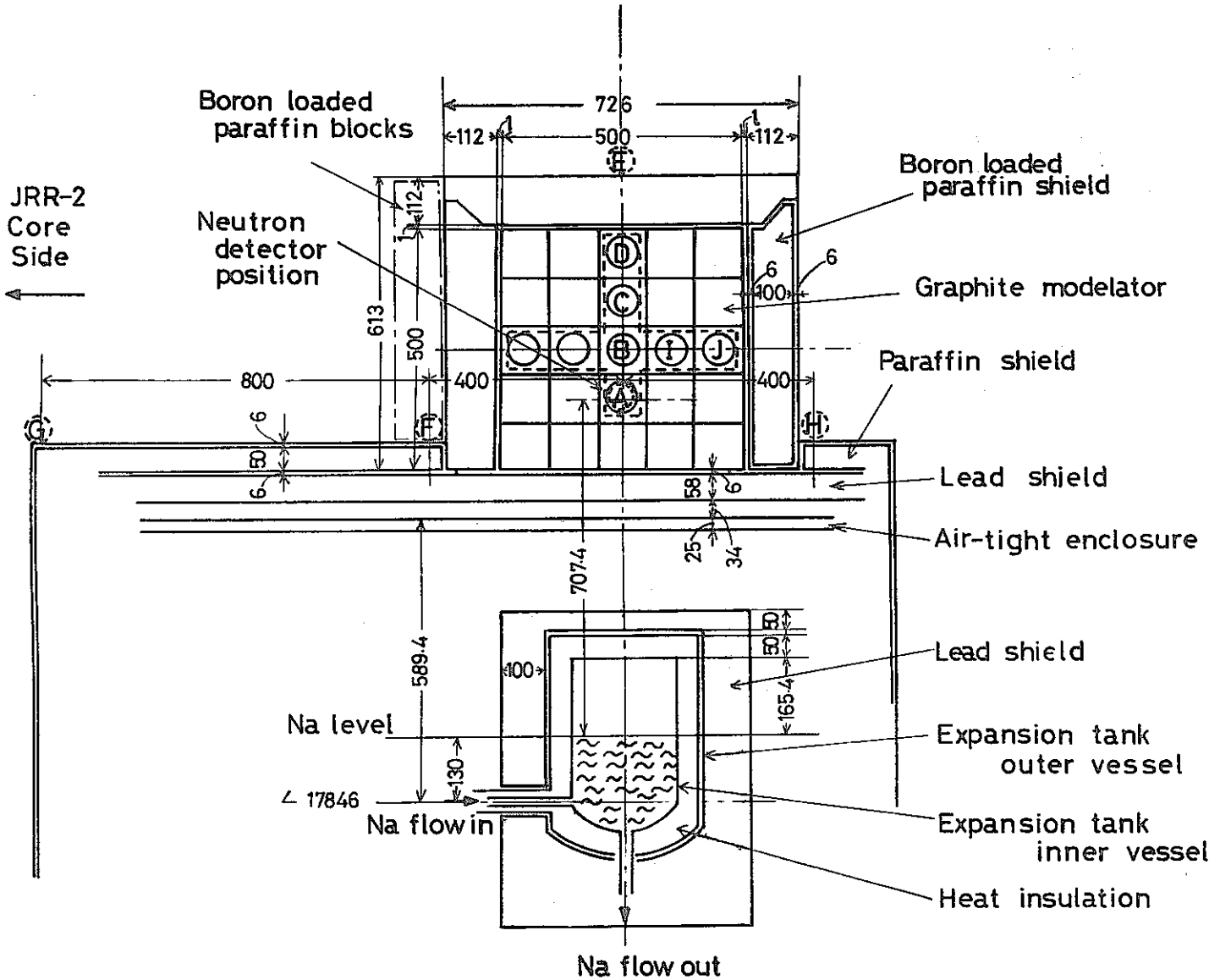

Fig2-4 Expansion tank and graphite moderator

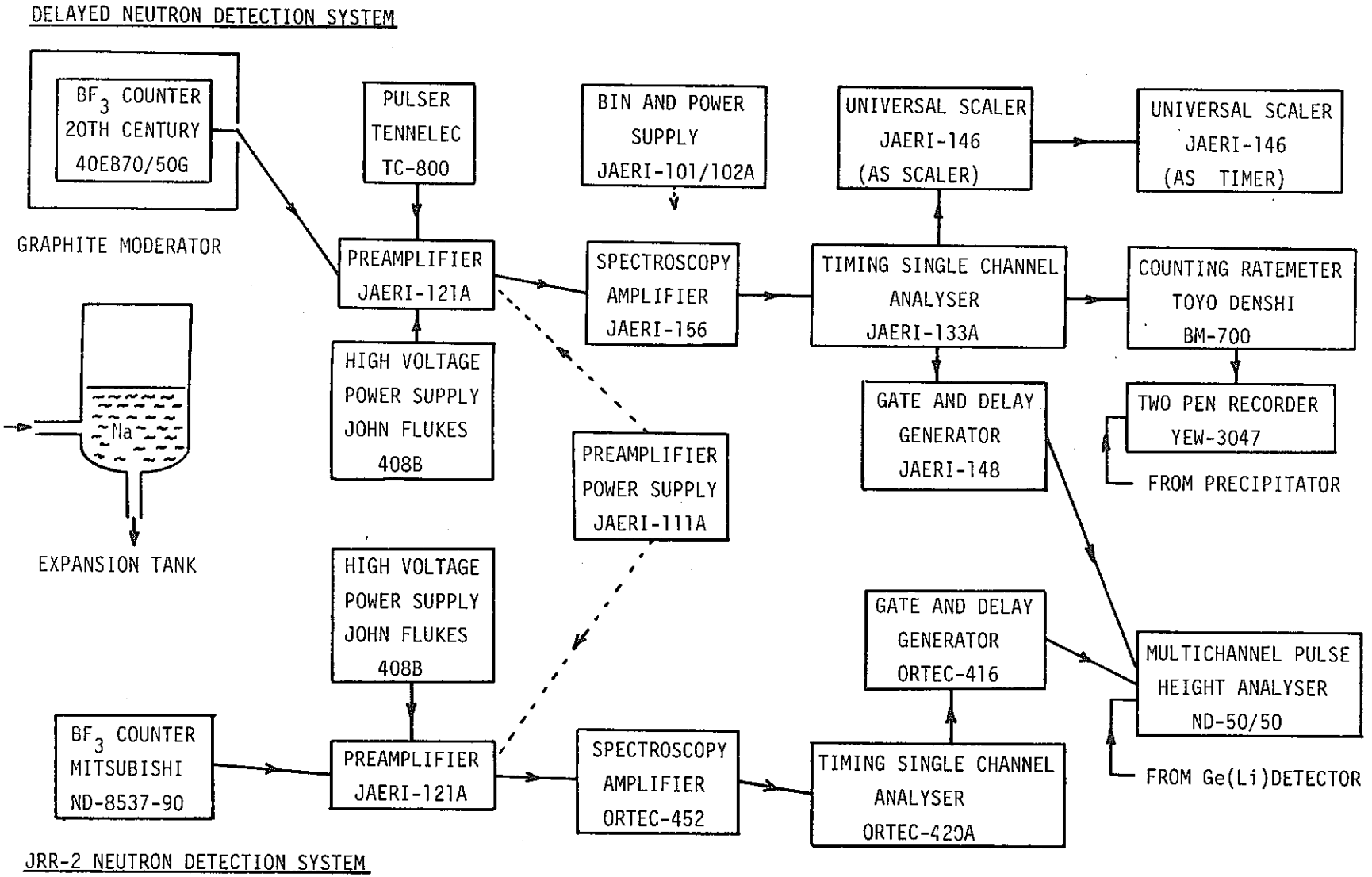

Fig.2-5 Schematic diagram of the electronics used in delayed neutron detector system in Sodium In-pile Loop

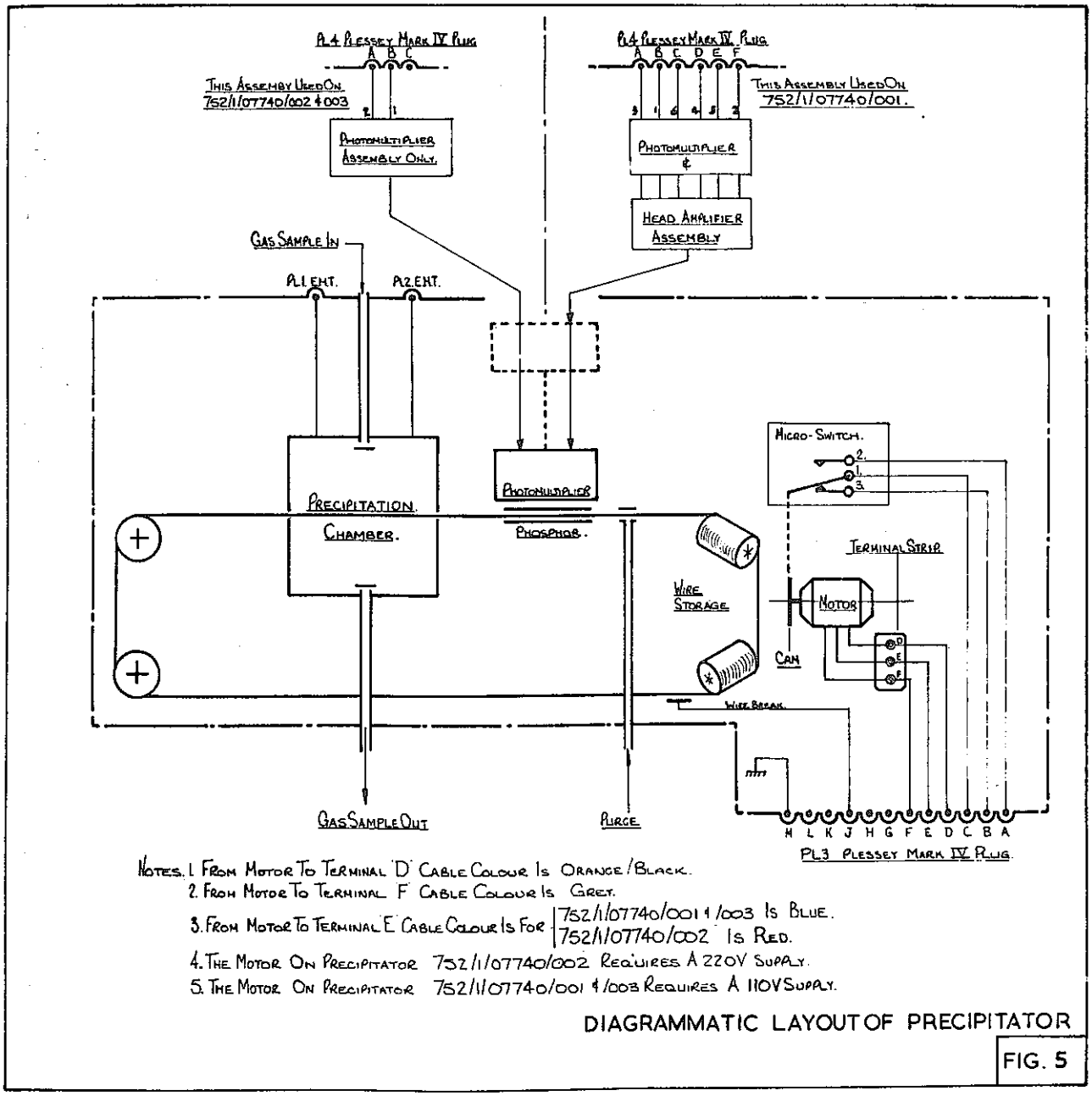

Fig.2-6 Diagrammatic Layout of Precipitator (Plessey Co.Ltd, Mark XI)

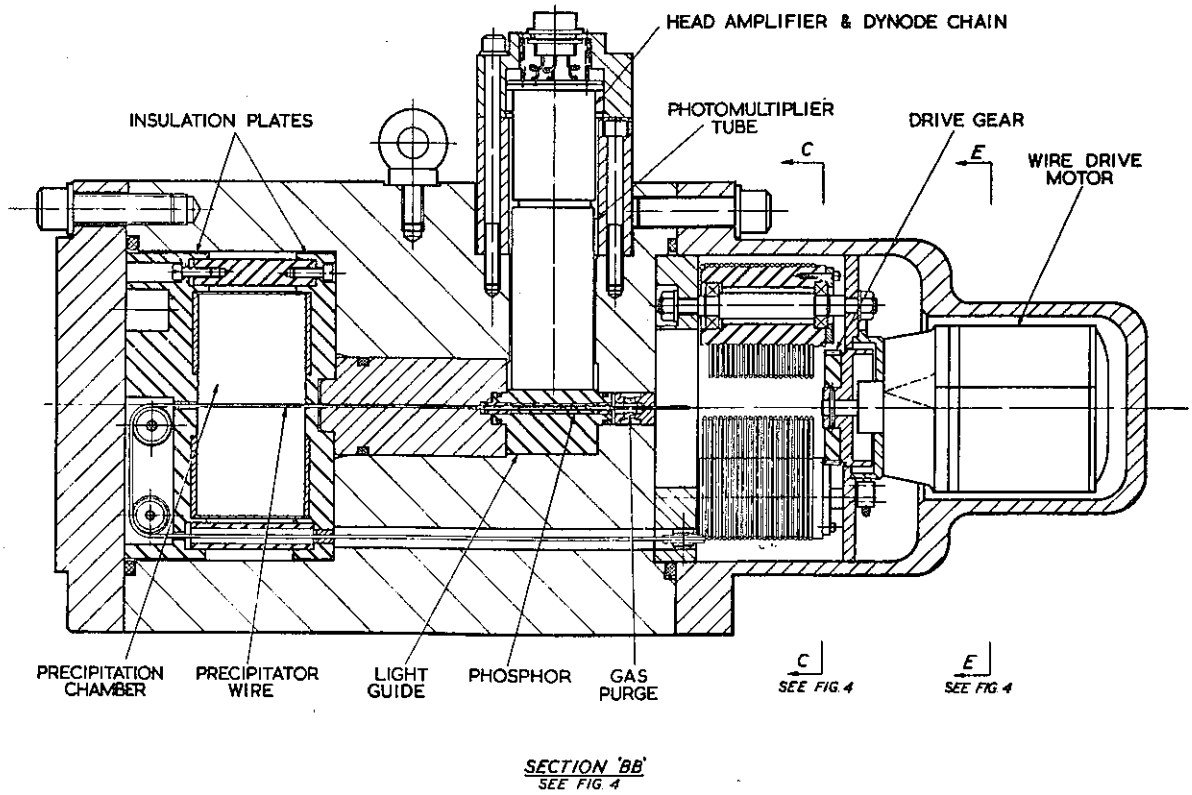

MARK ELEVEN PRECIPITATOR

FIG.3

Fig. 2-7 Cross section of precipitator (Plessey Co.Ltd. Mark XI)

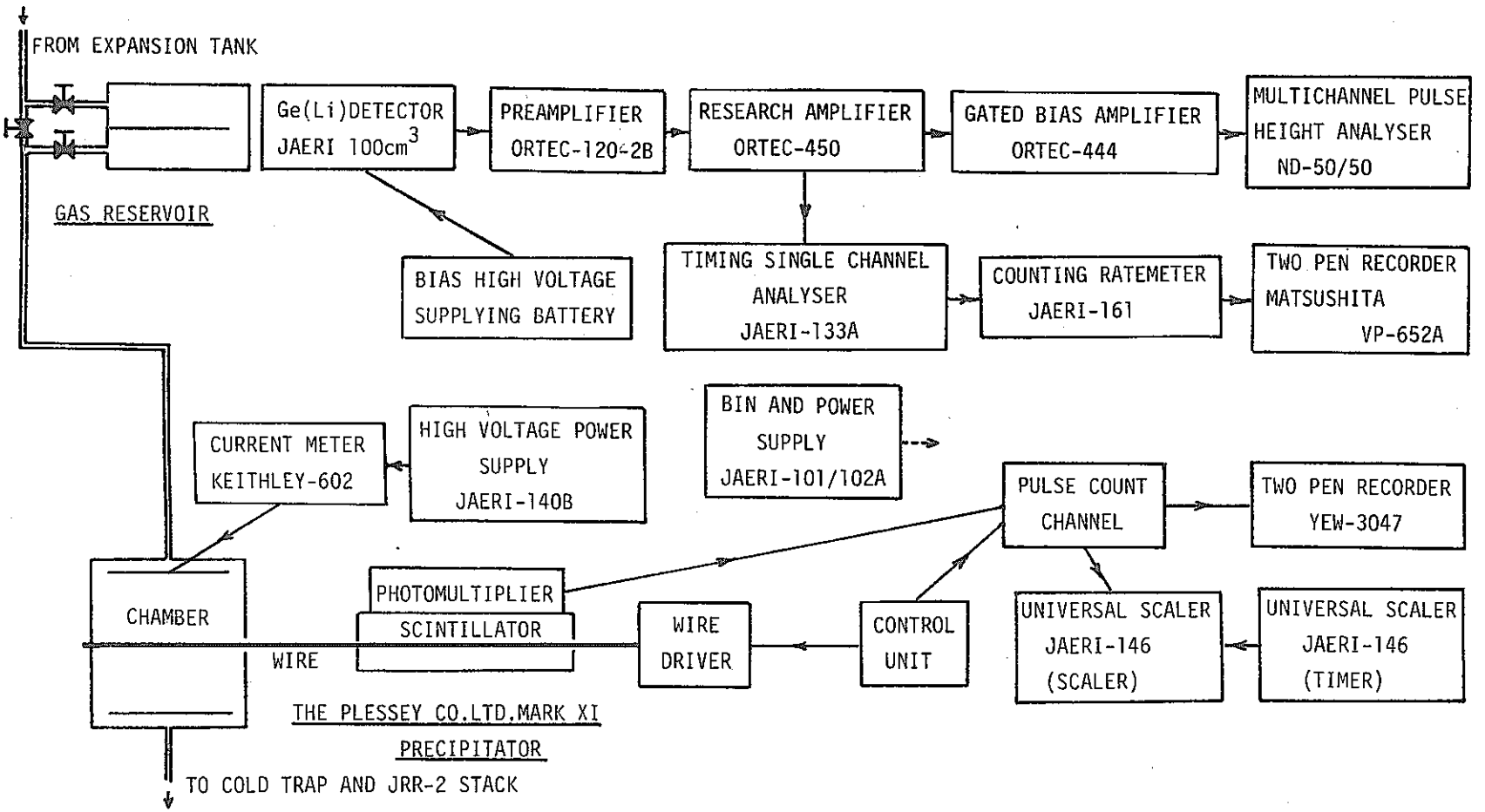

Fig.2-8 Schematic diagram of electronics used in gamma-ray spectrometry and precipitator of Sodium In-pile Loop

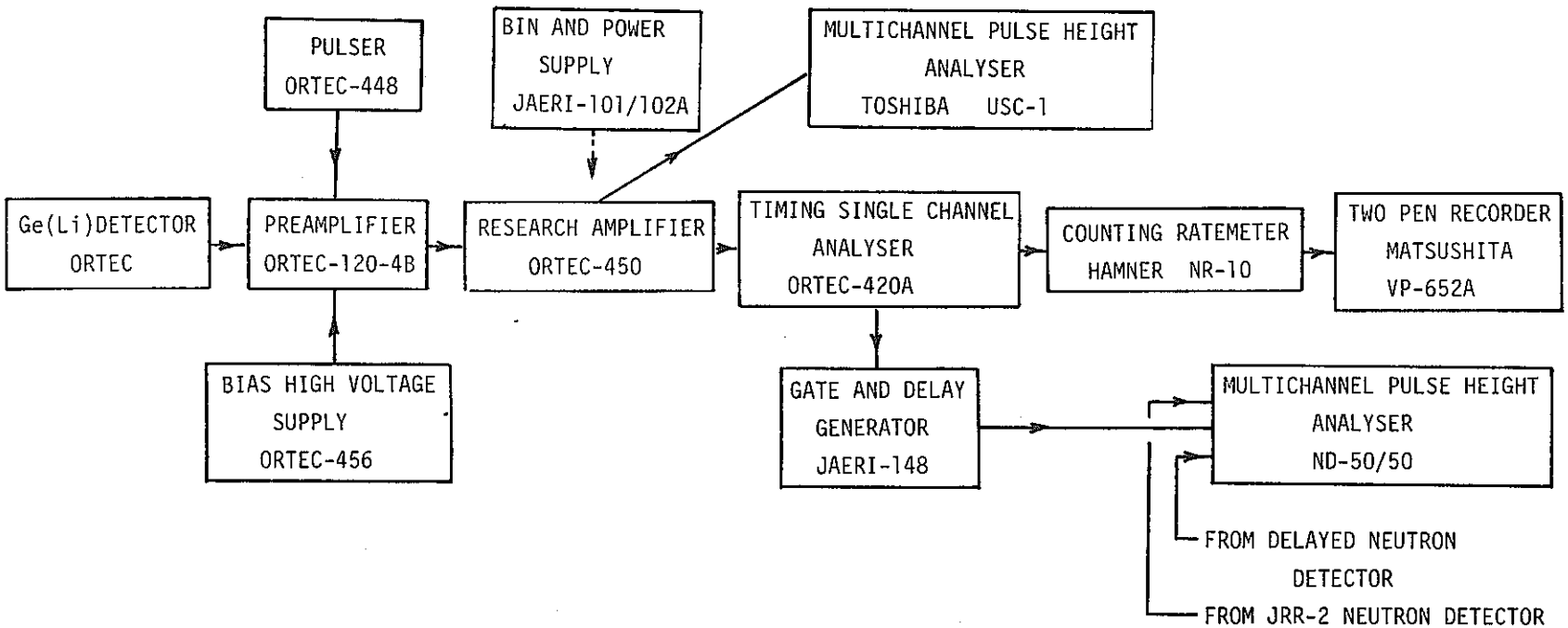

Fig.2-9 Schematic diagram of the electronics used in gamma-ray spectrometry of expansion tank gas

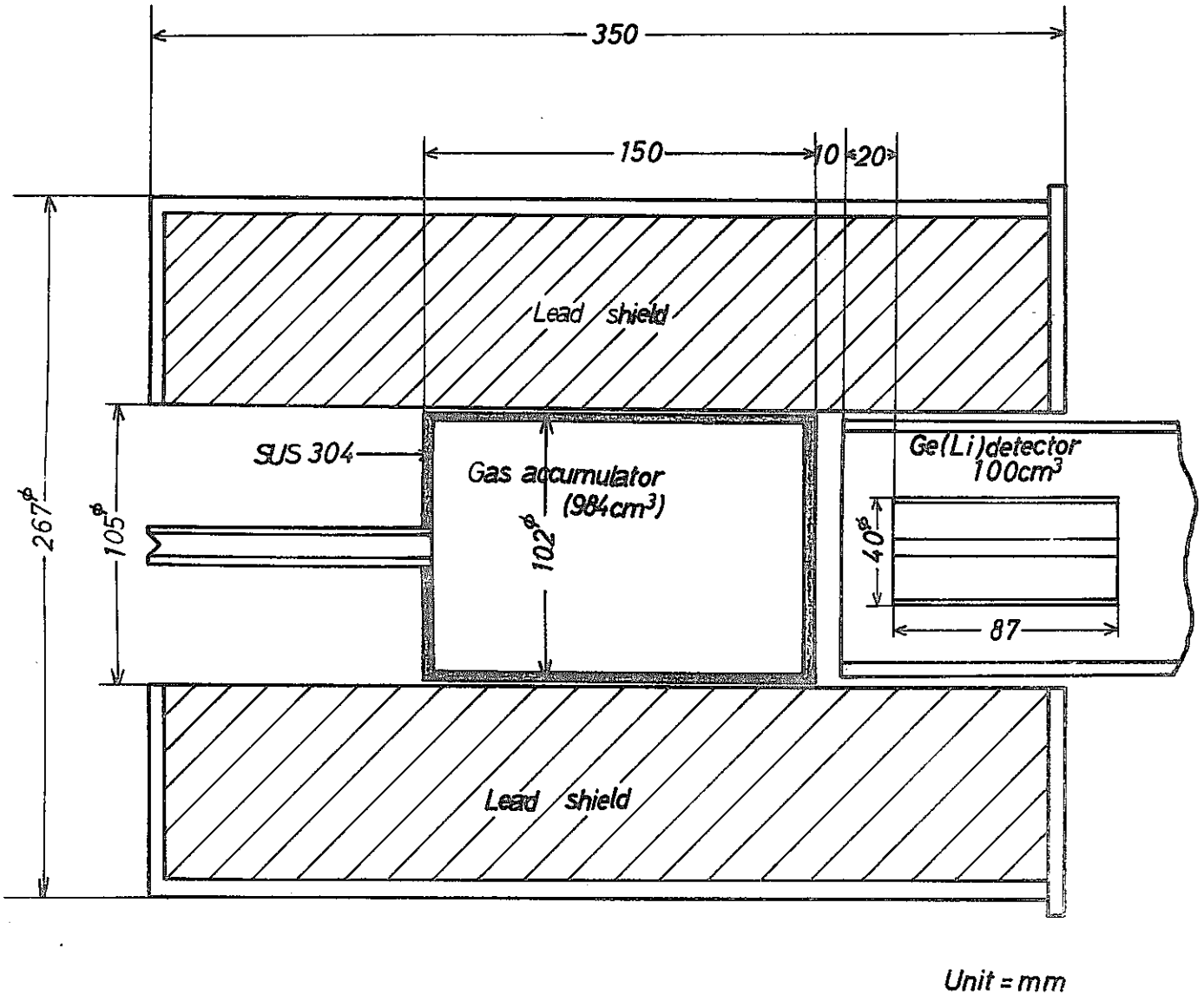

Fig.2-10 Dimensions of cover-gas reservoir and Ge(Li) gamma-ray detector

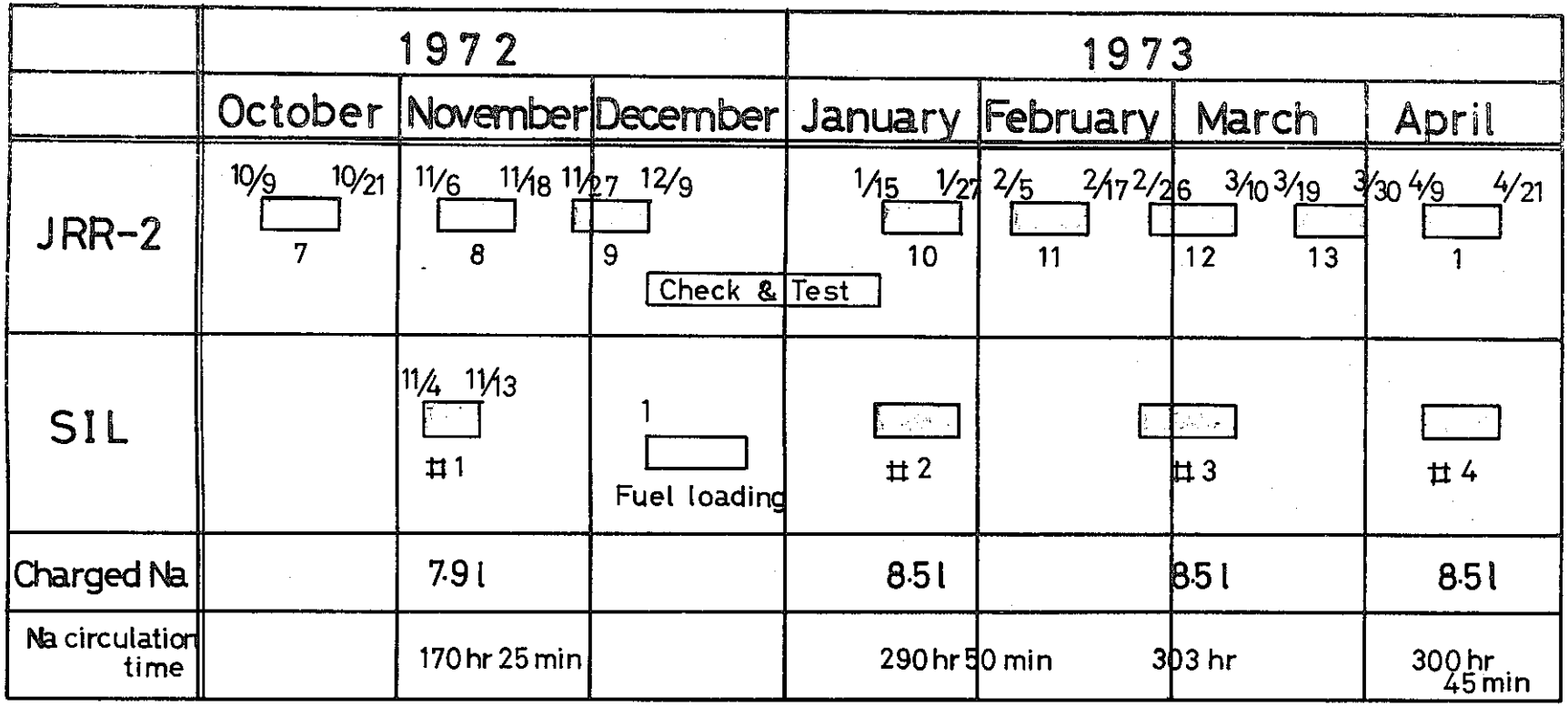

Fig 3-1 Time schedule of SIL experiment

	1973							
	May	June	July	August	Septemb.	October	Novemb.	Decemb.
JRR-2	5/7 5/19 (2) 5/28 6/9 (3) 6/18 6/30 (4) 7/9 7/21 (5) 7/30 8/11 (6) 6 weeks Check and test					10/1 10/13 (7) 10/22 11/3 (8)	11/12 11/24 (9)	12/3 12/15 (10)
S.I.L.		5	6	7		8	9	10
Charged Na		8.5l	8.5l	8.5l		8.5l	8.5l	8.5l
Na circulation time		306hr 50min	245hr 3min	298hr 1min		271hr 13min	295hr 23min	257hr 21min

	1974			
	January	February	March	April
JRR-2	No operation			
S. I. L.	No operation, Fuel unloading			

Fig.3-2 Time schedule of S.I.L. experiment

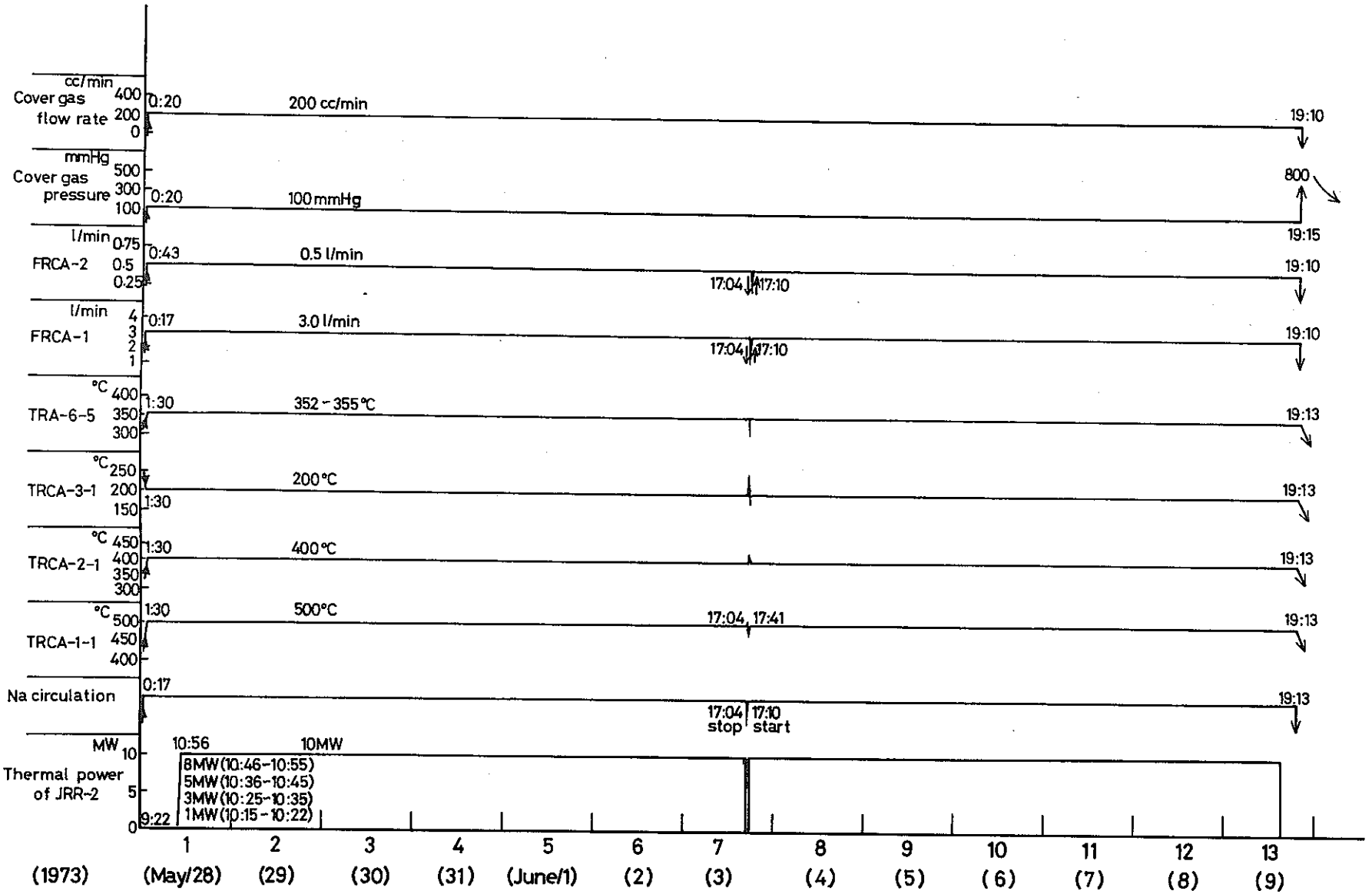

Fig.3-3 JRR-2 and Sodium In-pile Loop operating conditions of the 5th sodium circulation experiment (May 28 - June 9, 1973)

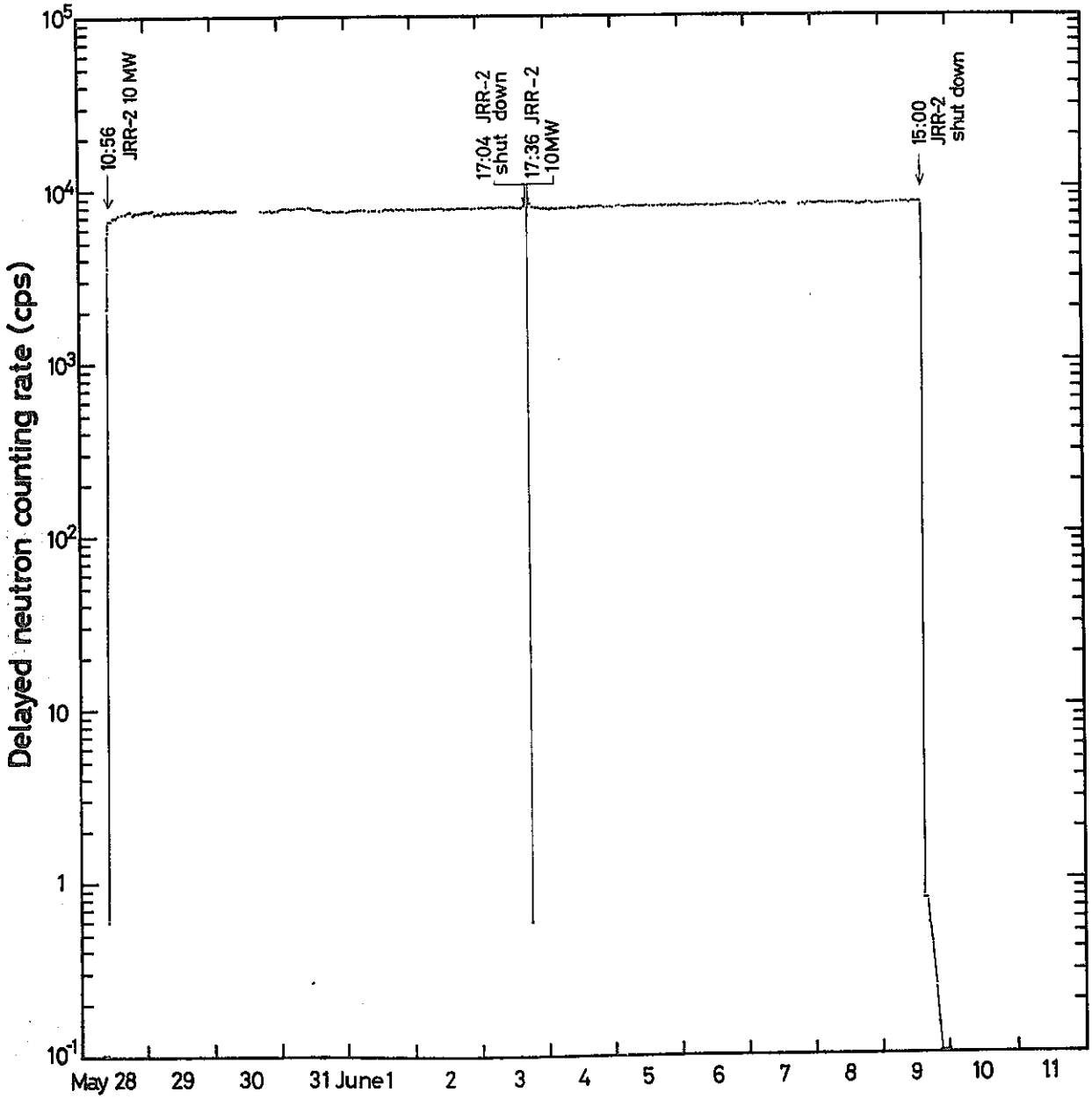

Fig.3-4 Delayed neutron counting rate change during the 5th sodium circulation experiment (May 28 ~ June 9, 1973)

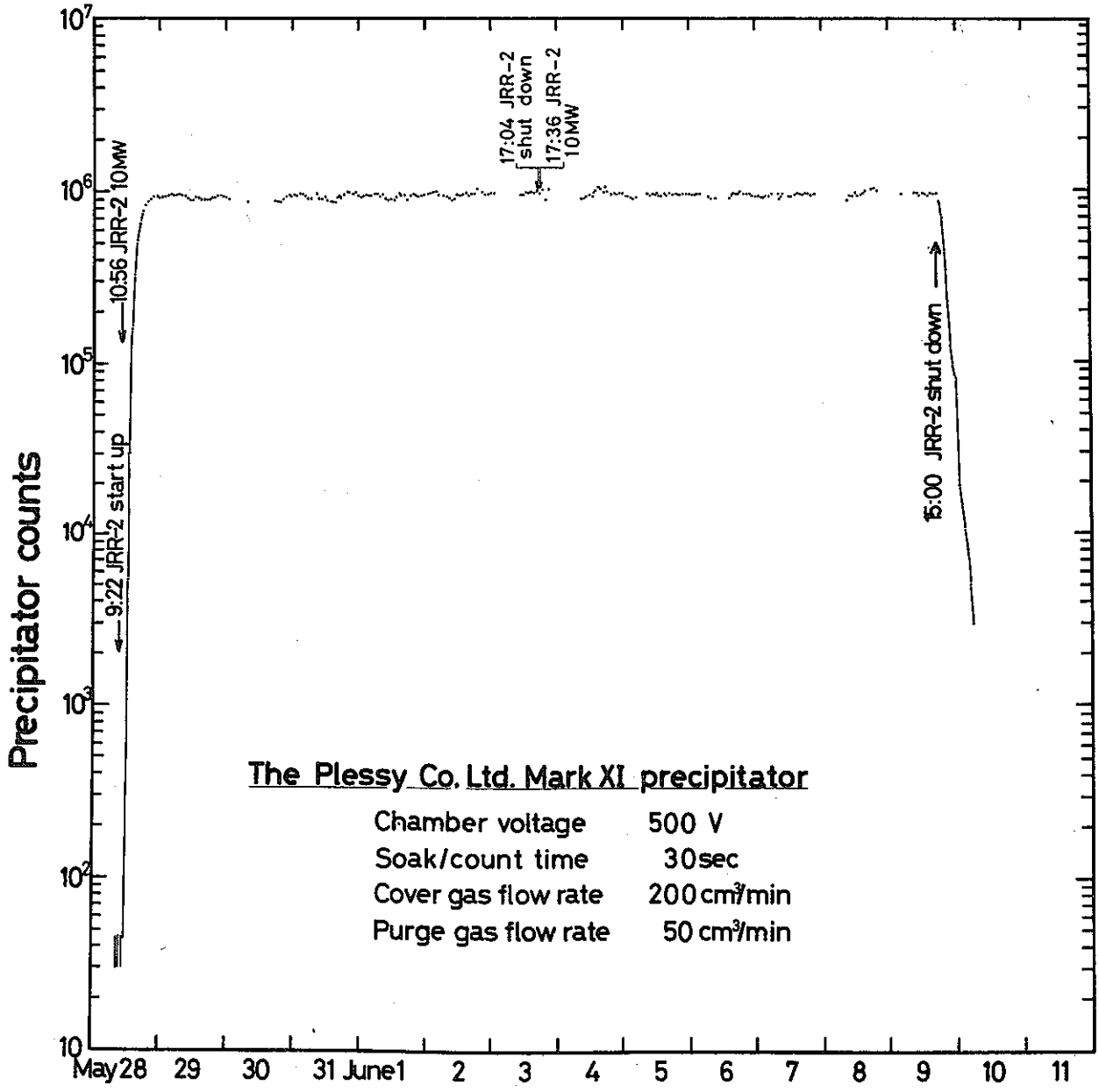

Fig.3-5 Precipitator count change during the 5th sodium circulation experiment (May 28 - June 10, 1973)

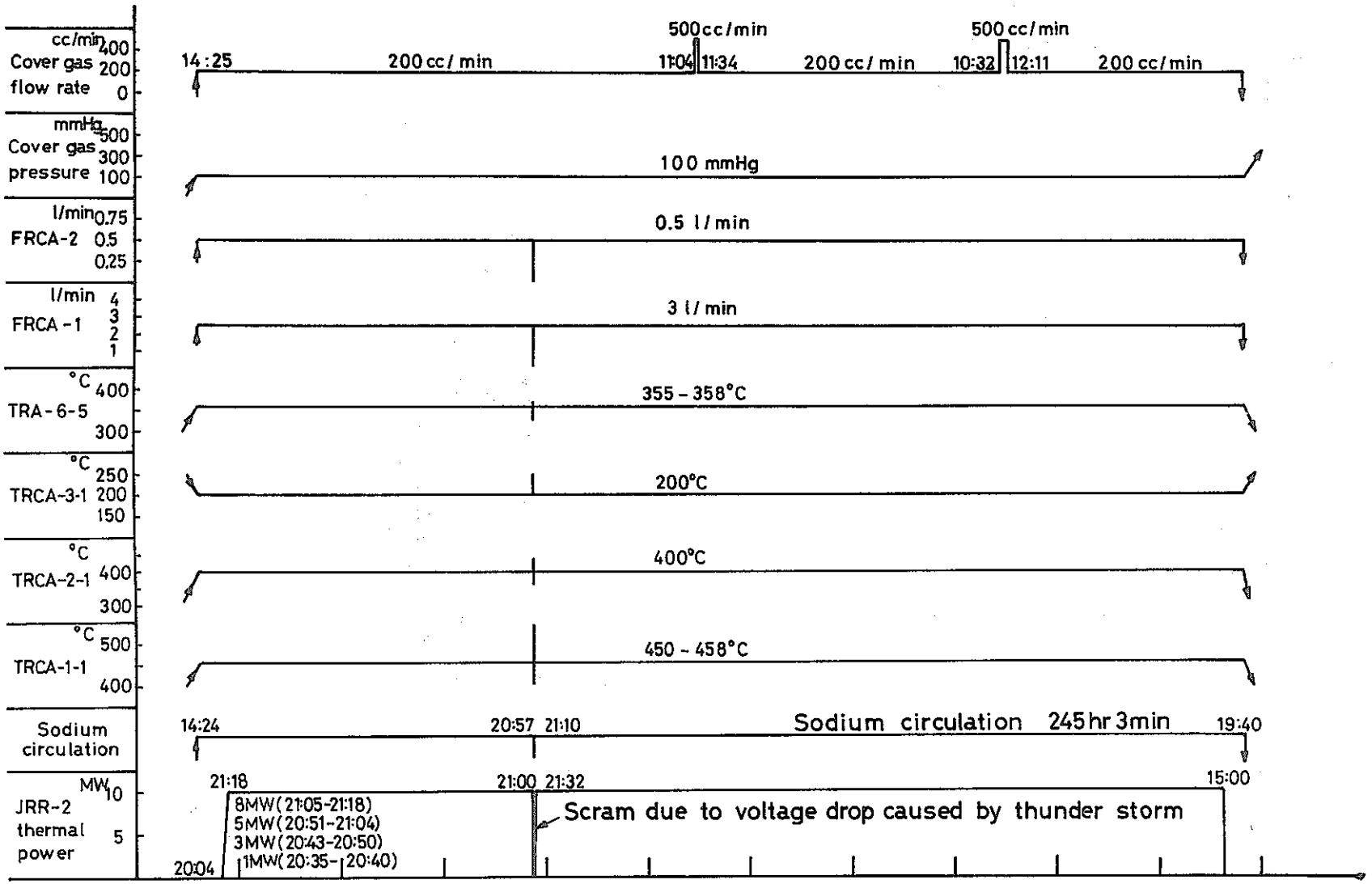

Fig.3-6 JRR-2 and SIL operation conditions during 6th sodium circulation experiment (June 20 - 30, 1973)

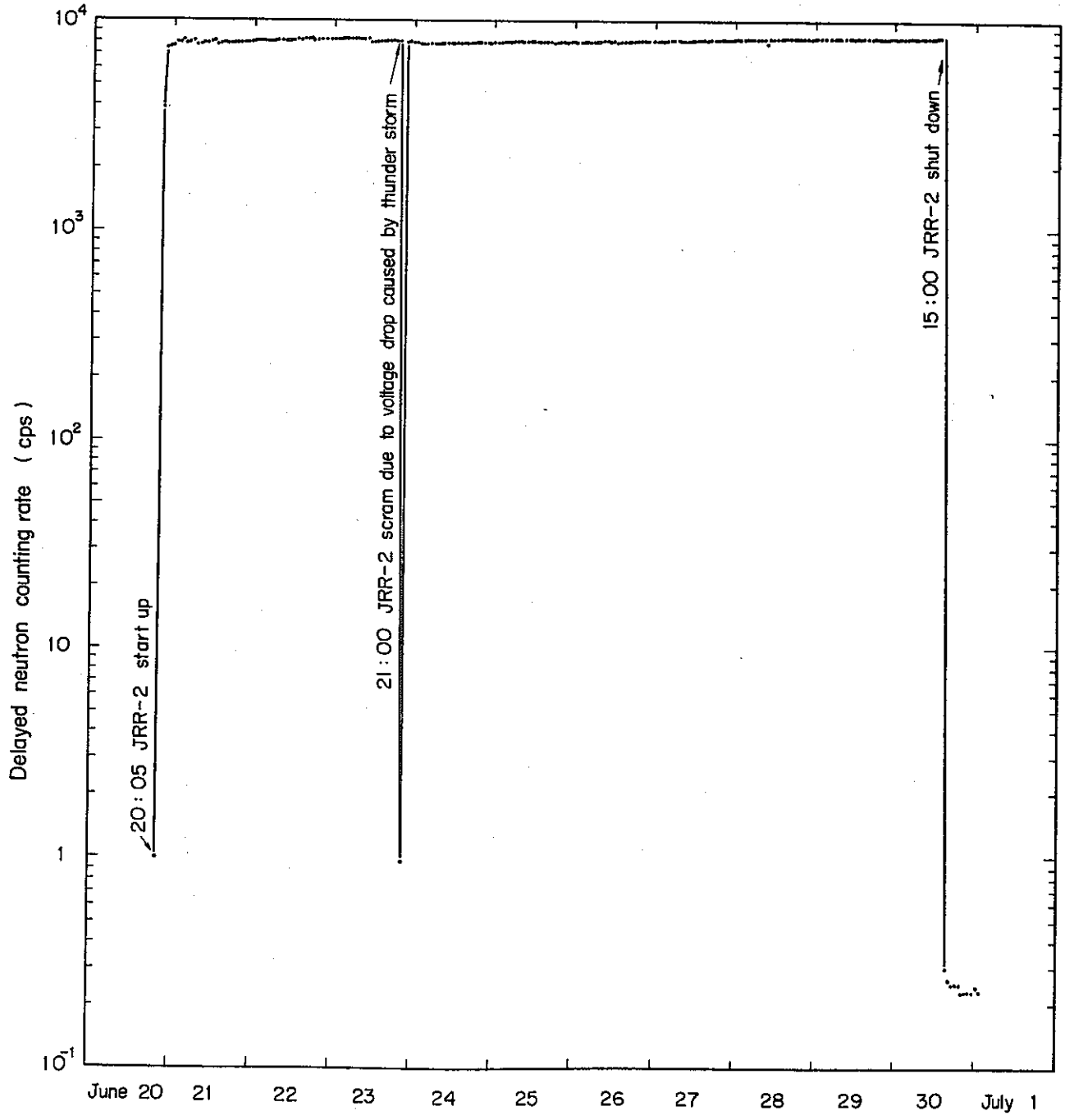

Fig.3-7 Delayed neutron counting rate change during 6th sodium circulation experiment (June 20 ~ July 1, 1973)

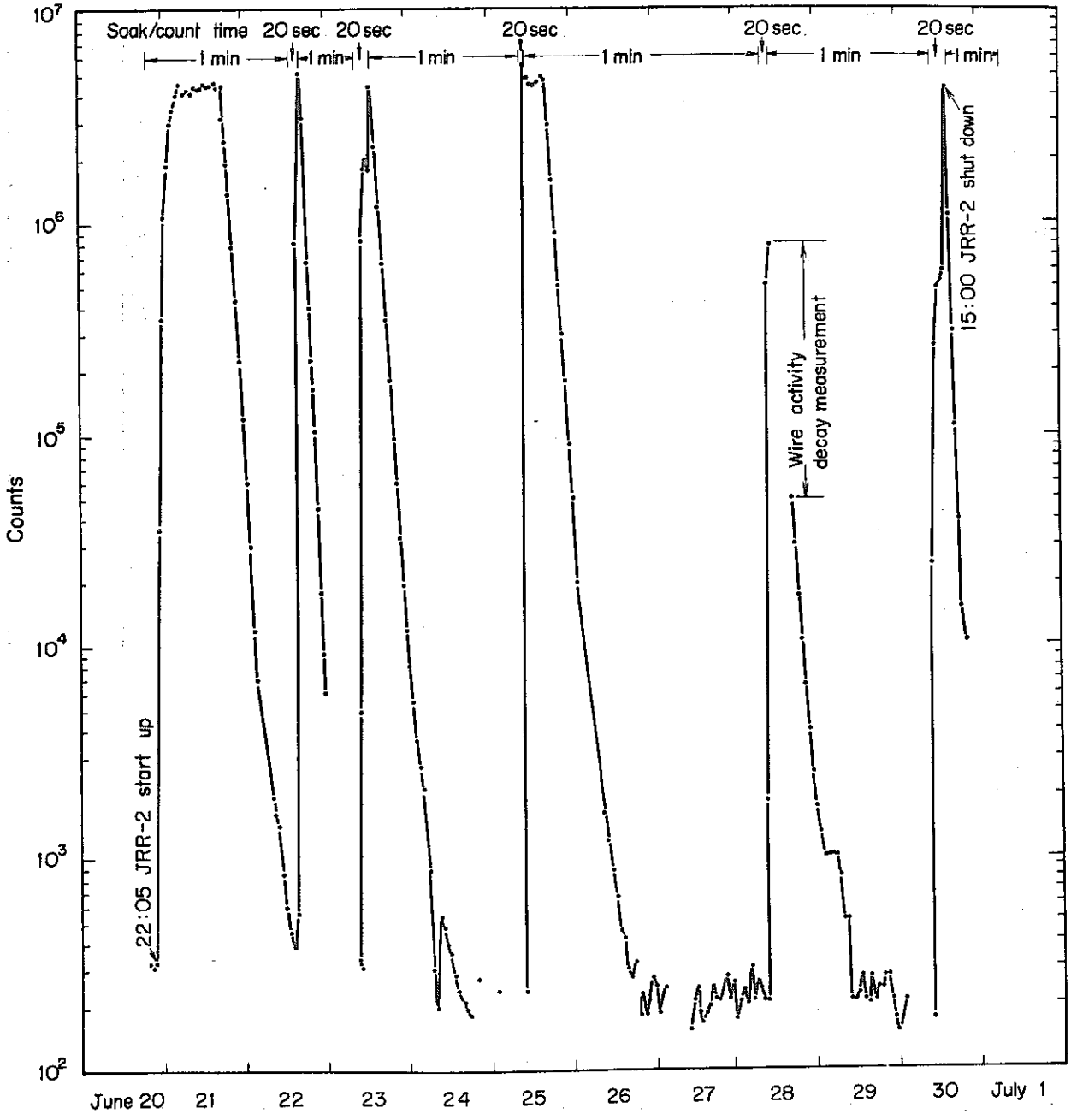

Fig. 3-8 Precipitator count change during 6th sodium circulation experiment (June 20 ~ 30, 1973)

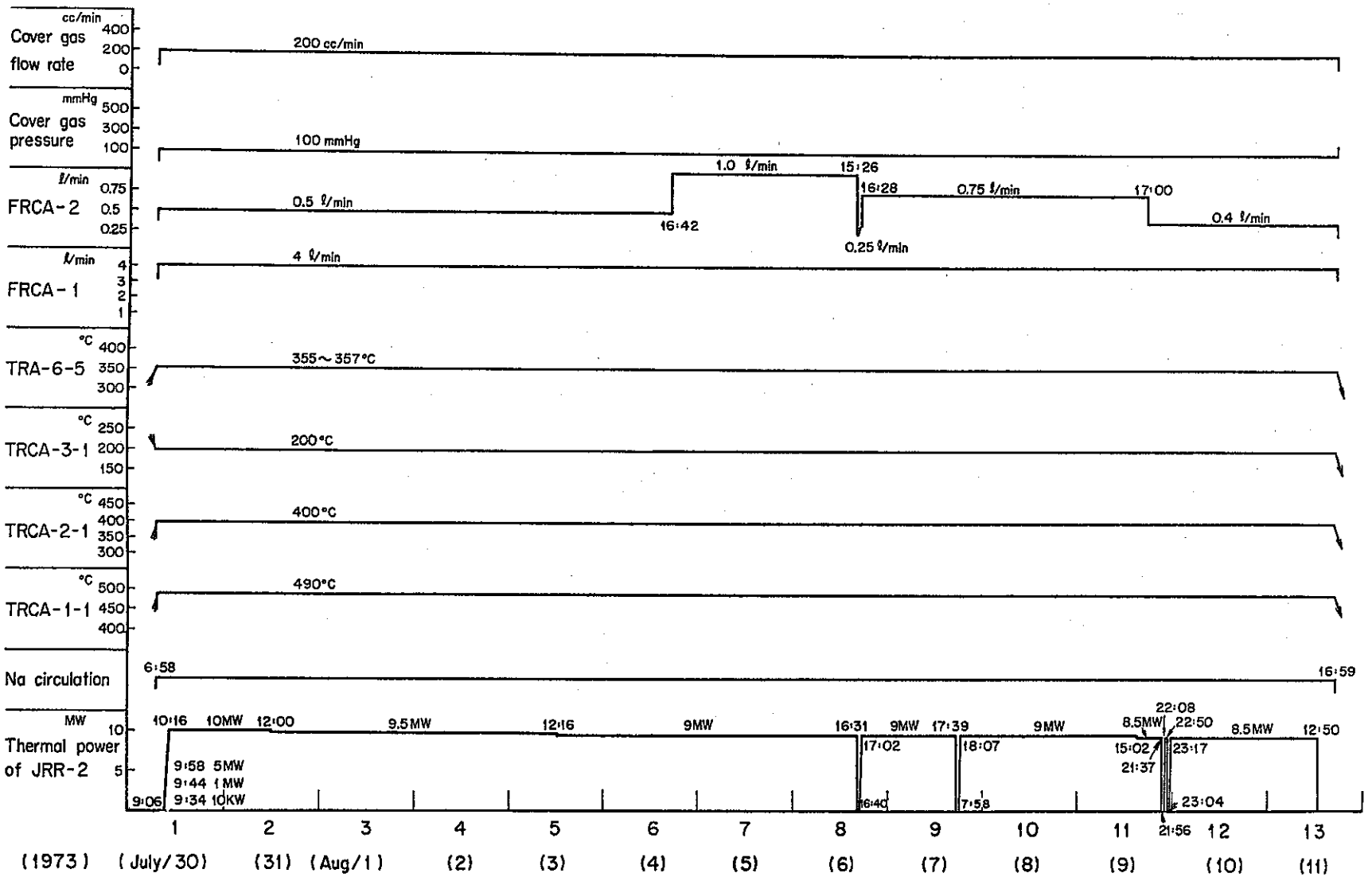

Fig.3-9 JRR-2 and Sodium In-pile Loop operating conditions of the 7th sodium circulation experiment (July.30 ~ Aug.11)

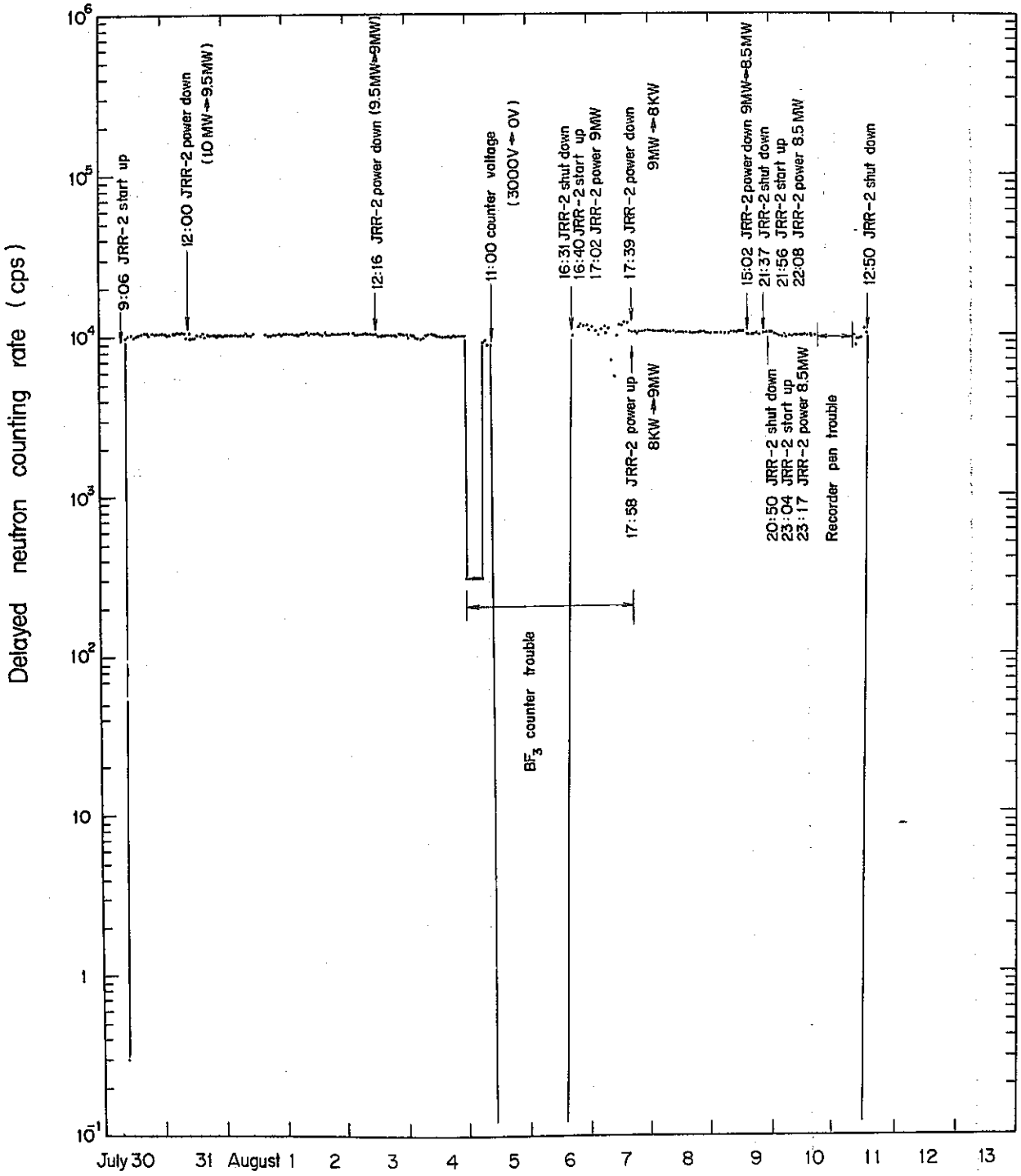

Fig.3-10 Delayed neutron counting rate change during 7th sodium circulation experiment (July 30 ~ August 11, 1973)

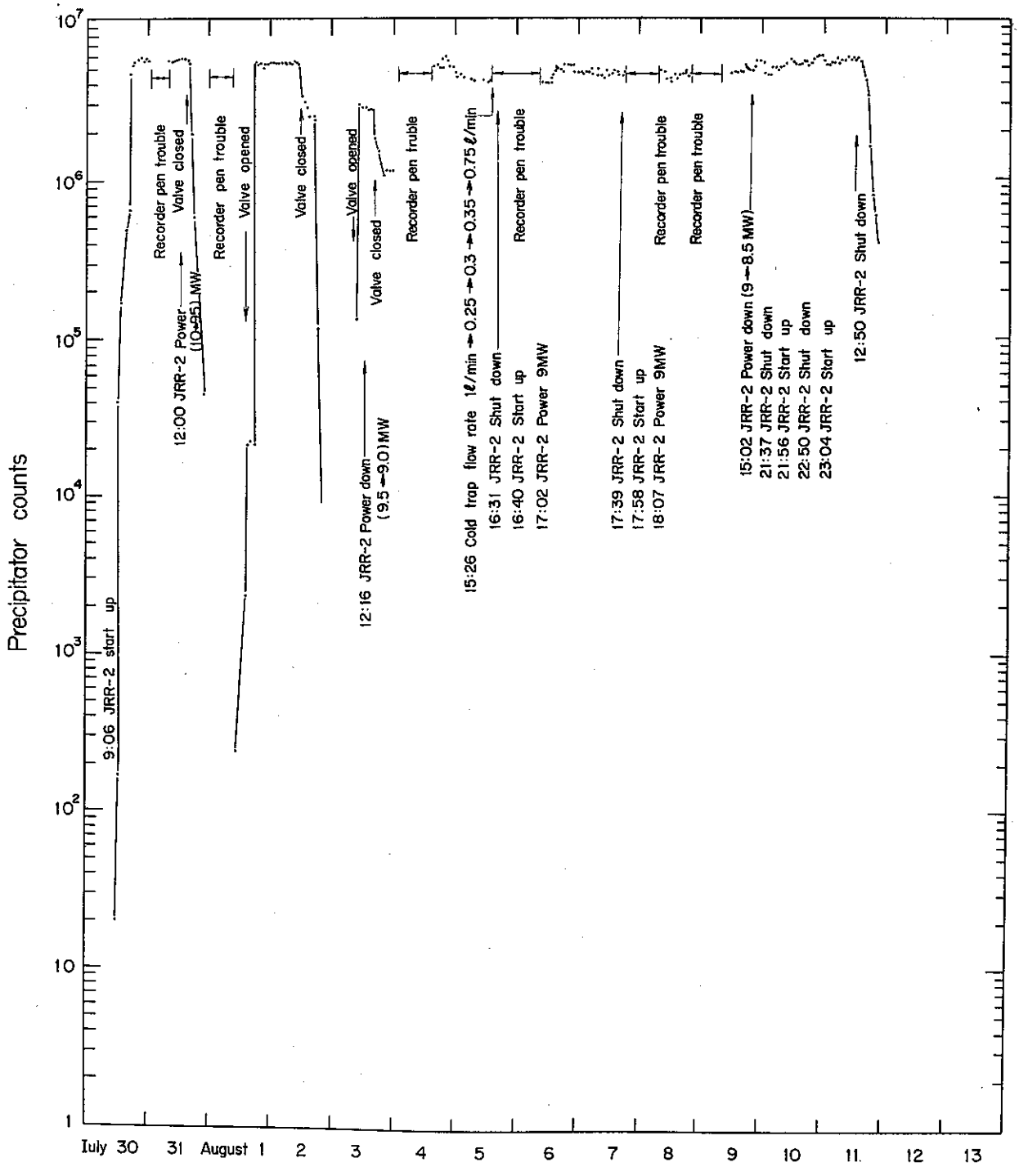

Fig. 3-11 Precipitator count change during 7th sodium circulation experiment (July 30 ~ August 11, 1973)

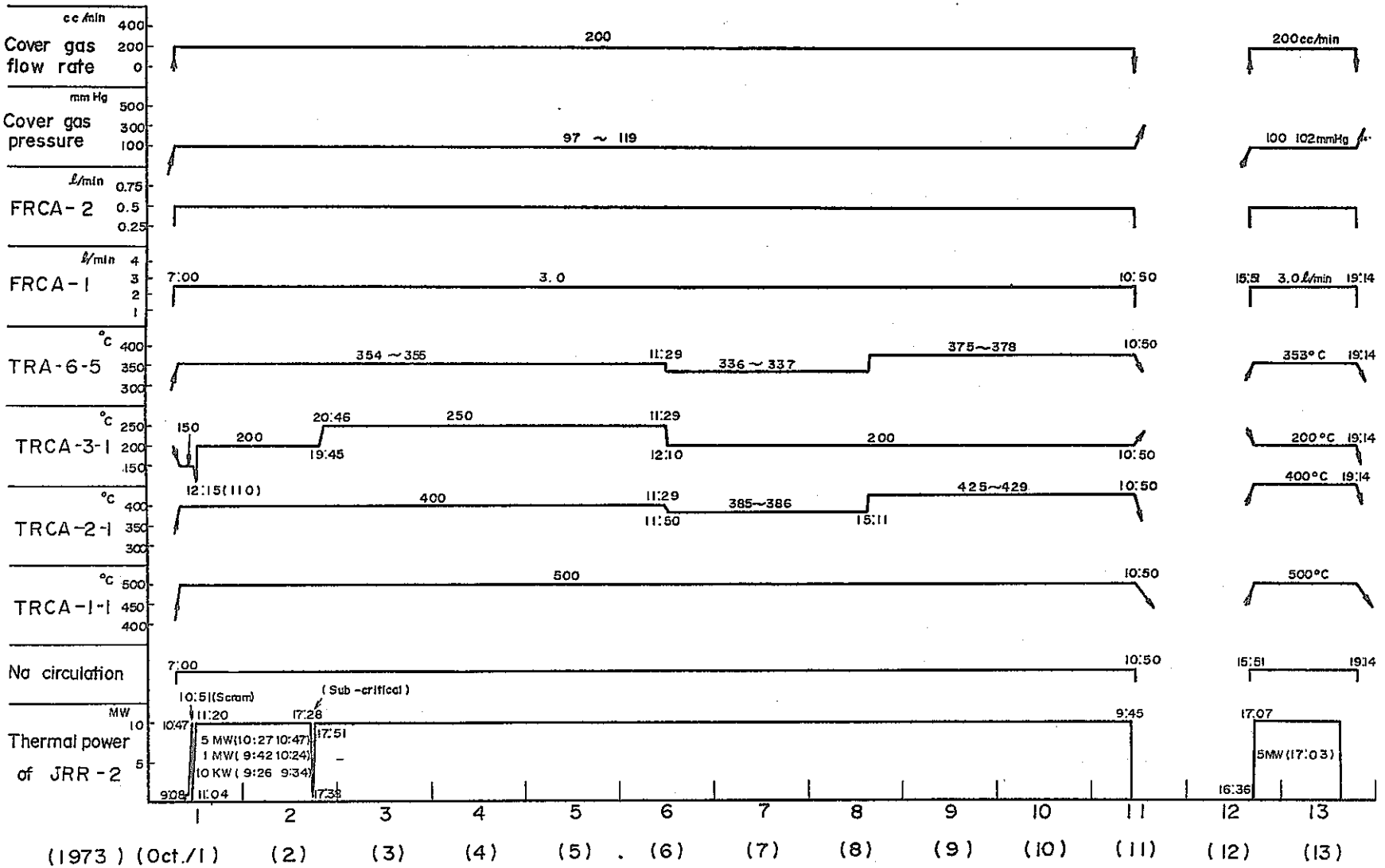

Fig.3-12 JRR-2 and Sodium In-pile Loop operating conditions of the 8th sodium circulation experiment (Oct. 1 ~ Oct. 13)

Fig.3-13 Delayed neutron counting rate change during 8th sodium circulation experiment

(October 1 ~ 15, 1973)

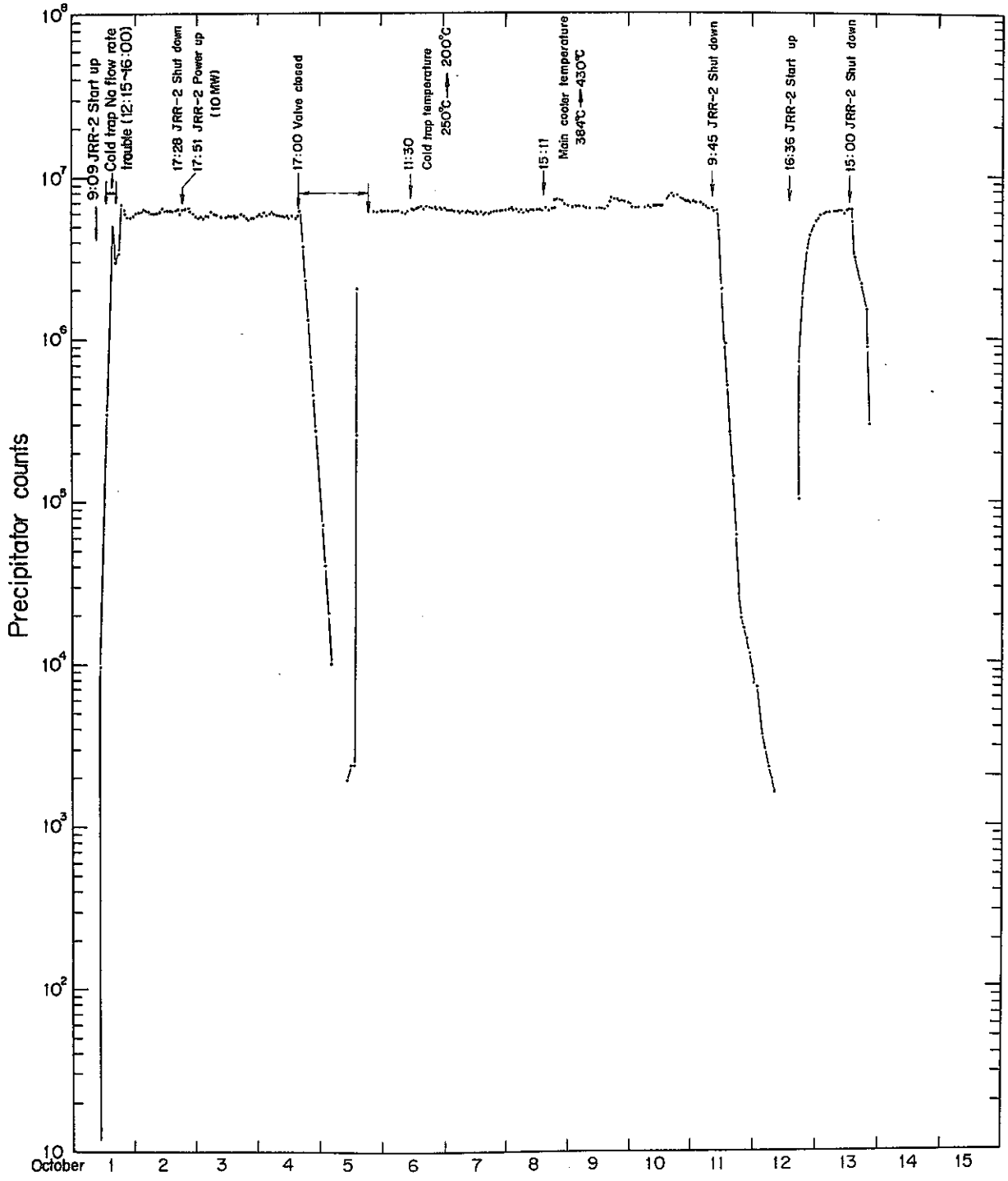

Fig. 3-14 Precipitator count change during 8th sodium circulation experiment (October 1 ~13, 1973)

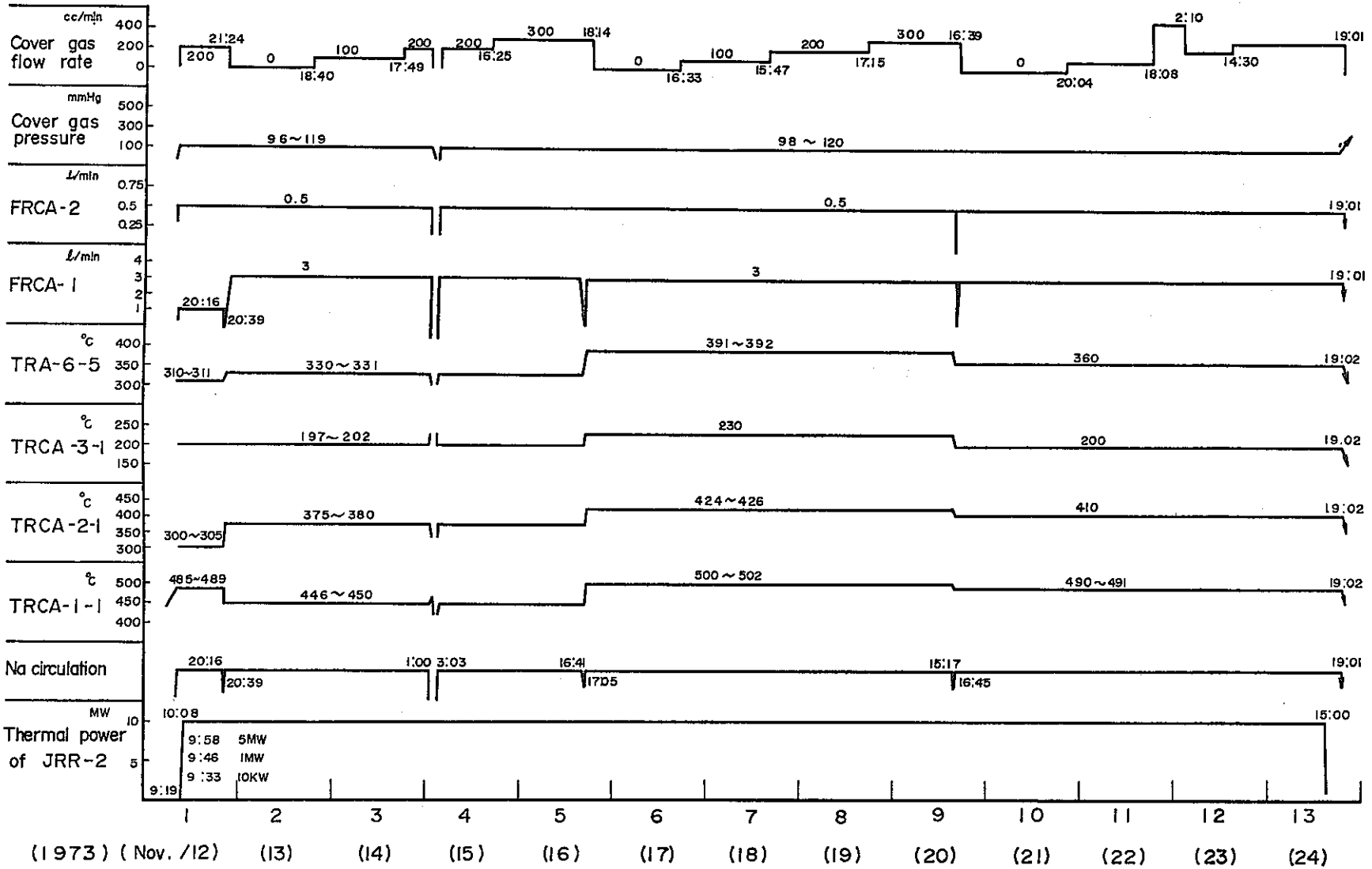

Fig.3-15 JRR-2 and Sodium In-pile Loop operating conditions of the 9th sodium circulation experiment (Nov. 12~ Nov. 24)

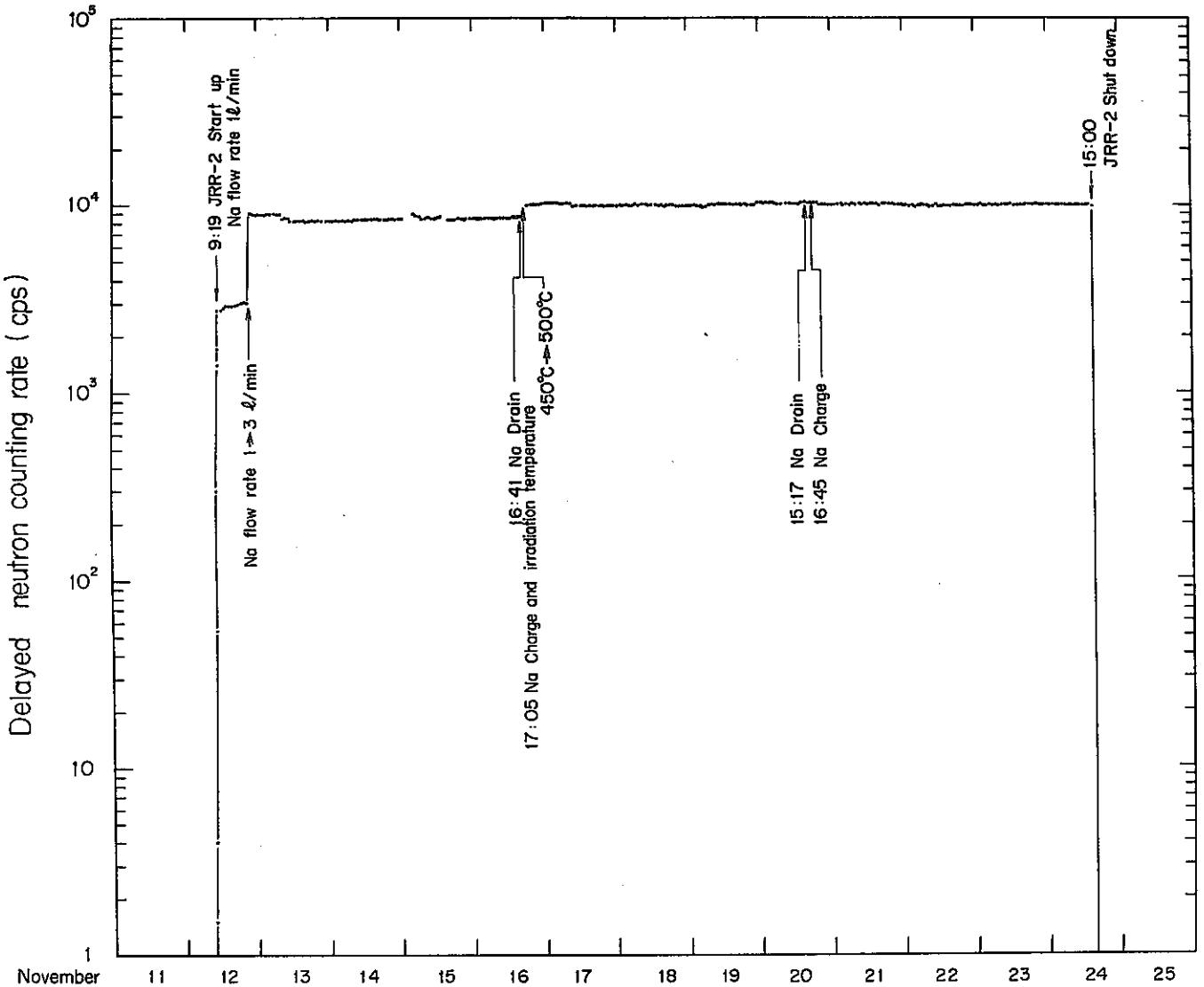

Fig.3-16 Delayed neutron counting rate change during 9th sodium circulation experiment

(November 12 ~ 24, 1973)

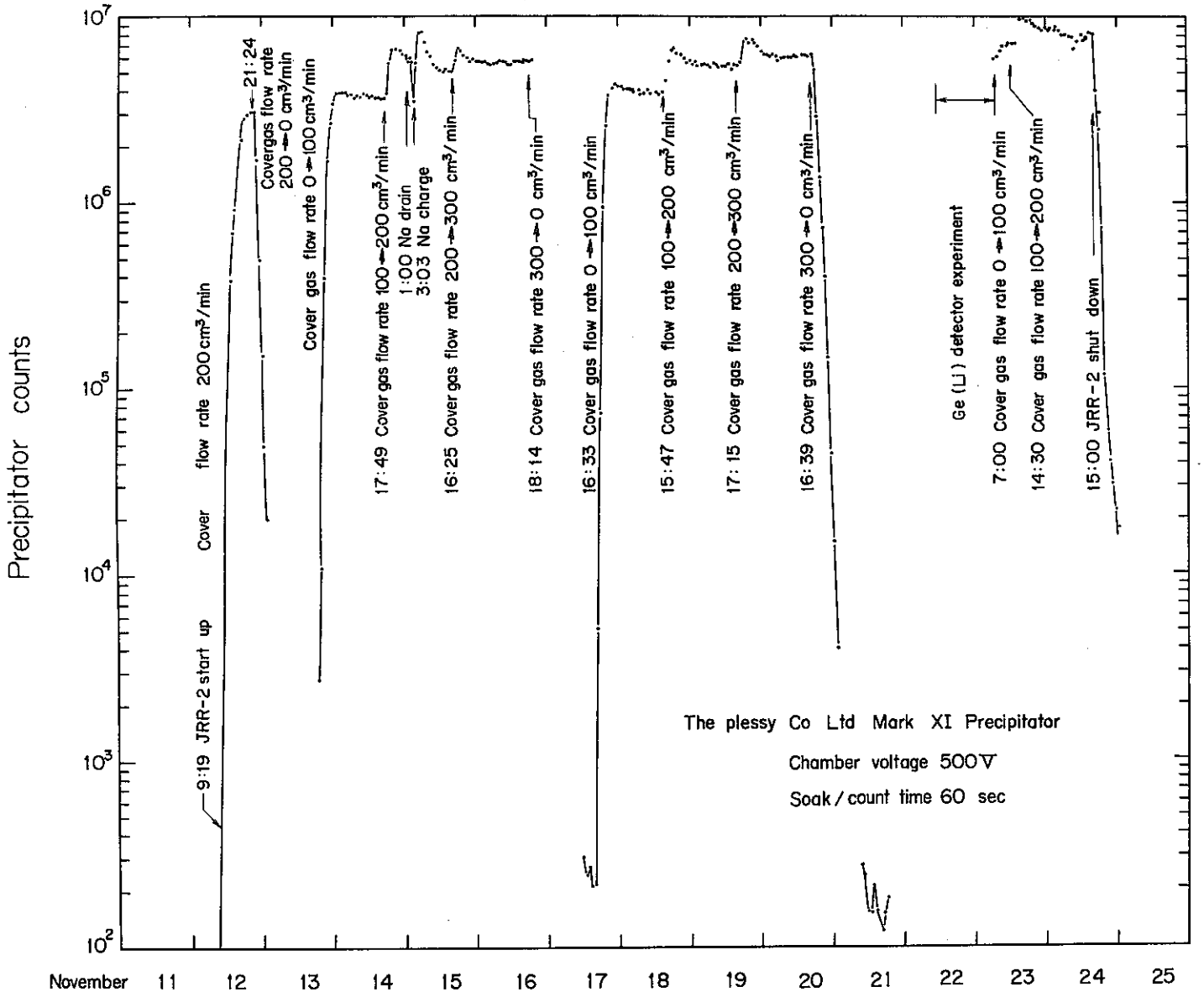

Fig.3-17 Precipitator count change during 9th sodium circulation experiment (November 12~24, 1973)

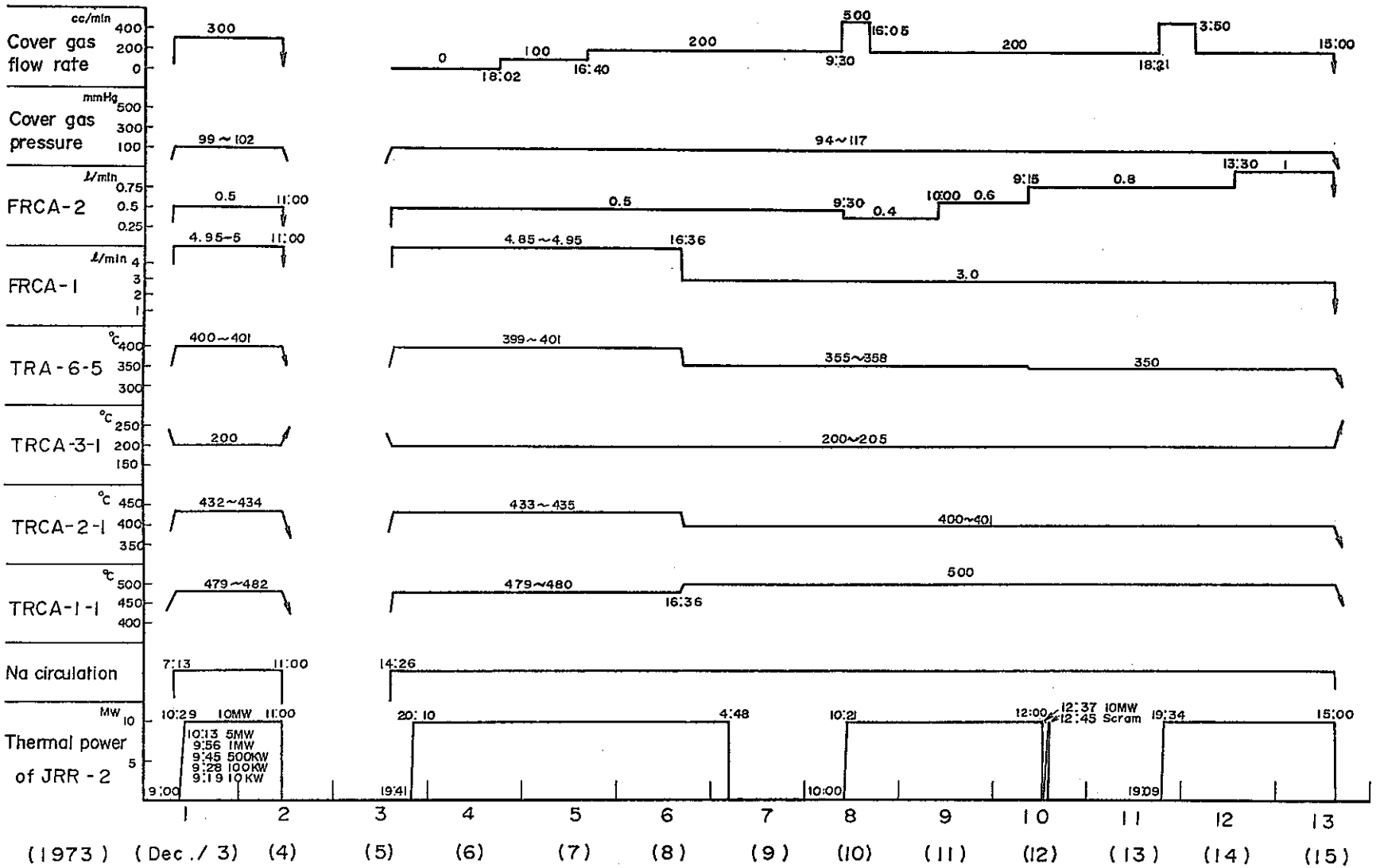

Fig. 3-18 JRR-2 and Sodium In-pile Loop operating conditions of the 10th sodium circulation experiment (Dec.3 ~ Dec.15)

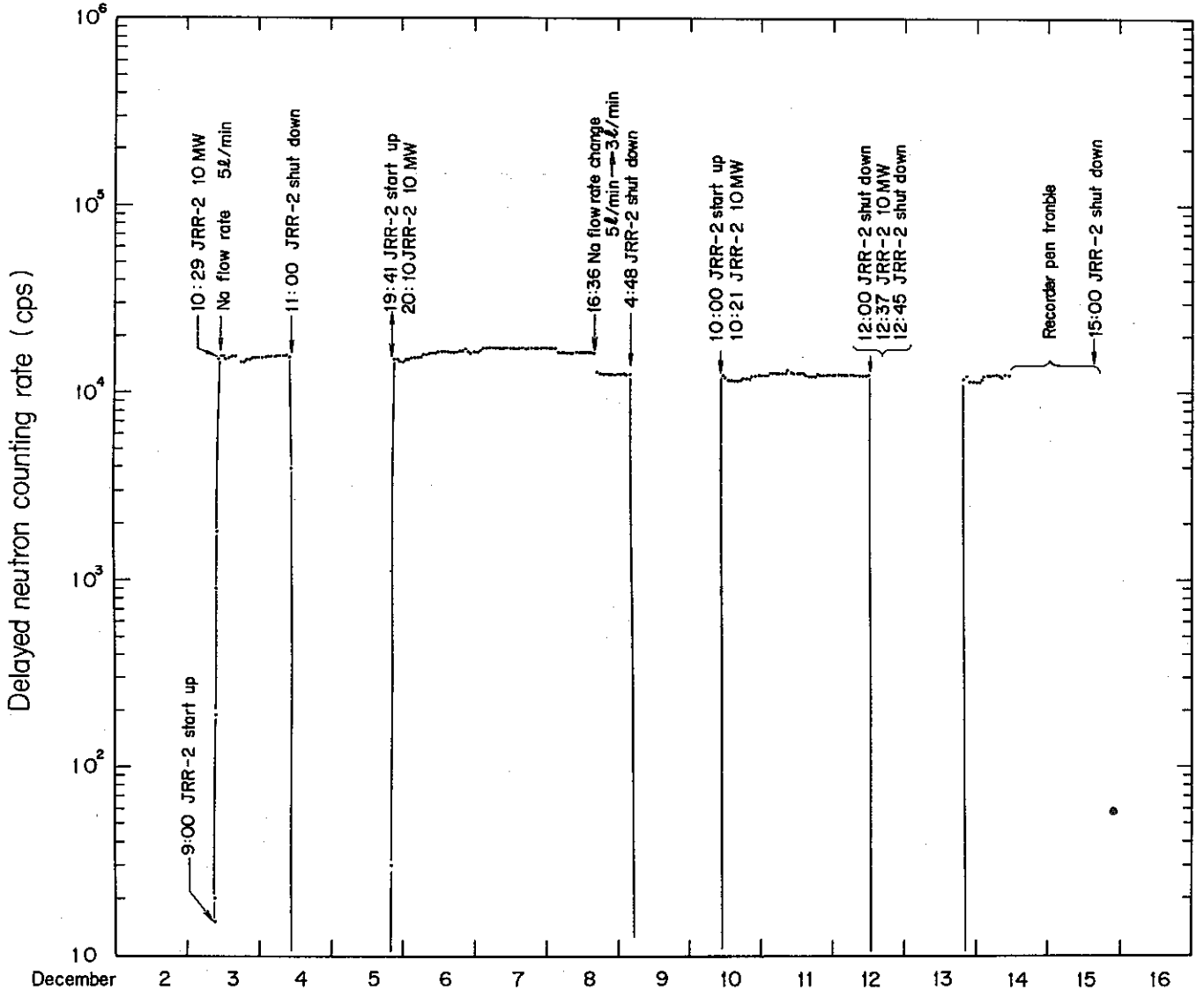

Fig. 3-19 Delayed neutron counting rate change during 10 th sodium circulation experiment (December 3~15, 1973)

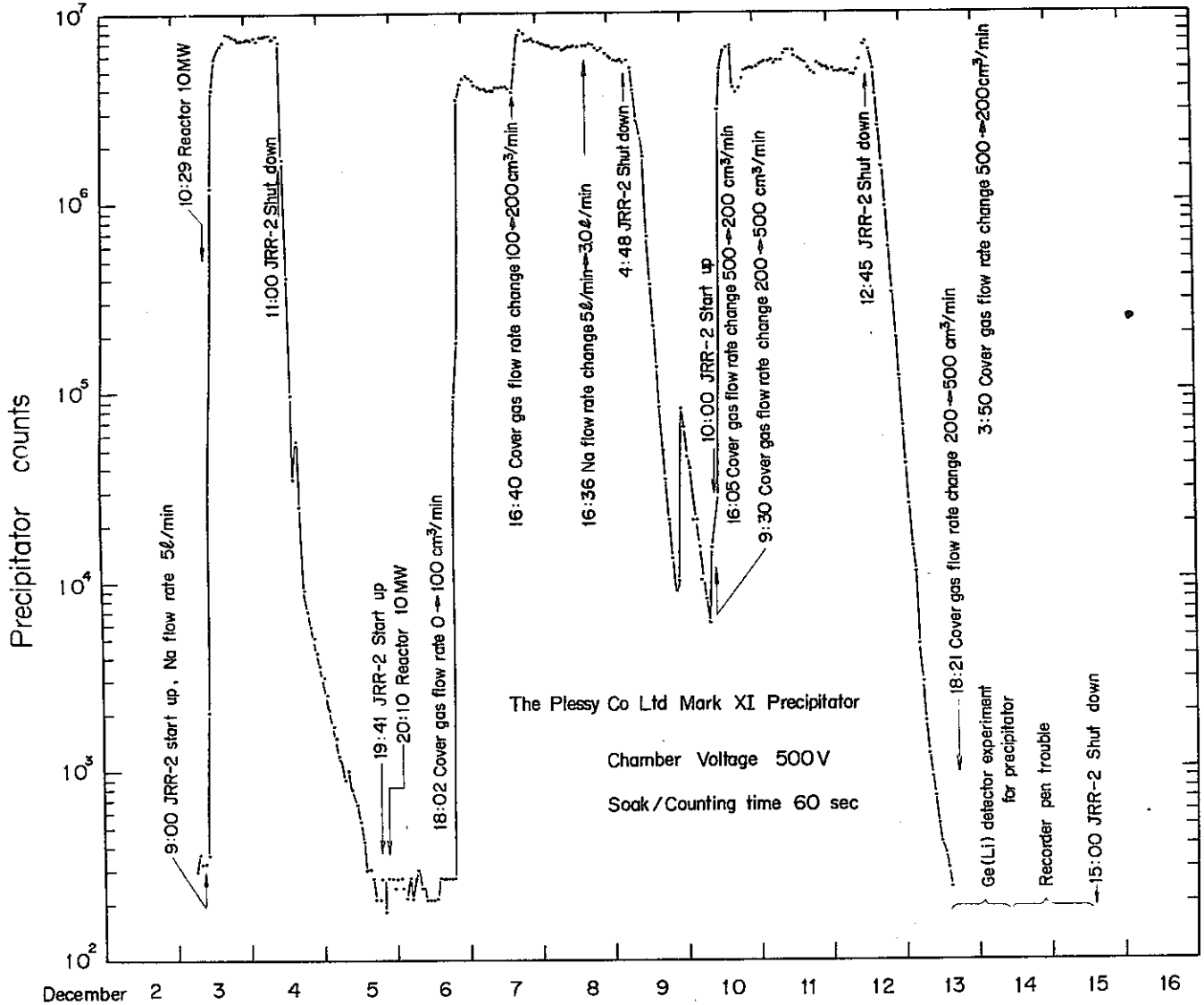

Fig. 3-20 Precipitator count change during 10 th sodium circulation experiment (December 3~15, 1973)

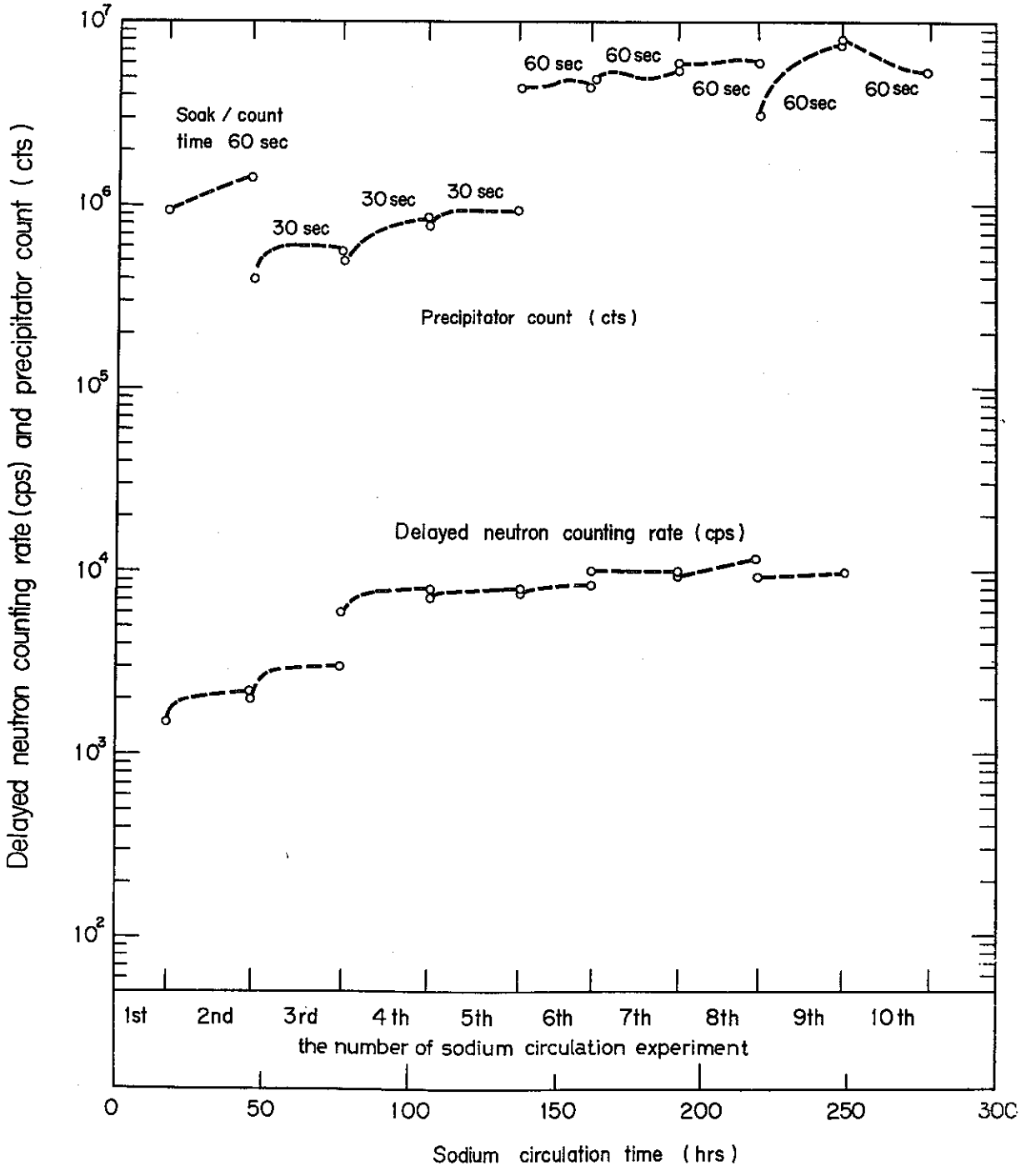

Fig. 4-1 Long-range change of delayed neutron counting rate and precipitator count at stationary conditions of JRR-2 and SIL operation

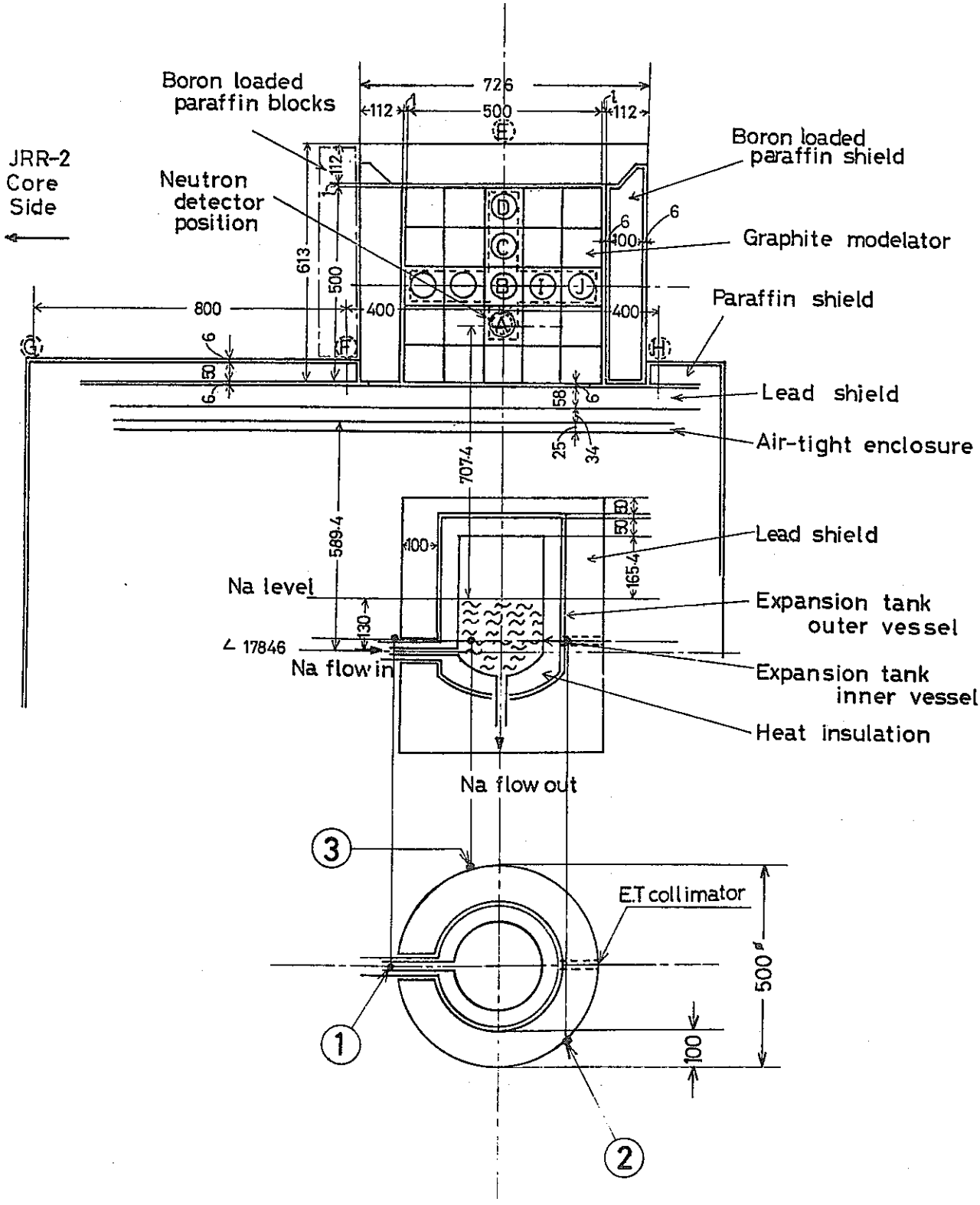

Fig. 4-2 Neutron source positions in the detection efficiency measurement of delayed neutron detection system

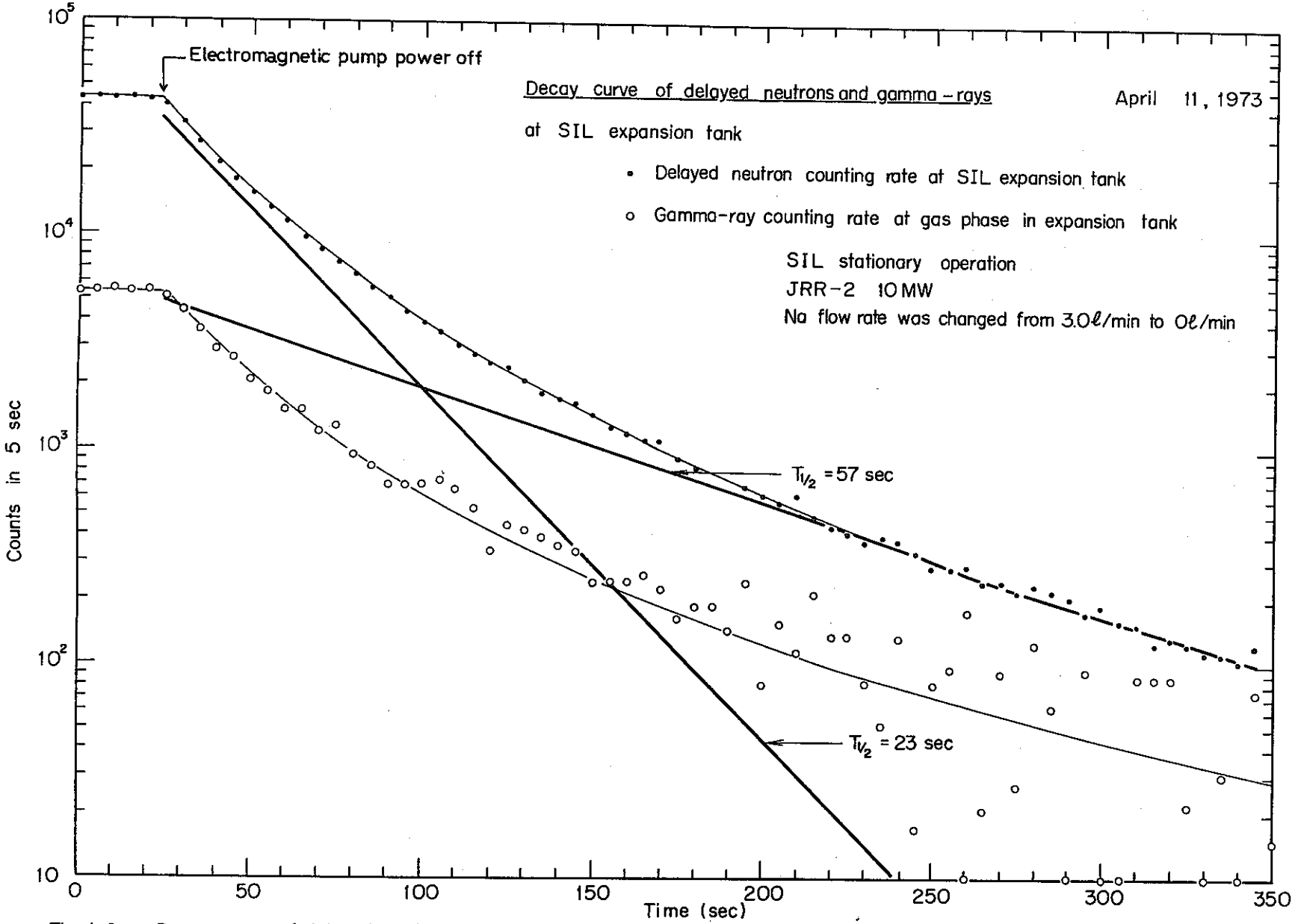

Fig. 4-3 Decay curve of delayed neutron counting rate after Na flow rate change from 3ℓ/min to 0 ℓ/min

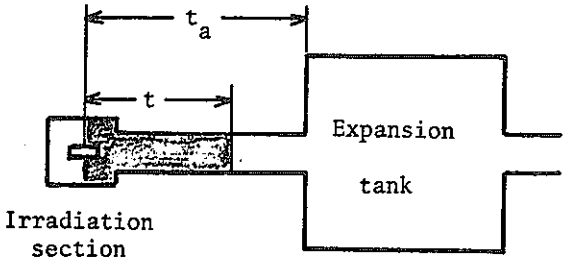

(1) $0 < t < t_a$

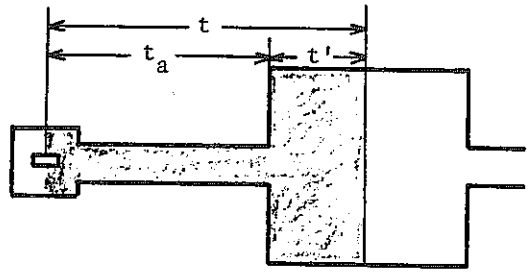

(2) $t_a < t < t_b$

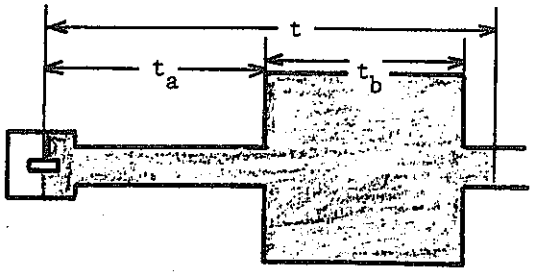

(3) $t_a + t_b < t < t_a + t_c$

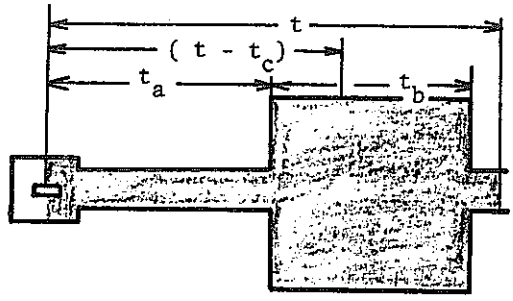

(4) $t_a + t_c < t < t_a + t_b + t_c$

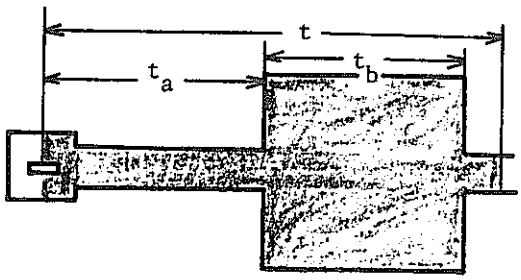

(5) $t > t_a + t_b + t_c$

t_a; sodium travel time from irradiation section to expansion tank inlet

t_b; sodium travel time in expansion tank

t_c; time needed for reactor start-up to reach full power

Fig.4-4 Front positions of delayed neutron emitters in sodium loop at various stages

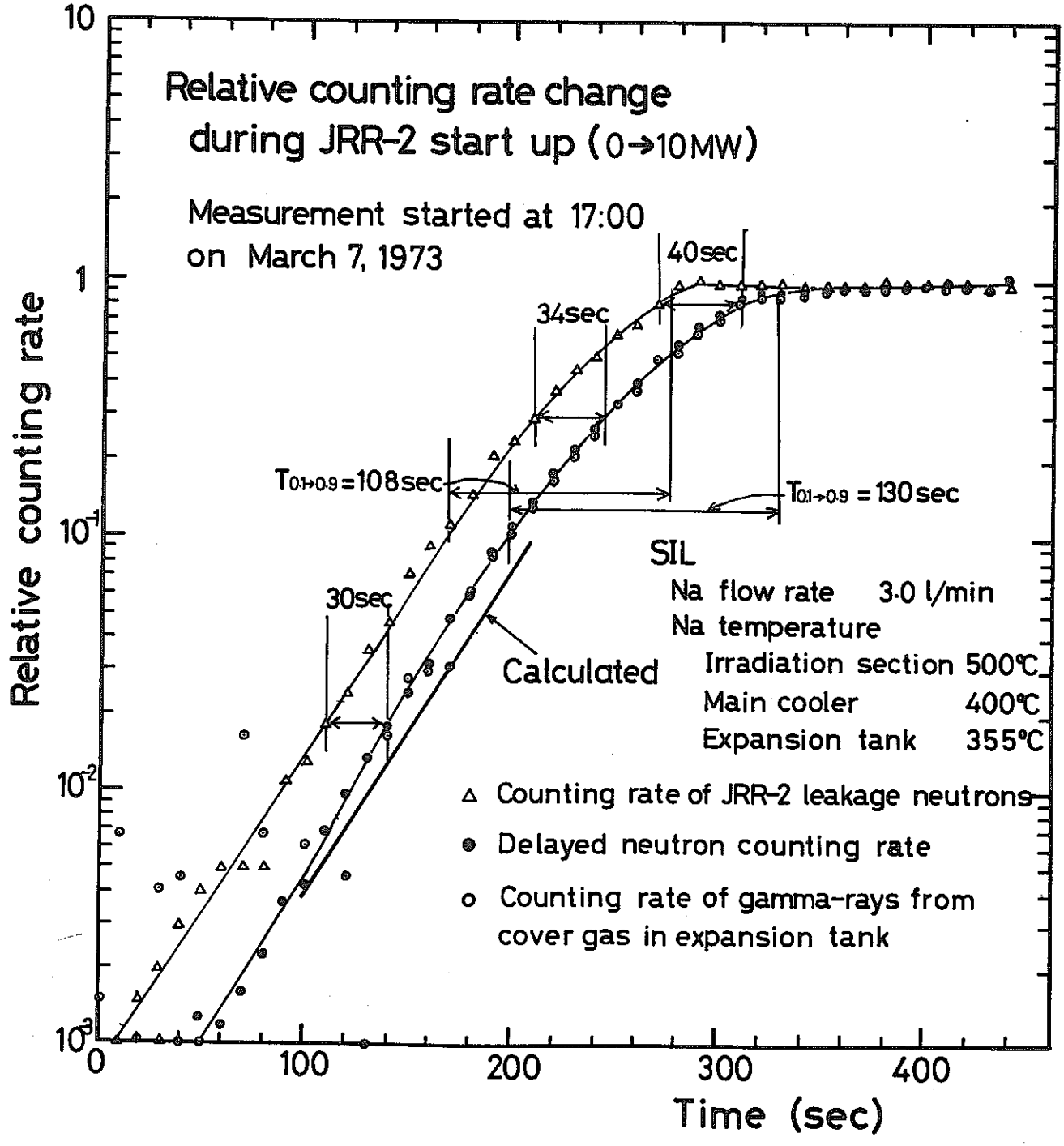

Fig4-5 Relative delayed neutron counting rate change during JRR-2 start up(0→10 MW)

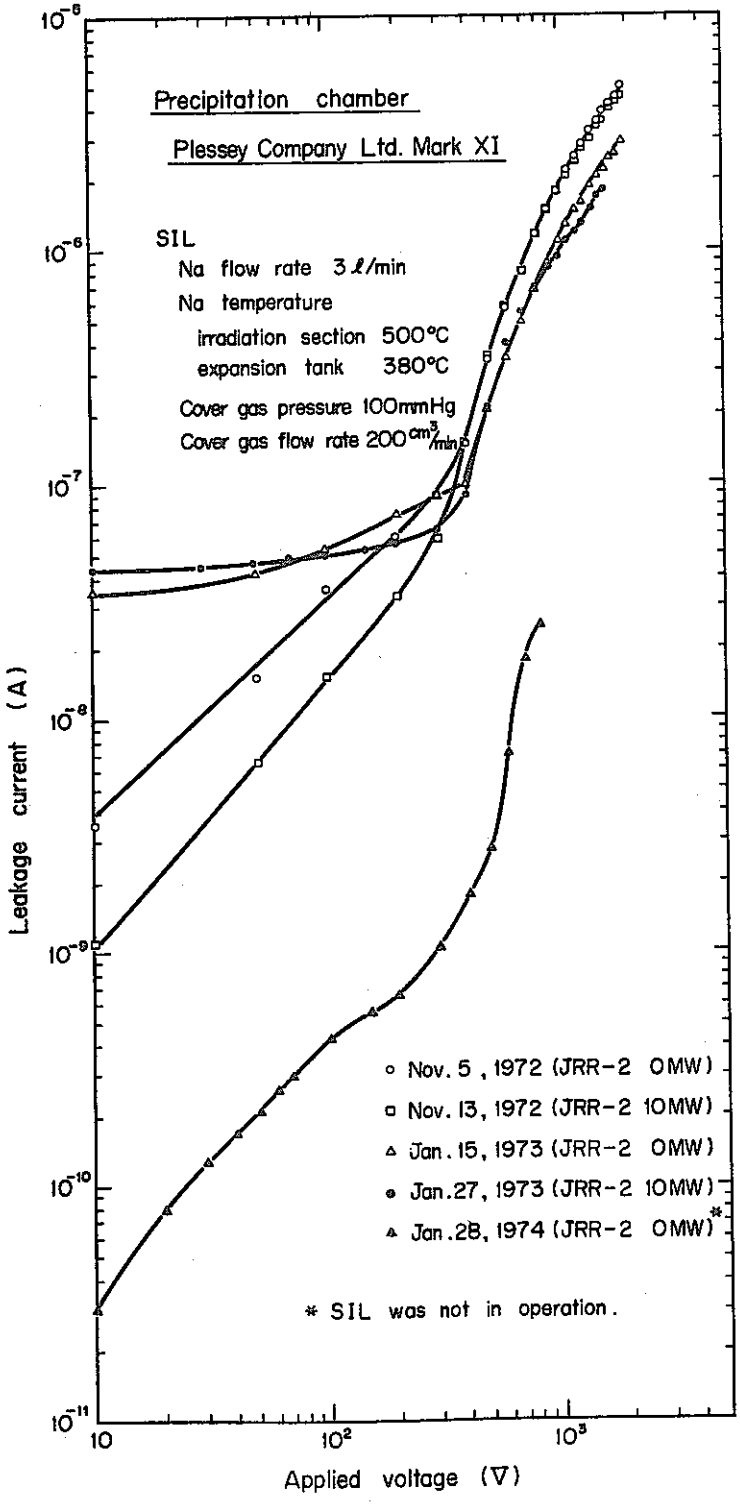

Fig. 5-1 Precipitator leakage current vs. applied voltage characteristics

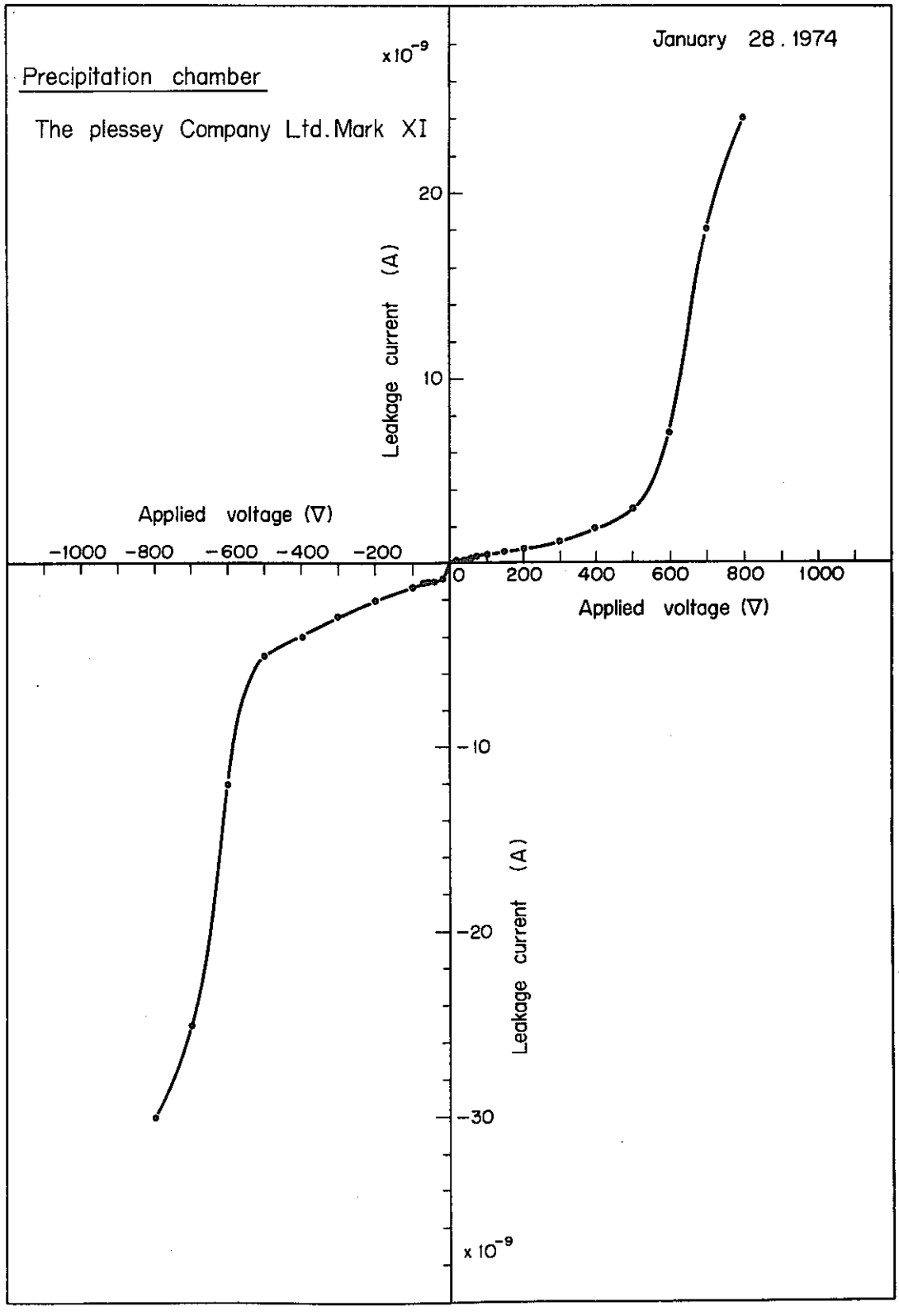

Fig. 5-2 Precipitator leakage current vs. applied voltage characteristics

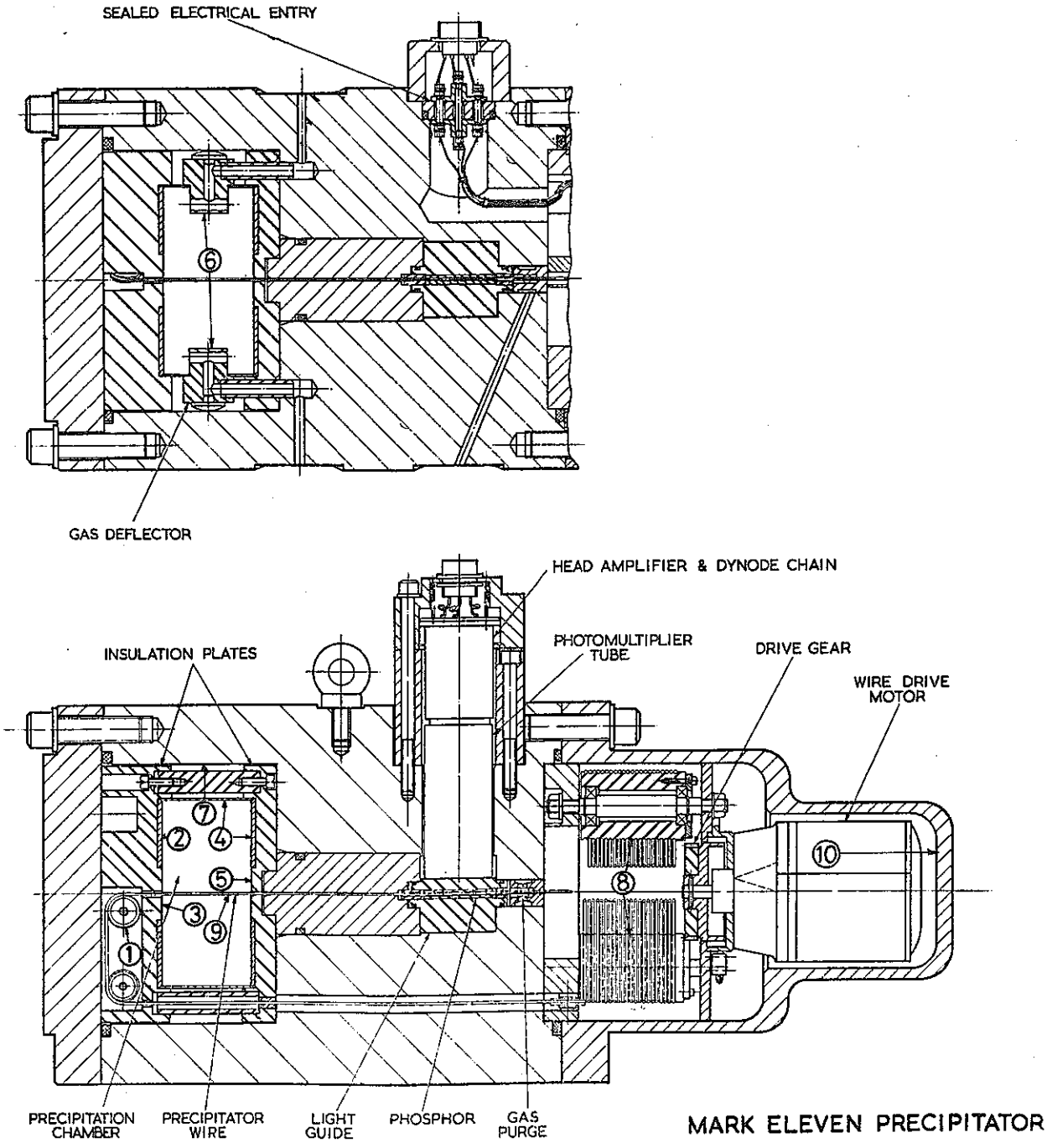

Fig.5-3 Sampled positions in the precipitator for measuring the amount of sodium deposition

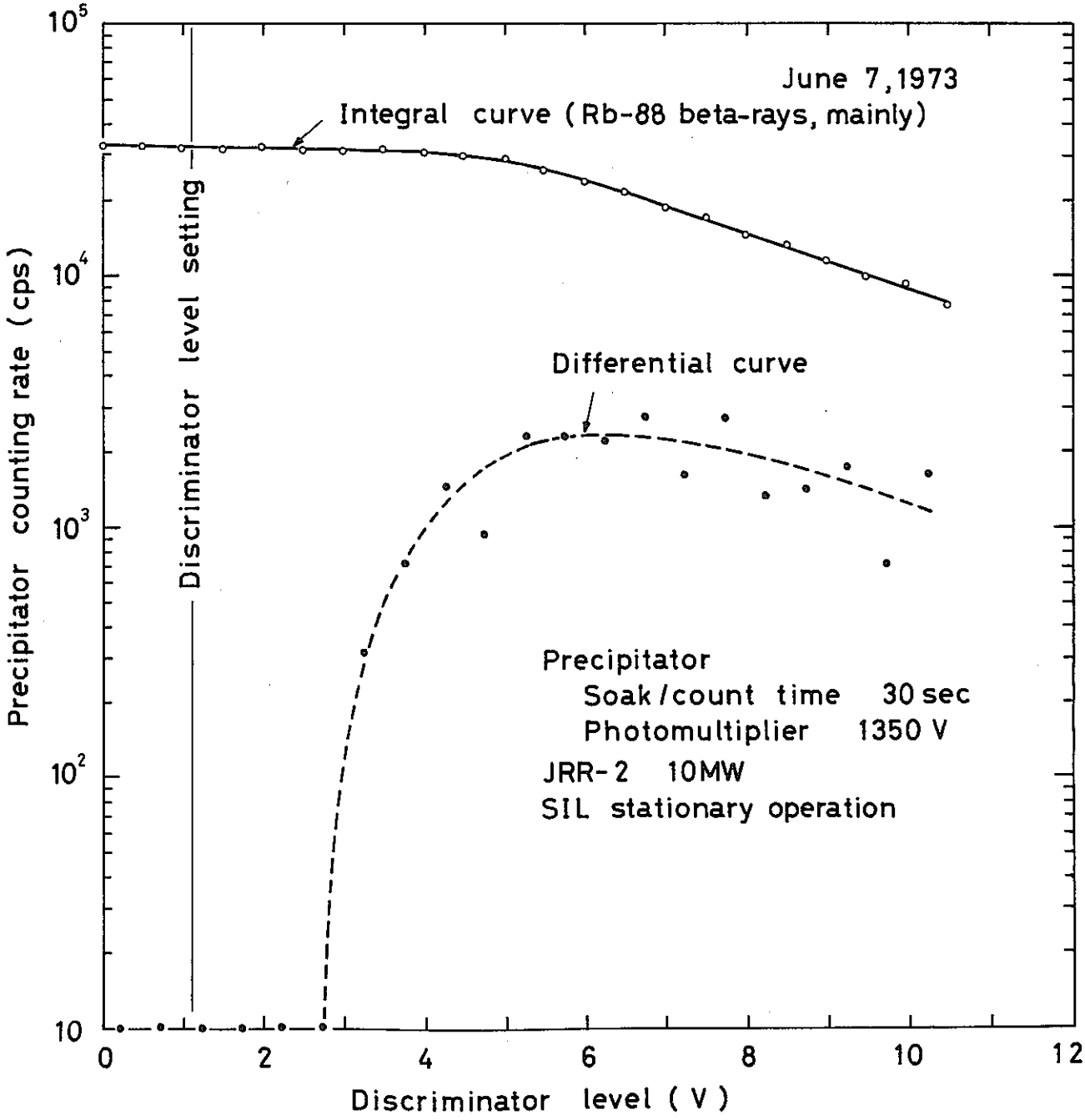

Fig.5-4 Discrimination curve of precipitator counting rate (photomultiplier voltage 1350 V)

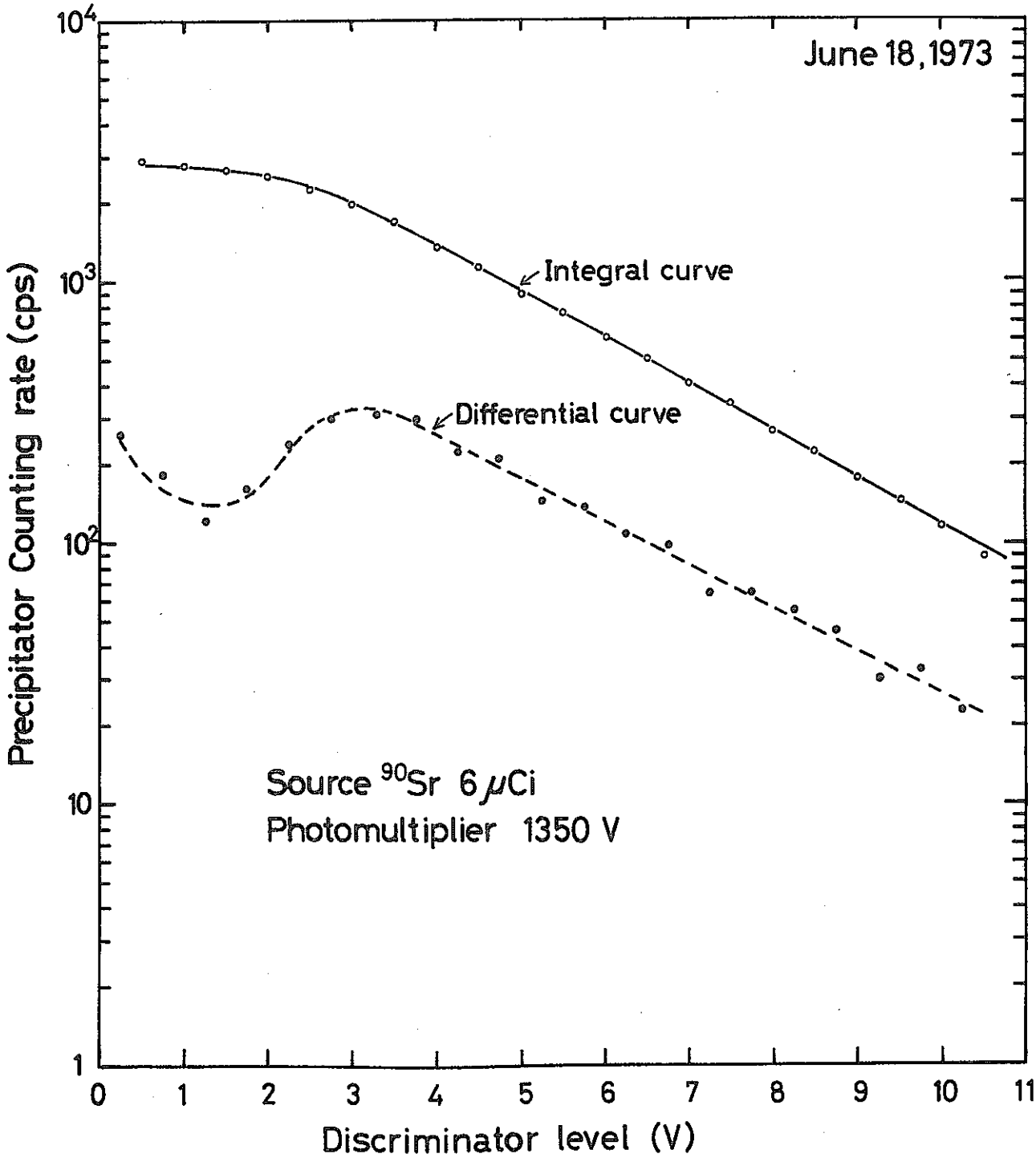

Fig. 5-5 Discriminator curve of precipitator counting rate for Sr-90 (Photomultiplier voltage 1350 V)

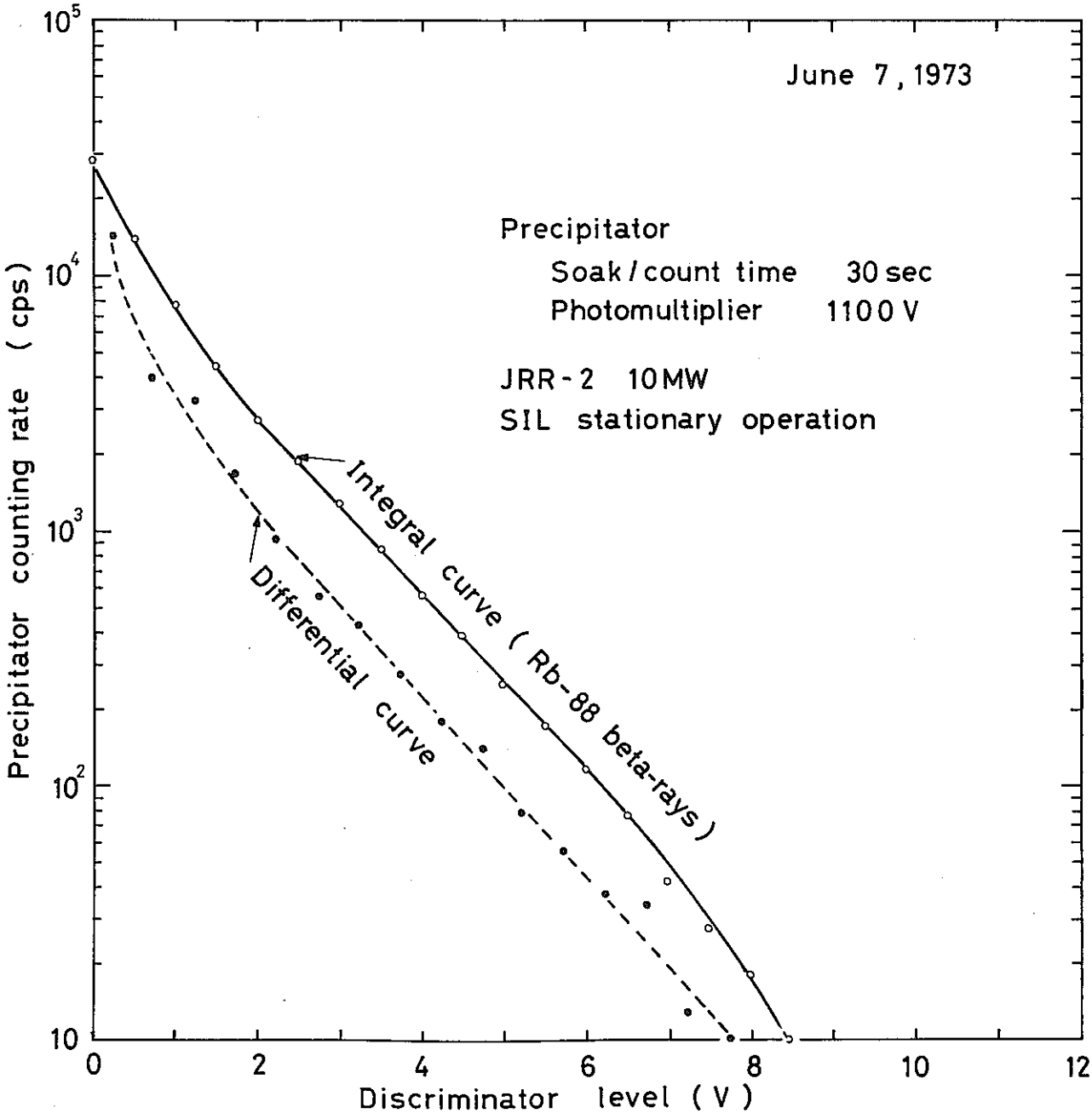

Fig.5-6 Discrimination curve of precipitator counting rate (photomultiplier voltage 1100V)

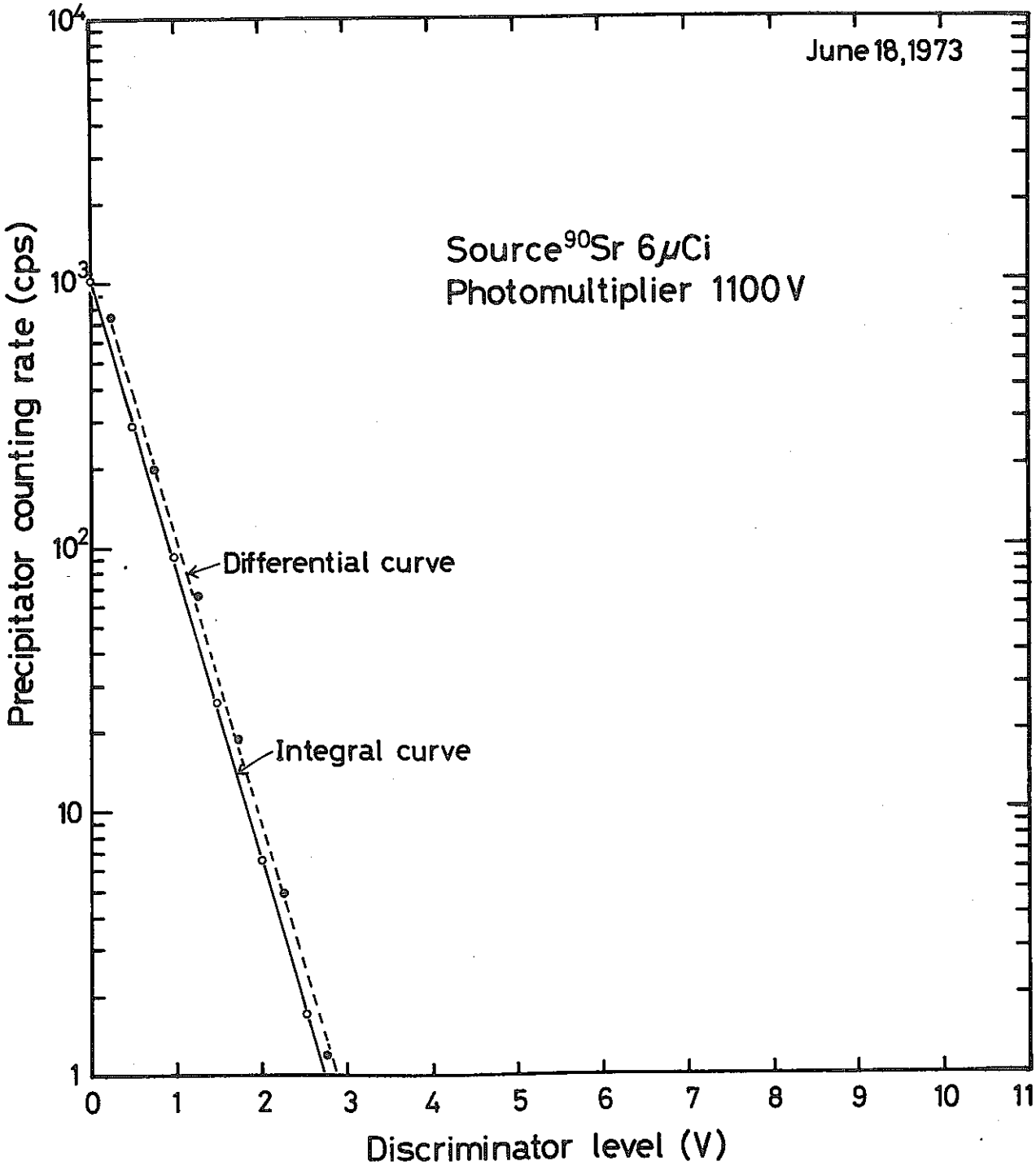

Fig.5-7 Discriminator curve of precipitator counting rate for Sr-90 (Photomultiplier voltage 1100 V)

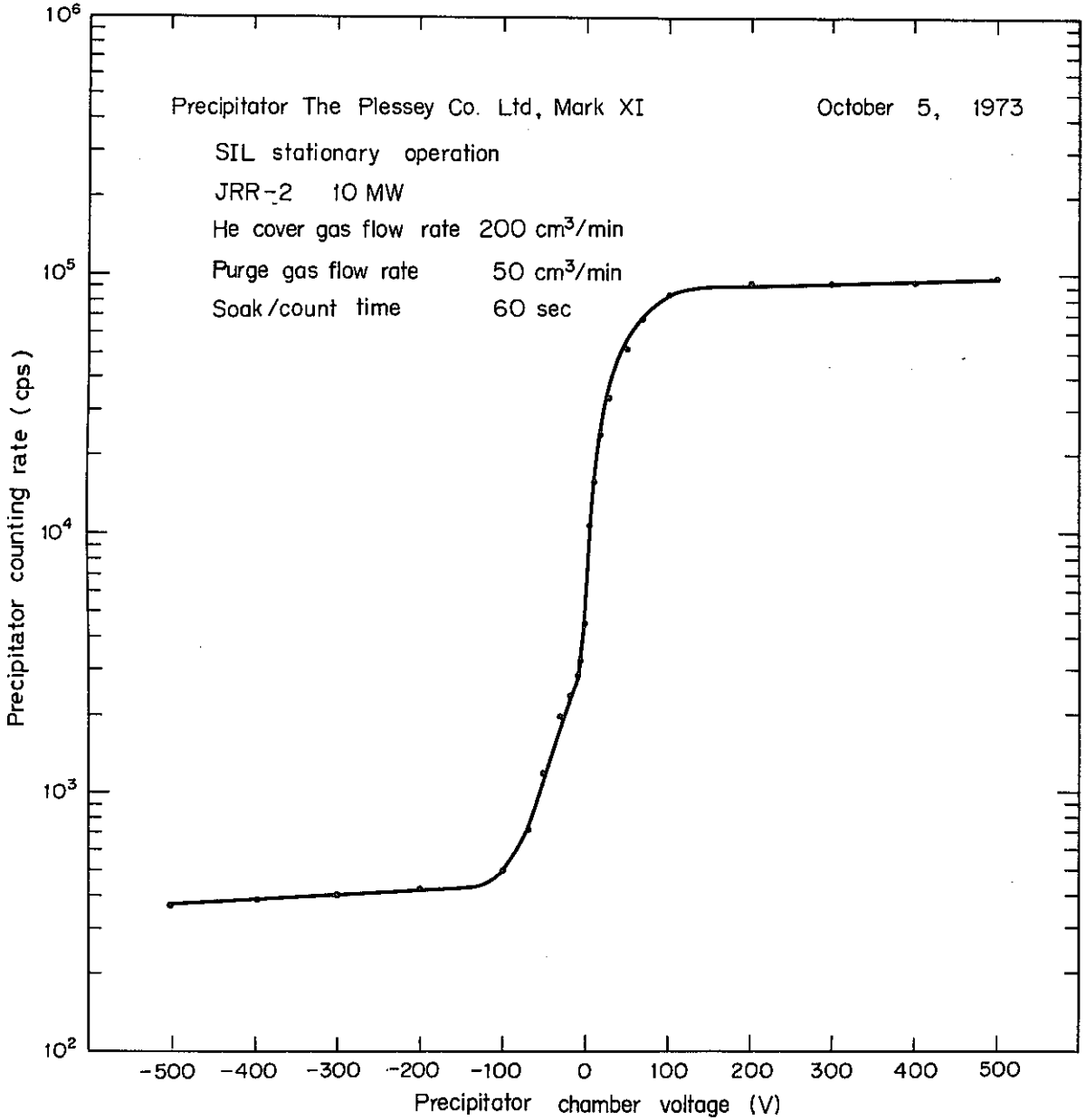

Fig.5-8 Precipitator counts vs. chamber voltage characteristics

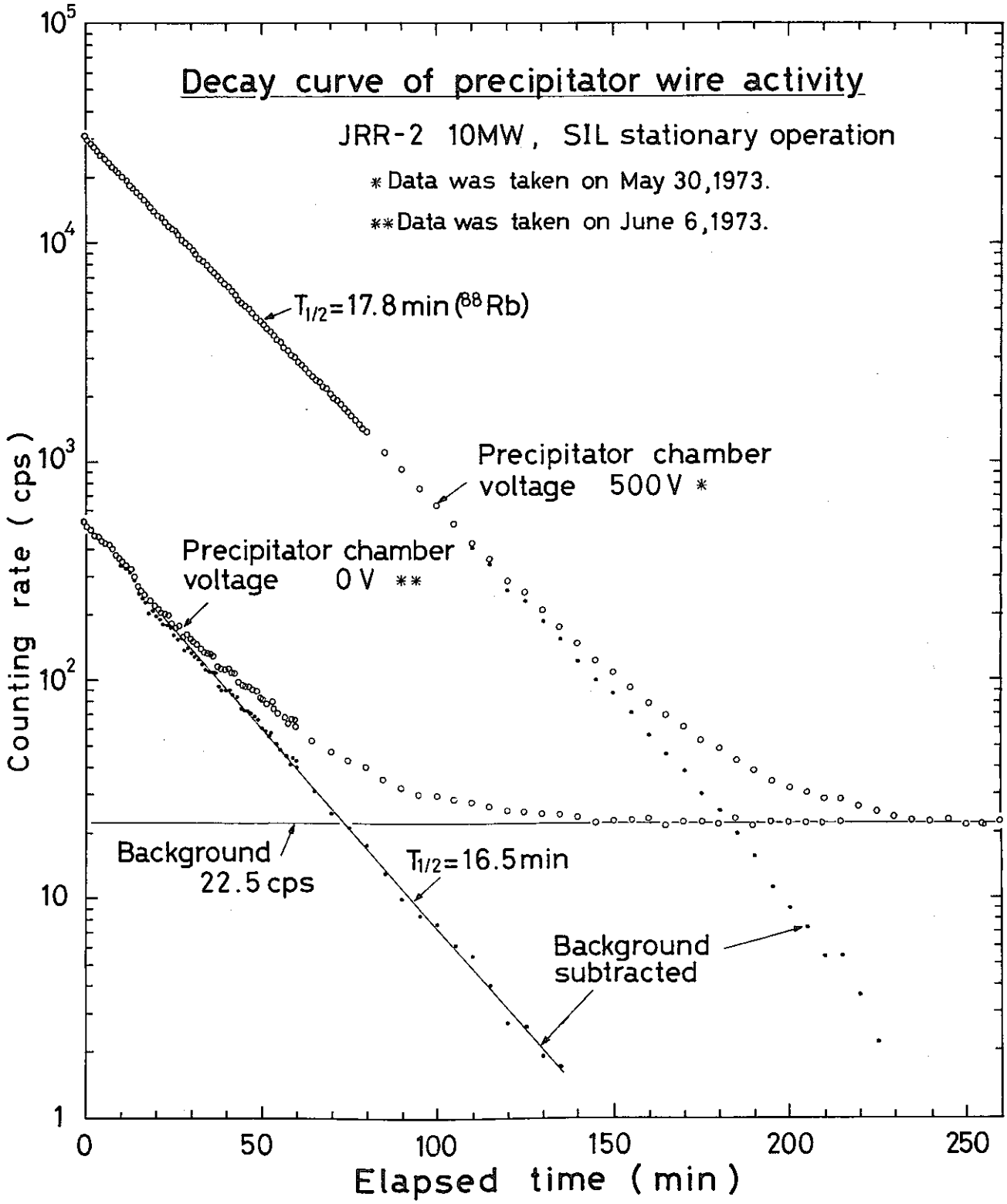

Fig.5-9 Decay curve of precipitator wire radioactivity

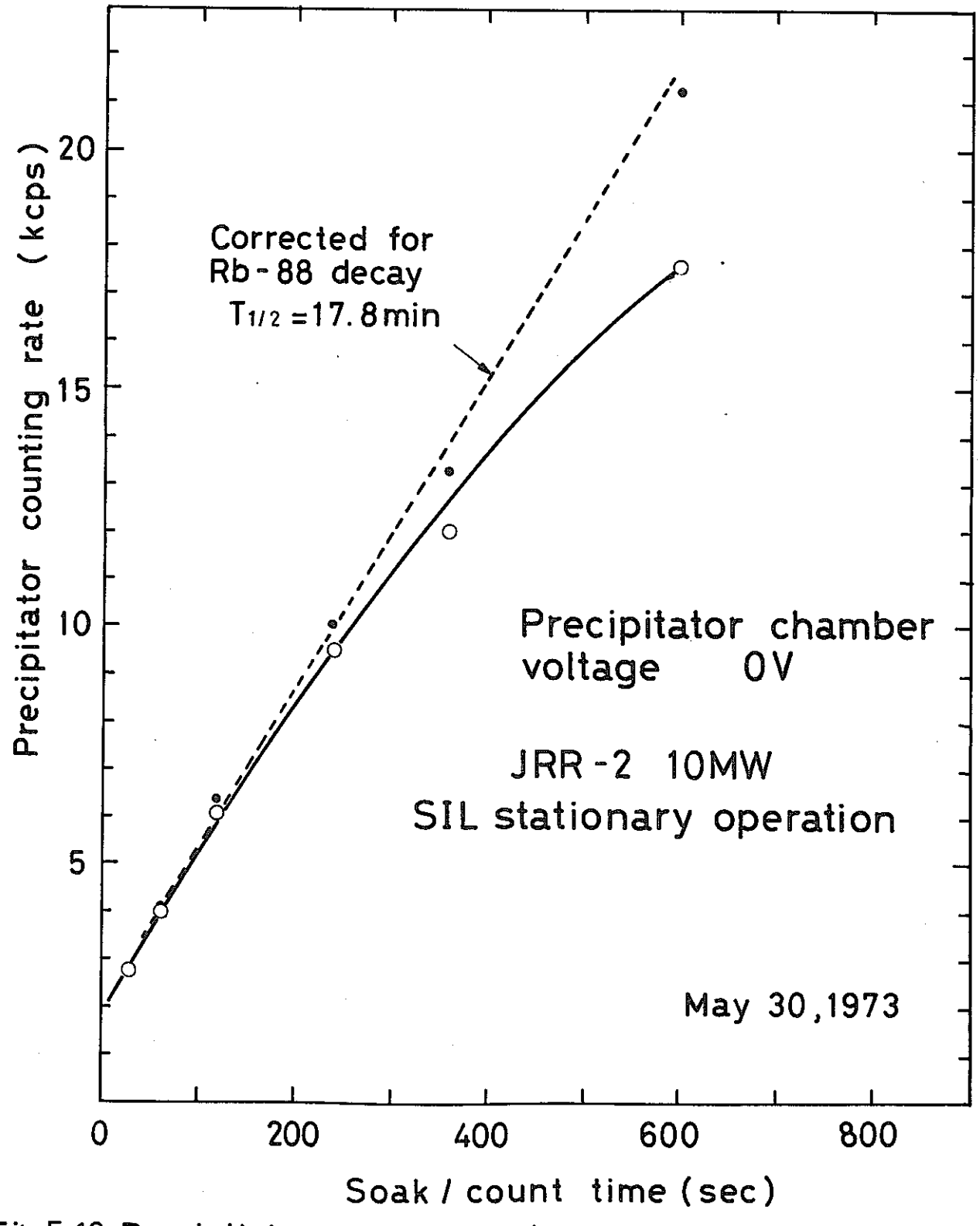

Fig.5-10 Precipitator counting rate -vs- soak/count time characteristics (precipitator chamber 0V)

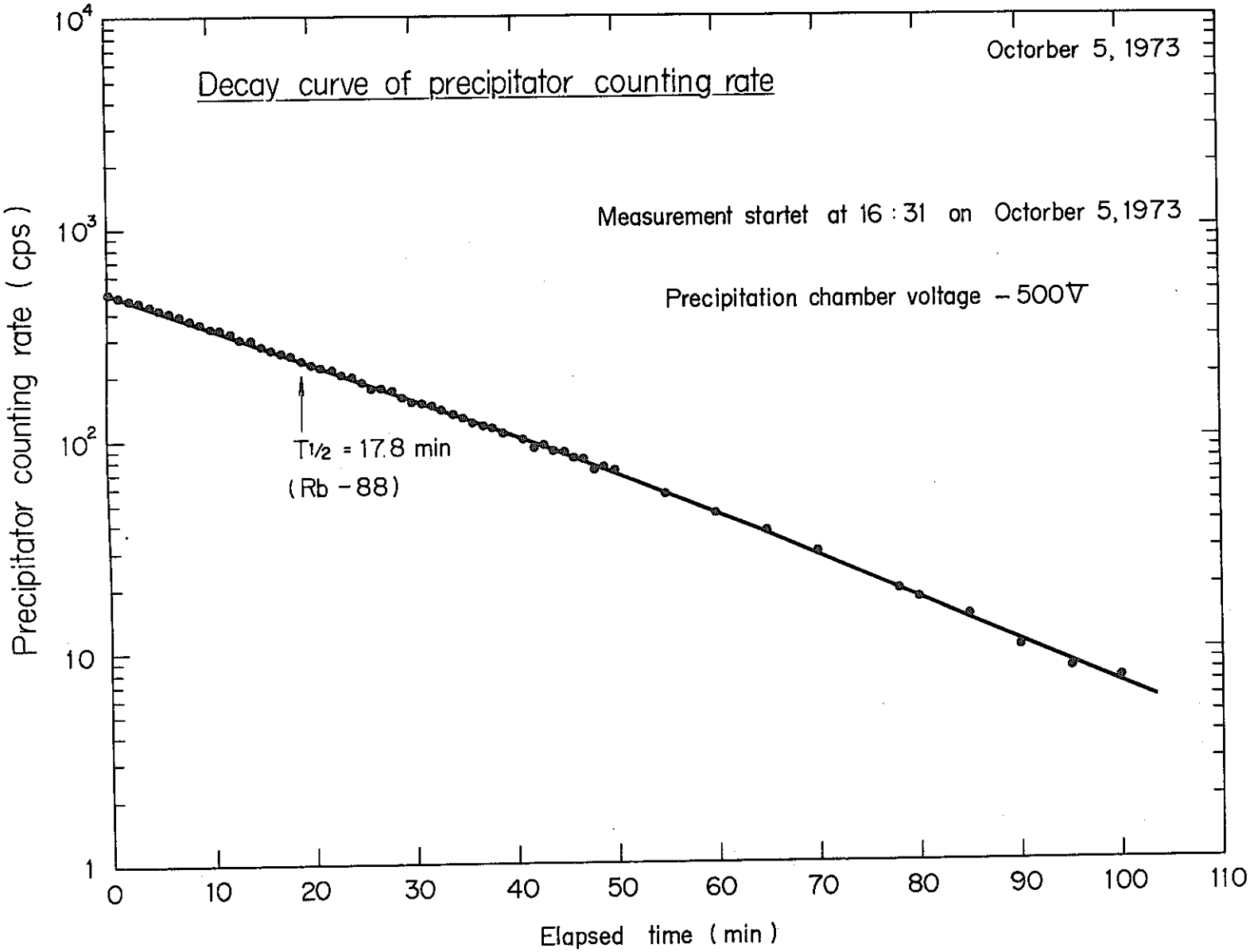

Fig. 5-11 Decay curve of precipitator wire radioactivity at precipitation chamber voltage-500V.

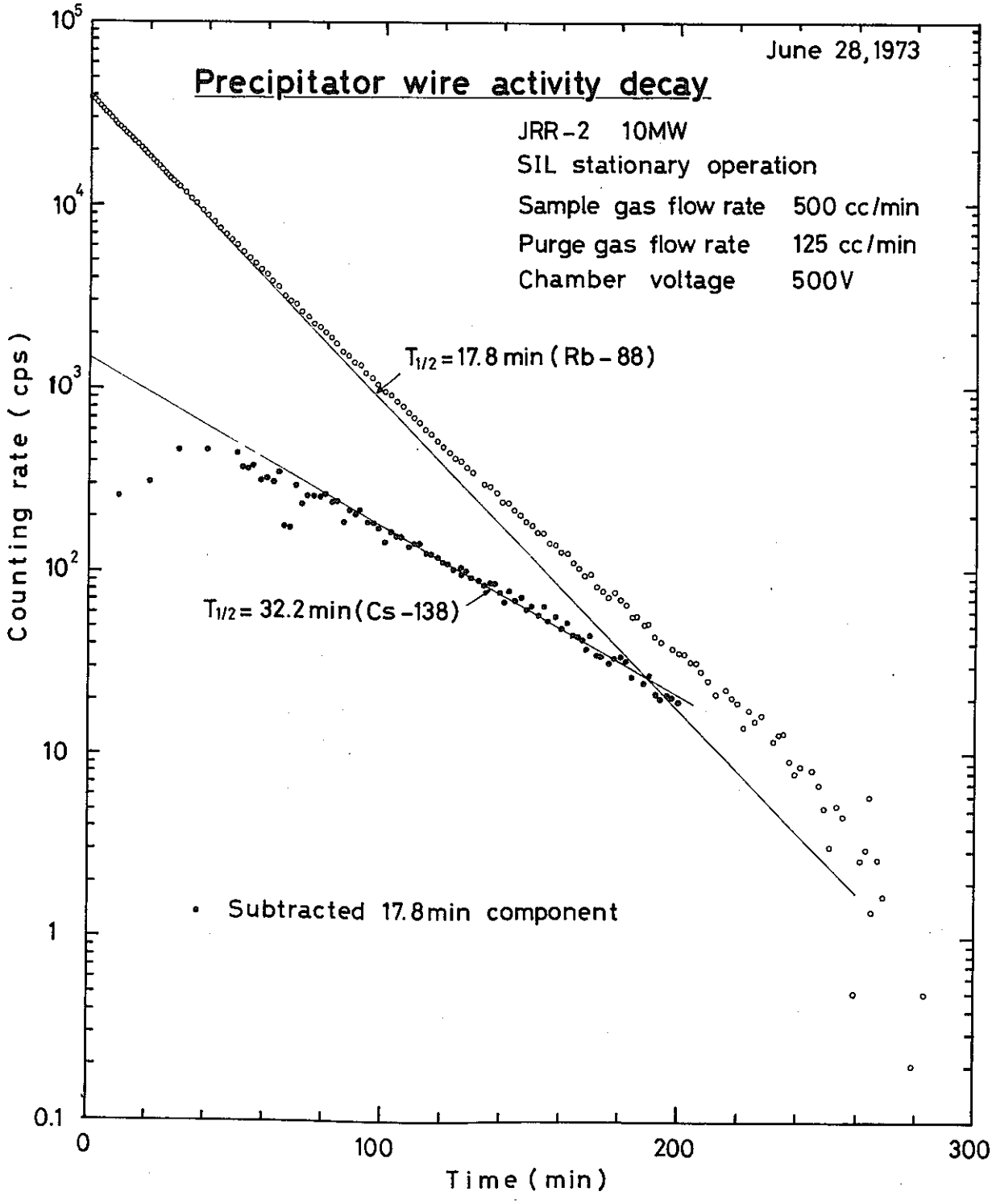

Fig.5-12 Activity decay of precipitator wire (500cc/min)

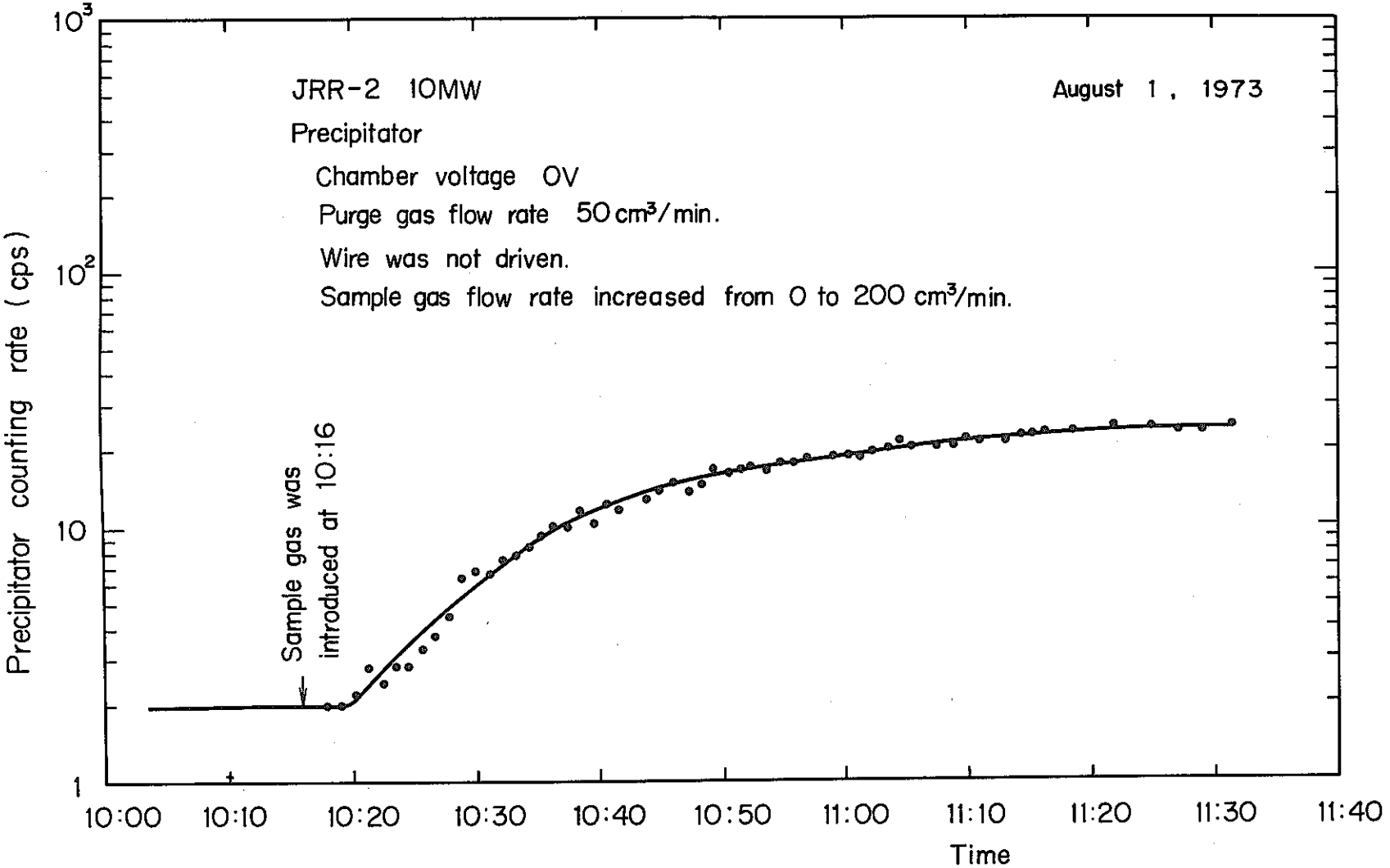

Fig.5–13 Change in precipitator counting rate after sample gas was introduced into precipitator chamber with OV and with no wire driven.

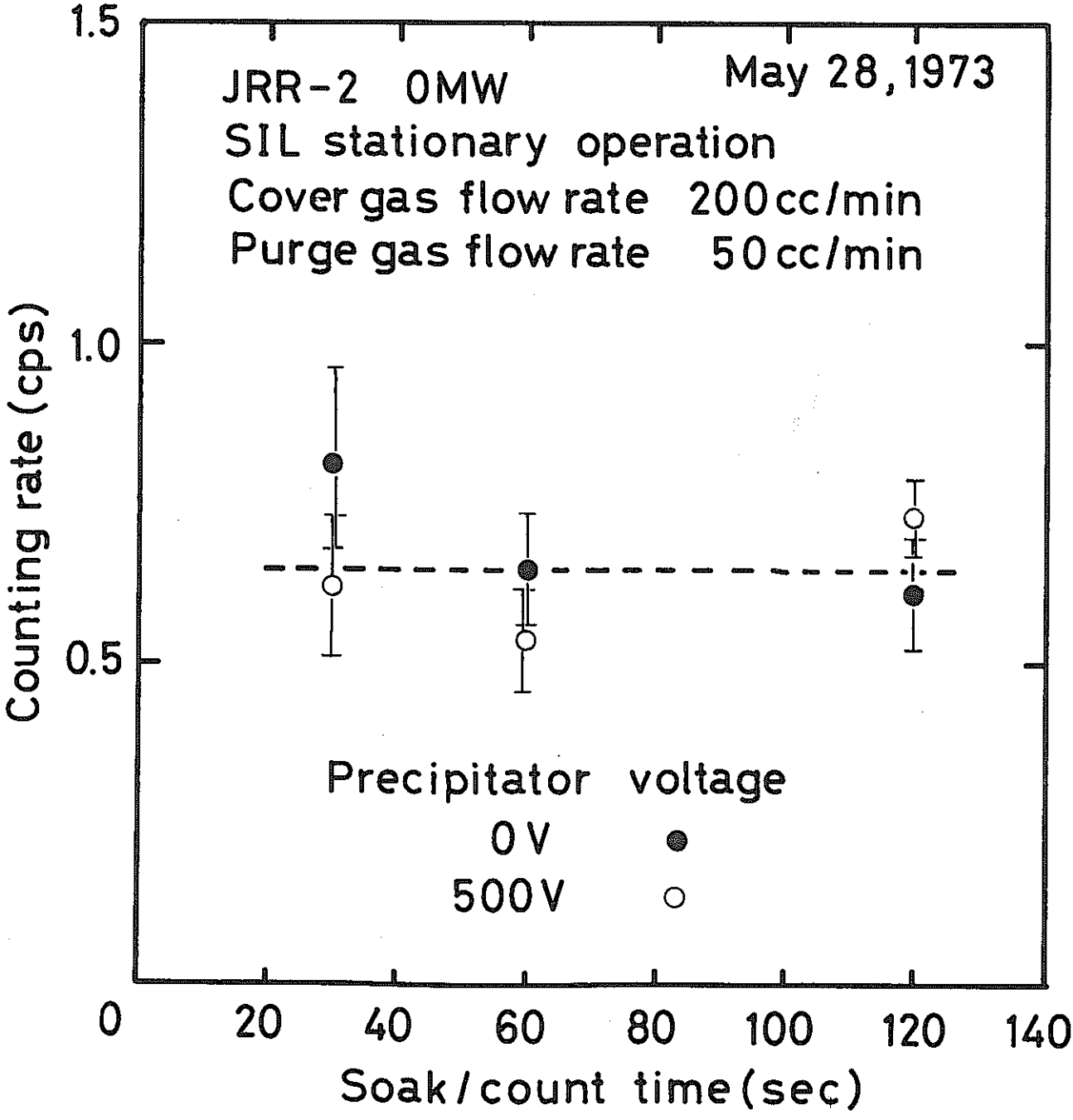

Fig.5-14 Precipitator background counting rate vs soak/count time characteristics

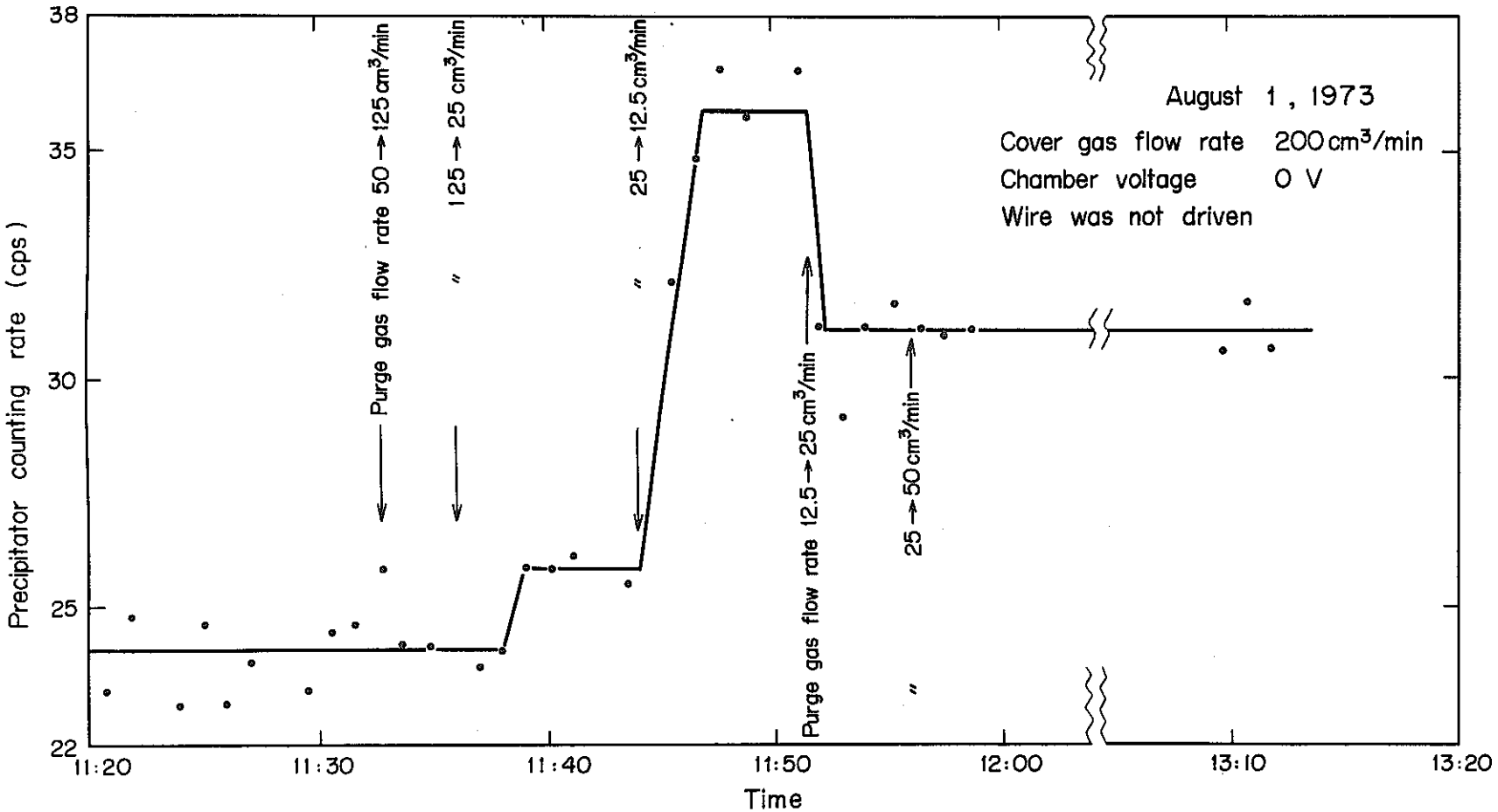

Fig. 5-15 Change in precipitator counting-rate when purge gas flow rate was changed

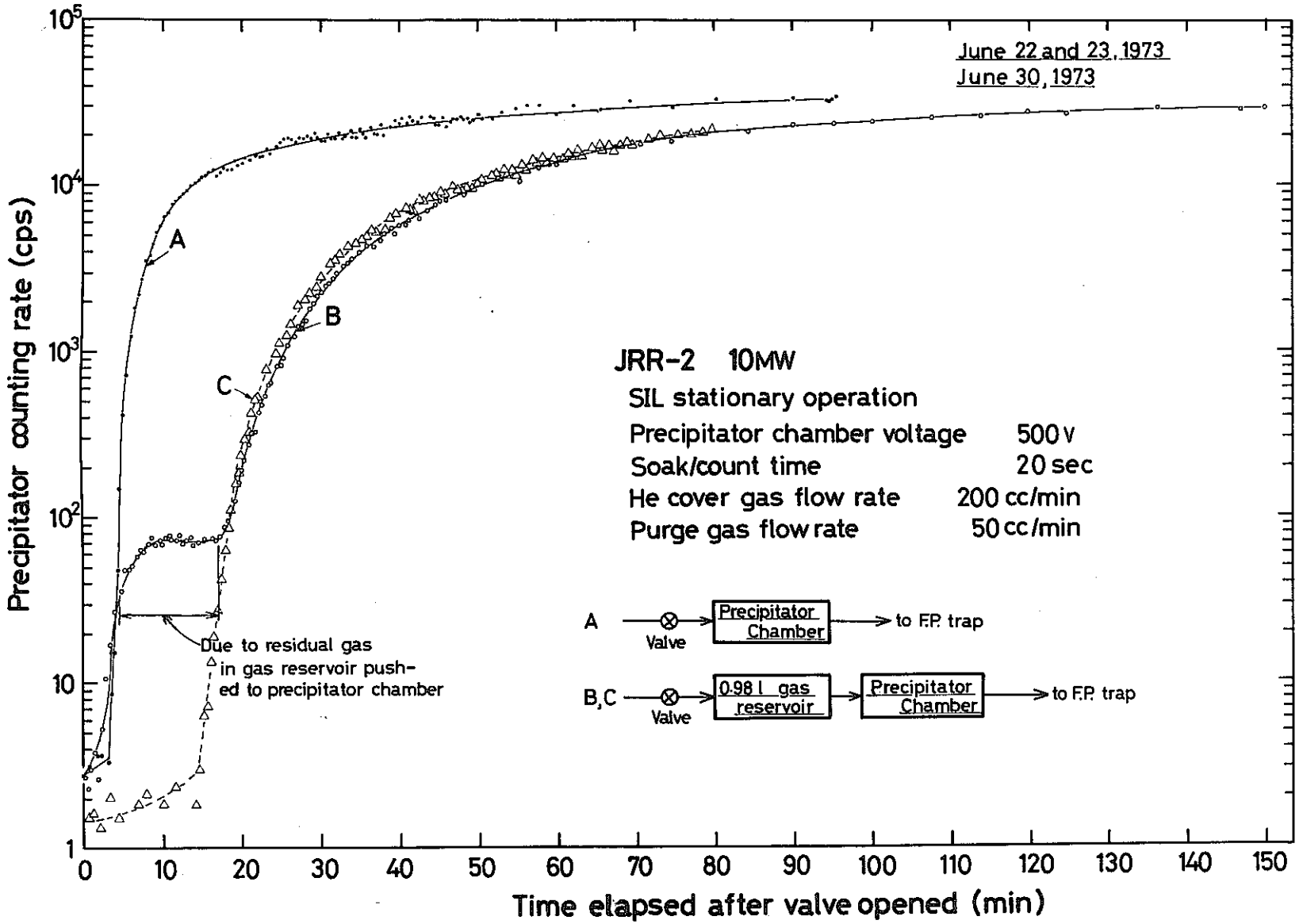

Fig.5-16 Precipitator counting rate change after valve was opened

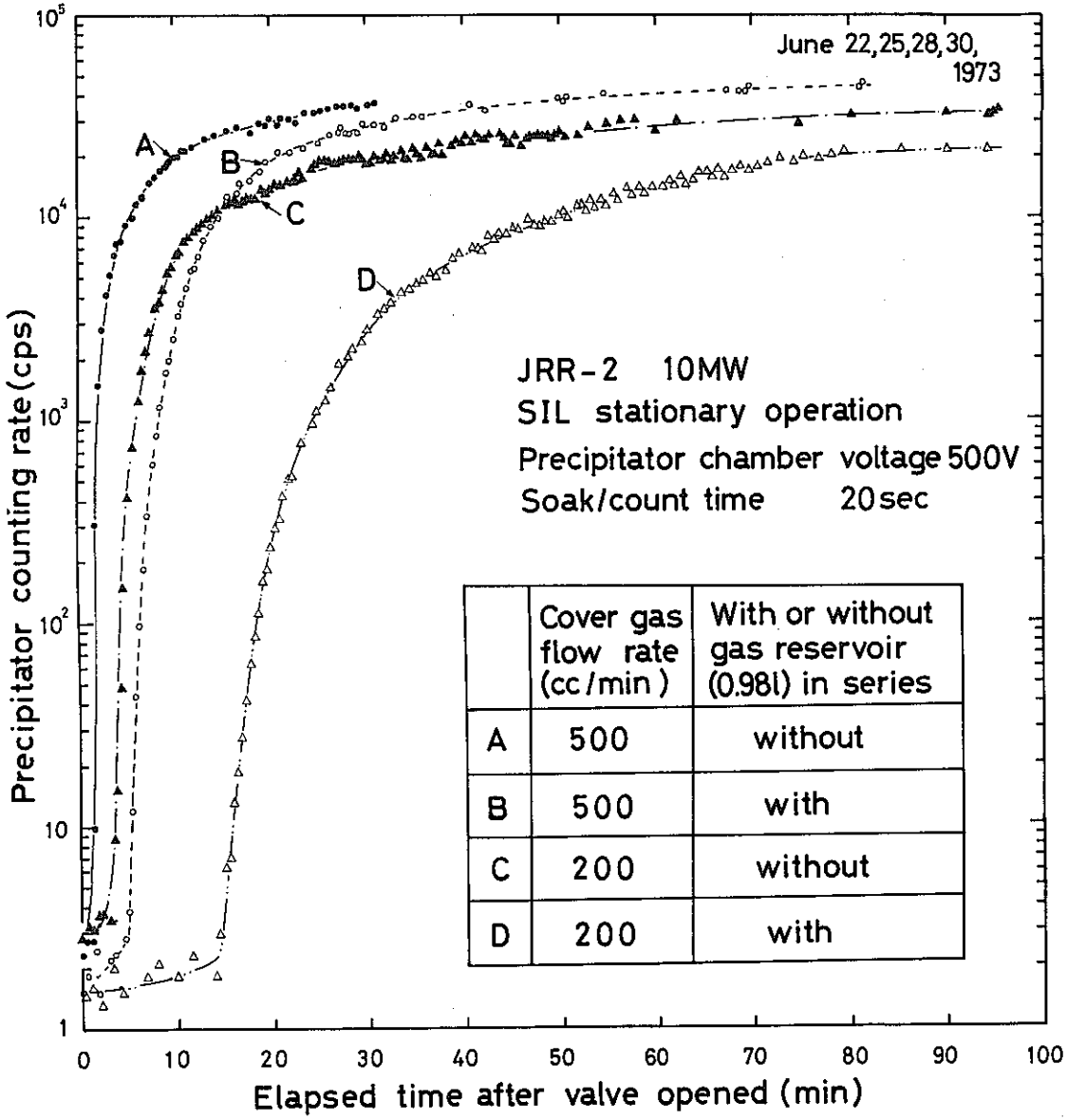

	Cover gas flow rate (cc/min)	With or without gas reservoir (0.98l) in series
A	500	without
B	500	with
C	200	without
D	200	with

Fig.5-17 Precipitator counting rate change after valve was opened

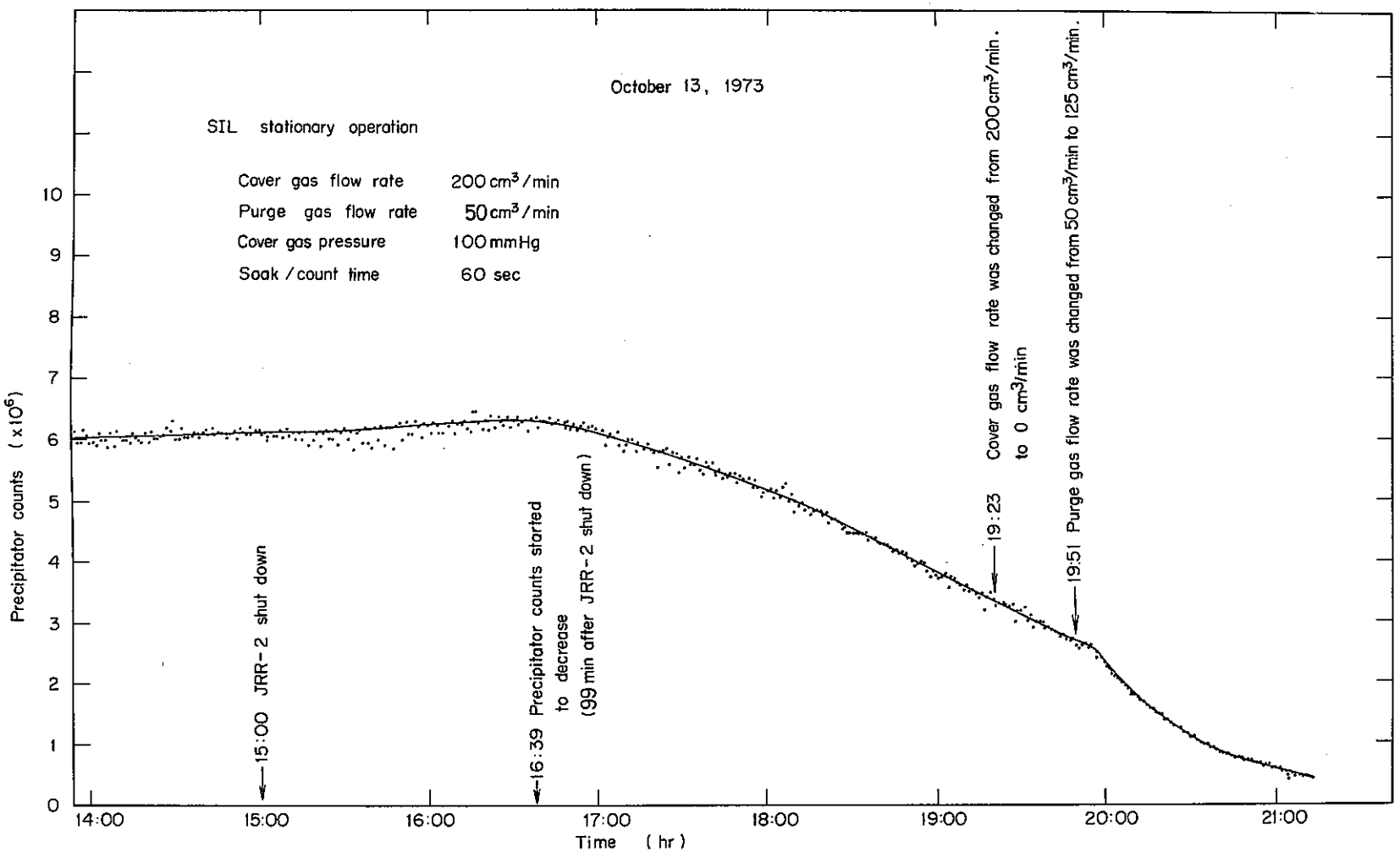

Fig.5-18 Precipitator counts change during JRR-2 shut down

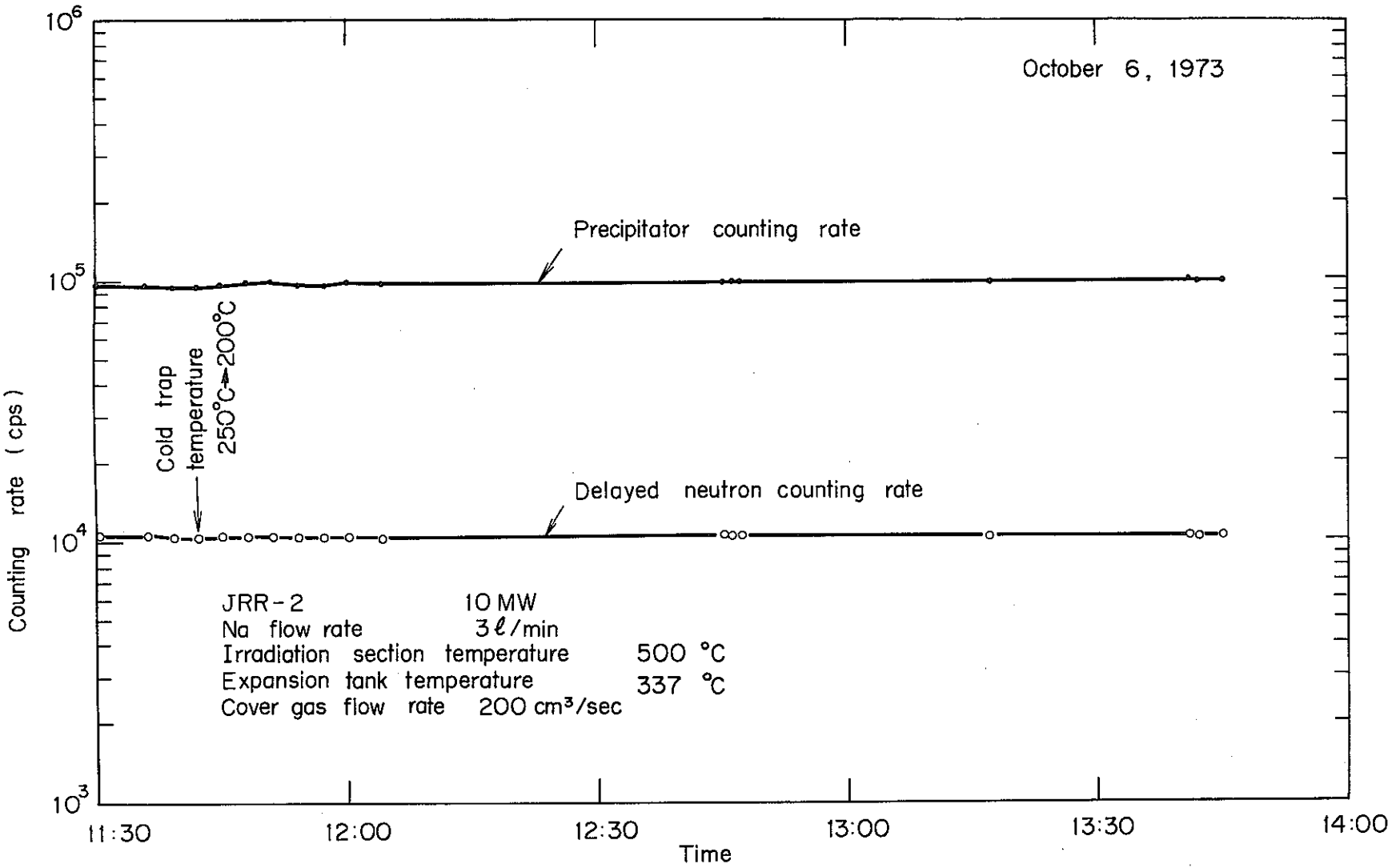

Fig. 5-19 Counting – rate change during cold trap temperature change

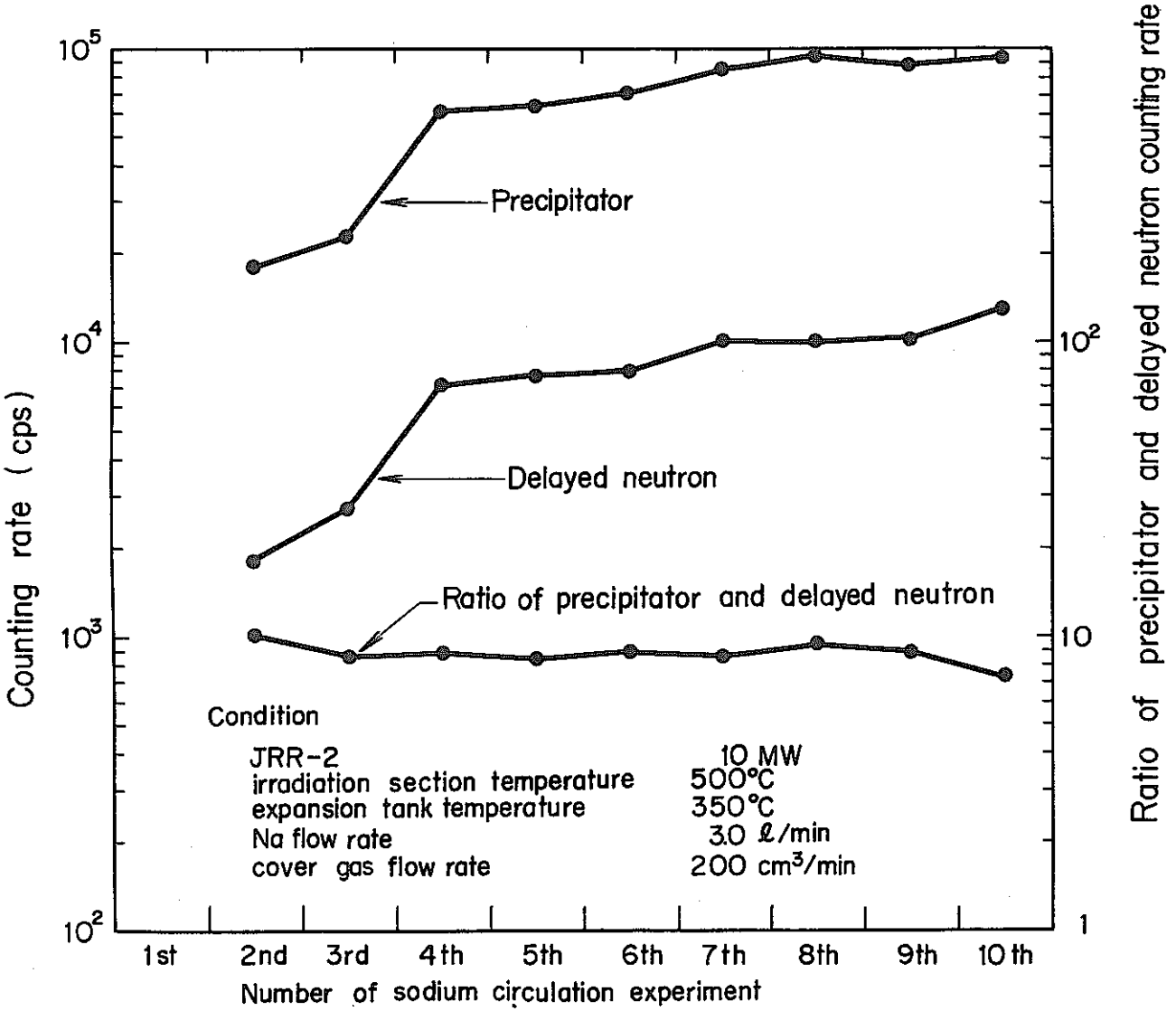

Fig. 5-20 Long-range counting-rate change of delayed neutron and precipitator detection systems

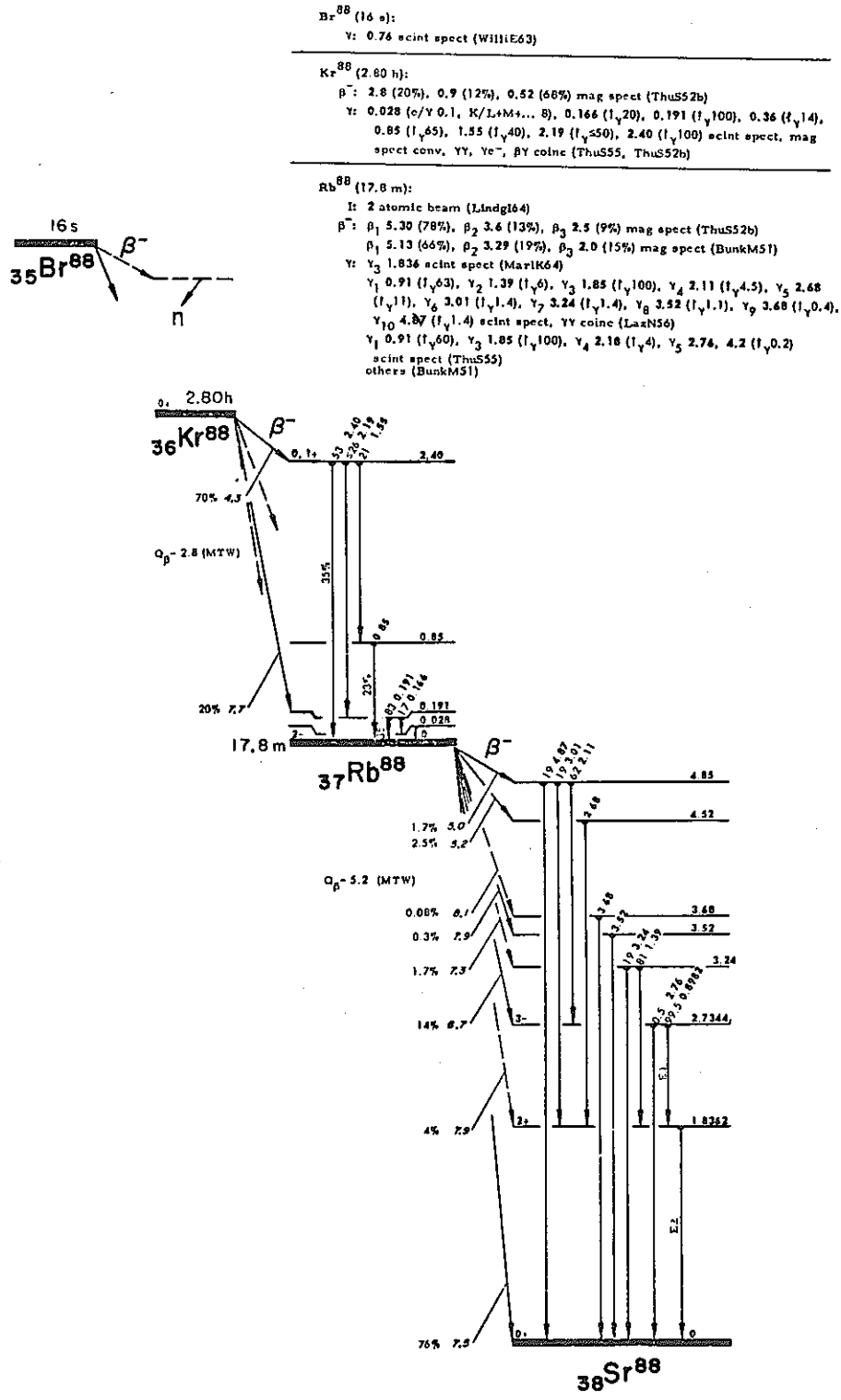

Fig.6-1 Decay scheme of Br-88, Kr-88, and Rb-88
(From Lederer, et al. Table of Isotopes 6th ed., John Wiley & Sons, Inc, 1968)

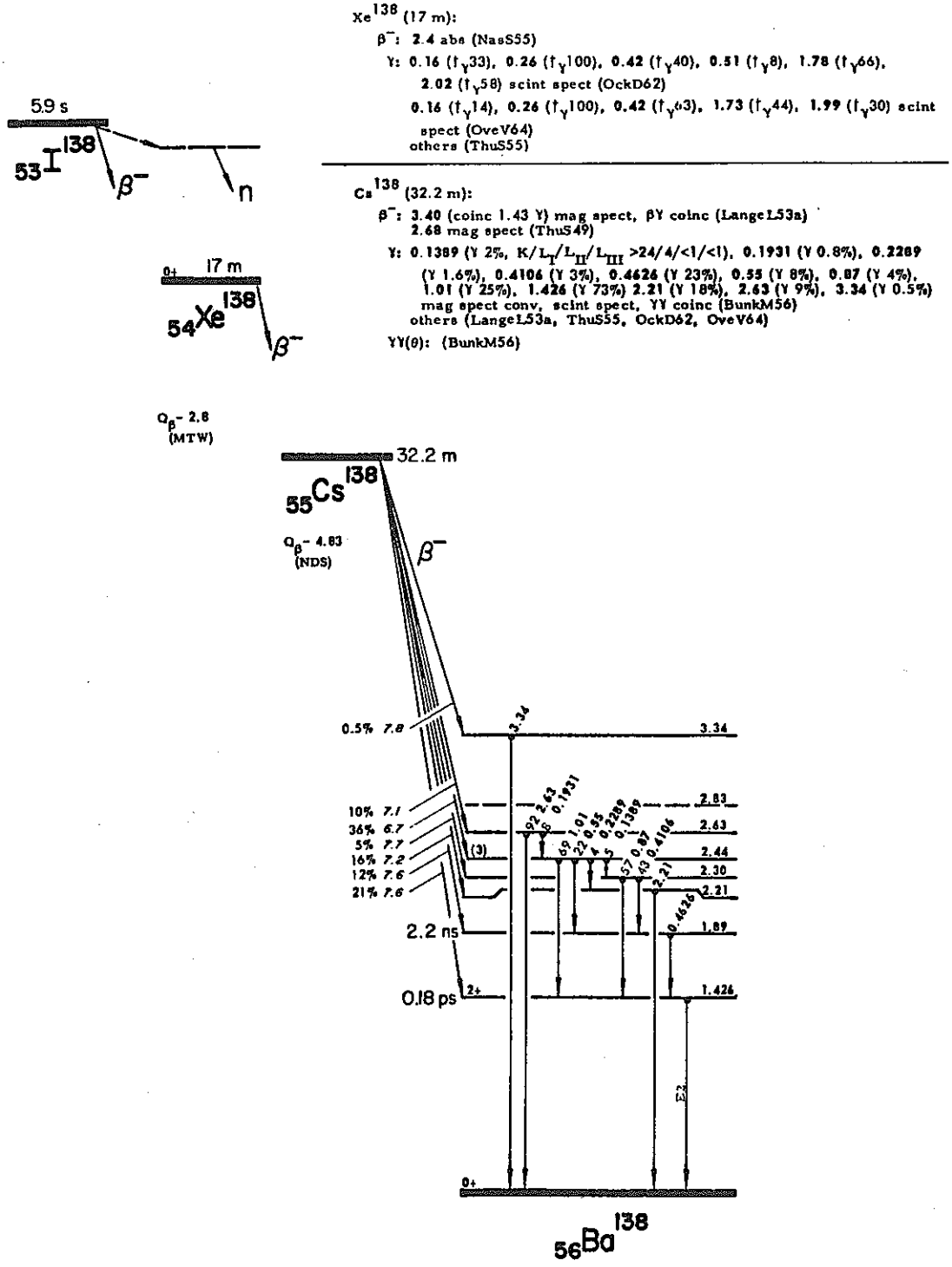

Fig.6-2 Decay scheme of I-138, Xe-138 and Cs-138
(From Lederer, et al, Table of Isotopes, 6th ed., John Wiley & Sons, Inc, 1968)

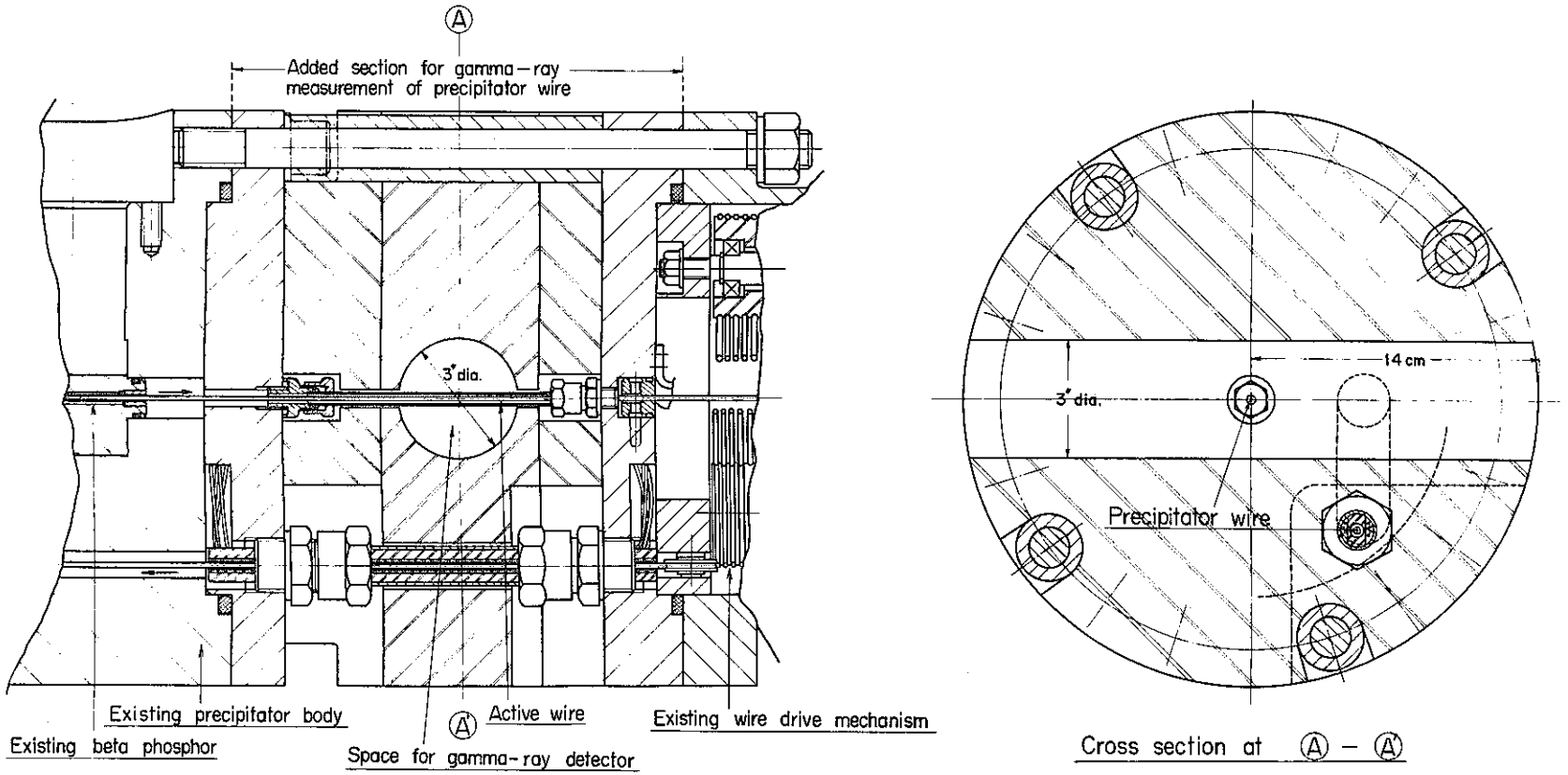

Fig.6-3 Added section for gamma-ray measurement of precipitator wire
(The Plessey Co., Ltd. Mark XI)

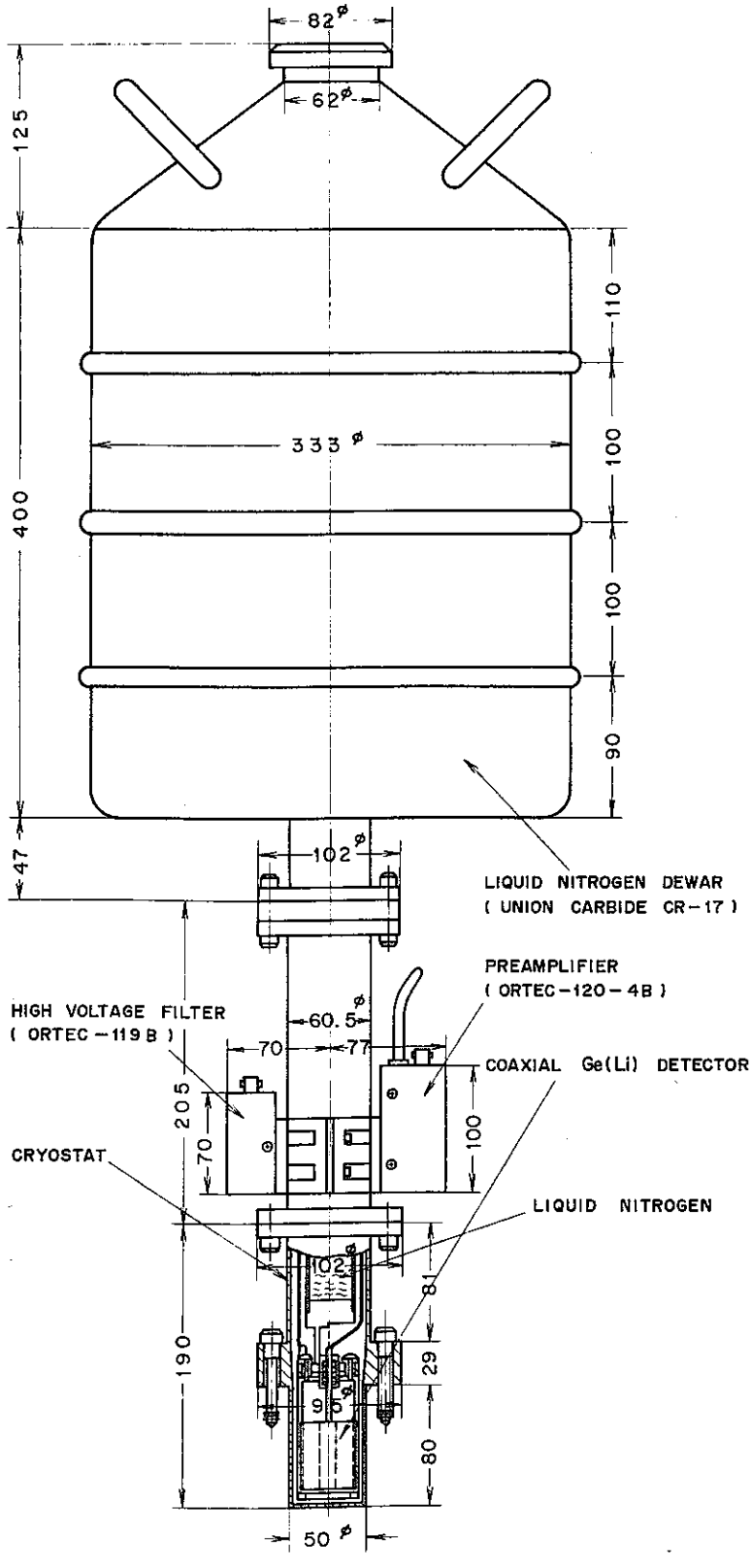

Fig.6-4 Ge (Li) detector, cryostat and Dewar

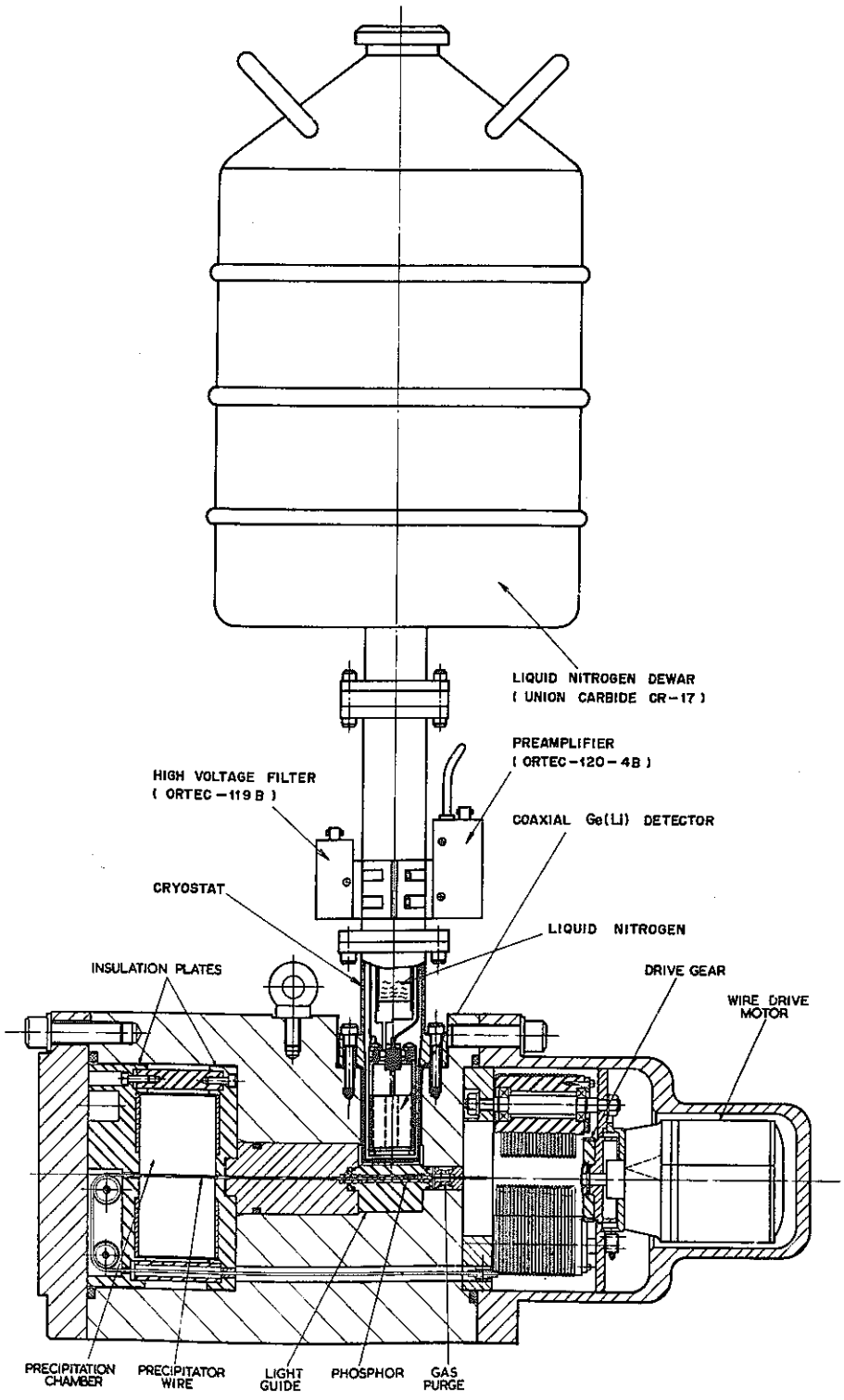

Fig.6-5 Precipitator with Ge(Li) detector for measuring gamma-rays from precipitator wire

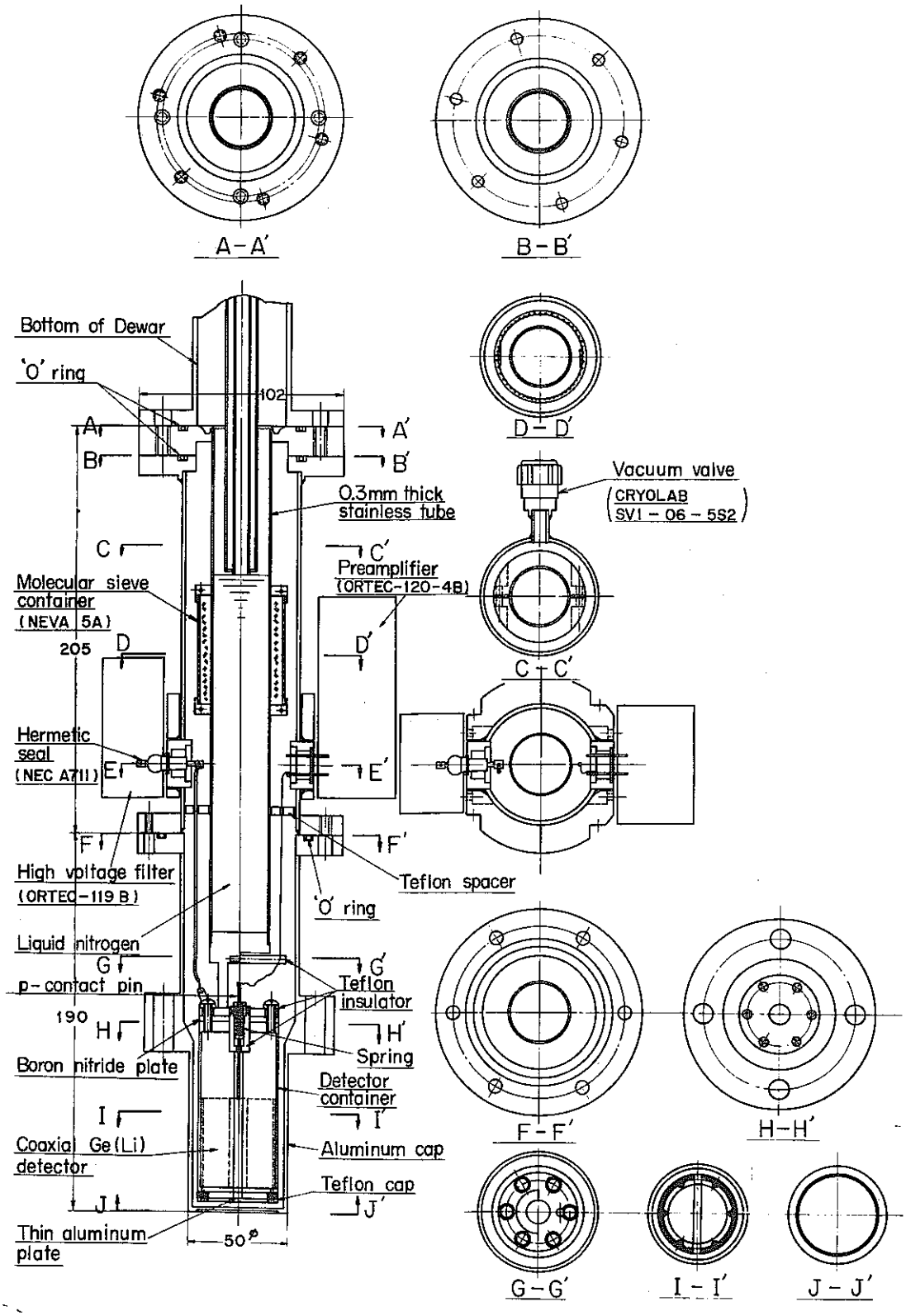

Fig. 6-6 Cross section of cryostat

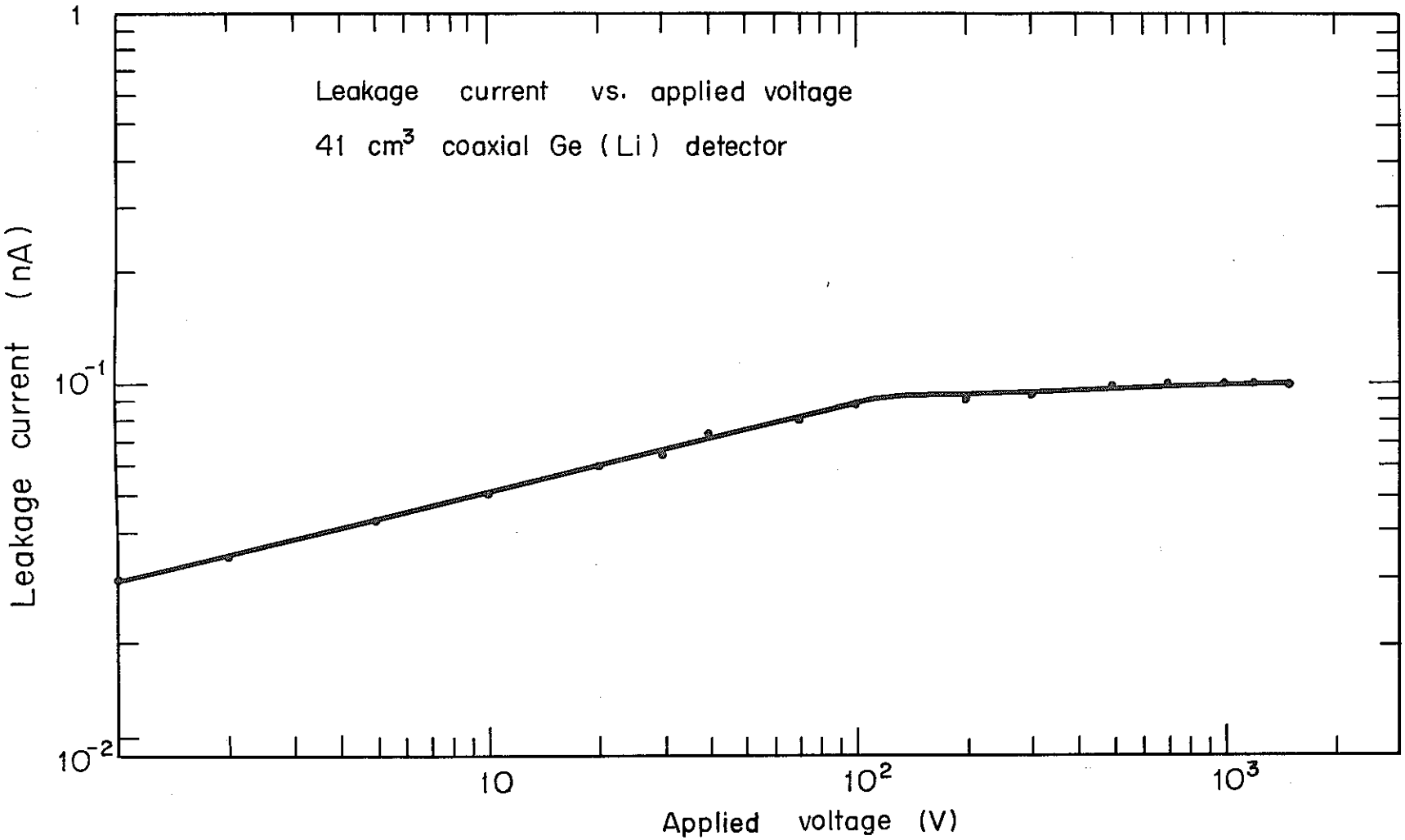

Fig. 6-7 Leakage current vs. applied voltage characteristics of 41 cm^3 coaxial Ge (Li) detector

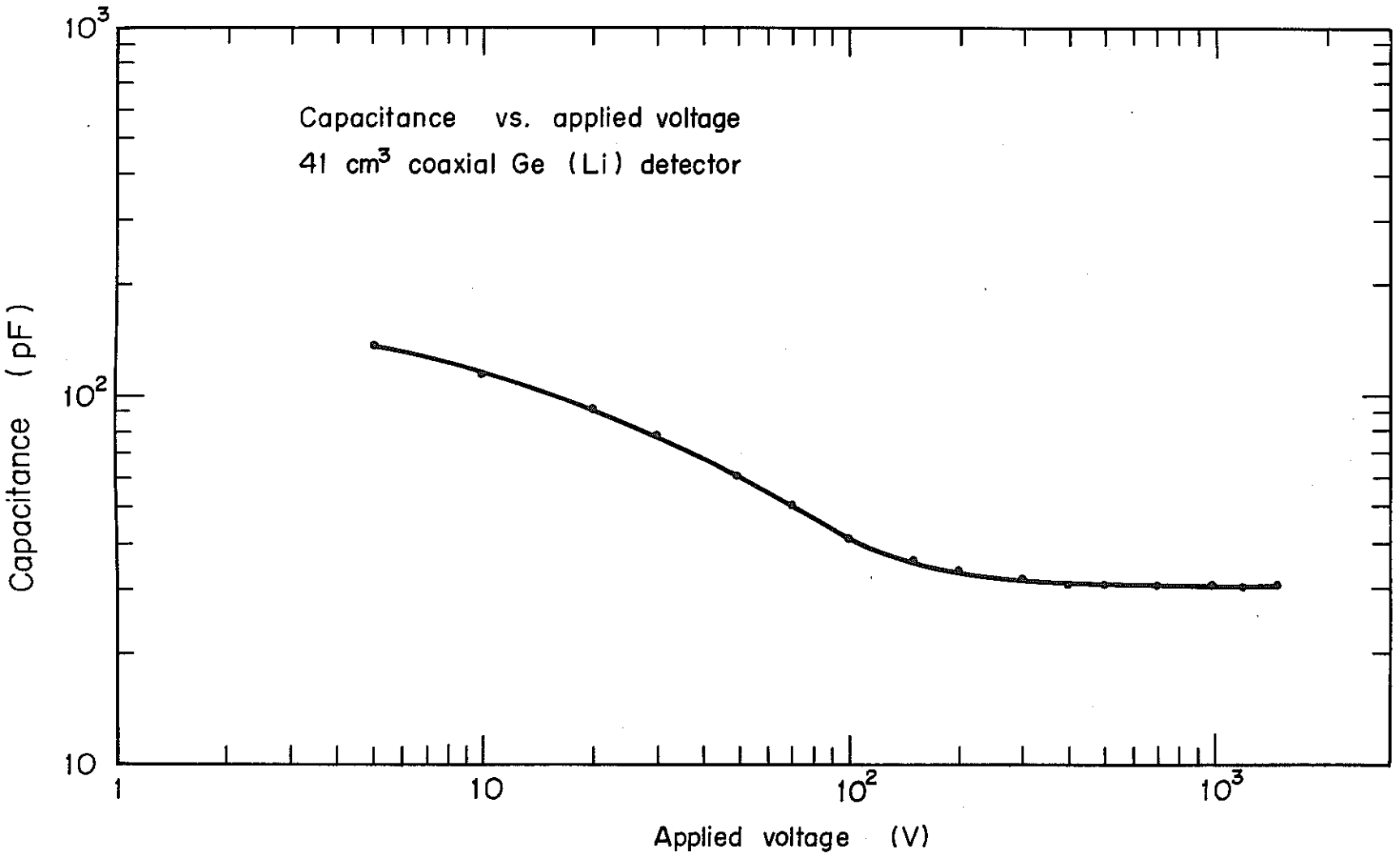

Fig. 6-8 Capacitance vs. applied voltage characteristics of 41cm³ Ge (Li) detector

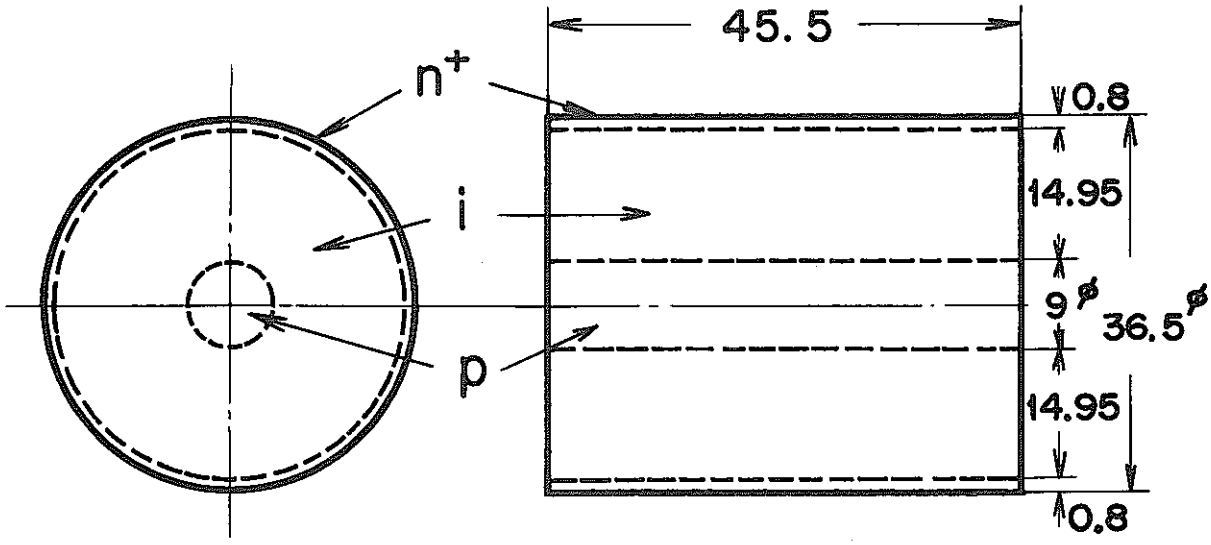

Crystal diameter	36.5	mm
n^+ - layer thickness	0.8	mm
p - region diameter	9.0	mm
i - region thickness	14.95	mm
Crystal length	45.5	mm
Sensitive volume	40.64	cm^3
Crystal volume	47.61	cm^3
Calculated capacitance	29.6	pF

Fig.6-9 Coaxial Ge (Li) detector

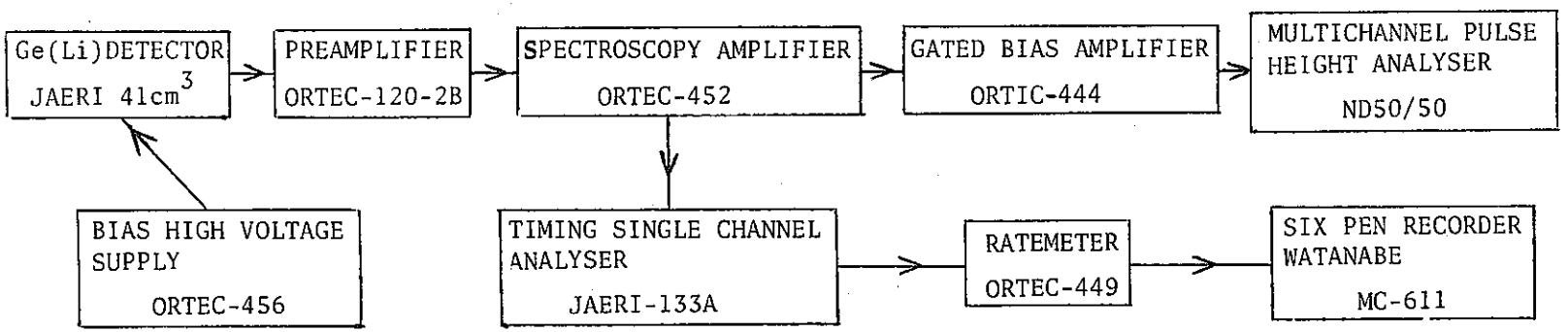

Fig. 6-10 Schematic diagram of electronics used in precipitator wire gamma-ray measurement

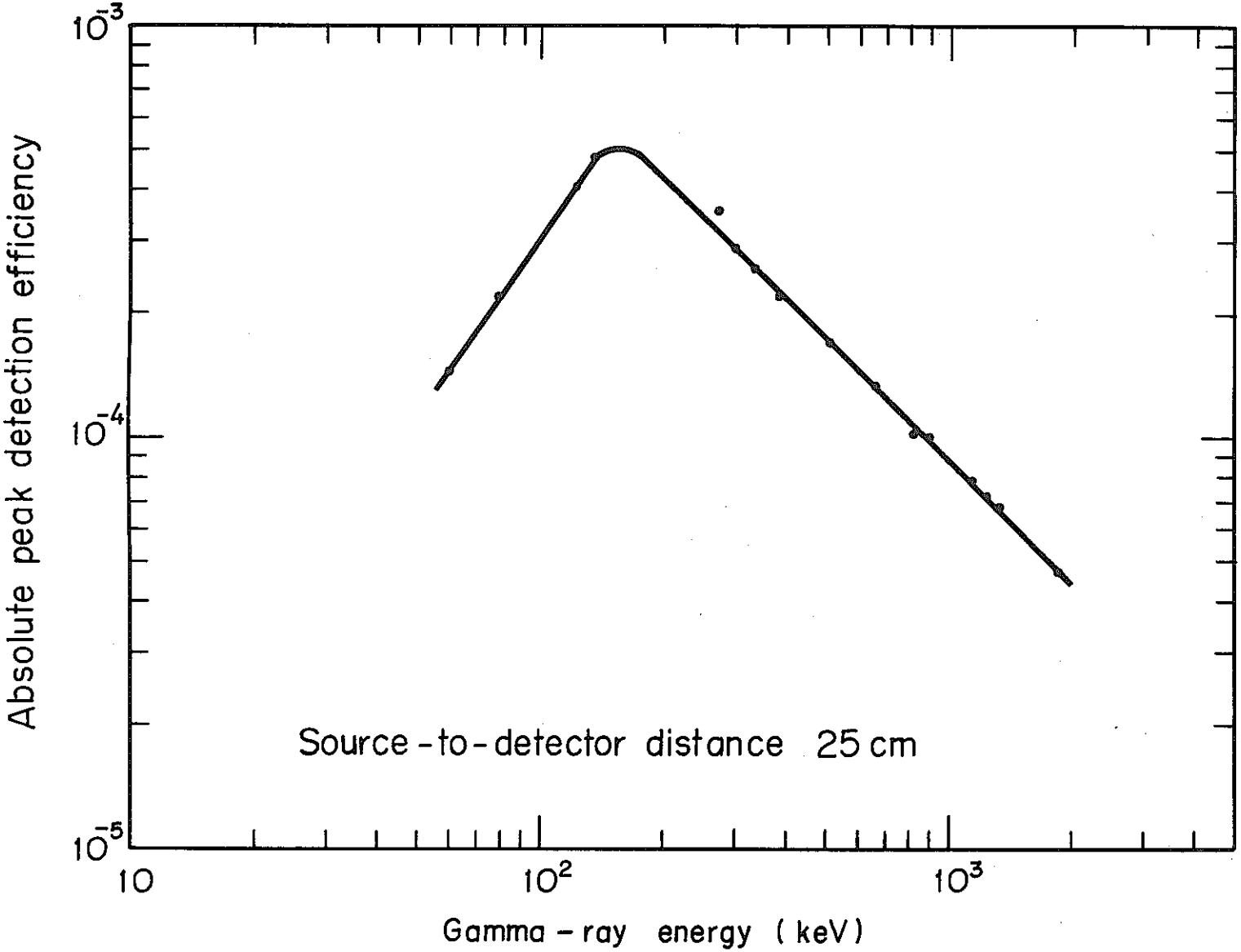

Fig. 6-11 Absolute peak detection efficiency of 41 cm^3 coaxial Ge(Li) detector

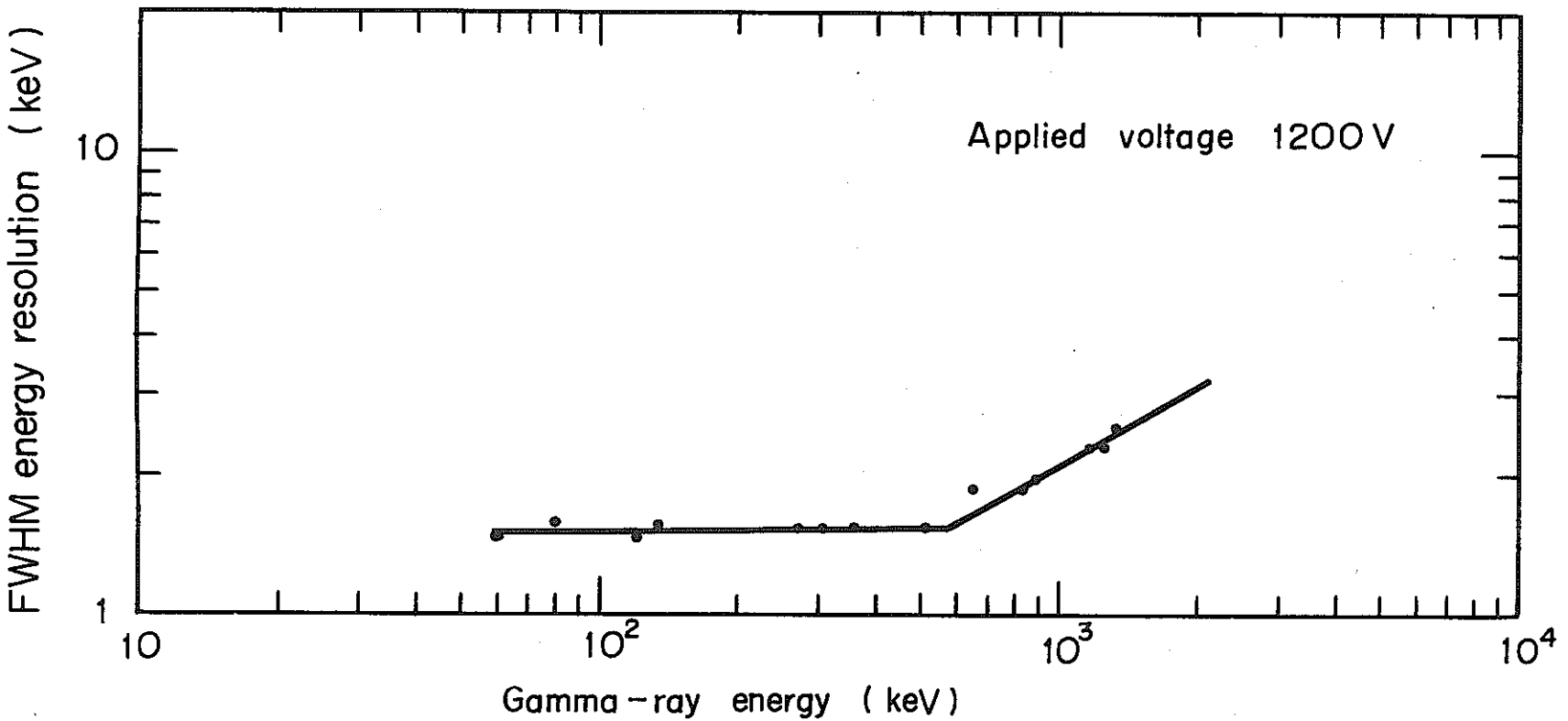

Fig. 6-12 FWHM energy resolution characteristics of 41 cm^3 coxial Ge (Li) detector

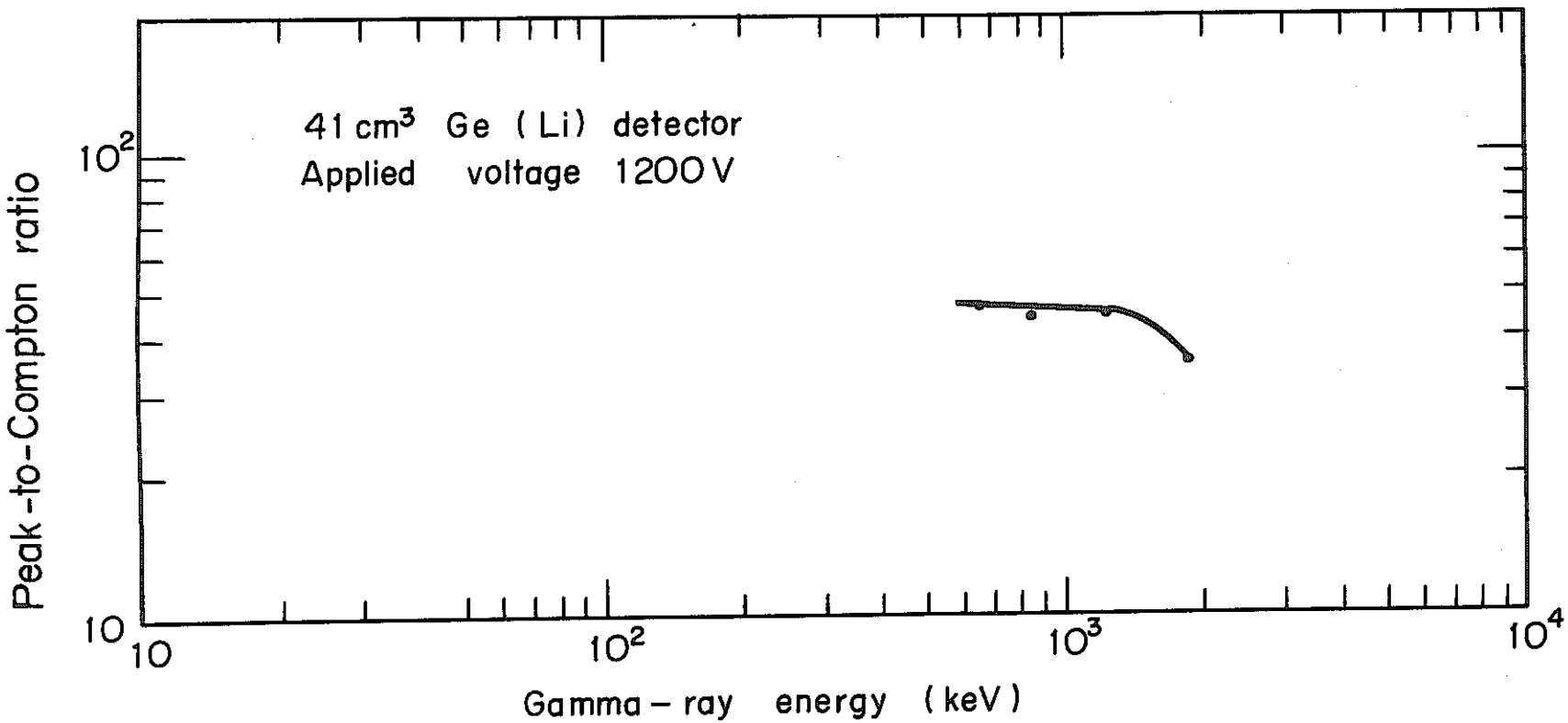

Fig. 6-13 Peak-to-Compton ratio of 41 cm³ coaxial Ge (Li) detector as a function of gamma-ray energy

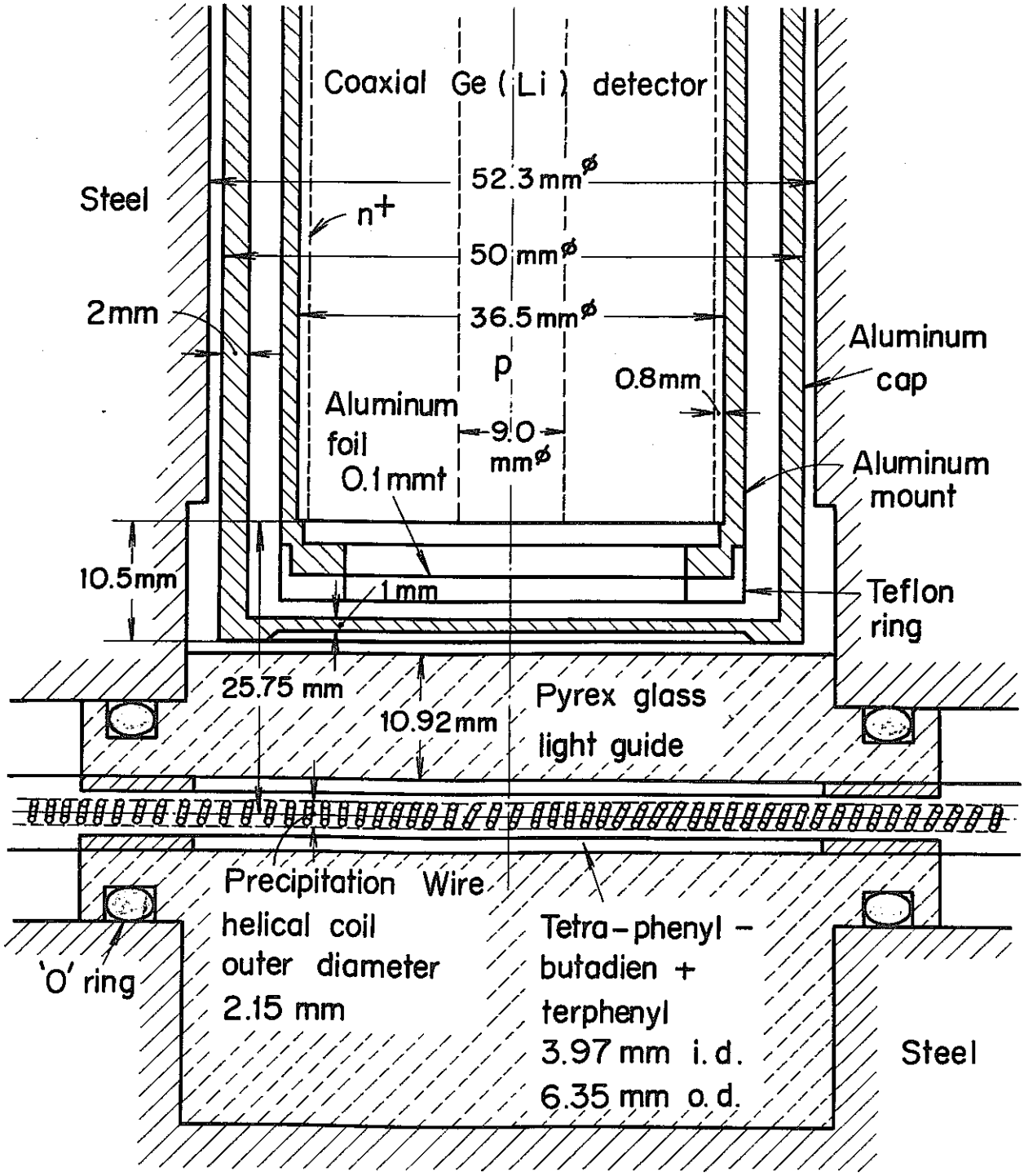

Fig. 6-14 Dimensional relation between Ge (Li) detector and precipitation wire

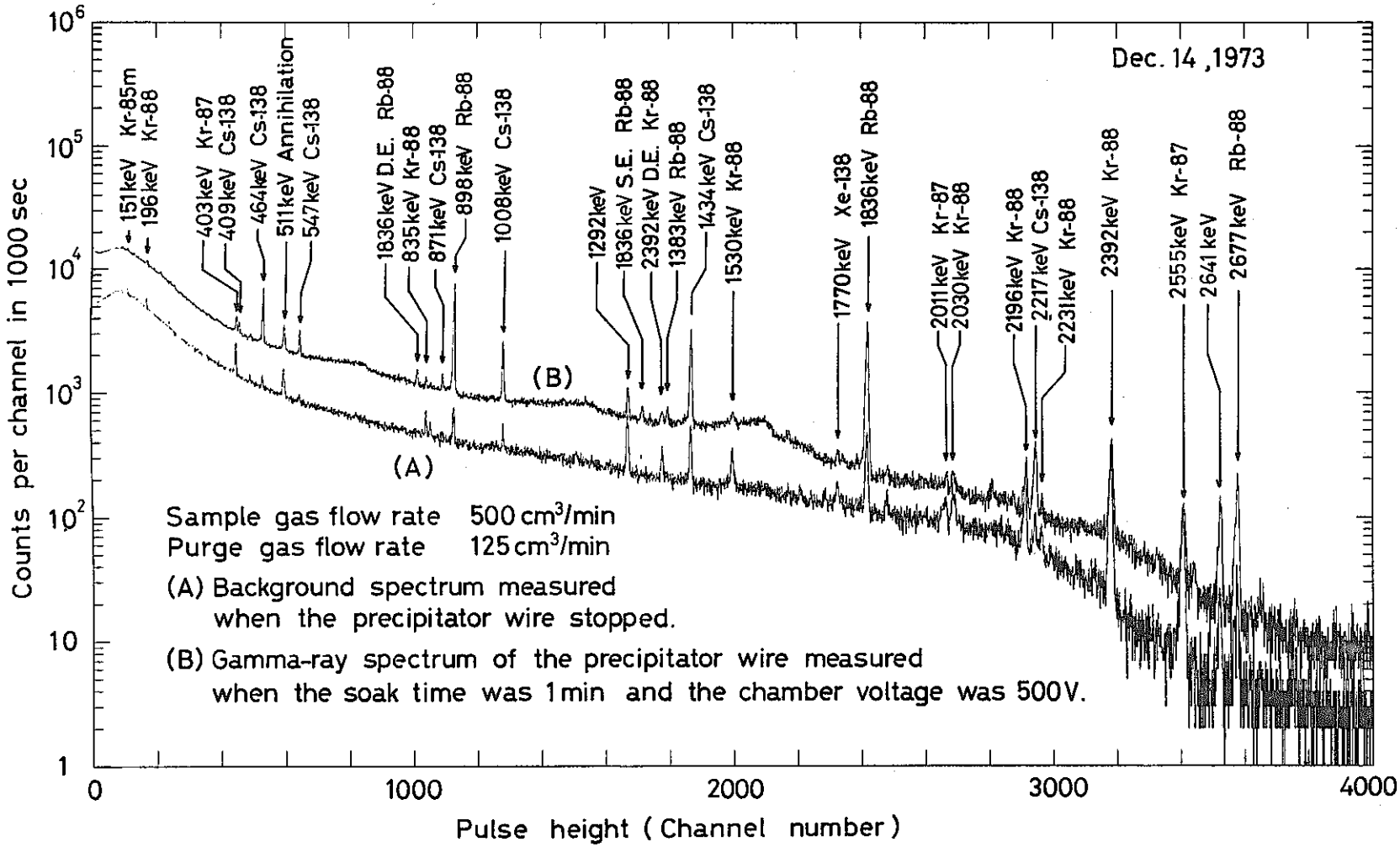

Fig.6-15 Gamma-ray spectra from precipitator wire

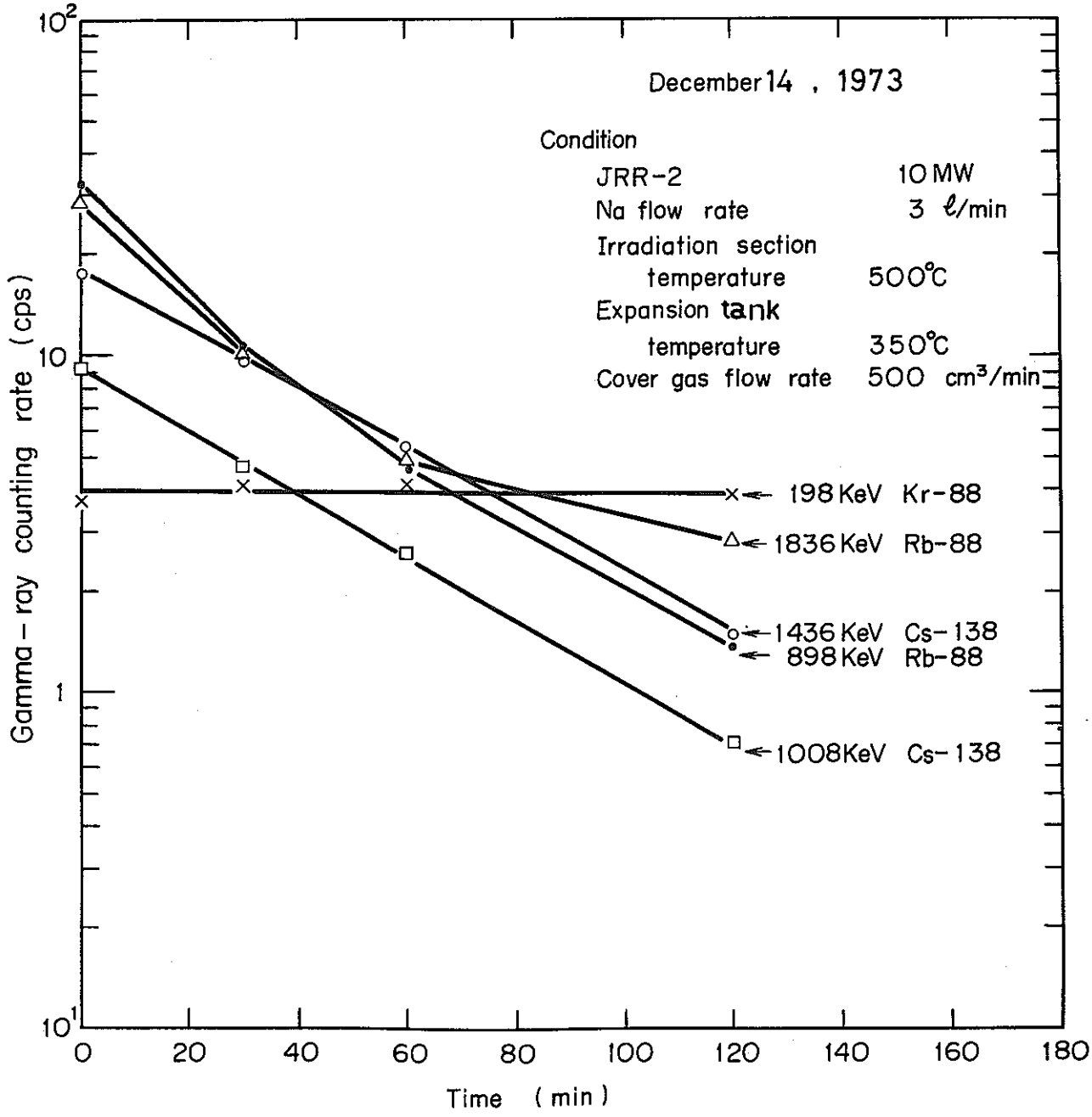

Fig. 6-16 Decay curve of precipitator wire activity measured by a coaxial Ge(Li) detector

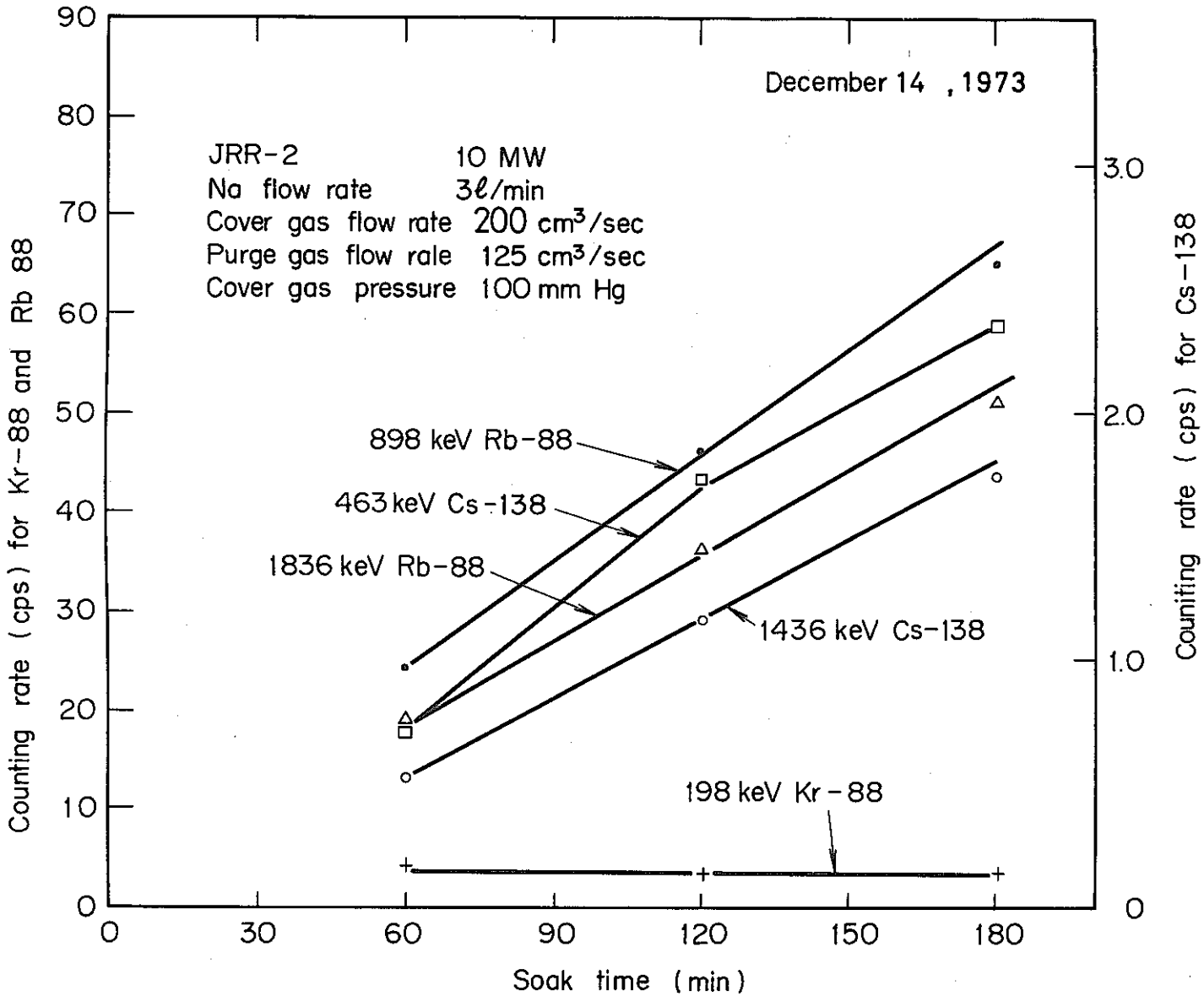

Fig. 6-17 Precipitator wire activity vs. soak time characteristics obtained by 41 cm³ Ge (Li) detector

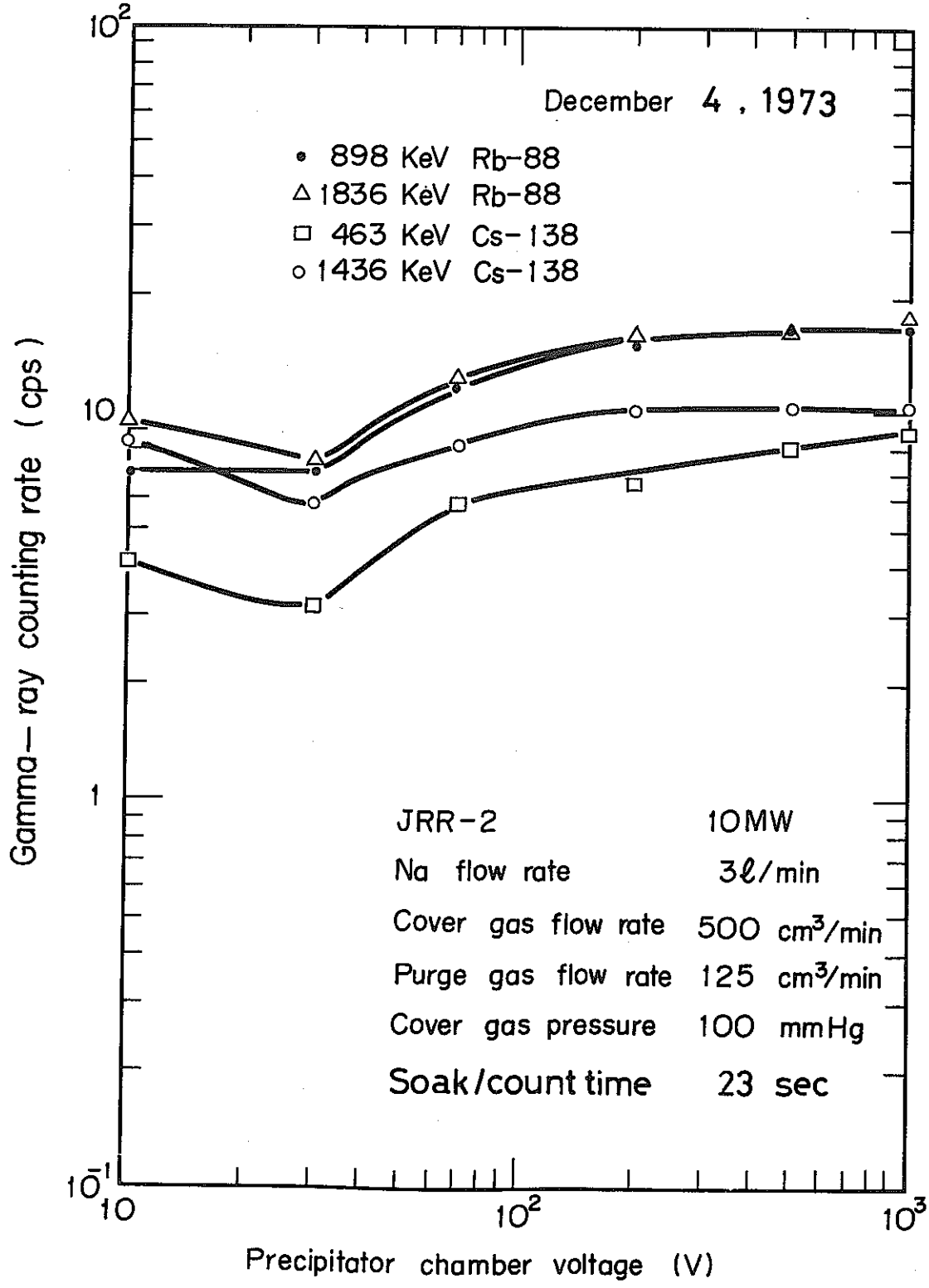

Fig. 6-18 Precipitator counts vs. chamber voltage characteristics obtained by using Ge (Li) detector

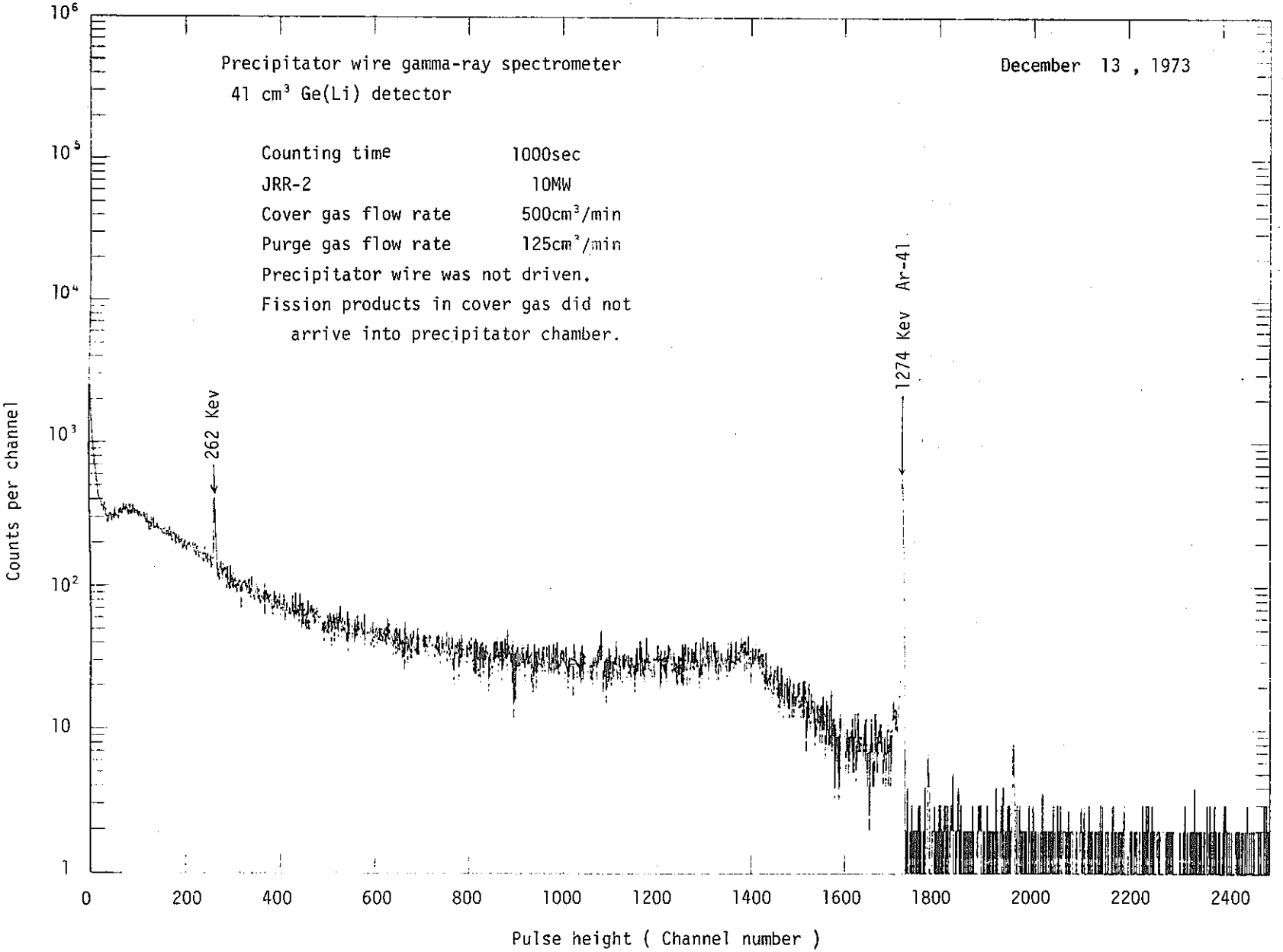

Fig.6-19 Pulse height distrifution of gamma-ray background in precipitator-wire gamma-ray spectrometer.

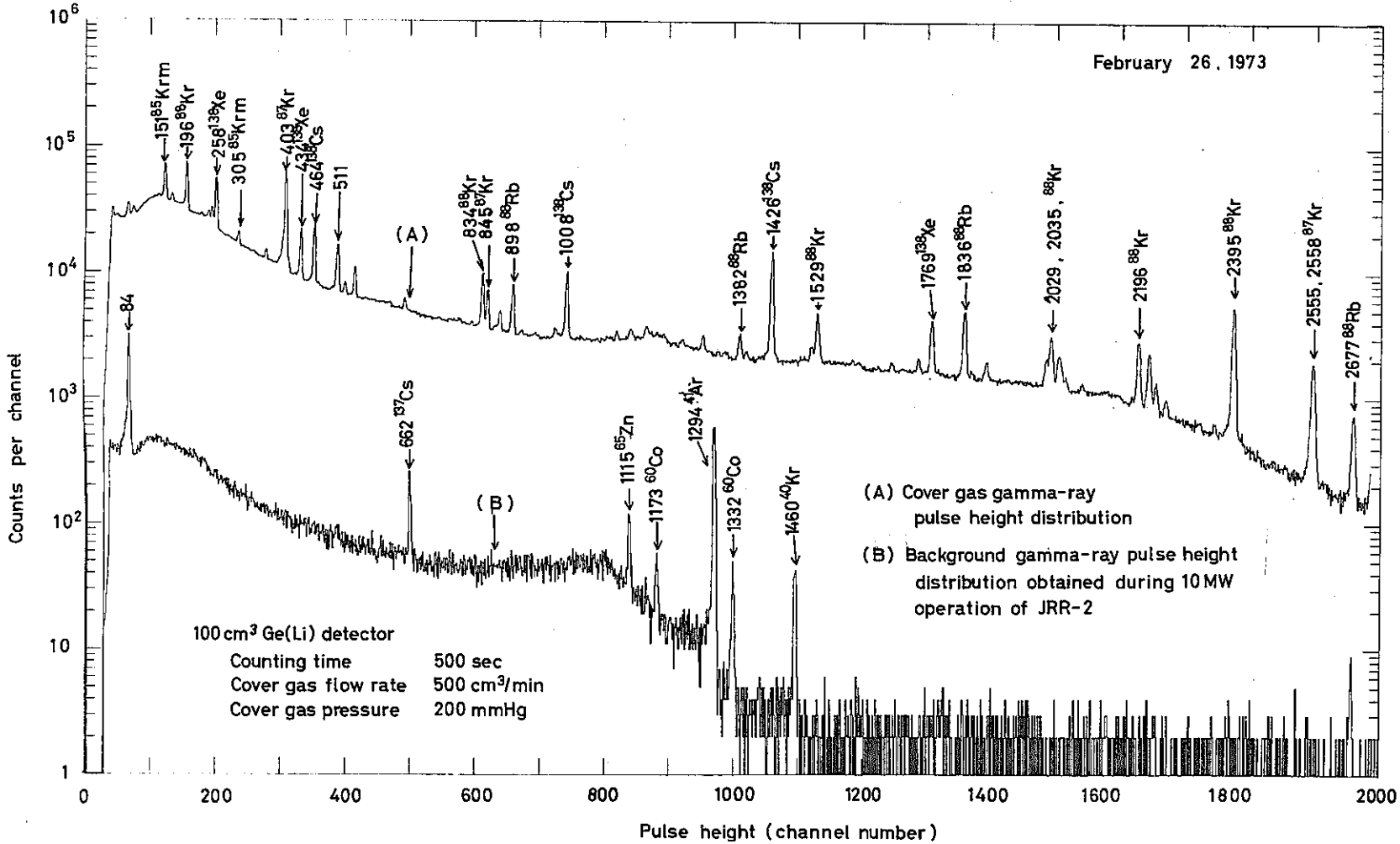

Fig 7-1 Pulse height distribution of gamma-rays from F.P. in cover gas measured by gas reservoir gamma-ray spectrometer